Characterisation of metacaspases of *Trypanosoma brucei*

A thesis submitted for the degree of Doctor of Philosophy in the Faculty of Veterinary Medicine, University of Glasgow

by

Matthew John Helms (B.Sc. Aberdeen 2001)

Wellcome Centre of Molecular Parasitology
Anderson College
University of Glasgow
Glasgow

October 2004

ProQuest LLC.
789 East Eisenhower Parkway
P.O. Box 1346
Ann Arbor, MI 48106 – 1346

Abstract

Metacaspases are proteins, with some sequence similarity to caspases, that have now been identified in plants, fungi and parasitic protozoa, but not mammals. Caspases are a conserved family of central effector cysteine peptidases involved in inflammatory disease, neurodegenerative disorders and apoptosis. Little was known about metacaspase function in any organism, although several studies have linked the metacaspases to apoptotic-like phenomena in both yeast and plants. Five metacaspase genes were identified in *Trypanosoma brucei* (*MCA1-MCA5*) whereas only one, syntenic with MCA5, has been identified in *Leishmania major*. *MCA2, MCA3* and *MCA5* encode for predicted cysteine peptidases, while *MCA1* and *MCA4* have substitutions at the putative active site residues which suggest that they may have a peptidase-independent function. *MCA2, MCA3* and *MCA5* also contain predicted WW binding domain motifs, suggesting the metacaspases may interact with other proteins.

Antibodies against MCA2, MCA3 and MCA5 were raised, and Western blotting revealed that MCA5 is expressed in both the bloodstream form (BSF) and procyclic form (PCF) while MCA2 and MCA3 expression is BSF specific *in vitro*. None of the proteins showed any large scale processing events, all being detected at around their predicted full-length masses. MCA2, MCA3 and MCA5 localised to the same compartment – vesicles located primarily between the nucleus and kinetoplast. Analysis revealed that the metacaspases co-localise with Rab11 in both PCF and BSF parasites. In BSF *T. brucei*, Rab11 positive recycling endosomes are involved in the recycling of both variable surface glycoprotein (VSG) and the transferrin receptor.

Metacaspase function was investigated by RNAi and subsequently gene knockouts. While the RNAi results were inconclusive, the gene knockouts revealed that *MCA2*, *MCA3* and *MCA5* are non-essential genes, both *in vitro* and *in vivo*. Upon generation of BSF *Δmca2/3Δmca5* parasites, an initial reduced growth rate was observed, although after successive passages growth rate returned to wild type levels. A comparative analysis of both VSG and transferrin receptor recycling processes revealed that these were the same in wild type and

Δ*mca2/3*Δ*mca5* BSF parasites. The possibility of metacaspase involvement in cell death processes was also examined. Parasites were exposed to heat shock and salt stress, but no differences between wild type and Δ*mca2/3*Δ*mca5* parasites were detected. These data suggest that the metacaspases are associated with Rab11 positive recycling endosomes, but are not essential for either VSG or transferrin receptor recycling, nor anti-VSG antibody or transferrin degradation.

Table of contents

List of figures

Chapter 1

Chapter 3

Chapter 4

Chapter 5

Acknowledgements

I would like to thank my supervisors, Jeremy Mottram and Graham Coombs for all their help, supervision and advice over the three years and for giving me the job in the first place.

Thanks to all the people in the lab who have helped over the years including Hubert Denise, Sebastein Besterio, Karen Grant, Dr Thesis aka Slyvan Enschalauer, Audry Ambit, Saj, Christina Naula, Felipe Gomez, Tansy Hamerton, Simon Lillico, Fiona Douglas and anyone else who's name I forgot.

A special thanks to Kirsten for keeping my spirits up when it was getting to me – and to the my parents (perhaps I've finally finished studying).

The research reported in this thesis is my own original work, except where otherwise stated, and has not been submitted for any other degree.

Matthew John Helms

October 2004

Abbreviations

BB	- Binding buffer
BSA	- Bovine serum albumin
BSF	- Bloodstream Form
B-PER	- Bacterial protein extraction reagent
CIP	- Calf intestinal phosphate
DABCO	- 4-diazabicyclo[2.2.2]octane
DAPI	- 4',6-diamidino-2-phenylindole
DMSO	- Dimethyl sulphoxide
EB	- Elution buffer
EDTA	- Ethylenediaminetetraacetic acid
EGTA	- Ethyleneglycol-bis(b-aminoethylether)-*N*,*N*,*N*',*N*'-tetraacetic acid
ECL	- Enhanced chemiluminescence
FITC	- Fluorescein isothiocyanate
HRP	- Horseradish peroxidase
IgA	- Immunoglobulin A
IgG	- Immunoglobulin G
IPTG	- Isopropyl-β-D-thiogalactopyranoside
LB	- Luria-Bertani medium
NaAc	- Sodium acetate
PBS	- Phosphate-buffered saline
PCR	- Polymerase chain reaction
PBST	- PBS 0.05% Tween 20
PCF	- Procyclic Form
Pfu	- *Pyrococcus furiosus* DNA Polymerase
PVDF	- Polyvinylidene Fluoride
SDS	- Sodium dodecyl sulphate
SDS-PAGE	- SDS-polyacrylamide gel electrophoresis
SSC	- Salt sodium citrate buffer
TAE	- TRIS acetate EDTA buffer
Taq	- *Thermus aquaticus* DNA polymerase
TBE	- TRIS borate EDTA buffer
TDB	- Trypanosome dilution buffer

TRIS	- Tris [hydroxymethyl] aminomethane
TRITC	- Tetramethylrhodamine isothiocyanate
TritonX-100	- t-Octylphenoxypolyethoxyethanol
Tween-20	- Polyoxyethylene sorbitan monolaurate
X-Gal	- 5-bromo-4-chloro-3-indolyl-β-[D]-galactopyranoside
ZPFM	- Zimmerman's post fusion medium
ZPFMG	- ZPFM glucose

Chapter 1

Introduction

1.1 Trypanosomiasis.

Certain species of parasitic trypanosomatid protozoa still represent a major problem in the developing countries of the world. Their associated diseases are the cause of both serious economic and medical problems throughout large areas of Africa, Asia and South America. Problem species include the African trypanosome *(Trypanosoma brucei)*, the South American trypanosome (*Trypanosoma cruzi*) and a widespread variety of species of *Leishmania*. The trypanosomatids have very ancient evolutionary origins, believed to have diverged early in evolution from the other eukaryotic lineages and are classified together in the Order Kinetoplastida. The Kinetoplastida are characterized by a number of peculiarities such as the presence of the kinetoplast, which contains the mitochondrial DNA and is found within the single large mitochondrion.

All members of the genus *Trypanosoma*, with the exception of *T. equiperdum*, have indirect, or heteroxenous, life cycles. Members of this genus parasitise all classes of vertebrates, residing in the blood and tissues of infected animals, although some also occupy intracellular locations, most notably *T. cruzi*. The vector for *T. brucei* transmission, which causes diseases in both humans (sleeping sickness) and livestock (nagana), is the tsetse fly. Sleeping sickness, a disease that in the 1960's was believed to be under control, is now a daily threat to more than 60 million people in 36 countries of sub-Saharan Africa, which include some of the least developed countries in the world. It is estimated that between 300,000 and 500,000 people may be affected by the disease (World Health Organisation - www.who.int). Following infection, the trypanosomes multiply in the blood and lymph glands before eventually invading the central nervous system (CNS) by crossing the blood-brain barrier. This invasion of the CNS results in often-irreversible neurological alterations and without treatment the patient falls into a coma and invariably dies.

There are three subspecies of *T. brucei*: *T. brucei brucei*, which is not human infective, and *T. brucei rhodesiense* and *T. brucei gambiense* that are. *T. brucei rhodesiense* infection results in an acute illness, lasting several months and is prevalent in countries of eastern and southern Africa. In contrast, *T. brucei gambiense* infection results in a more chronic illness lasting several years and is

prevalent in mainly western and central African countries. Death in *T. brucei gambiense* infections is often from secondary causes such as malnutrition or other parasitic infections prior to symptoms of late sage infection developing.

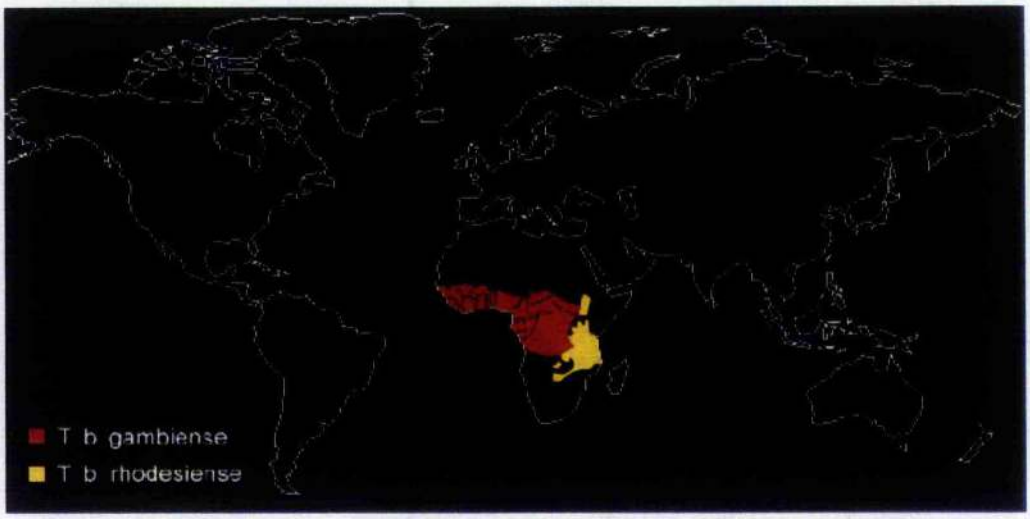

Figure 1.1: Geographical distribution of human infective *T. brucei* species.

The current treatment for trypanosomiasis is based on four main drugs, namely suramin, pentamidine, melarsoprol, and eflornithine. No new drugs have been developed in the last 25 years and most were introduced in the first half of the 20th century. Some of these drugs have very severe side effects and it is doubtful if they would be registered if developed today. Early stage infections are treated with pentamidine or suramin for *T. brucei gambiense* or *T. brucei rhodesiense* respectively. These treatments are usually effective and prevent disease progression. For late stage infections, the only effective drug for both human infective forms is the trivalent arsenical melarsoprol, due to its ability to cross the blood brain barrier. However, melarsoprol is also highly toxic, the most serious side effect is post treatment reactive encephalopathy (PTRE), which occurs in 5–10% of cases with a fatality rate of approximately 50% (Pepin and Milord, 1994). In addition to these problems, resistance to melarsoprol has also begun to emerge, with treatment failure rates of 30% reported among patients in Northern Uganda (Legros *et al.*, 2002). Eflornithine has been used successfully to treat late stage disease, especially in melarsoprol-refractory *T. brucei gambiense* infections, but seldomly for *T. brucei rhodesiense* which is more resistant to this drug (Burri and Brun, 2003).

However, eflornithine is expensive, difficult to administer and was non-profitable for drug companies. Only in recent years has this drug become available once more for treatment of the disease (Kennedy *et al.*, 2002).

Our understanding of the biology of the these organisms has been increased dramatically over the years but despite over a 100 years of research the diseases associated with these infections are still highly prevalent. The coming of genomics, however, has opened up new possibilities in kinetoplastid research and hopefully the coming decade will see major advances in the drugs available for treatment of these diseases.

1.2 Trypanosome biology.

The study of the cell biology of *T. brucei*, and indeed the kinetoplastids, has uncovered a number of strange and unique features. As described above, the Kinetoplastida possess a single large mitochondrion and in *T. brucei* this extends for virtually the length of the cell body (Figure 1.2). Located within the mitochondrion, is a specialised structure known as the kinetoplast, which contains the mitochondrial genome (kDNA) and within this structure a unique form of RNA editing occurs. The kDNA is made up of thousands of interlocked circular DNA molecules, composed of several thousand minicircles intertwined with a few dozen maxicircles. The maxicircles have a role similar to mitochondrial DNA in conventional eukaryotes, encoding for mitochondrial ribosomal RNA and subunits of the respiratory complexes. The minicircles, however, encode for guide RNAs that act as templates for the editing of maxicircle transcripts. This reaction is catalysed by a multi protein complex termed the editosome, and 16 proteins which make up this complex have been identified (Stuart and Panigrahi, 2002; Panigrahi *et al.*, 2003). This editing is essential for the generation of mature functional mRNAs, and involves the insertion or deletion of uridine residues at specific sites within the transcripts. The extent of editing of mitochondrial transcripts varies, from four uridine insertions to the insertion and deletion of hundreds of uridine residues (Benne *et al.*, 1986).

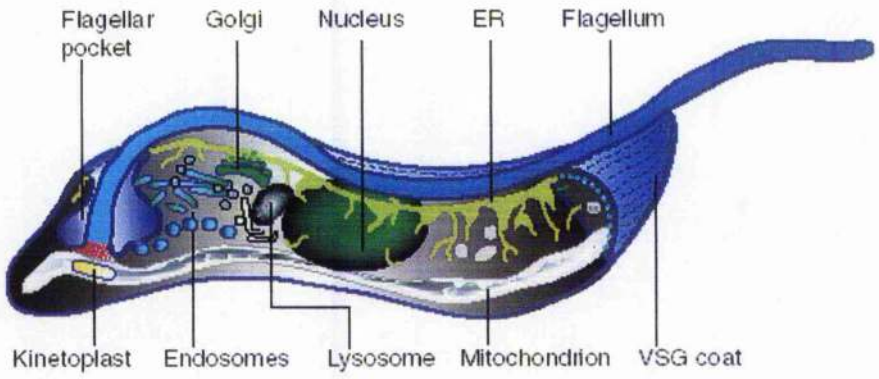

Figure 1.2: Illustration of bloodstream form (BSF) trypanosome, taken from Overath *et al.*, 2004).

Another unique structure to kinetoplastids are organelles termed glycosomes. These structures, related to peroxisomes of higher eukaryotes, have a specialised role in glucose metabolism (Clayton and Michels, 1996). In all Kinetoplastida studied, the major part of the glycolytic pathway is located within these organelles. Although glycolytic enzymes are the major enzymes found in glycosomes (up to 90% in Bloodstream form (BSF) *T. brucei*), other enzymes are also present which are common to peroxisomes, such as enzymes involved in fatty acid oxidation or lipid biosynthesis (Parsons *et al.*, 2001). In BSF *T. brucei*, in which the mitochondrion is not fully functional, the parasites use this organelle to facilitate ATP generation independent of oxidative phosphorylation. Although this rapid oxidation of glucose and production of ATP is much less efficient than oxidative phosphorylation, this is irrelevant due to the high availability of glucose available from the host's blood. Procyclic form (PCF) *T. brucei* have a more complex metabolic pathway that also involves the mitochondrion, although it has been suggested that the Kreb's cycle activity is not essential for energy production (van Weelden *et al.*, 2003).

With regard to the endocytic apparatus, it is believed that the trypanosomatids are similar to other eukaryotes. Homologues of several proteins associated with various components of the endosomal system have been described. These include BiP, an endoplasmic reticulem (ER) chaperone (Bangs *et al.*, 1993), the lysosomal protein p67 (Kelley *et al.*, 1999), and numerous Rab proteins which

are involved in vesicular trafficking (Field *et al.*, 1998; Field *et al.*, 1999; Jeffries *et al.*, 2001; Denny *et al.*, 2002; Jeffries *et al.*, 2002; Pal *et al.*, 2003; Dhir *et al.*, 2004). Through the study of the endocytic system in trypanosomatids it has been concluded that the system operates similarly to higher eukaryotes. For example, early endocytic vesicles are associated with Rab5 (Pal *et al.*, 2002) while recycling endosomes are associated with Rab11 (Jeffries *et al.*, 2001), and this has been observed across the genera (Gorvel *et al.*, 1991; Bucci *et al.*, 1992; Ullrich *et al.*, 1996; Green *et al.*, 1997).

In trypanosomatids, however, endo and exocytosis are limited to a region termed the flagellar pocket, an invagination of the plasma membrane representing approximately 0.5-3% of the cell surface. This is due to the presence of a sub-pellicular microtubule sheath underneath the plasma membrane but which is absent in the flagellar pocket region (Coppens *et al.*, 1987; Balber, 1990; Overath *et al.*, 1997). This pocket, from where the flagellum emerges, is located at the anterior end of the cell and is surrounded at its opening by a region referred to as an adhesion zone (Balber, 1990). This results in the formation of a secluded, yet extracellular, compartment (Brickman and Balber, 1993), with macromolecules entering or leaving the flagellar pocket having to pass through this adhesion zone.

To protect themselves from the harsh environments they inhabit, both life stages of *T. brucei* possess a densely packed surface coat. In the bloodstream and metacyclic forms, this is composed of more than 10^7 variable surface glycoprotein (VSG) molecules (Cross, 1975). This represents approximately 10% of the total cellular proteins and they are attached to the membrane via a glycosylphosphatidylinositol (GPI) anchor. The PCF coat is composed of an invariant surface molecule termed procyclin (Mowatt and Clayton, 1987; Richardson *et al.*, 1988), which, like VSG, is also attached to the membrane via a GPI anchor (Field *et al.*, 1991) and forms a protective surface coat (Ferguson, 1997)

1.3 Life cycle of *T. brucei*

1.3.1 Parasite development in mammalian host.

T. brucei is a digenetic pathogen whose complete life cycle involves alteration between mammalian host and insect vector, the tsetse fly. The parasites are transmitted to their mammalian hosts through an infected bite of a tsetse fly. The injected parasites termed metacyclic trypomastigotes initially form a lesion, and after multiplying for several days gain access to the blood through the lymphatic system. Initially, the parasites take on a long-slender form and rapidly divide, but as the parasitaemia advances these gradually differentiate into a non-proliferative short stumpy form. The stimulus which induces this change has been termed stumpy induction factor (SIF), although the identification of this molecule has eluded investigators. SIF is believed to be a trypanosome-produced factor which induces differentiation in a density-dependent manner (Vassella *et al.*, 1997). The slender form is exquisitely adapted for exploiting the rich source of glucose within the blood, rapid glycolysis occurring within the glycosomes (Opperdoes and Borst, 1977). Within the stumpy form, which accumulates at the peak of the parasitaemia, the mitochondrial respiratory chain which had been previously defunct becomes partially active (Feagin *et al.*, 1986; Michelotti and Hajduk, 1987; Bienen *et al.*, 1991). This is an essential change in the cellular biochemistry that enables the parasite to quickly adapt to the decrease in glucose concentrations experienced upon transfer to the insect host. Thus the parasite has fulfilled both rapid proliferation within the mammalian host and maximised the chances of successful transmission into the vector.

1.3.2 Antigenic variation.

Within the mammalian host, the trypanosomes are exposed to the immune system and evasion of this response is facilitated through the process of antigenic variation (Cross, 1975; Vickerman, 1978). Bloodstream and metacyclic form trypanosomes both possess a VSG coat, and while these molecules serve to protect the parasites from non-specific host immunity (Overath *et al.*, 1994), they are themselves highly immunogenic. The immune response mounted by the host results in the parasitaemia going into remission as

parasites are eliminated by complement-mediated lysis. However, through the process of antigenic variation a proportion of the parasites within the total population will have switched their variable antigen type (VAT). These different VAT's perform the same protective function, but provide the variation required to evade the immune response. This antigenic variation is behind the waves of parasitaemia observed in *T. brucei* infections. As the trypanosome population increases, attack by the immune system reduces the level of parasitaemia, subsequently followed by another wave of growth through VAT switching. Each VAT arises from the expression of a single *VSG* gene, from an estimated repertoire of approximately 1000 genes (Van der Ploeg *et al.*, 1982), although it is believed that only around 5% of these are functional (L. Marcello - personal communication). Many of these *VSG* genes are located in large arrays in the interior of chromosomes (Van der Ploeg *et al.*, 1982) while others are subtelomeric or found on minichromosomes. To ensure the exclusive expression of one *VSG* gene and maintain silence of all others, the parasites restrict transcription of *VSG* to transcriptionally active sites known as bloodstream expression sites (BSEs). For silent *VSG* genes to become active they must move to a BSE and this occurs via homologous recombination (Barry and McCulloch, 2001), the silent gene remaining intact while the active gene is replaced. The frequency of VAT switching is estimated at 1 switch per 10^3 cell divisions in pleomorphic trypanosomes (Turner and Barry, 1989) and this process appear to be spontaneous and independent of immunity (Hajduk *et al.*, 1992). However, the parasites also contain multiple copies of the BSEs within the genome, and only one BSE is active at anyone time. The exclusive expression from only one BSE is attained through a unique structure termed the expression site body (ESB) (Navarro and Gull, 2001). The ESB is believed to facilitate expression from a single BSE while excluding expression from all others. Also located at the BSEs are a number of expression site associated genes (ESAGs) (Cully *et al.*, 1985; Alexandre *et al.*, 1988; Pays *et al.*, 1989; Son *et al.*, 1989; Stadnyk *et al.*, 1991). These include a number of genes encoded for proteins destined for the cell surface, including *ESAG6* and *ESAG7*, which encode for the two subunits of the transferrin receptor (Steverding *et al.*, 1994; Salmon *et al.*, 1994).

1.3.3 Parasite development in tsetse fly vector.

Upon ingestion by a blood-feeding tsetse fly, parasites initially enter the lumen of the midgut where they experience radical changes in their environment, including a drop in temperature from 37°C to between 22-28°C, digestive enzymes and a reduction in glucose concentration. The short-stumpy form is able to make this transition very efficiently, while the majority of long-slender form trypanosomes ingested do not survive. As the availability of glucose reduces during blood meal digestion, oxidative phosphorylation takes over the energy requirements of the cell, utilising proline as fuel (Evans and Brown, 1972). Within 48-72 hours post-ingestion, the short-stumpy form begins to differentiate into the procyclic form (Vickerman, 1985), involving loss of VSG coat (Overath *et al.*, 1983), an increase in length, less dependence on glycosomal activity and expansion of the mitochondrion. The procyclic form also replaces the VSG coat with procyclin (Mowatt and Clayton, 1987; Richardson *et al.*, 1988). The procyclic form then invades the space between the peritrophic membrane and midgut epithelium (Evans and Ellis, 1983), where it resides and proliferates for the life span of the vector. A proportion of this population then further migrates towards the proventriculus, growing in length and ceasing division, at which stage they are termed mesocyclic trypanosomes. Invasion of the endoperitropic space then occurs, followed by movement into the salivary glands via the oesophagus, mouth parts and salivary ducts (Vickerman, 1985). Once within the salivary glands, several stages of differentiation occur. Initially they become epimastigotes, the main proliferative stage in the salivary glands, and attach to the epithelial cell microvilli by means of their flagellum. This is followed by differentiation into premetacyclic trypanosomes and subsequent differentiation into nascent metacyclic trypanosomes, involving cessation of cell division and acquisition of a VSG coat (Tetley and Vickerman, 1985). This form, while still attached to epithelial microvilli, possesses an acristate mitochondrion and functional glycosomes. Upon final transformation into mature metacyclic trypanosomes they detach from the epithelium, are free in the lumen of the salivary glands and are fully preadapted for life within a mammalian host.

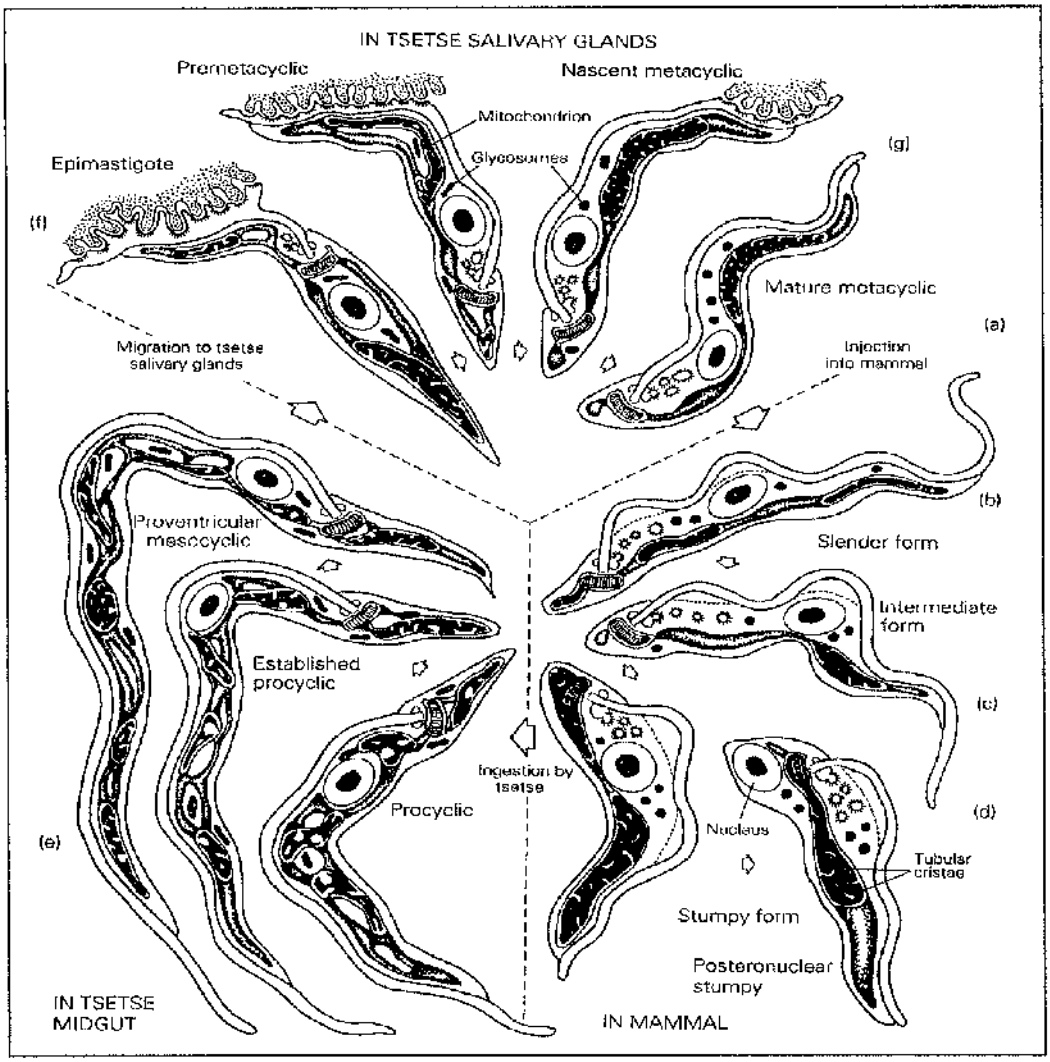

Figure 1.3: Diagrammatic representation of *T. brucei* life cycle, taken from Vickerman (1985).

1.4 Apoptosis and Programmed Cell Death (PCD).

The phenomena of programmed cell death (PCD) and apoptosis are mechanisms whereby specific cells in an organism are led down a suicidal pathway, which is more favourable than necrosis (Searle *et al.*, 1982). Necrosis is a passive, degenerative process induced by a cytotoxic event, commonly involving irreversible plasma membrane damage or inhibition of ATP synthesis. Such cytotoxic events lead to a collapse of membrane potential and result in a loss of ionic homeostasis (Choi, 1988). Unregulated increases in calcium concentrations result in a disruption of the cytoskeleton, along with the activation of degradative enzymes, and the influx of sodium results in a loss of cellular volume control and the cell ultimately ruptures, releasing its contents into the surrounding environment (Hall *et al.*, 1997). This can result in neighbouring cell damage or local inflammation and such a crude process can be very damaging to an organism or tissue. The actual resultant release of cellular contents can be more damaging than the initial cytotoxic insult.

PCD/apoptosis in comparison, are regulated forms of cell death that avoid the problems associated with necrosis (Syntichaki and Tavernarakis, 2002). Cells marked for destruction are removed without causing damage to local cells/tissues. The terms PCD and apoptosis are sometimes used collectively to refer to the same processes although this classification strictly is not correct. PCD should be thought of as cell death occurring during development under pre-determined genetic control, whereas apoptosis can be considered as an active process in which a specialised signalling pathway is responsible for the death of the cell (Kaufmann and Hengartner, 2001). While the stimuli for the two processes may be distinct, the intercellular effector pathways utilised to accomplish the cellular disassembly processes are similar. The effectors of these processes are the caspases, the targets of which have been studied extensively (Fischer *et al.*, 2003). Some of these include various members of the Bcl-2 family of proteins (Xue and Horvitz, 1997; Cheng *et al.*, 1997); these are mitochondrial-associated proteins involved in the regulation of among other things of the mitochondrial permeability transitional pore (MPTP). A nuclear protein, termed Acinus (apoptotic chromatin condensation inducer), has been identified that following caspase cleavage, elicits chromatin condensation and

nuclear fragmentation (Zamzami and Kroemer, 1999). Other targets include laminins, cytoskeletal proteins and DNA repair enzymes including poly (ADP-ribose) polymerase (Gu *et al.*, 1995).

Kerr *et al.* first described apoptosis morphologically in 1972 and in the past decade there has been a vast amount of research into the field. The onset of apoptosis/PCD is characterised by shrinkage of the cell and nucleus, together with condensation of nuclear chromatin, which is later followed by the complete break-up of nuclear material, termed karyorrhexis (Kerr *et al.*, 1972). The cell body becomes detached from the surrounding tissue and cellular extensions proceed to bud away from the plasma membrane. These apoptotic bodies, densely packed with intracellular organelles and fragments of nucleus, are rapidly phagocytosed by macrophages or neighbouring cells. This process usually occurs with no local inflammation or neighbouring cell damage and is thus the most common type of physiological cell death. Research into the processes behind PCD/apoptosis have clarified that it represents the facet of cell death that is actively driven by complex signalling pathways within the cells. On the flip side, necrosis represents a passive consequence of gross injury to the cell.

1.5 Apoptotic/PCD-like phenomena in single cell organisms.

Although apoptosis/PCD has only ever been fully characterised in multi-cellular organisms, there have been many claims of such pathways existing in single cell organisms also. The slime mould *Dictyostelium discoideum* spends the majority of its life cycle as a unicellular protist. However, under low nutrient conditions a dramatic transformation is induced, involving aggregation, differentiation and morphogenesis, resulting in the formation of a structure called a sorocarp. This is a multicellular fungus-like structure consisting mainly of spores and stalk cells. It is within these stalk cells that several features reminiscent to PCD have been observed (Cornillon *et al.*, 1994). Cytoplasmic and chromatin condensation was evident, although the presence of cellular vacuolisation and lack of DNA fragmentation do not agree with the classical definition of PCD. Caspase inhibitors have been used in an attempt to attenuate cell death within these stalk cells with no effect (Olie *et al.*, 1998) and recently it has been shown

that this type of cell death is independent of paracaspase activity, the sole caspase-like gene identified in *D. discoideum* (Roisin-Bouffay *et al.*, 2004).

The ciliated protozoon *Tetrahymena thermophila* contains two distinct nuclei separating somatic and germ line functions, termed macro- and micronuclei, respectively. During the sexual process of this organism the micronucleus, normally transcriptionally silent, gives rise to both new macro- and micronuclei. The macronucleus ceases transcription, progressively reducing in size, which is followed by rapid chromatin condensation and DNA fragmentation (Davis *et al.*, 1992). This apparent programmed nuclear death bears a resemblance to nuclear degeneration in eukaryotic cells undergoing PCD/apoptosis and suggests that some aspects of programmed death at least may be a common biological phenomenon.

PCD/apoptotic-like morphological and biochemical features have also been reported in the human intestinal protozoan parasite *Blastocystis hominis*, upon exposure to a cytotoxic monoclonal antibody (Nasirudeen *et al.*, 2001) and the drug metronidazole (Nasirudeen *et al.*, 2004). Several of the key features of apoptosis were reported: nuclear condensation, DNA fragmentation, reduced cytoplasmic volume, maintenance of plasma membrane integrity and the formation of apoptotic bodies.

In the human malarial parasite *Plasmodium falciparum* it has been shown that application of the drug chloroquine, results in the formation of oligonucleosomal DNA fragments within sensitive parasites (Picot *et al.*, 1997). More recently, it has been documented that apoptotic markers and caspase-like activity have been detected in *P. berghei* mosquito midgut stages both *in vitro* and *in vivo* (Al Olayan *et al.*, 2002).

1.6 Apoptotic/PCD-like phenomena in trypanosomatids.

1.6.1 Apoptotic/PCD-like phenomena in *Leishmania*.

Some of the morphological criteria associated with PCD/apoptosis have also been reported within various species of this kinetoplastid. Part of the life cycle involves a shift from 22-28°C to 34-37°C on movement from sandfly vector to mammalian host, and it is within this promastigote to amastigote transition that apoptotic-like features have been reported. In the case of *Leishmania amazonensis*, the resulting heat shock has been shown to induce apoptotic-like features within approximately 20% of dying promastigote cells (Moreira *et al.*, 1996). This process is dependent on calcium ions, as none of the structural features associated with apoptosis were observed in the presence of EGTA. The similarities with apoptosis include chromatin clumping, breakdown of nuclear membrane, DNA fragmentation and preservation of cytoplasmic organelles, although no membrane blebbing or apoptotic bodies were observed. This type of cell death is clearly distinct from the cell death within the remaining 80% of cells in which the cytoplasm swells, nuclear chromatin is dispersed in irregular clumps and there follows rupture and dissolution of almost all organelles. Late stationary cultures of *L. donovani* have been reported as displaying DNA laddering and nuclear chromatin condensation, followed by concurrent cleavage of a caspase substrate and loss of membrane integrity (Lee *et al.*, 2002). However, this apparent caspase activity was only partially reduced using caspase inhibitors, therefore it is possible that other, non-caspase-like peptidases are responsible for this activity. Also in *L. donovani*, it was shown that exposure to H_2O_2 resulted in nuclear condensation, DNA ladder formation, and induction of caspase-like activity (Das *et al.*, 2001), and pre-treatment with caspases inhibitors reduced the number of cells displaying these features. It has also been reported in *L. major* that treatment with staurosporine, a general protein kinase inhibitor believed to induce apoptosis in all nucleated mammalian cells (Weil *et al.*, 1996), resulted in almost the entire culture of promastigote cells dying within 5 days (Arnoult *et al.*, 2002). Cell shrinkage and DNA fragmentation were detected at 24 hours post-exposure, while membrane integrity was maintained over the same period. Nuclear degeneration was

reduced using a general caspase inhibitor, although there was no concurrent reduction in cell death, and similar results were obtained using the broad cysteine peptidase inhibitor E64. More recently, it has been claimed that camptothecin (CPT), an inhibitor of DNA topoisomerase I, induces PCD in both amastigote and promastigote forms of *L. donovani* (Sen *et al.*, 2004). Following application of CPT, the cleavage of PARP, a substrate of caspase-3 in higher eukaryotes (Tewari *et al.*, 1995), externalisation of phosphatidyl serine and genomic DNA fragmentation were presented as evidence pointing to a PCD-like phenomenon. In addition, a caspase-like activity was also detected using the caspase substrates DEVD-AFC and LEHD-AMC. Whether or not caspase-like activity is present within *Leishmania* is somewhat contentious at present, other researchers having shown that this apparent activity may be the result of cathepsin L-like cysteine peptidases (Zangger *et al.*, 2002). Cleavage of the caspase-3 substrate DEVD-AMC was observed in amastigote cell cultures, although this activity was absent in cysteine peptidase CPA and CPB double null mutants, which raises doubts about reports of other caspase-like activities in *Leishmania*.

1.6.2 Apoptotic/PCD-like phenomena in *Trypanosoma cruzi*.

The life cycle of this parasite also involves movement between insect vector and mammalian host, and is the causative agent of Chagas' disease in humans. Within the insect vector, the epimastigote form differentiates into the non-dividing metacyclic trypomastigote form, which are then infective for the vertebrate host. This differentiation has been associated with massive epimastigote death *in vitro*, displaying features similar to those seen during apoptosis (Ameisen *et al.*, 1996). Epimastigote cells in culture exponentially increase in number until a plateau is reached. During this exponential increase the differentiation into the trypomastigote form progressively increases, becoming maximal during the stationary period, when a large number of epimastigote cells begin to die. Examination of these dying cells revealed membrane blebbing, chromatin condensation and DNA fragmentation.

1.6.3 Apoptotic/PCD-like phenomena in *Trypanosoma brucei.*

Within *T. brucei*, again there are reports of apoptotic-like features being present under certain conditions. DNA isolated from procyclic form parasites incubated with the lectin Concanavalin A showed some evidence of genomic laddering and DNA fragmentation, while the kinetoplast DNA remained unaffected over the same period (Welburn *et al.*, 1996). Membrane integrity was maintained, and along with signs of chromatin rearrangement, was suggested to be the result of an active cellular death mechanism. This process was also shown to be associated with an increase in expression of two genes; prohibitin, belonging to a poorly characterised mitochondrial protein family with possible roles in cell cycle regulation, and TRACK, the suggested trypanosome receptor for activated kinase (Welburn and Murphy, 1998).

Other investigations have linked reactive oxygen species (ROS) to apoptotic-like cell death via a Ca^{2+}-dependent pathway. Procyclic trypanosomes exposed *in vitro* to xanthine and xanthine oxidase (XO), which results in the production of ROS, displayed several features similar to apoptosis (Ridgley *et al.*, 1999). At 5 hours post-induction, the cells displayed a complete loss of mobility, nuclear fragmentation, but no loss of membrane integrity. The intracellular addition of the calcium chelator EGTA attenuated all of these features, implicating calcium as a mediator. ROS and changes in calcium homeostasis in multicellular organisms have been linked to apoptosis (Lipton and Nicotera, 1998), and the delayed onset of permeability changes relative to loss of mobility and nuclear damage suggests the possibility of a regulated form of cell death.

There have been many suggestions as to why a single cell organism might want to regulate population size through a suicidal pathway. It has been suggested that an apoptotic-like pathway might be advantageous to unicellular organisms to regulate population size when resources are limited (Welburn *et al.*, 1997; Lee *et al.*, 2002; Al Olayan *et al.*, 2002). The idea is that a reduction in cell numbers is more beneficial to the population as whole if this aids in long term survival, and will increase the chance of successful transmission. It has also been proposed that death by an apoptotic-like mechanism might prevent the

release of immunogenic antigens, and therefore reducing the scale of the immune response raised against the organism (Lee *et al.*, 2002).

While there are numerous reports of apoptotic like phenomena within the lower eukaryotes there is still no definitive proof that single celled organisms have within them a mechanism for suicide. While the evidence might point to the possibility of such a mechanism, as yet no pathways or proteins have been identified which could facilitate such a process. If indeed there is an apoptotic-like machinery within single celled organisms it has yet to be identified and it is likely to be very different to that seen in higher eukaryotes, and until such system has been characterised, all the evidence must be seen as circumstantial.

1.7 Clans and families of peptidases.

Peptidases represent approximately 2% of the of the total number of proteins present in all types of organism (Barrett, 2004). The MEROPS database (merops.sanger.ac.uk) is an integrated source of information about peptidases, with each peptidase assigned to a family on the basis of statistically significant similarities in amino acid sequence. Families that are believed to have the same lineage are grouped into Clans, defined by MEROPS as peptidases that have arisen from a single evolutionary origin and contain similar tertiary structures and/or share common protein sequence motifs around the catalytic residues.

There are four major catalytic mechanisms by which peptidases cleave peptide bonds. These are cysteine, serine, aspartic and metallopeptidases. The catalytic mechanisms for cysteine and serine peptidases are similar, in that both a nucleophile and proton donor are required. In cysteine peptidases the nucleophile that attacks the peptide bond is the sulfhydryl group of the cysteine residue, while in serine peptidases this is the hydroxyl group of the serine residue. The histidine residue functions as the proton donor in both types of peptidase. The aspartic and metallopeptidases are catalytically very different to both the cysteine and serine peptidases, in that the nucleophile which attacks the peptide bond is an activated water molecule. In aspartic peptidases, there are usually two aspartate residues which act together to bind and activate the catalytic water molecule. With metallopeptidases, a metal ion, usually zinc, is

held in place through several amino acid residues, and in turn activates a water molecule.

Within the cysteine peptidases there have been identified several Clans (Figure 1.4), the most characterised of which are Clan CA and Clan CD. Clan CA, which contains 27 families, is typified by the plant enzyme papain. Papain, classified in family C1, was the first clearly recognised cysteine peptidase. It was also the first cysteine peptidase to have its three dimensional structure determined (Drenth *et al.*, 1968), and consequently is considered the archetypal cysteine peptidase. Indeed, family C1 is referred to as the papain family but it also includes the mammalian cathepsins B, C, K, L and S. Besides the cysteine and histidine residues of papain and related peptidases, there are other conserved residues important in catalysis. A glutamine residue that aids in formation of the "oxyanion hole", an electrophilic centre that stabilises the reaction intermediates, and a conserved asparagine/aspartate thought to orientate the imidazole ring of the catalytic histidine residue. The order of these residues in the polypeptide sequence is Gln, Cys, His, Asn/Asp. Members of Clan CA are all irreversibly inhibited by the compound E-64 (L-trans epoxysuccinyl-leucylamido-(4-guanidino)-butane).

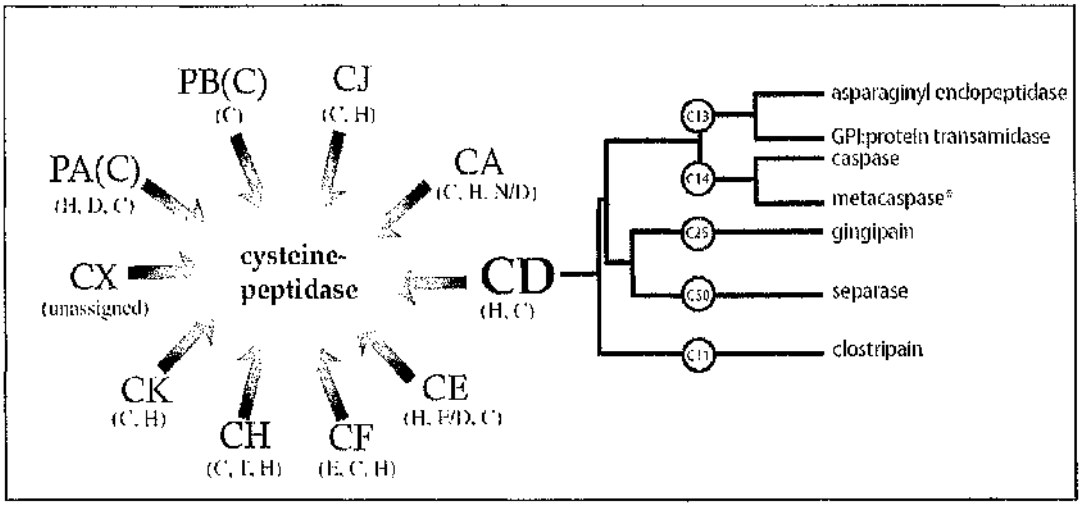

Figure 1.4: Classified Clans of cysteine peptidases, taken from Mottram *et al.*, 2003.

Clan CD enzymes are distinct from those of Clan CA in that only two residues, histidine and cysteine, are involved in the catalysis and are they located in the polypeptide in the order His, Cys. The Clan CD peptidases are unaffected by the 'classical' cysteine peptidase inhibitor E-64. The reason for this insensitivity is the strict substrate specificity of the Clan CD enzymes. Clan CA peptidases have a preference for large or hydrophobic residues at the S2 sub-site, but have little selectivity at the S1 sub-site. Thus, these peptidases readily accommodate the leucine located at the P2 of E-64 and are unaffected by the lack of a P1 residue. In contrast, most Clan CD enzymes have very strict, unequivocal specificity at the S1 sub-site for a single amino acid. For Clan CD peptidases, a productive interaction between the S1 sub-site of the enzyme and the P1 of the substrate is vital for binding. For this reason, E-64, which has no corresponding P1 residue, cannot bind, and so does not inhibit Clan CD peptidases. The lack of a selective, irreversible inhibitor initially hampered progress in the biochemical and cellular characterization of Clan CD peptidases. However, recent work has uncovered selective inhibitors of Clan CD peptidases, the aza-peptide epoxides, which inhibit caspases and asparaginyl endopeptidases, but not Clan CA enzymes (Asgian *et al.*, 2002). This class of inhibitor should pave the way towards elucidating the cellular functions of Clan CD enzymes and chemically validating them as drug targets. To date, Clan CD contains the sub families C11 (clostripains), C13 (legumains, GPI8), C14 (caspases), C25 (gingipain R) and C50 (separins) (Figure 1.4).

1.8 Clan CD peptidase family.

1.8.1 Caspases.

The caspases are the most well-known and characterised members of Clan CD due to their involvement in apoptosis and programmed cell death (PCD). Caspases (cysteinyl aspartate-specific proteinases) are a class of cysteine peptidases that form a central part of the cellular machinery, converting an apoptotic signal into the cellular disassembly process, and as the name suggests the substrate specificity at the P1 position is an aspartate residue. Cysteine peptidases were first implicated in cell death when it was discovered that CED-3, a gene product involved in PCD in the nematode *Caenorhadbitis elegans*

(Ellis and Horvitz, 1986), was structurally similar to the mammalian interleukin-1β-converting enzyme (ICE) (Yuan *et al.*, 1993). Subsequently, it was shown that overexpression of either *ICE* or the *C. elegans CED-3* gene induced apoptosis in fibroblasts (Miura *et al.*, 1993). These enzymes, subsequently categorised as caspases, became the first of a large family of related peptidases to be discovered which are widely distributed across the genera.

In addition to their sequence similarity to CED-3/ICE, all caspases contain a conserved QACXG pentapeptide motif surrounding the active site cysteine residue, together with conservation of other residues which participate directly in catalysis (Nicholson and Thornberry, 1997). Caspases are expressed constitutively as relatively inactive proenzymes, varying in size between 30 and 50 kDa and containing three domains: an amino terminal domain of varying size, a small subunit (~10 kDa) and a large subunit (~20 kDa).

Caspases can be activated through a variety of stimuli and a system has evolved to link upstream signalling pathways with downstream executioner processes. The caspases that perform these upstream functions are termed initiator caspases, such as caspase-8, -9 and -10, while downstream caspases are known as executioner caspases, such as caspase-3 and caspase-7 (Chang and Yang, 2000). Initiator caspases possess long prodomains and typically possess one of two identified domains. The first is the death effector domain (DED), identified in caspase-8 and caspase-10, linking ligand activated death receptors such as CD95 or TNFR1 (Boldin *et al.*, 1996) to caspase activation. The second domain, termed a caspase recruitment domain (CARD), is present in CED-3 and caspases-1, -2, -4, and -9 and is involved in interaction with Apaf-1 following release of cytochrome c from the mitochondria (Duan and Dixit, 1997). In response to upstream apoptotic signals, it has been proposed that the initiator caspases through an proximity-induced dimerisation model autocatalytically process and become active (Boatright *et al.*, 2003). Once activated, initiator caspases specifically cleave and hence activate effector caspase proenzymes. Processing of the proenzymes occurs at specific aspartate residues and results in cleavage into three domains (Ramage *et al.*, 1995). This results in removal of

the prodomain and the formation of a heterodimer composed of the large and small subunits. The X-ray crystal structure has been determined for several activated human caspases, including caspase-3 (Rotonda *et al.*, 1996), caspase-7 and -8 (Wei *et al.*, 2000), and caspase-9 (Renatus *et al.*, 2001). Thus, structures have been solved for human initiator and effector caspases. These structures reveal that the heterodimer of large and small subunits associates with another heterodimer to form a tetramer, with both the large and small subunits contributing residues that form the active site pocket.

There is believed to be a hierarchy within the caspases, the initiator caspases, following activation, subsequently cleaving and activating the downstream executioner caspases resulting in a branched cascade of caspase activation. These executioner caspases then induce apoptosis/PCD through the cleavage of various structural and repair proteins, such as keratin, nuclear lamins and poly (ADP-ribose) polymerase (PARP) (Utz and Anderson, 2000; Fischer *et al.*, 2003). The highly specific cleavage of a specific subset of proteins, is in agreement with the observation that apoptosis/PCD is not the result of indiscriminate protein degradation but rather a change in cellular metabolism leading to a co-ordinated cell suicide.

1.8.2 Other Clan CD peptidases.

The Gingipains, cysteine peptidases of the bacterium *Porphyromonas gingivalis,* a major pathogen in periodontal disease, have been identified as key virulence factors in this bacterium (Potempa and Travis, 1996). Gingipain R falls into Clan CD and is particularly interesting due to the possession of a catalytic domain very similar to that of the caspases. This protein has been crystallised and shows topological homology with caspase-1 (Eichinger *et al.*, 1999), with identically positioned cysteine and histidine residues, an equivalent oxyanion hole and a similarly placed and shaped S1 pocket. However, with the caspases the S1 pocket is optimised for aspartate side chains, while with Gingipain R arginine is the favoured amino acid. Clostripain, another bacterial peptidase identified from the bacterium *Clostridium histolyticum* (Mitchell and Harrington, 1968) also shows a strict specificity for arginine at the S1 pocket (Mitchell, 1977). The legumains are cysteine peptidases that were first

identified in the leguminous seed of the mouth bean, *Vigna aconitofolia* (Kembhavi *et al.*, 1993). This was later shown to be homologous to an enzyme from *Schistosoma mansoni* (Hara-Nishimura *et al.*, 1993) and homologues have also been identified in mammals (Chen *et al.*, 1997), all showing specificity for asparagine at the P1 position. Along with the legumains in the C13 family are classified the glycosylphosphatidylinositol (GPI) transamidases, and as this class of peptidase has been identified within the trypanosomatids are discussed in more detail below. As are the separases, the most recently classified members of Clan CD, which are essential for correct sister chromatid separation during mitosis in eukaryotic cells (Uhlmann *et al.*, 1999; Nasmyth, 1999).

1.9 Importance of cysteine peptidases in parasitic protozoa.

There are more than 500 types of cysteine peptidases currently known (Barrett and Rawlings, 2001; Rawlings *et al.*, 2004) and many have been shown to carry out vital functions or be involved in disease processes (Lecaille *et al.*, 2002). Cysteine peptidases of parasitic protozoa have been implicated in a variety of biological events, including invasion of host cells, immune evasion, pathogenesis and virulence (Mottram *et al.*, 1998; Rosenthal, 1999; Frame *et al.*, 2000; Klemba and Goldberg, 2002; Sajid and McKerrow, 2002; Denise *et al.*, 2003), and some have also been validated as drug targets of high promise (McKerrow *et al.*, 1999; Sajid and McKerrow, 2002). Most cysteine peptidases of parasitic protozoa that have been characterized are located in Clan CA, family C1. This family includes cruzain of *Trypanosoma cruzi* (Eakin *et al.*, 1992), CPA (Souza *et al.*, 1994), CPC (Bart *et al.*, 1995), the CPB (Robertson and Coombs, 1994) multigene family of *Leishmania mexicana*, and the falcipains of *Plasmodium falciparum* (Francis *et al.*, 1996; Shenai *et al.*, 2000).

Clan CA enzymes are believed to represent excellent drug targets with which to rationally design inhibitors to treat parasitic infections. The inhibition of the *T. brucei* cathepsin-L like cysteine peptidase rhodesain with selective dipeptidyl inhibitors was shown to have anti-trypanosomal activities comparable with those of drugs used in the treatment of sleeping sickness (Nkemgu *et al.*, 2003). A separate study has also reported the screening of a library of thiosemicarbazone cysteine protease inhibitors against the parasitic cysteine peptidases cruzain,

falcipain-2, and rhodesain from *T. cruzi*, *P. falciparum*, and *T. brucei*, respectively. Some of the compounds tested effectively inhibited the enzymes, were parasiticidal and displayed no observable toxicity in mice (Greenbaum *et al.*, 2004). Thus, it is believed that the development of specific peptidase inhibitors may aid in the creation of new treatments for parasitic infections.

The advent of extensive genome sequence data has led to the identification in parasitic protozoa of cysteine peptidases belonging to Clan CD, and their discovery has led to a reassessment of the importance and roles of cysteine peptidases in parasitic protozoa. Moreover, it appears that these enzymes have much greater substrate specificity and therefore functions than the Clan CA enzymes, and so perhaps provide better targets for drug attack.

1.10 Clan CD peptidases identified in *T. brucei*.

1.10.1 Glycosylphosphatidylinositol (GPI) transamidases.

GPI8 is essential for the attachment of GPI anchors to VSG and procyclin in both the BSF and PCF life stages of *T. brucei*, respectively (Lillico *et al.*, 2003). The use of GPI anchoring to attach proteins to the cell surface is widespread throughout eukaryotes, and GPI8 has been identified as being essential for this process in both yeast (Benghezal *et al.*, 1996) and mammalian cells (Yu *et al.*, 1997). In *T. brucei*, GPI8 has been shown to be essential for BSF but not for the PCF survival *in vitro*, although the PCF parasites were unable to establish an infection *in vivo* (Lillico *et al.*, 2003). Within the biosynthetic pathway there are numerous proteins involved in the formation of the GPI anchor.

It has been shown that the human and *Saccharomyces cerevisiae* GPI complex is well conserved, containing five homologous components (Hong *et al.*, 2003). The human components, GAA1, GPI8, PIG-S, PIG-T, and PIG-U are homologous to yeast Gaa1p, Gpi8p, Gpi17p, Gpi16p, and Cdc91p, respectively. Within *T. brucei*, it is believed that the GPI complex shares only three components with humans and *S. cerevisiae*, *Tb*GPI8, *Tb*GAA1 and *Tb*GPI16. Additionally, however, there are two specific components termed trypanosomatid transamidase 1 (TTA1) and TTA2 (Nagamune *et al.*, 2003).

The GPI8 protein shows a high level of sequence identity with the legumains and thus has been classified within the C13 family. Whether they should be classified separately is open to debate, as they are clearly distinct from the legumains in the functions they perform. Legumains are general proteolytic enzymes with various functions across the genera (Manoury *et al.*, 1998; Muntz and Shutov, 2002), while GPI8 is universally involved in the attachment of GPI-anchors to polypeptides (Benghezal *et al.*, 1996; Yu *et al.*, 1997; Lillico *et al.*, 2003).

1.10.2 Separases.

An enzyme of such importance to the effective functioning of the eukaryotic cell cycle would be expected to be present in parasitic protozoa, and indeed a separin gene has been identified in *T. brucei* (Mottram *et al.*, 2003). This gene encodes for a large protein of >1000 amino acids with two major domains, a conserved cysteine peptidase domain at the C-terminus and a less conserved N-terminal securin-binding domain (Ross and Cohen-Fix, 2002). Securin is a regulatory protein that inhibits the activity of separase until all pairs of chromatids have established bipolar spindle attachments (Hornig *et al.*, 2002). Separases are thought to have specific cleavage sites (hydrolysis at the C-terminal side of arginine residues), with only a few substrates present in the cell (Ross and Cohen-Fix, 2002).

1.10.3 Metacaspases.

The metacaspases, which were first identified in 2000 by researchers in California (Uren *et al.*, 2000), have not yet officially been classified within Clan CD by MEROPS. Several sequences with distant but significant similarities to caspases had previously been identified in human and *Dictyostelium discoideum* databases (Aravind *et al.*, 1999). Further iterative database searches using these sequences identified two novel families of caspase-like proteins which were termed the paracaspases and the metacaspases (Uren *et al.*, 2000). Until these discoveries, no caspases-like peptidases had been identified in plants, fungi, or protists. Based upon domain structure and sequence similarity, the metazoan and *Dictyostelium* sequences identified were classified as paracaspases while sequences from plants, fungi and protozoa were termed metacaspases (Uren *et*

al., 2000). Interestingly, no metacaspase genes have been identified in mammals suggesting that they might provide a good drug target.

1.11 Functions of metacaspases.

1.11.1 Functions of plant metacaspases.

Plant metacaspases have been classified into two types (Uren *et al.*, 2000). Type-I metacaspases contain a pro-domain that is proline rich and contains a zinc finger motif with similarities to that in LSD1, a protein involved in the hypersensitivity response pathway. The hypersensitive response is a plant response to infection by microbial pathogens and is often accompanied by rapid cell death in and around the initial infection site. This response is associated with restricted pathogen growth and has been suggested to represent a form of PCD (Greenberg, 1996). Type-II metacaspases do not posses a prodomain, but have an insertion of approximately 180 amino acids (Uren *et al.*, 2000). A type-II metacaspase, termed *Le*MCA1, has been cloned from the tomato plant (*Lycopersicon esculentum*) and gene expression during cell death in *Botrytis cinerea* infected tomato leaves observed (Hoeberichts *et al.*, 2003). Infection of *Arabidopsis thaliana* with *B. cinerea* has been shown to induce an oxidative burst accompanied by the activation of hypersensitive cell death (Govrin and Levine, 2000). As in *A. thaliana*, it is believed that *B. cinerea* infection induces the hypersensitive sensitive response and *Le*MCA1 mRNA was only detected in infected leaves. Thus it was suggested that the metacaspases have a caspase-like role in the plant hypersensitivity response.

A further role for the metacaspases in cell death in plants has been reported using the model system of somatic embryogenesis in the Norway spruce (*Picea abies*). In this developmental pathway, autophagic cell death has been implicated in the transition from proembryogenic mass (PEM) to somatic embryo and correct embryonic pattern formation (Filonova *et al.*, 2000). A type-II metacaspase cDNA was identified from embryogenic cell cultures and *in situ* hybridization analysis revealed accumulation of metacaspase mRNA in embryonic tissues and structures committed to death (Suarez *et al.*, 2004). Silencing of the metacaspase gene by RNAi was accompanied by loss of

embryonic pattern formation. This silencing also resulted in a reduction in VEIDase activity, a caspase-like activity previously reported to be essential for embryo development (Bozhkov *et al.*, 2004). It was suggested that the plant metacaspases are part of the developmental cell death machinery, involved in maintenance of the balance between death and proliferation required for plant embryogenesis

In *A. thaliana* there have been nine metacaspase genes identified, three of which were classified as type-I metacaspases, while the remaining six are type-II metacaspases. Expression of N-terminally tagged type-II metacaspases in *E. coli* revealed that there was an apparent autocatalytic processing similar to caspases (Vercammen *et al.*, 2004), which was absent following substitution of the putative active site cysteine residues. Analysis of the cleaved fragments revealed that this autoprocessing occurred after either a conserved arginine or lysine residue. Additionally, it was demonstrated that the activity of the recombinant enzymes was dependant on this autoprocessing, and that all substrates tested with either arginine or lysine at the P1 position were cleaved efficiently. No cleavage of classical caspase substrates was detected using the recombinant enzymes. It is interesting to note that no processing pattern was detected when type-I metacaspases were overexpressed, presumably due to fact that the cleavage site identified is located in the insert region characteristic of type-II metacaspases. These findings suggest that the metacaspases, like other Clan CD peptidases, are specific for the P1 residue. However, unlike the caspases they display a preference for the basic amino acids similar to the separases, clostripains and gingipains.

1.11.2 Functions of yeast metacaspases.

Potential roles for metacaspase involvement in cell death in *Saccharomyces cerevisiae* have also been reported (Madeo *et al.*, 2002; Herker *et al.*, 2004; Wadskog *et al.*, 2004). Yeast possesses a single metacaspase gene and the overexpression of an epitope tagged metacaspase (YCA1) revealed apparent processing, which was absent when substitution of the putative active site residues was performed (Madeo *et al.*, 2002). Following exposure of yeast to H_2O_2, a stimulus previously suggested to induce apoptotic-like death in yeast

(Madeo *et al.*, 1999), caspase-like activity was detected using FITC-VAD-fmk, a fluorescent inhibitor which should only bind to active caspases. Additionally, the overexpression of YCA1 for 44 hours resulted in the appearance of apoptotic markers. Fragmented DNA and chromatin condensation were observed in 90% and 20% of the cells, respectively. Both of these phenomena were almost completely abolished by the co-incubation with the caspase inhibitor z-VAD-fmk. It has also been also proposed that high salinity is able to induce apoptosis in yeast, with ectopic expression of the anti-apoptotic protein Bcl-1 enhancing NaCl tolerance (Huh *et al.*, 2002), and an increased sensitivity to NaCl stress observed following deletion of the *SRO7* gene (Wadskog *et al.*, 2004). *SRO7* is the yeast homologue of a *Drosophilia* tumour suppressor gene required for development of epithelial cell polarity (Bilder *et al.*, 2000). On exposure to growth inhibiting concentrations of NaCl, the Δ*sro7* cells displayed a rapid loss in viability that was accompanied by markers of apoptosis (Wadskog *et al.*, 2004). The additional deletion of *YCA1*, was shown to reduce the fast initial drop in viability and reduce DNA fragmentation. Caspase-like activity was also observed using FITC-VAD-fmk, while only basal activity was detected in Δ*yca1* mutants. Further reports of metacaspase involvement in apoptotic-like cell death have also been claimed in yeast with regard to chronological aging. A hypothesis has been suggested whereby certain yeast cells commit altruistic suicide to spare resources for other younger and fitter cells in aging cultures (Herker *et al.*, 2004). An analysis of chronologically aged cultures revealed that markers of apoptosis (DNA fragmentation, chromatin condensation and phosphatidly serine externalisation) were all present together with caspase-like activity, assessed using FITC-VAD-fmk.

However a recent paper has questioned the validity of using fluorochrome-conjugated caspase inhibitors, such as FITC-VAD-fmk, to detect caspase-like activity in dying yeast cells. It was demonstrated that dead or inviable yeast cells non-specifically bind fluorescent-conjugated caspase inhibitors (Wysocki and Kron, 2004). An exponentially growing culture of wild type yeast cells was split, with one half incubated at 80°C for 5 minutes to rapidly kill the cells and denature all proteins. Staining of both live and heat-killed cells with FITC-

VAD-fmk revealed that the heat-killed cells accumulated the fluorescent caspase inhibitor. A separate study examining the specificity of caspase inhibitors such as z-VAD-fmk has also highlighted potential problems with the interpretation when using these small peptide inhibitors. It was shown that a range of these peptides linked to chloromethylketone (cmk) or fluoromethylketone (fmk) groups efficiently inhibited legumain and various cathepsins in addition to the caspases (Rozman-Pungercar *et al.*, 2003). These findings suggest that the detection of caspase-like activity, in the previously described reports, may not have been due to metacaspase activity. Rather they may have been due to non-specific interactions with FITC-VAD-fmk inhibitor, or the detection of Clan CA peptidases with z-VAD-fmk.

Additional to work on the endogenous yeast metacaspase, it has also been reported that the heterologous expression of a *T. brucei* metacaspase (*Tb*MCA4) in *Saccharomyces cerevisiae* resulted in growth inhibition, mitochondrial dysfunction and cell death (Szallies *et al.*, 2002). All five *T. brucei*, as well as the single *Schizosaccharomyces pombe* metacaspase, were expressed, but of these, only *Tb*MCA4 resulted in any phenotypic consequences and these were lost following mutation of the putative active site residues. Both endogenous and *T. brucei* metacaspase GFP fusion proteins showed apparent nuclear localisation, and the endogenous metacaspase displayed a genetic interaction with WWM1. This protein was identified as a potential hydrophilin, these proteins are often involved in osmotic stress responses (Garay-Arroyo *et al.*, 2000). Interestingly, WWM1 overexpression resulted in a growth arrest, similar to effects of *Tb*MCA4 expression, and which was suppressed by concurrent expression of the endogenous metacaspase.

In addition to reports where the metacaspase have been suggested to play a role in cell death, there are examples of apoptotic-like phenomena reported in yeast unrelated to metacaspase function. In both *Saccharomyces cerevisiae* and the filamentous fungus *Aspergillus nidulans*, induction of cell death with markers typically associated with apoptosis were shown to be unaffected by deletion of the single metacaspase present in both organisms (Cheng *et al.*, 2003; Wysocki and Kron, 2004). Whether or not apoptosis actually exists in yeast is open to

debate, there is evidence to suggest that such a process may exist, although the majority of the components required for apoptosis in multicellular organisms are absent from the yeast genome. If such a pathway does exist in yeast, it is likely to be a much more primitive form and definitive linkage of metacaspase function to such a phenomenon has not been demonstrated.

That the metacaspases might function as a part of this controversial process is a tempting hypothesis to postulate. Investigations into their functions in both yeast and plants have suggested that the metacaspases might be involved in cell death processes (Madeo *et al.*, 2002; Szallies *et al.*, 2002; Hoeberichts *et al.*, 2003; Herker *et al.*, 2004; Wadskog *et al.*, 2004; Suarez *et al.*, 2004). The apoptotic pathways are extremely complex in higher eukaryotes, utilising numerous different signalling pathways and domain aggregations (Koonin and Aravind, 2002). Assuming that the metacaspases do represent the ancestral caspases, it is possible that during evolution they were recruited to the developing process of PCD/apoptosis and at which time they diverged and diversified to become modern day caspases.

Other than in yeast, there have been no documented functions assigned to the metacaspases in any single cell organisms. Their functions in protozoa may, or may not be, similar to that in yeast, but, whatever the case, this novel family of peptidases demands study and may well offer opportunities for further insights into the cell biology of the trypanosomatids.

Aims of the project:

1) To identify and characterise the metacaspase genes of *T. brucei*
- expression profile and localisation

2) To analysis of metacaspase function through RNAi

3) To analysis of metacaspase function through targeted gene disruption

Chapter 2

Materials and methods

Details of oligonucleotide sequences together with a list of buffers and solutions used follow these methods.

2.1 Culturing, harvesting and cryopreservation of trypanosomes.

Genetic knockouts in the bloodstream form (BSF) were performed in *Trypanosoma brucei* strain *427*. These were maintained at 37°C with 5% CO_2 in HMI-9 (Hirumi and Hirumi, 1989) supplemented with 10% (v/v) heat-inactivated fetal calf serum (FCS) (Gibco) and 10% (v/v) serum plus (JHR Biosciences). Genetic knockouts in the procyclic form (PCF) were performed in *T. brucei* EATRO795. These were cultured at 27°C in complete SDM79 medium (Brun and Schonenberger, 1979) supplemented with 10% (v/v) heat-inactivated FCS (Gibco). For the RNAi study, the procyclic 427 pLew13 pLew29 and the bloodstream form 427 pLew13 pLew90-6 cell lines were used (Wirtz *et al.*, 1999) and maintained as above.

Final antibiotic concentrations used for maintenance and selection of transgenic trypanosomes were as follows. In the BSF: hygromycin (Roche) at 5 μg ml^{-1} , neomycin at 2 μg ml^{-1}(Calbiochem), blasticidin (Calbiochem) at 2 μg ml^{-1}, puromycin (Calbiochem) at 2 μg ml^{-1} and phleomycin (Cayla) at 2.5 μg ml^{-1}. In the PCF: hygromycin (Roche) at 50 μg ml^{-1}, neomycin (Calbiochem) at 15 μg ml^{-1}, zeocin (Cayla) at 10 μg ml^{-1}.

Harvesting of the BSF and PCF parasites was performed by centrifugation at 1500g or 1000g for 5 mins at room temperature, respectively. Culture medium was removed and cells resuspended in an equal volume of sterile PBS. Parasites were then centrifuged once more before use in downstream applications.

Cryopreservation of both BSF and PCF parasites was performed as follows. Typically, a 10 ml culture of mid logarithmic phase parasites was harvested as previously described and re-suspended in an equal volume of appropriate culture medium supplemented with 10% (v/v) sterile glycerol (Sigma). 1 ml aliquots were then transferred into cryovials (Sterillin) and slow-frozen at -80°C. The following day cryovials were transferred to liquid nitrogen for long term storage.

Recovery of trypanosomes was performed by thawing at room temperature prior to immediate transfer to appropriate medium.

2.2 Transfection and cloning of parasites.

Transfection and cloning of PCF parasites was performed as follows. Parasites were grown to a mid logarithmic density of approximately 8 x 10^6 cells ml^{-1} and 3×10^7 parasites harvested as previously described. Parasites were then resuspended in 0.5 ml Zimmermans post fusion medium (ZPFM) in a 0.4-cm pulse cuvette (Bio-Rad) with between 1 to 5 µg of linearised plasmid DNA. Cuvettes were then pulsed twice using a Bio-Rad pulser II set at 1.5 kV, 25 µF before immediate re-suspension of parasites in 5 ml of SDM-79 prewarmed to 27°C. After overnight recovery, appropriate antibiotics and a final concentration of 25% (v/v) conditioned medium was added to cultures. Conditioned medium was taken from a wild type culture grown to excess of 2 x 10^7 cells ml^{-1}, the parasites were removed by centrifugation and the medium passed through a 0.22 µm filter. Various dilutions of the transfected parasites were then plated out on 96-well plates, the plates were sealed with parafilm, placed in an airtight box and incubated at 27°C for several weeks or until clonal populations grew.

Transfection and cloning out of BSF parasites was performed as follows. Parasites were grown to a mid logarithmic density of 1 x 10^6 cells ml^{-1} and 5×10^7 parasites harvested as previously described. Parasites were then resuspended in 0.5 ml ZPFMG in a 0.4-cm pulse cuvette (Bio-Rad) with between 5 - 20 µg of linearised plasmid DNA. Cuvettes were then pulsed once using a Bio-Rad pulser II set at 1.2 kV, 25 µF before immediate re-suspension of parasites in 50 ml of HMI-9 prewarmed to 37°C. After overnight recovery, appropriate antibiotics were added to the cultures. Various dilutions of the transfected parasites were then plated out on 24-well plates and incubated at 37°C, 5% CO_2 until clonal populations grew up.

2.3 PCR reactions.

PCR reactions were performed using two different enzymes, Taq (*Thermus aquaticus*) (Abgene) or the high-fidelity Pfu (*Pyrococcus furiosus*) (Stratagene)

depending on the requirements. PCR was typically performed in 20 µl reactions with the following constituents: 50 ηg template DNA, 5 ρmol of each primer, 0.3 units of Taq or 1 unit of Pfu and 2 µl of respective 10x PCR mix. Reaction mixtures were overlaid with mineral oil and reactions performed in a PCR Express machine (Hybaid).

2.4 DNA gel electrophoresis.

Gel electrophoresis was performed using agarose from either Gibco or SeaKem in conjunction with 0.5x TRIS borate buffer (TBE) or 1x TRIS acetate buffer (TAE), respectively. TBE buffer was used for day to day analysis, while TAE buffer was used when DNA was to be excised from the gel or for Southern blotting. The molecular weight marker used was a 1 kb ladder (Invitrogen) at a concentration of 0.5 µg per lane.

DNA was visualised by the addition of ethidium bromide (Sigma) to the gel mix at a final concentration of 0.5 µg ml^{-1}. Visualisation was by exposure to UV light using a Gel Doc 2000 (BioRad).

DNA was extracted from agarose gels using a Gel Extraction Kit (Qiagen) as specified in the manufacturer's instructions. When DNA was to be used for further cloning steps, or for use in transfections, the DNA was subsequently ethanol-precipitated. This was performed by the addition of 2.5 volumes 100% ethanol and 10% 3 M NaAc (pH5.2) and incubated at -20°C for 30 mins prior to centrifugation at 18,000g for 10 mins. The resultant pellet was then washed twice in 70% (v/v) ethanol and re-suspended in a suitable volume of sterile water and kept at -20°C until required.

2.5 Cloning of PCR products.

PCR products, generated as described previously, were ligated into either pGEM-T Easy vector (Promega) or pCR-Script (Stratagene) depending on whether amplification was performed using Taq or Pfu, respectively, and according to the manufacturer's guidelines. These ligations were then used to transform heat-shock competent XL-1 blue cells (Stratagene) according to the manufacturer's guidelines, and transformants selected by their ability to grow on LB (Luria-

Bertani) agar plates supplemented with 50 μg ml^{-1} ampicillin. The presence of PCR products within vectors was initially determined by blue/white selection of colonies using 0.5 mM IPTG and 80 μg ml^{-1} X-gal, following which positives were screened by colony PCR using the SP6 and T7 (pGEM-T) or T3 and T7 (pCR-Script) RNA Polymerase Promoter Sequencing Primers.

2.6 Colony PCR.

Bacterial colonies were screened for DNA insertion as follows: using a 200 μl pipette tip, white colonies were selected from agar plates and suspended in 20 μl of sterile distilled water. 2 μl were then used to substitute for template DNA in a PCR reaction using Taq DNA polymerase as described above. PCR products were analysed on an agarose gel as described previously. Clones of interest were then used to inoculate 5 ml of LB medium and incubated overnight at 37°C at 220 rpm. Cells were cryopreserved by addition of 1 ml of overnight bacterial culture to 1 ml of a 2% (w/v) peptone 40% (v/v) glycerol solution and placed at -70°C for long term storage.

2.7 Plasmid preparation.

Plasmid preparation from bacterial cultures was performed in two ways depending on the amount of DNA required. For general cloning or sequencing, plasmids were prepared from 5-10 ml overnight bacterial cultures using a MiniPrep kit (Qiagen) according to the manufacturer's guidelines. If larger amounts of DNA were required, for transfections for example, 50 ml bacterial cultures were grown and DNA extracted using a MidiPrep kit (Qiagen) according to the manufacturer's guidelines.

2.8 Plasmid generation.

2.8.1 *MCA2/3* RNAi construct.

A 668 base-pair fragment, sharing 100% identity with *MCA2* and *MCA3*, was amplified by PCR from genomic DNA (strain 427) with Pfu (Stratagene) using the primer pair OL905 (*Bam*HI) and OL906 (*Hin*dIII). The engineered restriction sites added are indicated in brackets. This fragment was cloned into pCR-script and sequenced to ensure fidelity before excision with *Bam*HI and *Hin*dIII. This

fragment was then cloned into pGL571 pre-digested with *Bam*HI and *Hin*dIII to generate pGL671. For transfection purposes, pGL671 was digested with *Not*I and purified by agarose gel electrophoresis as previously described.

2.8.2 *MCA5* RNAi construct.

A 416 base-pair fragment of *MCA5* was amplified by PCR from genomic DNA (strain 427) with Pfu (Stratagene) using the primer pair OL944 (*Bam*HI) and OL945 (*Hin*dIII), the engineered restriction sites added are indicated in brackets. This fragment was cloned into pCR-script and sequenced to ensure fidelity before excision with *Bam*HI and *Hin*dIII. This fragment was then cloned into pGL571 pre-digested with *Bam*HI and *Hin*dIII to generate pGL714. For transfection purposes, pGL714 was digested with *Not*I and purified by agarose gel electrophoresis as previously described.

2.8.3 *MCA2/3/5* RNAi construct.

The 668 base pair *MCA2/3* fragment was excised from pGL670 with *Hin*dIII and cloned into pGL714 pre-digested with *Hin*dIII to generate pGL905. For transfection purposes, pGL905 was digested with *Not*I and purified by agarose gel electrophoresis as previously described.

2.8.4 *MCA2 & MCA3* knockout constructs.

The 5' flank of *MCA2* and the 3' flank of *MCA3* were amplified by PCR from genomic DNA (strain 427) with Pfu (Stratagene) using the primer pairs OL969 (*Xba*I) / OL970 (*Xba*I) and OL971 (*Apa*I) / OL972 (*Apa*I), respectively, the engineered restriction sites added are indicated in brackets. These fragments were then cloned into pCR-script and sequenced to ensure fidelity before excision of the 5' and 3'flanking regions with *Xba*I and *Apa*I, respectively. These were then cloned sequentially into pGL699 pre-digested firstly with *Xba*I and subsequently with *Apa*I to generate pGL802, the *BSD MCA2/3* knockout construct. Exchange of resistance genes was achieved by excising the *PAC* gene from pGL698 using *Eco*RI and cloning into pGL802 pre-digested with *Eco*RI, generating pGL808, the *PAC MCA2/3* knockout construct. For transfection purposes, pGL802 and pGL808 were digested with *Not*I/*Xho*I and appropriate fragments purified by agarose gel electrophoresis as previously described.

2.8.5 *MCA5* knockout construct.

The 5' and 3' flanks of *MCA5* were amplified by PCR from genomic DNA (strain 427) with Pfu (Stratagene) using the primer pairs OL1135 (*Not*I) / OL1131 (*Xba*I) and OL1132 (*Apa*I) / OL1134 (*Apa*I), respectively, the engineered restriction sites added are indicated in brackets. These fragments were then cloned into pCR-script and sequenced to ensure fidelity before excision of the 5' and 3' flanking regions with *Not*I/*Xba*I and *Apa*I, respectively. These were then cloned sequentially into pGL802 pre-digested firstly with *Not*I/XbaI and subsequently with *Apa*I to generate pGL904. The primer pairs OL1307 / OL1308 and OL1309 / OL1310, engineered to contain *Eco*RI restriction sites, were used to amplify both the *HYG* and *NEO* resistance genes, respectively, from pGL893 and pGL227. These were then inserted into pCR-Script, sequenced to ensure fidelity before excision with *Eco*RI and cloned individually into pGL904 pre-digested with *Eco*RI to generate pGL905 and pGL906. For transfection purposes, pGL906 and pGL907 were digested with *Not*I/*Eco*RV and appropriate fragments purified by agarose gel electrophoresis as previously described.

2.8.6 Generation of recombinant MCA5 expression vector.

MCA5 was amplified by PCR from genomic DNA (strain 427) with Pfu using the primer pair OL1029 (*Ase*I) and OL1030 (*Xho*I), the engineered restriction sites added are indicated in brackets. This fragment was then cloned into pCR-script and sequenced to ensure fidelity before excision with *Ase*I and *Xho*I. This fragment was then used to ligate into the *E. coli* expression vector pET-28a(+) pre-digested with *Nde*I and *Xho*I to generate pGL805.

2.8.7 *MCA2*, *MCA3* and *MCA5* re-expression constructs.

MCA2 and *MCA3* ORF's were excised from pGL863 and pGL864, respectively, using *Nde*I and *Xho*I while *MCA5* was excised from pGL805 using *Ase*I and *Xho*I. Fragments were then blunt ended using Klenow (NEB) as stated in manufacturer's guidelines. These fragments were then cloned individually into pGL884 pre-digested with *Eco*RV and dephosphorylated with calf intestinal alkaline phosphate CIP (NEB) as stated in manufacturer's guidelines to generate pGL867, pGL868 and pGL927. For transfection purposes, pGL867 and pGL868

were digested with *Xba*I/*Hin*dIII, while pGL927 was digested with *Bam*HI and *Hin*dIII, and appropriate fragments purified for transfection.

2.8.8 HA-tagged MCA2 & MCA3 constructs.

Equal molar concentrations of OL1225 and OL1226 were heated together at 95°C for 10 mins and subsequently allowed to cool slowly to room temperature to allow annealing to occur. These complementary primers encode for the last 12 amino acids of *MCA2* and *MCA3* with the addition of the sequence for an hemagglutin (HA) epitope tag. Additionally, these were engineered, once annealed, to possess overhanging sequences compatible with *Bgl*II and *Xho*I restriction digests. These annealed primers were then cloned into pGL863 and pGL864 pre-digested with *Bgl*II and *Xho*I, which removes the last 12 base pairs of both *MCA2* and *MCA3* respectively, to generate pGL865 and pGL866. These modified genes were then excised from pGL865 and pGL866 with *Nde*I and *Xho*I and fragments blunt ended using Klenow (NEB) as stated in manufacturer's guidelines. These fragments were then cloned individually into pGL884 pre-digested with *Eco*RV and dephosphorylated with CIP (NEB) as stated in manufacturer's guidelines to generate pGL878 and pGL879. For transfection purposes, pGL878 and pGL879 were digested with *Bam*HI and *Hin*dIII and appropriate fragments purified for transfection.

2.9 DNA Sequencing and analysis.

Sequencing of cloned DNA was performed by the University of Glasgow Molecular Biology Support Unit (MBSU) using an ABI automatic sequencer. Raw sequence data were imported, edited and individual sequence fragments compiled into contigs using AlignX (Informax Inc.). Homology searches were carried out through the Gene DB (http://www.genedb.org) and National Centre for Biotechnology Information (NCBI) [http://www.ncbi.nlm.nih.gov] BLAST servers.

2.10 Expression and purification of recombinant MCA5 in *Escherichia coli.*

The *MCA5* expression vector pGL805 was transformed into *E. coli* BL21 cells (Stratagene) and 500 ml of LB inoculated. Once the OD reached approximately 0.6, expression was induced with a final concentration of 1mM IPTG. At 4 hours

post-induction, cells were harvested by centrifugation at 5000g for 10 mins at 4°C. The pellet was then lysed in 40 ml of Bacterial Protein Extraction Reagent (B-PER) (Pierce) on a rotary shaker for 15 mins at room temperature, followed by centrifugation at 24,000g for 10 mins. The resultant pellet was then resuspended in 30 ml B-PER with the addition of 200 μg ml^{-1} lysozyme (Sigma) and incubated at room temperature for 10 mins. A further 10 mins centrifugation at 24,000g was performed and the resultant pellet washed twice in 20 ml of a 1:10 dilution of B-PER. A series of washes with different solutions was then used:

- 1 x H_20
- 1 x 50 mM Tris, 5 mM EDTA, 5% (w/v) sucrose, pH 8
- 1 x 75 mM Tris, 500mM NaCl, 0.1% Tx100, pH 7.5
- 1 x H_20
- 1 x 100 mM Tris, 5 mM EDTA, 1 M Urea, pH 8
- 2 x H_20

The pellet was finally re-suspended in 10 ml 8 M urea, 100 mM NaH_2PO_4, 10 mM Tris, pH 8, and left on a rotary shaker overnight at 4°C. Protein purification was then performed using nickel agarose beads (Qiagen) as per manufacturer's guidelines for purification under denaturing conditions and eluted in 4 x 0.5 ml fractions of first buffer D and then buffer E (see section 2.27). The fraction with the highest concentration of purified protein was identified and a volume of this elution fraction containing approximately 800 μg of protein electrophoresed via SDS-PAGE and the MCA5 band excised. This material was then frozen in liquid nitrogen, ground with a pestle and mortar, resuspended in PBS and sent for antibody production in sheep at Diagnostics Scotland.

2.11 Affinity purification of anti-MCA2/3 antiserum.

Anti-MCA2/3 antiserum raised against a 80mer peptide with 100% identity between MCA2 and MCA3 (Figure 3.5B) had previously been generated (N.Fasel, University of Lausanne, Switzerland). Generation of an affinity matrix using the peptide was performed using an Amino Link Immobilisation Kit (Pierce) as detailed in the manufacturer's guidelines. 2 ml of the antiserum was mixed with 2 ml of Binding buffer (BB) (Pierce) and the column left on a rotary

shaker for 1 hour at room temperature. The column was then drained and washed with 15 ml of BB. Antibodies were then eluted with 4 ml of Elution buffer (EB) (Pierce) into 0.5 ml of a 10X PBS solution. Eluted antibodies were then concentrated by centrifugation in a 2 ml 10,000 MW exclusion concentrator (VivaScience) with 10 ml 1x PBS added during the concentration process to lower the salt concentration. A volume of approximately 300 µl was then mixed with glycerol to a final concentration of 50% and stored at -20°C.

2.12 Electrophoresis of proteins.

SDS-PAGE gels were cast and run according to the method of Laemmli as adapted for the BioRad Mini-PROTEAN II system. Typically, resolving gel acrylamide concentration was 12% (w/v) and SDS-PAGE running buffer was made as a 10X stock and used at 1X concentration. Cell pellets were resuspended in Laemmli sample buffer containing 0.25% Triton-X100 and samples heated at 100°C for 5 mins. Usually, gels were run at 180V until the dye front reached the bottom of the gel, although occasionally migration was allowed to progress further for better separation of closely migrating proteins.

2.13 Coomassie staining of gels.

Protein gels were simultaneously fixed and stained by immersion in Coomassie stain solution for 1 hour at room temperature. Gels were destained with several changes of destain solution until optimum staining/background was observed, following which they were washed in several changes of distilled water and vacuum dried.

2.14 Western blotting of gels and immuno-detection of proteins.

Protein gels were equilibrated in transfer buffer for 15 mins and then blotted onto PVDF membrane (Pierce) using a Trans-Blot Semi-Dry Electrophoretic Transfer Cell (BioRad) set at 10V, 15mA for 30 mins. After transfer of proteins, the membrane was stained with Ponceau Red (Sigma) to visualise the molecular weight marker and to check for efficient transfer of proteins. The membranes were then destained with water, followed by blocking with 5% (w/v) dried skimmed milk powder in PBS with 0.05% Tween-20 (Sigma) (PBST) for 1 hour at room temperature or overnight at 4°C. Membranes were then incubated with

varying titres of primary antibody/antiserum in PBST on a roller for 1 hour at room temperature. Membranes were then washed 3 x with 5 ml PBST for 5 mins each and then incubated with secondary antibody-HRP conjugates (Promega) in PBST on a roller for 1 hour at room temperature. Blots were developed by incubation with SuperSignal Chemiluminescent Substrate Stable Peroxide Solution (Pierce) and SuperSignal Chemiluminescent Substrate Luminol/Enhancer (Pierce) for 1 min. Membranes were then encased in plastic film and exposed to X-Ray film for varying periods of up to 5 mins depending on intensity of the signal.

2.15 Immunofluorescence microscopy.

Logarithmic phase BSF or PCF parasites were harvested as previously described and resuspended in PBS. Cells were then spread onto slides and allowed to settle until an appropriate cell density was achieved, following which slides were air dried and subsequently fixed and permeabilised in first -20°C methanol for at least 15 mins followed by -20°C acetone for 2 mins. After drying, slides were blocked with 5% (w/v) dried skimmed milk in PBST for 30 mins in a dark moist chamber. Slides were then incubated with varying titres of primary antibodies/antiserum in PBST for 30 mins at room temperature. Slides were washed thoroughly with 10 ml PBST and incubated with appropriate secondary antibody fluorophore conjugates (Molecular Probes/Sigma). Following thorough washing with 10 ml PBST, slides were mounted with PBS/50 % (v/v) glycerol containing 2.5 % (w/v) 1, 4-diazabicyclo[2.2.2]octane (DABCO) (Sigma) as antifade and 1 μg ml^{-1} 4',6-diamidino-2-phenylindole (DAPI) (Sigma) to label DNA. Microscopy was carried out using a Zeiss UV microscope and images were captured with an Orca-ER camera (Hammamatsu) and Openlab software v 3.1.5 (Improvision).

Tomato lectin staining was performed on live mid-logarithmic phase BSF parasites. Cells were washed in serum-free HMI-9 medium and resuspended in 100 μl of prewarmed serum-free HMI9 at 1 x 10^7 cells ml^{-1}. 1 μl of FITC-tomato lectin (Sigma) was added and incubated in the dark at 4°C for 30 mins, washed and followed by a further incubation for a 30 mins period at 4°C in serum-free HMI9. Lysosomes were also selectively stained using live mid-logarithmic phase

BSF parasites. Cells were washed and resuspended in 100 µl of serum-free HMI9 at 1 x 10^7 ml^{-1}. 1 µl of Lysotracker Red DND-99 (Molecular Probes) was added and incubated at 37°C for 20 mins. Following incubation with either tomato lectin or Lysotracker, parasites were washed, re-suspended in PBS and air dried onto slides as previously described. Golgi apparatus staining was performed on fixed parasites previously adhered to slides. 1 µl of Bodipy-Texas Red ceramide (Molecular Probes) was added to 1 ml of 1.8% (w/v) fatty acid free BSA (Sigma) in PBS, applied to slides and incubated for 1 hour in a dark moist chamber.

2.16 Preparation of *T. brucei* genomic DNA for PCR.

Typically 10 ml of mid-logarithmic phase BSF or PCF were harvested and washed in PBS as previously described. Cell pellets were then re-suspended in 0.5 ml TELT (Medina-Acosta and Cross, 1993) and incubated at room temperature for 5 mins. 0.5 ml of a 1:1 ratio of phenol/chloroform was added and gently mixed for 5 mins, followed by a centrifugation at 16,000g for 5 mins. The aqueous phase was extracted and a further 0.5 ml of phenol/chloroform added and gently mixed for 5 mins followed by a further centrifugation at 16,000g for 5 mins. The aqueous phase was then extracted and DNA ethanol precipitated by the addition of 2.5 volumes of 100% EtOH with 10% (v/v) 3 M sodium acetate and centrifuged at 16,000g for 30 mins at 4°C. The resultant DNA pellet was then washed twice in 70% (v/v) EtOH, air dried for 5 mins and re-suspended in sterile distilled water. DNA was quantified spectrophotometrically at 260 nm and stored at 4°C.

2.17 Preparation of *T. brucei* genomic DNA for Southern blotting.

1 x 10^8 parasites were harvested and washed in PBS as previously described. Cells were then re-suspended in 3 ml NTE and 150 µl of a 10% SDS solution added, gently mixed and incubated for 15 mins at 37°C. 150 µl of 10 mg ml^{-1} RNase A (Sigma) was then added and incubated for 1 hour at 37°C. Subsequently 120 µl of 5 mg ml^{-1} Proteinase K (Sigma) was added and incubated overnight at 37°C. 1 volume of phenol was then added and gently mixed for 15 mins at room temperature followed by centrifugation at 2000g for 15 mins at 4°C. The aqueous phase was then extracted, mixed with 1 volume of chloroform, mixed gently for

15 mins at room temperature followed by centrifugation at 2000g for 15 mins at 4°C. The aqueous phase was extracted and mixed with 3 ml of isopropanol by gently inverting the tube until DNA became visible as white fluff. This material was then removed using a blue tip, transferred into 70% (v/v) EtOH and centrifuged at 16,000g for 5 mins at 4°C. After 1 further wash in 70% (v/v) EtOH the DNA pellet was air dried and resuspended in sterile distilled water. DNA was quantified spectrophotometrically at 260 nm and stored at 4°C.

2.18 Southern blotting.

Southern blotting was performed as follows. Following agarose gel electrophoresis of restriction enzyme digested DNA, a photograph was taken of the gel with a ruler laid alongside. The gel was then immersed in depurination buffer for 15 mins and then rinsed 3x in water. Next the gel was immersed in denaturation buffer for 30 mins and rinsed 3x in water. Finally the gel was immersed in neutralisation buffer for 30 mins. The DNA was transferred onto Hybond XL membrane (Amersham) soaked in neutralisation buffer by blotting overnight using 20x SSC as the transferrant. DNA was then fixed to the membrane using a UV Stratalinker 2400 (Stratagene). The membrane was then incubated with 10 ml of hybridisation mix with the addition of 200 μg ml^{-1} denatured salmon sperm (Sigma) at 65°C for 2 hours on a rotary shaker. 25 ηg of labelled probe was then added to the hybridisation mix and left incubating with the blot overnight at 65°C on a rotary shaker. The blot was then rinsed with 2 x SSC/0.1% SDS prior to washing for 30 mins with the same solution at 65°C. The blots were then sequentially washed with 1 x SSC/0.1% SDS, 0.5 x SSC/0.1% SDS and 0.1 x SSC/0.1% SDS all for 30 mins at 65°C. The membrane was then sealed in plastic film, a storage phosphor screen exposed for 2 days and developed using a Typhoon 8600 variable mode imager.

2.19 VSG recycling pathway.

BSF parasites were harvested at mid logarithmic growth phase, and after three washes with ice-cold trypanosome dilution buffer (TDB) the cell density adjusted to 1 x 10^8 cells ml^{-1} in ice-cold TDB. The parasites surface coat was then labelled using a final concentration of 1 mM sulfo-NHS-SS-biotin (Pierce) for 10 mins on ice and the reaction terminated by the addition of 10 mM Tris-HCl, pH 8.5. After

three washes with ice-cold TDB, parasites were re-suspended to a density of 1 x 10^7 ml^{-1} in pre-warmed HMI9 and endocytosis allowed for 5 mins at 37°C followed by three washes with ice-cold TDB at 4°C. Biotin probe remaining on the surface was then cleaved through incubation of parasites with HMI-9, 10% (v/v) fetal calf serum, 50 mM glutathione, pH 9, on ice for 10 mins. Parasites were washed a further three times in ice cold TDB before returning to HMI9 for 1 hour at 37°C. Samples were taken at various points for analysis by Western blot and immunofluorescence analysis (IFA) and processed as previously described. VSG-biotin was detected using either a streptavidin-Texas Red conjugate (Molecular Probes) or a streptavidin-HRP conjugate (Sigma).

2.20 Anti-VSG221 degradation.

BSF parasites were harvested at mid logarithmic phase and re-suspended at 1 x 10^7 cells ml^{-1} in HMI-9. Parasites were then labelled with rabbit anti-VSG221 antibodies at 4°C for 30 mins. Parasites were then washed three times in ice cold serum-free HMI9 and incubated at 37°C for 30 mins. Following this incubation period, parasites were prepared for analysis by both Western blot and IFA as previously described. The culture medium following this period was also TCA precipitated. 1 volume of a 0.5 mg ml^{-1} TCA solution was added to 4 volumes of culture medium, gently mixed and incubation on ice for 10 mins. Following centrifugation at 18,000g for 5 mins, the pellet was washed twice in ice cold acetone and briefly air dried before re-suspension in 1 x Laemmli sample buffer. Rabbit anti-VSG antibodies were detected directly using a anti-rabbit IgG-HRP conjugate (Promega).

2.21 Transferrin uptake assay.

BSF parasites were harvested at mid logarithmic phase and washed twice in ice-cold serum-free HMI9. Cell density was adjusted to 1 x 10^7 parasites ml^{-1} and a final concentration of 50 μg ml^{-1} transferrin-biotin conjugate (Molecular Probes) added. Individual 250 μl aliquots of the cell suspension were then placed at 37°C for 5, 10, 15 and 60 mins before centrifugation at 1500g and washing of cell pellets three times in ice-cold PBS and prepared for Western blot analysis. Following the 60 mins incubation, one aliquot was washed three times in ice-cold

HMI9 before incubation in HMI9 for 10 mins at 37°C. Following this, the parasites were centrifuged at 1500g for 5 mins at 4°C, washed three times in ice-cold PBS and prepared for Western blot analysis. Transferrin–biotin conjugate was detected using streptavidin-HRP conjugate (Sigma).

2.22 Heat shock experiments.

BSF and PCF parasites were harvested at mid logarithmic phase and re-suspended at 5 x 10^5 or 5 x 10^6 cells ml^{-1} in HMI9 or SDM79, respectively. PCF parasites were exposed to either a 37°C or 42°C heat shock for 2 hours. BSF parasites were exposed to a 42°C heat shock for 2 hours. Following heat shock, the parasites were prepared for Western blot analysis as previously described. BSF recovery from heat shock was examined by monitoring the growth rate of parasites over several days following the initial heat shock.

2.23 Salt stress experiments.

BSF parasites were harvested at mid logarithmic phase and re-suspended at 4 x 10^5 cells ml^{-1} in HMI9 with the addition of 125 mM NaCl and cell numbers were monitored over a 5 hour period. Following this period, parasites were washed three times in HMI9 and resuspended to 5 x 10^4 cells ml^{-1} and recovery monitored over a period of several days.

2.24 Reactive oxygen species experiments.

BSF and PCF parasites were harvested at mid logarithmic phase and re-suspended at 5 x 10^5 or 5 x 10^6 cells ml^{-1} in HMI9 and SDM79, respectively. A final concentration of 1 μM xanthine (Sigma) was added to the cultures together with the addition of a 1/1000 dilution of xanthine oxidase (Sigma). BSF and PCF cultures were incubated in these conditions for 2 and 4 hours, respectively, before washing in PBS and being prepared for Western blot analysis as previously described.

2.25 Concanavalin A experiments.

PCF parasites were harvested at mid logarithmic phase and re-suspended at 5 x 10^6 cells ml^{-1} in SDM79. A final concentration of 50 μg ml^{-1} Concanavalin A (Con A) was added and parasites incubated for 6 and 24 hour periods. After this

period, parasites were washed in PBS and prepared for Western blot as previously described.

2.26 Oligonucleotide sequences.

OL15	CCGTGGGCTTGTACTCGGTCA
OL16	ACCCGCAAGCCCGGTGCCTGA
OL536	TTGAGACAAAGGCTTGGCCAT
OL537	GGTTATGTGTGGGAGGGCTAA
OL905	AGGATCCATGGGTCGCGACACCTCTTC
OL906	GAAGCTTAGCGCCTGTAGAACCCGTACC
OL944	GCGAATTCATGGACGCAGCTCTCGCTTTGC
OL945	GCAAGCTTACATCGTACACAAGCCATGCC
OL969	AATCTAGAGCGGCCGCAAGGGGTGACGAAACAGGAGC
OL970	AATCTAGACTCATCCGCATATGTATTCG
OL971	TTGGGCCCGTTTCTGCCCTTTGGTTCGC
OL972	AAGGGCCCCTCGAGTTATGTCCAATAGCGGTGGC
OL1130	AAGCGGCCGCCTTGTTCTCCCTTTCGTGTGGC
OL1133	ATGGGCCCGATATCTTTCGTCTCCTTTCCGTTGACC
OL1307	GCGAATTCATGAAAAAGCCTGAACTCACCGC
OL1308	GCGAATTCCTATTCCTTTGCCCTCGGACG
OL1309	GCGAATTCATGGGATCGGCCATTGAACAAGATGG
OL1310	GCGAATTCTCAGAAGAACTCGTCAAGAAGG
OL1373	GCGATATCATGGACGCAGCTCTCGCTTTGC
OL1374	GCGATATCTCACTTGCGGCCGGGTTTACC
OL1029	GCATTAATGACGCAGCTCTCGCTTTGC
OL1030	GCGAATTCTCACTTGCGGCCGGGTTTACCCTG
OL1131	AGTCTAGAGCTTCACCCTCTTTTCCCGAAC
OL1132	ATGGGCCCATGTCTATGACCCACCCTTCCC
OL1134	ATGGGCCCGATATCAGTCGGAAGTGGTCACATGACC
OL1135	AAGCGGCCGCATGTTTCGTATCCGAGGGTTGG
OL1151	GAGTGGCTTTTGGAACAAGAGC
OL1152	TAGCACCAACACAAAGCGATGC
OL1225	GATCCATCCAATACCCCTACGACGTCCCGGACTATGCCTAGC
OL1226	TCGAGCTAGGCATAGTCCGGGACGTCGTAGGGGTATTGGATG
SP6	ATTTAGGTGACACTATAGAATAC
T3	AATTAACCCTCACTAAAGGG
T7	GTAATACGACTCACTATAGGGC

2.27 Buffers and solutions.

Coomassie Stain

Methanol	50% (v/v)
Acetic acid	10% (v/v)
Coomassie Brilliant Blue	0.125% (w/v)

Destain

Methanol	10% (v/v)
Acetic acid	10% (v/v)

Buffer D for protein elution

Urea	8 M
NaH_2PO_4	0.1 M
Tris	10 mM
pH 5.9	

Buffer E for protein elution

Urea	8 M
NaH_2PO_4	0.1 M
Tris	10 mM
pH 4.5	

Denhardts (50x)

Ficol 400	1% (w/v)
Polyvinylpyrrolidone (PVP)	1% (w/v)
BSA	1% (w/v)

DNA denaturation solution

NaCl	1.5 M
NaOH	0.5 M

DNA denaturation solution

HCl	0.25 M

DNA loading buffer (6x)

Ficoll	15 % (w/v)
Orange G	0.2 % (w/v)
Xylene cyanol	0.1 % (w/v)

DNA neutralisation solution

NaCl	3 M
Tris (pH 7.5)	1 M

Ethidium bromide

10 mg ml^{-1} stock solution in dH_2O

Hybridisation solution

SSC	6 x
SDS	1% (w/v)
Denhardts	5 x
EDTA	5 mM
NaH_2PO_4	20 mM
pH 6.5	

Laemmli sample buffer (4x)

SDS	4 % (w/v)
Glycerol	10 % (v/v)
2-mercaptoethanol	10 % (v/v)
Trizma base	0.125 M
Bromophenol blue to colour	
pH 6.8	

Luria-Bertani (LB) medium

	g/litre
Bacto-tryptone	10
Bacto-yeast extract	5
NaCl	10

Solutes were dissolved in 950 ml deionised water and the pH adjusted to 7.0 with 5 M NaOH. The volume was adjusted to 1 litre prior to autoclaving.

LB agar

LB medium as described above with addition of 15 g litre^{-1} bacto-agar

NTE

Tris	10 mM
NaCl	100 mM
EDTA	5 mM
pH 7.5	

Phosphate buffered saline (PBS)

KH_2PO_4/K_2HPO_4 (pH 7.4)	10 mM
NaCl	137 mM

***Pfu* DNA polymerase reaction buffer**

KCl	50 mM
Tris-HCl (pH 9.0)	10 mM
Triton®X-100	0.1% (v/v)

SSC (20x)

NaCl	3 M
Trisodium citrate	3 M

TAE (50 x)

Tris	2 M
Sodium acetate trihydrate	2 M
EDTA	50 mM
pH 7.2	

TBE (0.5 x)

Tris	20 mM
Boric acid	20 mM
EDTA	0.5 mM
pH 7.2	

***Taq* DNA polymerase reaction buffer**

KCl	50 mM
Tris-HCl (pH 9.0)	10 mM
Triton®X-100	0.1% (v/v)

TDB (Trypanosome dilution buffer)

KCl	5 mM
NaCl	80 mM
$MgSO_4$	1 mM
Na_2HPO_4	20 mM
NaH_2PO_4	2 mM
Glucose	20 mM
pH 7.4	

TELT

Tris	50 mM
EDTA	62.5 mM
LiCl	2.5 M
Triton X-100	4% (w/v)
pH 8.0	

Western running buffer (10X)

Tris	250 mM
Glycine	1.92 M
SDS	87 mM

Western transfer buffer

Tris	48 mM
Glycine	39 mM
SDS	15 mM

ZPFM

NaCl	132 mM
KCl	8 mM
Na_2HPO_4	8 mM
KH_2PO_4	1.5 mM
Mg acetate	0.5 mM
Ca acetate	90 µM
pH 7	

ZPFMG

NaCl	132 mM
KCl	8 mM
Na_2HPO_4	8 mM
KH_2PO_4	1.5 mM
Mg acetate	0.5 mM
Ca acetate	90 µM
Glucose	55 mM
pH 7	

Chapter 3

Characterisation of metacaspases

3.1 Analysis of metacaspase genes in *T. brucei.*

The identification of metacaspase genes within plants, fungi and protozoa (Uren *et al.*, 2000) allowed the discovery of several metacaspase genes within *T. brucei.* BLAST searches of the *T. brucei* genome database (www.genedb.org), using the *Saccharomyces cerevisiae* metacaspase sequence, identified five distinct metacaspase genes, all present as single copies. An independent study also identified these same five genes within the *T. brucei* genome (Szallies *et al.*, 2002). *MCA1* (Tb11.02.0730) is located on chromosome 11, *MCA2* (Tb06.3A7.310) and *MCA3* (Tb06.3A7.290) are both located on chromosome 6, *MCA4* (Tb10.70.5250) is located on chromosome 10, while *MCA5* (Tb09.211.4760) is located on chromosome 9. A cartoon representation of the five predicted proteins illustrates that MCA1-4 have a similar domain structure, while MCA5 is unique in that it possesses a C-terminal extension (Figure 3.1). Alignments of the metacaspases with human caspase-3 identified the putative active site histidine and cysteine residues (Szallies *et al.*, 2002; Mottram *et al.*, 2003). These active site histidine and cysteine residues are highlighted in figure 3.1. Of note is that MCA1 and MCA4 have cysteine to serine substitutions while MCA1 also has a histidine to tyrosine substitution. Post-translational modification software - NetOGlyc, NetNGlyc, SignalP (ca.expasy.org) - predicts that MCA1, MCA2 and MCA3 have 1 predicted N-glycosylation site each, MCA4 has none while MCA5 has eight predicted sites. The software also predicts the presence of a signal peptide on MCA5, while the probability of the other metacaspases possessing one is very low. Also identified within the metacaspases of *T. brucei* are possible Class III WW binding domain motifs. WW binding domains act as ligands for WW domains, which are modules mediating protein-protein interactions in a diverse range of cellular processes (Sudol and Hunter, 2000). Class III WW binding domains are characterised by poly-proline motifs flanked by arginine or lysine residues (Macias *et al.*, 2002). Motifs fulfilling these requirements were identified in the N-terminal regions of MCA1, MCA2 and MCA3 and the C-terminal extension of MCA5. An alignment of the amino acid sequences of these five proteins highlights in more detail these features, together with illustrating the major blocks of homology between the metacaspases (Figure 3.2).

Examination of the amino acid sequence of the MCA5 C-terminal extension reveals that it is both proline-rich and contains repeating stretches of sequences of proline, glutamine, alanine and tyrosine residues. A BLAST search of this extension was performed in June 2004 against the *T. brucei* predicted peptide database at GeneBD (www.genedb.org) and produced two significant hits. These are both hypothetical proteins (Tb11.33.0008 and Tb10.389.1920) located on chromosome 11 and 10, respectively. An alignment of these two hypothetical proteins with the MCA5 C-terminal extension shows that they share a high level of sequence identity over these repeating motifs (Figure 3.3). Particularly of note is the motif QPPxxA, which is repeated five times in all three proteins. These two identified hypothetical proteins are also highly similar around the region that aligns with the MCA5 extension.

A comparison of the active site regions of the *T. brucei* metacaspases with metacaspases from other protozoa and fungi reveals some interesting features (Figure 3.4). Firstly, the histidine to tyrosine substitution observed in TbMCA1 is also present in one of the two metacaspases identified in both *Plasmodium falciparum* and *P. berghei* (named MCAy). Interestingly, these two metacaspases also have a substitution at the predicted active site cysteine residue, with a threonine in this position. Secondly, adjacent to the predicted active site cysteine in all the *T. brucei*, *T. cruzi* and *L. major* metacaspases is a second cysteine residue, which might in reality be the active site cysteine. However, in yeast and *P. falciparum* (MCAx) there is a serine residue located at this position, although in *P. berghei* (MCAx) there is a cysteine at this position and the alignment reveals a proline at the predicted active site position. Uniquely, the *Theileria annulata* metacaspase has no cysteine residue in either the putative or adjacent position, instead encoding for a serine residue at the putative active site location.

T. brucei MCA2 (Tb06.3A7.310) and *MCA3* (Tb06.3A7.290) are found adjacent to each other, localised to chromosome 6 (Figure 3.5A). Located 5' of this locus is a putative cysteinyl-tRNA synthetase gene while 3' there is a putative ATP-dependent RNA helicase gene. Alignment of predicted MCA2 and MCA3 protein sequences show that these two genes are also highly homologous, sharing 91% identity at both the DNA and protein level (Figure 3.5B). The divergence

between the two proteins occurs almost exclusively within the N-terminal region of the proteins, where MCA3 also has a small extension of 10 amino acids relative to MCA2. Taken together, the sequential positioning and high homology displayed between *MCA2* and *MCA3* is strong evidence for a past gene duplication event giving rise to the current genomic locus.

A phylogenetic analysis of metacaspase genes from *Trypanosoma brucei*, *T. cruzi*, *Leishmania major*, *P. falciparum*, *P. berghei*, *Theileria annulata* and yeast was generated using the central catalytic domain only using alignX (InforMax) (Figure 3.6). As expected *Tb*MCA5 groups with MCA5 homologues identified in both *L. major* and *Trypanosoma cruzi*. This was predicted due to high sequence identity and synteny around the respective genomic loci of the three trypanosomatid species. Genomic synteny was also identified between the *TbMCA2* and TbMCA3 locus and *T. cruzi* MCAx and MCAy locus (these two genes are also present as a tandem repeat) and the phylogenetic analysis confirmed their close relationship. Not surprisingly, the metacaspases in apicomplexa parasites form a subgroup, but which, interestingly, groups closer to yeast than the trypanosomatid metacaspases. The analysis also suggests that this grouping of apicomplexan and yeast metacaspases is most similar to the MCA5 homologues identified in *T. brucei*, *T. cruzi* and *L. major*.

3.2 Analysis of MCA2 and MCA3 expression in *T. brucei*.

To generate specific antibodies against MCA2 and MCA3, an 80-mer peptide was generated that encompassed both the histidine and cysteine catalytic residues of MCA2 (N. Fasel, University of Lausanne, Switzerland). MCA2 is virtually identical to MCA3 over this region with only one alanine to valine substitution (Figure 3.5B). This peptide was then used to immunise a rabbit at Diagnostics Scotland and affinity purification of the antiserum performed using an affinity matrix generated with the 80-mer peptide used in the immunisation.

Western blot analysis was then used to determine the expression profile of MCA2 and MCA3 in both procyclic (PCF) and bloodstream (BSF) life stages *in vitro*. Analysis of whole cell lysates was able to detect several proteins recognised by the affinity purified antibody (Figure 3.7). One protein, estimated to be 48 kDa,

and a less abundant protein estimated, at around 35 kDa, were detected in both the PCF and BSF parasite cell extracts. However, unique to the BSF cell lysates were two further proteins detected at around the predicted sizes of MCA2 and MCA3 (of 38 and 39 kDa, respectively). The confirmation of the identity of these proteins as MCA2 and MCA3 was performed by both RNAi and gene knockouts (Chapters 4 and 5). While these two proteins closely match the predicted sizes of MCA2 and MCA3, there appears to be a difference in size greater than 1 kDa. The detection of MCA2 and MCA3 at around their predicted full-length sizes suggested, however, that these two proteins do not undergo any large scale processing events. The identities of the 35 and 48 kDa proteins are unknown but the masses do not correspond to the predicted sizes of any other identified metacaspases within *T. brucei*.

While the anti-peptide antibodies were sufficient for the identification of MCA2 and MCA3 by Western blot analysis, they were not suitable for use in immunofluorescence studies, as they also detected the proteins of 48 and 35 kDa, as discussed above. Therefore, it was decided to generate HA epitope tagged versions of MCA2 and MCA3 to allow the specific detection of the proteins. The HA tag is derived from an epitope of the influenza hemagglutinin protein, which has been used successfully to epitope-tag proteins in *T. brucei* (McManus *et al.*, 2001; Wang *et al.*, 2003). The sequence for an HA tag was cloned, in frame, onto the 3' terminal end of both MCA2 and MCA3. These tagged genes were then sub-cloned into a trypanosome expression vector designed to integrate and drive expression from the αβ tubulin array (Figure 3.8A), which was kindly provided by R. McCulloch, University of Glasgow. These two separate constructs were subsequently transfected into wild type BSF parasites and clonal populations obtained, using the *BLE* gene as the resistance marker.

Western blot analysis of whole cell lysates was then used to determine if expression of MCA2HA and MCA3HA was successful. Probing with a mouse monoclonal anti-HA antibody detected one major protein in both MCA2HA and MCA3HA transfectants (Figure 3.8B). The addition of an HA-tag adds approximately 1 kDa to the mass of subject protein. Therefore, the predicted

sizes of MCA2HA and MCA3HA are 39 and 40 kDa, respectively, closely matching the Western blot results. This demonstrated that expression of MCA2 and MCA3 with the addition of an HA tag was successful and that it was possible to detect specifically these proteins individually in BSF parasites.

3.3 Cellular localisation of *T. brucei* metacaspases.

The specific detection of MCA2HA and MCA3HA enabled the study of the cellular localisation of MCA2HA and MCA3HA using immunofluorescence analysis (IFA). BSF parasites expressing either MCA2HA or MCA3HA were prepared for analysis and stained with mouse anti-HA monoclonal antibodies (Figure 3.9). The IFA images revealed that both MCA2HA and MCA3HA localised within several punctate regions, located exclusively between the nucleus and kinetoplast. This labelling suggests that MCA2HA and MCA3HA are associated with an organellar structure, present between the nucleus and kinetoplast and that the proteins are not located in the cytosol.

It was planned to produce recombinant MCA5 for both antibody production and for biochemical studies. Full-length MCA5 was cloned into the pET-28(a)+ expression vector and used to transfect BL21 *E. coli*; this vector is designed for expression of subject protein with the addition of a polyhistidine tag at the N-terminus. Induction of expression at 37°C with 1 mM IPTG resulted in a very good expression level of His tagged protein, however, unfortunately these conditions resulted in 100% insoluble material. All subsequent attempts at producing soluble enzyme by altering both the IPTG concentration and/or induction temperature were unsuccessful; the protein being always found exclusively in the pellet fraction. Further avenues were also pursued in an effort to produce soluble protein. The polyhistidine tag was moved to the C-terminus, with no success in terms of solubility, while various truncated forms of MCA5-His were also expressed, but again only insoluble material was produced.

Despite this failure to produce soluble protein, the insoluble protein was still suitable for antibody production. The full-length MCA5 recombinant protein with a N-terminal histidine tag, of predicted size 58 kDa, was used for this

purpose. A 500 ml culture of MCA5-His expressing BL21 *E. coli* was grown and expression induced with 1 mM IPTG at 37°C, as these conditions had been observed to produce the highest levels of recombinant protein. At 4-hours post induction, the bacteria were harvested, inclusion bodies extracted and extensively washed to remove contaminants. These inclusion bodies were then solubilised in 8 M Urea at 4°C overnight. To purify MCA5-His from native inclusion body proteins, the material was passed through a nickel-agarose column. After washing, elution from the column was performed via a drop in pH to break the physical bond between nickel-agarose and the polyhistidine tag. Two separate pH values where used in the elution, pH 6.3 and pH 4.5, and fractions collected. A coomassie stain of SDS PAGE gels of these elution fractions shows that the majority of MCA5-His was eluted in the pH 4.5 fraction (Figure 3.10)

It was clear, however, that there were still several non-desirable contaminating proteins within the purified material. Therefore, a volume of eluted protein, containing approximately 800 μg of recombinant protein, was electrophoresed via SDS-PAGE and the MCA5-His protein excised. This material was subsequently ground into a paste and resuspended in PBS. This suspension was then sent for antibody production in sheep at Diagnostics Scotland.

Western blot analysis was performed to determine the expression profile of MCA5 in both PCF (strain EATRO 795) and BSF (strain 427) life stages *in vitro*. Analysis of whole cell lysates revealed that the antiserum recognised a single 60 kDa protein, present in both PCF and BSF extracts (Figure 3.11). The predicted size of MCA5 is 55 kDa. The specificity of this antiserum was confirmed by both RNAi and gene knockout (Chapters 4 and 5). This constitutive expression of MCA5 in both life stages is distinct to that observed for MCA2 and MCA3, which appear to be BSF-specific. MCA5 was detected at approximately its predicted size, so no large-scale processing events were evident, as had been observed also for MCA2 and MCA3.

The high specificity of the sheep polyclonal anti-MCA5 antiserum enabled its use directly in immunofluorescence studies, with no further purification being

necessary. Both wild type PCF (strain EATRO 795) and BSF (strain 427) were prepared for IFA and stained with the sheep polyclonal anti-MCA5 antiserum (Figure 3.12). MCA5 displayed a punctate distribution localised primarily between the nucleus and kinetoplast in both PCF and BSF parasites, consistent with an organellar location. The pattern of staining was similar to that observed with MCA2HA and MCA3HA. Interestingly, while total protein levels were very similar in both life stages when examined by Western blot (Figure 3.11), this compartment was stained much less extensively in the PCF compared to BSF parasites.

The localisation studies previously described for MCA2HA, MCA3HA and MCA5 all pointed to their association with an organellar structure situated between the nucleus and kinetoplast. However, the individual experiments did not reveal whether these individual metacaspases are localised to separate compartments or are present within the same structures. Therefore double-labelling experiments with MCA2HA or MCA3HA and MCA5 were performed to determine if the metacaspases are co-localised. BSF parasites expressing MCA2HA or MCA3HA were prepared for IFA and probed with mouse monoclonal anti-HA antibodies and sheep polyclonal anti-MCA5 antiserum (Figure 3.13). A very high level of co-localisation was observed for both MCA2HA and MCA3HA with MCA5. Assuming that the HA-tagged MCA2 and MCA3 are targeted to the same compartment as the native proteins, this result demonstrates that MCA5 is associated with the same structures as MCA2 and MCA3 in BSF parasites.

3.4 Identification of metacaspase positive compartment.

While the IFA studies showed that the metacaspases are associated with an organellar compartment localised between the nucleus and kinetoplast, it does not provide any real insights into the possible functions or roles of the proteins. Therefore the organellar compartment in which the metacaspases are localised was investigated by utilising various commercially available markers. Between the nucleus and kinetoplast in *T. brucei* there are several well-characterised organellar structures for which fluorescent markers are available. For initial studies the endosomal system and the Golgi apparatus were examined.

3.4.1 Early endosomes.

The early endosomes of *T. brucei* can be labelled for detection by IFA using a tomato lectin fluorophore conjugate (Nolan *et al.*, 1999; Jeffries *et al.*, 2001). This lectin binds selectively to poly-N-acetyllactosamine (pNAL) residues present on proteins located in early endosomal membranes. BSF parasites were incubated with this lectin for 1 hour at 4°C to allow up-take and association with early endosomal membranes. Parasites were then prepared for IFA and stained with sheep polyclonal anti-MCA5 antiserum (Figure 3.14A). Examination of the merged image of tomato lectin and anti-MCA5 labelling clearly shows that there is no co-localisation between these two compartments, ruling out metacaspase association with the tomato lectin-labelled component of the early endosomal system in *T. brucei*.

3.4.2 Lysosomes.

To label the lysosomal compartment of *T. brucei* we utilised the commercially available probe Lysotracker. This molecule, upon uptake, is targeted to the lysosomal compartment where the reduction in pH results in a large increase in fluorescence, thus allowing the specific detection of this compartment (Magez *et al.*, 1997). BSF parasites were incubated with Lysotracker for 1 hour at 37°C to allow sufficient material to accumulate in the lysosome. Parasites were subsequently prepared for IFA and stained with sheep polyclonal anti-MCA5 antiserum (Figure 3.14B). Analysis of the merged image of lysosomal and anti-MCA5 labelling clearly shows that there is no co-localisation between these two compartments, thus ruling out metacaspase association with the lysosome in *T. brucei*.

3.4.3 Golgi apparatus.

Having ruled out metacaspase association with both the early endosomes and the lysosome, it was investigated whether the metacaspases are associated with the Golgi apparatus. To label this compartment we utilised the probe BODIPY-Ceramide, a reliable marker of the mammalian Golgi apparatus and also shown to specifically label the Golgi apparatus in *T. brucei* (Field *et al.*, 2000). Wild type

BSF parasites were incubated with the BODIPY-Ceramide dye for 1 hour at 37°C to allow accumulation within the Golgi apparatus. Parasites were then prepared for IFA and stained with sheep polyclonal anti-MCA5 antiserum (Figure 3.14C). There was no co-localisation between the BODIPY-Ceramide and MCA5, suggesting that the Golgi is not the location of the metacaspases.

3.4.4 Recycling endosomes.

Having ruled out metacaspase association with early endosomes, the lysosomal compartment and Golgi apparatus, an analysis of recycling endosomes was carried out with an antibody specific to recycling endosomes in *T. brucei*. This antibody was raised against *Tb*Rab11, a small GTPase known to localise to recycling endosomal membranes in *T. brucei* (Jeffries *et al.*, 2001). To determine if the metacaspases localised to this compartment of the endosomal system, PCF and BSF wild type parasites were prepared for IFA. These were then labelled with immunopurified polyclonal rabbit anti-*Tb*Rab11 antibodies and sheep polyclonal anti-MCA5 antiserum (Figure 3.15). MCA5 labelling was consistent with previous observations (Figure 3.12) and Rab11 labelling gave a very similar pattern to that seen with MCA5, in that many more structures were labelled in the BSF compared to PCF parasites. Furthermore, upon the merging of MCA5 and Rab11 labelling, a very high level of co-localisation in both PCF and BSF parasites was revealed. This evidence is highly suggestive that the metacaspases are associated with the recycling compartment in *T. brucei*. Interestingly, Rab11 is the only characterised Rab family member that displays a stage-regulated expression in *T. brucei*, exhibiting a much higher expression level in the BSF (Jeffries *et al.*, 2001). This observation was confirmed by performing Western blot analysis on total cell extracts prepared from the PCF and BSF parasite cultures used in the IFA analysis. Rab11 expression in the BSF was greatly increased relative to the PCF (Figure 3.16).

3.4.5 MCA5 positive structures traffic recycled material.

Although immunofluorescence analysis suggested that the metacaspases are associated with recycling endosomes in *T. brucei*, we wanted to confirm this by determining if MCA5 positive structures were also trafficking recycled material.

To investigate this, we utilised the anti-VSG antibody recycling pathway for which Rab11 positive endosome involvement has been documented (Pal *et al.*, 2003). It is known that, *in vivo*, host anti-VSG antibodies bound to the parasite's surface are rapidly internalised as part of the normal VSG recycling process (Russo *et al.*, 1993). Initially these antibodies enter Rab5 positive early endosomes (Pal *et al.*, 2003), prior to their secretion via Rab11 positive recycling endosomes (Jeffries *et al.*, 2001).

Therefore a co-localisation of internalised anti-VSG antibodies with MCA5 would further confirm metacaspase association with recycling endosomes. Wild type BSF parasites were labelled with rabbit polyclonal anti-VSG antibodies at 4°C prior to a 30 mins incubation at 37°C. Parasites were then prepared for IFA and stained with sheep polyclonal anti-MCA5 antiserum. Internalised rabbit anti-VSG antibodies were detected using an anti-rabbit TRITC conjugate, while anti-MCA5 labelling was detected using an anti-sheep FITC conjugate (Figure 3.17). Internalised anti-VSG antibodies were located between the nucleus and kinetoplast, consistent with uptake by the endosomal system. No surface labelling remained, suggesting that the majority was internalised over this 30 min period. A merged image of internalised anti-VSG antibodies and MCA5 labelling, however, showed only a partial co-localisation between anti-VSG and MCA5 signals. This is not unexpected, and could be due to the dynamics of the endosomal system. It is feasible to suggest that some of the labelled anti-VSG antibody would be associated with early endosomes and therefore would not be detected when staining with MCA5. Conversely, not all recycling endosomes would be trafficking these internalised antibodies, especially after a 30 min chase when, as suggested by the lack of surface labelling, the recycling process was almost complete. Therefore, this partial co-localisation of MCA5 with material known to be recycled, taken together with the identification of MCA5 association with Rab11 positive endosomes, is further evidence of metacaspase association with recycling endosomes in *T. brucei*.

3.5 Attempts to activate processing of metacaspases.

It is known that caspases require processing prior to their becoming active and it has also been reported that the yeast metacaspase may undergo possible caspase-like processing (Madeo *et al.*, 2002). From the Western blot analysis (Figures 3.7 and 3.11) it appears that the *T. brucei* metacaspases do not undergo any such processing events in parasites grown under normal *in vitro* conditions. It is possible, however, that the metacaspases require a stimulus, such as a stressful event, to trigger their processing and activation. In an attempt to investigate this hypothesis, we exposed both PCF and BSF parasites to a variety of stressful conditions - ones documented to induce apoptotic-like cell death in protozoa (Moreira *et al.*, 1996; Welburn *et al.*, 1999; Ridgley *et al.*, 1999). Heat shock was performed on PCF parasites by incubating at either 37°C or 42°C for 2 hours, while BSF parasites were incubated at 42°C for 2 hours. PCF and BSF parasites were also exposed to reactive oxygen species. These were generated by the addition of both xanthine and xanthine oxidase to the culture medium. Additionally PCF parasites were also treated with the lectin Concanavalin A and incubated for 6 and 24 hours. Following these stimuli, whole cell lysates were prepared and analysed by Western blot to determine if any processing of the metacaspases was evident. No processing events were detected, the sizes of MCA2, MCA3 and MCA5 were unchanged in all lysates analysed (not shown).

3.6 Discussion.

3.6.1 Characterisation of metacaspases

We have been able to identify five distinct metacaspase genes (*TbMCA1-TbMCA5*) within the *T. brucei* genome. Analysis of the predicted proteins revealed that MCA1, MCA2, MCA3 and MCA4 are all roughly equivalent in size, ranging between 38 and 40 kDa. MCA2 and MCA3 share a very high level of sequence identity, 91% at the protein level, and their sequential positioning on chromosome 6 is consistent with a gene duplication event. The region of divergence between these two proteins is located at the N-terminal domain, where MCA3 has a 10 amino acid extension. This is suggestive that the N-terminal region may be important for some differential function or targeting of the two proteins, although neither MCA2 nor MCA3 are predicted to posses signal peptides. The maintenance of almost 100% sequence identity over the remainder of the two proteins, however, allows us to speculate that they will have very similar, if not identical, substrate recognition. It is possible, however, that this divergence at the N-terminus affects neither the localisation nor activity of the peptidases and is not important to their function. In fact, the syntenic *T. cruzi MCA2* and *MCA3* homologues, *MCAx* and *MCAy*, are of equal size with no N-terminal extension on either.

The identification of five metacaspase genes in *T. brucei* is of interest as this is the largest known repertoire of metacaspase genes of any protozoon. Searches of genome databases for other protozoa identified MCA2, MCA3 and MCA5 homologues within *T. cruzi*, while *L. major* possesses a sole MCA5 homologue. These homologous genes also display strong genomic synteny between these three trypanosomatids.

MCA5 is different from the four other metacaspases from *T. brucei* in that it possesses a large C-terminal extension of roughly 15 kDa. This extension is proline-rich and contains stretches of repeating sequence. Protein BLAST searches of this region against the *T. brucei* database identified two proteins that displayed strong similarity with the aforementioned repeating sequences, however, no functions have been assigned to these hypothetical proteins. If the

functions of these proteins were known this may help to understand the role of this C-terminal extension of MCA5. The fact the repeating motif QPPxxA was identified in the MCA5 C-terminal extension and two further hypothetical *T. brucei* proteins, which, apart this modular homology, do not have any identity to the metacaspases, leads us to believe that this repeating module may fulfil some form of specialised role within the parasites. MCA5 also possesses a predicted N-terminal signal sequence, but there is no experimental evidence to confirm whether this is a true targeting signal.

Of the metacaspase genes examined experimentally in *T. brucei*, we have shown that MCA2 and MCA3 expression is stage-regulated while MCA5 is constitutively expressed *in vitro*. MCA2 and MCA3 were detected on SDS-PAGE gels by Western blotting at around their predicted sizes of 38 and 39 kDa, respectively, demonstrating that neither protein undergoes any large-scale processing events *in vitro*. However, there does appear to be a greater separation than 1 kDa between the two proteins as assessed by SDS-PAGE and this might suggest some differential post-translational modifications. MCA2 and MCA3 both have a single predicted N-glycosylation site and neither are predicted to possess a signal peptide. MCA5 was detected at around 60 kDa, which is significantly larger that its predicted size of 55 kDa. This increase in size may be the result of post-translational modifications, MCA5 being predicted to contain 8 possible N-glycosylation sites. Many cysteine peptidases are processed upon maturation, with cleavage of the N-terminal most common. The papain family of cysteine peptidases, for example, undergoes cleavage of N-terminal polypeptide extensions of various lengths which act as potent inhibitors toward the cognate enzyme (Fox *et al.*, 1992). Caspase maturation also involves proteolytic removal of a pro-domain together with cleavage into two subunits; these subunits subsequently dimerise to form the active enzyme (Rotonda *et al.*, 1996).

If such a process were occurring to the metacaspases of *T. brucei*, we would not expect them to migrate so closely to their predicted molecular weights. We cannot rule out, however, that the metacaspases are capable of being processed under certain conditions, and that normal *in vitro* culture conditions do not stimulate their activation. Our attempts to induce processing were based on the

hypothesis that the metacaspases may be involved in the apoptotic-like cell death that has been reported in trypanosomes and that they remain inactive until a specific stimulus provokes their activation. While the stimuli used did not induce any possessing, it is possible that certain stimuli may do so. The trigger for processing of the metacaspases may only be present under certain *in vivo* conditions, for example. Future analysis of extracts made from parasites isolated from either the mammalian host or insect vector may be able to address this possibility. Alternatively the metacaspases may bear no similarity, with regard to processing, to the caspases, being active as full-length proteins and requiring no processing to become active. Numerous unsuccessful attempts have been made to produce soluble recombinant metacaspase enzyme for use in biochemical studies to address this question (S.J Sanderson, unpublished). Future work, however, may reveal whether the *T. brucei* metacaspases are active as full-length proteins or require processing to become active.

The expression of MCA5 is distinct from that of MCA2 and MCA3 in that this protein was detected at approximately equivalent levels in both PCF and BSF parasites. Therefore MCA5 is constitutively expressed in *T. brucei*, while MCA2 and MCA3 are only present in the BSF life stage. This suggests that MCA2 and MCA3 fulfil a specialised role in the BSF, while the function of MCA5 might be more basal. Interestingly, the only metacaspase gene identified to date in the *L. major* sequencing projects has been an *MCA5* homologue and despite almost completion of the database, homologues of *MCA1-4* have not been identified. However, three metacaspase genes have been identified in the *T. cruzi* sequencing database (www.genedb.org). This organism possesses homologues of *MCA2*, *MCA3* and *MCA5*. *MCA1* and *MCA4* homologues have not been identified. These observations further support the idea that *MCA5* is the basal metacaspase in all trypanosomatids and that the requirement for further metacaspase genes may be specific to trypanosomes.

This hypothesis can be extended further than the trypanosomatids to encompass other protozoa and yeast. Examination of the Apicomplexa genome databases (www.genedb.org) reveals that two metacaspase genes are present in several *Plasmodium* species, while *Theileria annulata* appears to have a single

metacaspase. Within the genomes of both *Saccharomyces cerevisiae* and *Schizosaccharomyces pombe* there is also a single metacaspase gene, which is mirrored in the filamentous fungus *Aspergillus nidulans*. An alignment and compilation of a phylogenetic tree of all identified metacaspases from protozoa and yeast supports the idea that *MCA5* represents the basal metacaspase gene. *Tb*MCA5 is grouped along with the homologues from *T. cruzi* and *L. major* as expected. The metacaspases from *Plasmodium, Theileria* and Yeast are all more divergent, highlighted by their separation from the kinetoplastid metacaspases. However, these sequences share more in common with the MCA5 homologues than with any of the other metacaspases found in the trypanosomatids.

Analysis of the metacaspase protein sequences also led to the identification of predicted Class III WW binding domain motifs. There are four classes of these binding motifs; Class I is represented by the minimal core consensus Pro-Pro-X-Tyr, Class II by Pro-Pro-Leu-Pro, Class III by polyproline stretches flanked by either an Arg or Lys residue and Class IV by phosphor-Ser/Thr-Pro (Sudol and Hunter, 2000). These binding domains act as ligands for WW domains. The initials WW derives from the presence of two signature tryptophan residues that are spaced 20-23 amino acids apart, there is also a conserved proline residue (Bork and Sudol, 1994; Andre and Springael, 1994). These WW domains fold as stable, triple stranded Þ-sheets (Macias *et al.*, 1996) that bind to proteins with WW binding domains which are rich in proline. They act as modules mediating protein-protein interactions in a diverse range of cellular processes (Sudol *et al.*, 2001; Ingham *et al.*, 2004). There is only one published example of a protein with a WW domain in *T. brucei*; *Tb*ZFP2 was shown to possess the characteristic dual tryptophan residues and conserved proline. The protein with which ZFP2 interacts, with via this domain, has not been identified (Hendriks *et al.*, 2001). However, there are seven proteins within *T. brucei* that are predicted to possess WW domains (www.genedb.org). Six of these are hypothetical proteins, while one has been annotated as a putative myosin IB heavy chain. The absence of ZFP2 from this list highlights that the prediction software is unable to detect all of the WW domains present within *T. brucei* and suggests that more proteins containing WW domains may be present.

We have identified possible WW binding motifs in the N-terminal region of MCA1, MCA2 and MCA3 while in MCA5 a similar motif is located within the C-terminal extension (Figure 3.2). The minimum number of proline residues flanked by an arginine or lysine residues required to fulfil a Class III binding site is two. MCA2 possesses three prolines flanked by an arginine residue, while MCA3 possesses four prolines flanked by a lysine residue. Interestingly, MCA1 possesses the bare minimum requirement of two prolines and is flanked by both a lysine and arginine residue, while MCA4 does not meet the requirement, with only one proline residue. At the relative N-terminal position of MCA5, there is also only one proline residue, however, located at the distal end of the C-terminal extension there are five prolines flanked by a lysine residue. We can speculate from this that MCA1, MCA2 and MCA3 may have functional WW binding domains, while MCA4 has lost the WW domain binding activity. MCA5 meanwhile, has a predicted functional WW binding site within its unique C-terminal extension and therefore appear to have either lost, or not acquired, a binding site at its N-terminal region. The presence of these WW binding motifs suggests the metacaspases interact with other WW domain containing proteins as part of their normal function. The identification of numerous proteins possessing WW domains in the *T. brucei* database allows for this possibility and future experiments may be able to identify these partners.

Interestingly, recent two-hybrid screens have revealed that the yeast metacaspase (Mca1p, YOR197p) interacts with several proteins and among them Wwm1p (YFL010p) (Uetz *et al.*, 2000; Ito *et al.*, 2001). Additionally, the toxic effect of overexpression of Wwm1p in yeast was suppressed by the simultaneous overexpression of the yeast metacaspase (Szallies *et al.*, 2002). Wwm1p was characterised as a potential hydrophilin, which have been implicated in osmotic stress responses (Garay-Arroyo *et al.*, 2004). Wwm1p possesses an N-terminal WW domain and intriguingly shares some level of sequence identity to the *Tb*MCA5 C-terminal extension. The relevance of these observations to the situation in trypanosomes is unclear. The observations do suggest, however, some level of commonality between the metacaspase functions from protozoa to yeast.

It has been reported that yeast metacaspase showed proteolytic activity towards the mammalian caspase substrates VEID-AMC and IETD-AMC. This activity was completely abrogated by the addition of z-VAD-FMK, a broad-range caspase inhibitor (Madeo *et al.*, 2002). Additionally, the mutation of the putative active site cysteine residue to alanine was shown to reduce this caspase-like activity (Madeo *et al.*, 2002). Also in yeast, where the ectopic expression of *Tb*MCA4 was reported to cause a loss of respiratory competence, the mutation of either of the putative active residues independently to alanine resulted in loss of this phenotype (Szallies *et al.*, 2002). These observations suggest that the metacaspases do possess peptidase activity and that the conserved histidine and cysteine residues function as the catalytic dyad. Examination of these putative active site residues within *Tb*MCA1 and *Tb*MCA4 initially suggested that they might not possess cysteine peptidase activity. Alignment of the *T. brucei* metacaspases with human caspase-3 and metacaspases from yeast and *Plasmodium falciparum* revealed that both *Tb*MCA1 and *Tb*MCA4 have a serine substitution at the putative active site cysteine residue (Mottram *et al.*, 2003). Additionally, *Tb*MCA1 also has a tyrosine substitution at the putative active site histidine position. However, positioned immediately adjacent to this serine substitution in both *Tb*MCA1 and *Tb*MCA4 is located another cysteine residue. This second cysteine residue is conserved in all trypanosome and *Leishmania* metacaspases; however a serine is located at this position in yeast and *Plasmodium falciparum*. This raises two possibilities for *Tb*MCA4 if it retains peptidase activity as reported (Szallies *et al.*, 2002); firstly, that either of the adjacent positions can function as the active site cysteine, or, secondly, that it is an example of a mixed type peptidase. There is a precedent for this, Serine repeat antigen 5 (SERA5) from *P. falciparum* possess a central domain with a high level of sequence identity to papain and appears to be a Clan CA, family C1 cysteine peptidase. However, the protein has a serine residue at the position of the active site cysteine and it has been reported that this enzyme domain retains catalytic activity (Hodder *et al.*, 2003).

While it is possible that *Tb*MCA4 is an active peptidase, it is highly unlikely that *Tb*MCA1, which also has the putative active site histidine replaced by a tyrosine residue, will be an active peptidase. The histidine residue is essential due to its

imidazolium group, required for stabilisation of the thiolate ion involved in the nucleophilic attack of the peptide bond. Tyrosine lacks this imidazole group and therefore it is predicted that *Tb*MCA1 cannot possess peptidase activity.

This raises the possibility that either *Tb*MCA1 and/or *Tb*MCA4 are examples of "dead" peptidases. Sequence identity between *Tb*MCA1, *Tb*MCA4 and the other *T. brucei* metacaspases remains high, especially around the active sites. This suggests that, although they may no longer possess peptidase activity, their function may still be reliant on substrate binding. A catalytically inactive structural homologue of caspase-8, termed I-FLICE, has been shown to inhibit both TNFR1 and CD95 induced apoptosis in mammalian cells (Hu *et al.*, 1997). The conserved catalytic cysteine residue is absent from I-FLICE and there is a lack of conservation at key residues involved in substrate binding, however I-FLICE was able to form complexes with caspase-8. It was reasoned that I-FLICE, a naturally occurring inactive caspase, acts as a dominant negative inhibitor of apoptosis. Whether the "dead" metacaspases MCA1 or MCA4 act in a similar was is unknown. No information is available concerning the expression profile of either gene, and there remains the possibility that they are simply pseudogenes.

Interestingly, a histidine to tyrosine substitution is not unique to *Tb*MCA1. *P. falciparum* contains two metacaspases genes, one encodes for a protein with the putative histidine and cysteine residues, while the other encodes for a protein with tyrosine and threonine at these respective positions. As was the case with *Tb*MCA1, it is extremely unlikely that this *P. falciparum* metacaspase will possess peptidase activity. However, the presence of a tyrosine residue in both *P. falciparum* and *T. brucei* "dead" metacaspases may signify that this residue has a specialised role. For two divergent protozoa to both select the same residue at this equivalent position, and to then maintain it is unlikely by chance. It is also suggestive that both the tyrosine residue at this position and these "dead" peptidase themselves have an important role to play in the parasites. More generally, from the data currently available in genome sequencing projects, we can predict the possibility of "dead" metacaspases in *T. brucei*, *Plasmodium*, and *Theileria annulata* but not in yeast, *Trypanosoma cruzi* or *Leishmania*.

3.6.2 Metacaspase localisation.

The apparent organellar localisation of the metacaspases was initially surprising, based on what is known about caspases. Caspases are located free within the cytoplasm and are not associated with any known organellar structures (Miossec *et al.*, 1996). This initial observation of the metacaspases highlighted a major difference in the location of these proteins relative to the caspases, and suggested that they do not fulfil homologous roles. The only other analysis of metacaspase localisation has been performed in yeast. In *Saccharomyces cerevisiae* a global analysis of protein localisation, using GFP as a label, localised the single yeast metacaspase to both the nucleus and cytoplasm (Huh *et al.*, 2003), while the ectopic expression of a *Tb*MCA4-GFP fusion in yeast also revealed apparent nuclear localisation (Szallies *et al.*, 2002). These observations are different from what we have observed and it would be interesting to compare the localisation of metacaspases from *T. brucei* with other protozoa and plants.

The findings that MCA2, MCA3 and MCA5 all occupy an organellar location raised the question of whether these three proteins are found in distinct compartments or are located together within the same compartment. As the MCA2/3 antibody detected several other proteins, this question was addressed using epitope-tagged versions of MCA2 and MCA3. These co-localisation studies revealed that MCA2, MCA3 and MCA5 are all located within the same structures in BSF parasites. The use of epitope-tagged versions of MCA2 and MCA3, however, raises the possibility of the incorrect targeting of these proteins. It is known that the addition of epitope tags can interfere with the cellular targeting machinery or affect protein-protein interactions, resulting in the incorrect localisation of tagged proteins. The co-localisation of MCA2HA and MCA3HA with MCA5 in BSF parasites provides good evidence that the HA tag does not alter the normal targeting of the metacaspases. It is extremely unlikely that the addition of an epitope tag would result in the targeting of MCA2HA and MCA3HA to the same compartment in which native MCA5 is localised.

One intriguing feature was turned up by our IFA comparison of the distribution of MCA5 in PCF and BSF parasites. Although Western blot analysis had revealed that MCA5 was expressed at equivalent levels in both PCF and BSF life stages

this was not directly mirrored when we performed IFA on the parasites. MCA5 labelling was shown to be much more extensive in the BSF as compared to the PCF. This suggests that the metacaspase positive compartment may be more active in the BSF.

An organellar system that is more active in BSF compared to PCF is the endosomal system. The main reason for this increased endosomal activity is primarily for the rapid recycling of the VSG surface coat. Recent studies showed that the parasites are able to endocytose an area equivalent to the whole plasma membrane within 12 minutes (Engstler *et al.*, 2004). Indeed, the BSF has one of the fastest rates of membrane turnover recorded. This contrasts with the PCF, where the rate of endocytosis is substantially lower (Liu *et al.*, 2000).

Therefore, with our hypothesis in mind regarding greater metacaspase requirement in the BSF and the location of the metacaspases within an organellar structure, we investigated various components of this system. However, initial attempts proved unsuccessful with regard to identification of the metacaspase compartment. Several compartments were ruled out; the data showing that the metacaspases were not associated with the early endosomal, the lysosomal (also termed late endosomes), or the Golgi compartments.

Another component of the endosomal system known to be highly active in the BSF is the recycling system (Engstler *et al.*, 2004). BSF parasites, which are exposed to the immune system within the mammalian host, use antigenic variation as the primary defence mechanism to evade attack. To ensure that host anti-VSG antibodies do not reach levels sufficient to clear the infection, the parasites periodically express distinct VSG isoforms during the course of infection (Pays *et al.*, 1994). However, host antibodies may be generated faster than the switching of VSG and it is believed that the rapid trafficking and recycling of VSG is also likely to be an important defence against the immune system (O'Beirne *et al.*, 1998). The processes of exo- and endocytosis are highly polarised in trypanosomatids, and are limited to the flagellar pocket from where endocytosis of VSG occurs constitutively in *T. brucei* (Russo *et al.*, 1993). VSG is a very stable molecule and therefore the majority of the internalised VSG is

recycled back to the surface (Seyfang *et al.*, 1990), while in contrast, the anti-VSG antibodies are extensively degraded. The addition of anti-VSG antibodies *in vitro* results in their rapid internalisation, degradation and recycling (O'Beirne *et al.*, 1998).

This recycling of VSG and anti-VSG antibodies has been shown to be mediated via two distinct compartments; internalisation occurring via Rab5 positive early endosomes and the recycling via Rab11 positive recycling endosomes (Pal *et al.*, 2003). Rab proteins, a subgroup of the Ras superfamily of small GTPases, localise to the external membrane of specific compartments and are involved in the regulation of vesicle trafficking (Nuoffer and Balch, 1994). They are believed to be essential for correct vesicular trafficking and different members localise to specific membrane structures (Novick and Brennwald, 1993). For example, Rab5 is found uniquely on early endosomal membranes (Bucci *et al.*, 1992), while Rab11 has been shown to associated with recycling endosomes (Ullrich *et al.*, 1996) in mammalian cells. *T. brucei* Rab11 has also been characterised and shown to be associated with recycling endosomes, trafficking both VSG and the transferrin receptor in the BSF (Jeffries *et al.*, 2001).

The lack of co-localisation of MCA5 with tomato lectin had previously excluded the possibility of metacaspase association with early endosomes. Using an antibody raised against *Tb*Rab11, however, it was demonstrated that MCA5, and by inference MCA2 and MCA3, co-localise with Rab11 in both life stages. Rab11 is the only known Rab protein shown to be under life stage regulation in *T. brucei,* the expression levels of Rab11 being notably higher in the BSF compared to the PCF (Jeffries *et al.*, 2001). This was also confirmed in our studies. This differential expression is thought to be due, partially at least, to the increased requirement of recycling processes in the BSF as previously discussed. Recycling in PCF parasites is not well characterised, this life stage expresses neither VSG nor the transferrin receptor, and no surface molecules that are actively recycled have been identified (Borst and Fairlamb, 1998). It has been suggested, therefore, that the *Tb*Rab11 compartment represents a developmentally regulated organelle dedicated principally to BSF recycling processes, and contributes to the survival of *T. brucei* within the mammalian host (Jeffries *et al.*, 2001).

Our own analysis of Rab11 labelling by IFA confirms the study of Jeffries *et al.* (2001) that BSF parasites have a much more extensive recycling compartment than PCF parasites. This reflects the higher expression levels of *Tb*Rab11 observed in BSF parasites and the much more active recycling processes which occur in this life stage. It is probable therefore that the metacaspases are involved somehow in the recycling of proteins in *T. brucei*, and it is logical to suggest that a greater complement of metacaspases may either be required or be more advantageous to the parasites. While Rab11 expression is upregulated to meet the increased recycling demands in BSF parasites, the strategy taken with relation to the metacaspases associated with these endosomes might not be to increase expression, but to increase the number of genes expressed.

One question that clearly arises from the identification of MCA2, MCA3 and MCA5 within the Rab11 positive compartment in the BSF is how they are targeted to that location. As previously discussed, MCA2 and MCA3, only diverge significantly at their N-terminal region. It was initially believed that the small extension present on MCA3 might have been involved in differential targeting between MCA2 and MCA3. This does not appear to be the case, however, as both of proteins are associated with the same compartment. The N-terminal region of MCA5, which itself is predicted to be a possible signal peptide, has no sequence identity to the N-terminal regions of either MCA2 or MCA3. These three proteins are targeted to the same compartment, therefore, without the presence of a conserved N-terminal targeting sequence. There are various models suggested to explain how proteins are concentrated and targeted to differential organelles of the endocytic and secretory systems in eukaryotic cells (van Vliet *et al.*, 2003). It is known that the targeting of proteins to specific locations occurs primarily at the trans-Golgi network (TGN) where cytosol-oriented sorting signals direct cargo to the appropriate export site (Traub and Kornfeld, 1997). Targeting signals that act as address codes, directing proteins to various intracellular compartments including endosomes and lysosomes, have been identified. They use a tyrosine-based sorting signal that conforms to a YXXØ motif (where Ø is an amino acid with a bulky hydrophobic side chain) (Marks *et al.*, 2004). While such mechanisms have yet to be identified in protozoa, it is likely that there is a

conserved motif within MCA2, MCA3 and MCA5 that is responsible for their targeting to the same compartment.

Immuno-electron microscopy data would be useful to support the localisation studies performed. Immunofluorescence analysis shows that the metacaspases are associated with an organellar structure; however, this technique is unable to ascertain where exactly within these structures the metacaspases are located. We predict that these proteins are located within the lumen of these structures as they have no transmembrane domains or membrane attachment motifs. Indeed, preliminary data suggest that MCA5 is located within the lumen of these Rab11 positive vesicles (Tetley, unpublished).

In addition, the partial co-localisation of MCA5 with internalised anti-VSG221 antibodies confirmed that the metacaspase-positive compartment does indeed traffic molecules that are known to be recycled. These findings raise the possibility that the metacaspases may be involved in the cleavage and/or degradation of proteins contained within these recycling endosomes. Anti-VSG antibodies have been shown to be extensively degraded prior to secretion (Pal *et al.*, 2003), and the addition of a cocktail of peptidase inhibitors resulted in a build up of internalised anti-VSG antibodies (Russo *et al.*, 1993). The enzymes responsible for this degradation have not been identified and no peptidases have been shown to reside within either the early or recycling endosomes in *T. brucei*. Therefore, the peptidases responsible for the degradation of anti-VSG antibodies may well be present within either the early or recycling endosomes. Interestingly, the slowing of recycling processes in *T. brucei* by the expression of mutant versions of Rab5 and Rab11 proteins were reported to increase the degradation of recycled material (Pal *et al.*, 2003), presumably due to an increased transit time through the endosomal system and greater exposure to proteolytic enzymes.

Caspases are highly specific in respect to their substrate specificity (Stennicke and Salvesen, 1998), and a similar feature has recently been demonstrated in the plant metacaspases (Vercammen *et al.*, 2004). One of the features of the Clan CD family of cysteine peptidase that have been classified so far is that they will only accept one specific residue at the P1 position. For example, caspases will only

cleave following an aspartate residue, while legumains require an asparagine residue at the P1 position. There is one known exception to this rule, GPI8 is able to accept a range of residues in the P1 position (Eisenhaber *et al.*, 2001). If the metacaspases do indeed follow this general rule, as recent evidence suggests, they would be expected to have specific substrate specificity and not make for an effective general degradative enzyme.

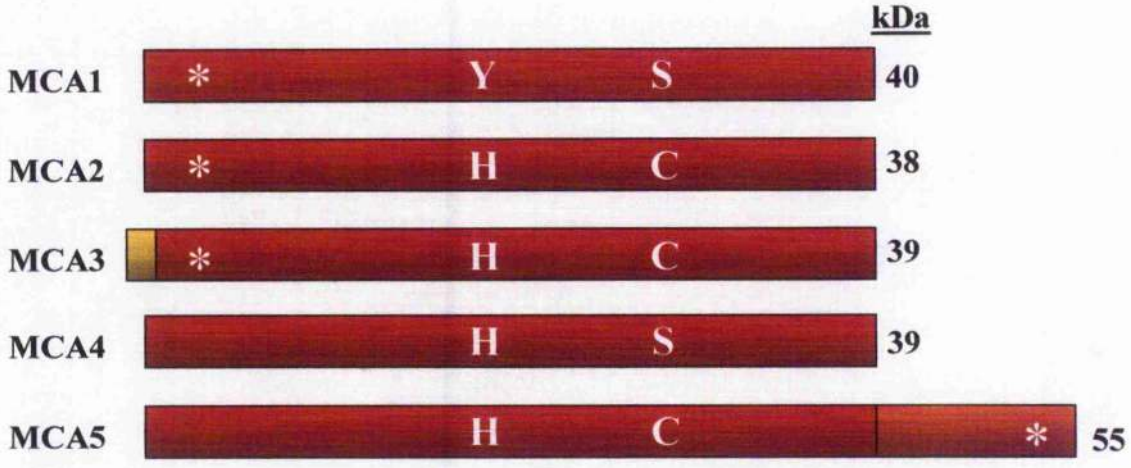

Figure 3.1: Domain structure and predicted molecular masses of the *Trypanosoma brucei* MCA family.
The putative active site histidine (H) and cysteine (C) residues are indicated. These are substituted by tyrosine (Y) or serine (S) in MCA1 and MCA4. Predicted Class III WW binding domain motifs are indicated (*) together with C-terminal extension of MCA5 (orange) and N–terminal extension of MCA2 relative to MCA3 (yellow).

Figure 3.2: Amino acid sequence alignment of *T. brucei* metacaspases.
MCA1, MCA2, MCA3, MCA4 and MCA5 were aligned using Align X (InforMax Inc.). Putative active site residues are highlighted by a blue box, a red box highlights regions identified as possessing predicted Class III WW binding domain motifs, and the black box highlights a predicted signal peptide. Non-similar residues are black, conservative or similar residues are blue, and identical residues are red with grey background.


MCA2 (1) ----------MCSLITQLCDAGQLADYVGLGWLNAVSSQPYLVQALGLQPPPRRVDVDAAFRDAKGLHGHQPWVAT-PLPGQTVRALFI
MCA3 (1) -MAVDPRCLLSLCSTISKASSAKGTNDFVKIGMELWQTAQPYLVQALGLQPPPPKVDVDAAVANAGDAHGEQPWVAT-PLPGQTVRALFI
MCA1 (1) MSSEKVAGYVQCVVGIIFGVVTGGASIYVTIAMELLQVAVPYVLVTLGLQRRPXKGGVDKAMAEAESVX-AEVMKKP-SKQQRSFRALFI
MCA4 (1) -----MGGCVSTALKVGAETVAEGHIDLISFAINYFKNAVPYIVKYLGRQQRPKEVDMEATLTEAKESKGFQPWKIS-CQPKGAVRGLFI
MCA5 (1) ----------MDAALALLFGQVATAVLPYVVNSIGRVPRPKRVDVKKAMGEAHQCRPVVPYRAPRPYTEGRVKALFI
MCA2 (79) GINYYGTSAALSGCCNDVKQMLATLQKKGLPINEAVILVDEDNFPGRTDQPTRDNIVRYMAWLVKDAKPGDVLFFHYSGHGTQCKSRGDS
MCA3 (89) GINYYGTSAALSGCCNDVKQMLATLQKKGLPINEAVILVDEDNFPGRTDQPTRDNIVRYMAWLVKDAKPGDVLFFHYSGHGTQCKSRGDS
MCA1 (89) GIDYKGTPAELRGCQADAVMMAGTMEKIGIPITERCVXMDTDDPRFNAIKPTRANILQHMAWLVKDAKPGDALFLHYSGYGAQVRAEEDK
MCA4 (85) GVNYGNTEAQLSGCCNDIMMMIGALQKRNFPLTEVVILADKEDVPGRTGEPTRANILRYLAWLAQDAQPNDVLFFHYSGHGTRANARDDD
MCA5 (68) GINYTGSSAQLGGCVNDVMHMLQTLQRIEFPISECCILVDDRRFPNFTAMPTRENIIKYMAWLVYDVRPGDVLFFHFSGHGAETKGGRDS
MCA2 (169) DEKYDQCIAPVDFQKSGCIVDDDIHKLLFSRLPEKVRLTAVFDCCHSGSIMDLPFTYVCSGGEQASGTPHMKRIREGNDVLGDVMMISGC
MCA3 (179) DEKYDQCIAPVDFQKSGCIVDDDIHKLLFSRLPEKVRLTAVFDCCHSGSIMDLPFTYVCSGGEQASGTPHMKRIREGNDVLGDVMMISGC
MCA1 (179) EEEFDQCIVPCDYEENGCILDNELHEIIS-TLPRGVRLTAVFDCSHAGTLLDLPFSLICSSN-DCSAVGEMKRIRTGGDVNAHVLMFSAC
MCA4 (175) CEEYDQCIVPMDYVENGCIVDNEIHEILVSQLPKGVRLTAVFDCSHSGSMLDLPYAYVCDSSKDGSGSCGMKRVREDNDVQADVLMISAC
MCA5 (158) NEKMDQCLVPLDYDKAGAILDDDLFELMIKGLPAGVRMTAVFDCCHSASLLDLPFAFVAGRNVSSNQRHEMRMVRKDNYSRGDVVMFSGC
MCA2 (259) ADEQTSADVKNTATFGTGSTGAGGAATQCITCMLMNNQSLSYGKLLIETRDMLKRKGFKQVPQLSASKAIDLDQTFSLTEMFSVDRSIQ-
MCA3 (269) ADEQTSADVKNTATFGTGSTGAGGAATQCITCMLMNNQSLSYGKLLIETRDMLKRKRFKQVPQLSASKAIDLDQTFSLTEMFSVDRSIQ-
MCA1 (267) GDDEAAADLPNAGDFVEGASGSGGAATQCFISMLLNKTPGTIYSLLSTTRDKLREKGFKQSPXMSASRCLSLXEKFTLTELFSVAEPCPN
MCA4 (265) ADDEAALGVDNTQDFYESGKDSGGAATFCLTAMMMREEPLTFLDLLVHTREMLKSRGFTQVPHLSASKPINLMQRFSLEGLFPQERTLL-
MCA5 (248) EDSGTSADVTNTSSFGNGTVAAGGAATQAFTWALLNTTGYSYIDIFMKTREVLRQKGYKQVPQLSSSKPVDLYKQFSLFGPLTMNASLVQ
MCA2 (348) ----------
MCA3 (358) ----------
MCA1 (357) ILTGEPRWKTTPLGGK----------
MCA4 (354) ----------
MCA5 (338) HLPQEYVQPWAPHPAYQQPHEATLPASVSQPHSQPVMGIPVASTSNGKSNPGVSDGGRASGEVYPPTQYPSSHPAPQQQAYYQPPQQAYY
MCA2 (348) ----------
MCA3 (358) ----------
MCA1 (373) ----------
MCA4 (354) ----------
MCA5 (428) QPPQQAYYQPPQQAYYQPPQQAYYQPPQQAYYQPEPHHQPAPPPPPKKENKPARPGYPMSYCMKFSQGKPGRK

Figure 3.3: Amino acid sequence alignment of *T. brucei* MCA5 C-terminal extension with two predicted proteins.
The MCA5 C-terminal extension was used in a Blast Search against the *T. brucei* predicted protein database at GeneDB. Two proteins were identified that share sequence identity with this region and were aligned with the C-terminal extension of MCA5 using Align X (InforMax Inc.) Non-similar residues are black, conservative or similar are residues are blue, and identical residues are red with grey background.

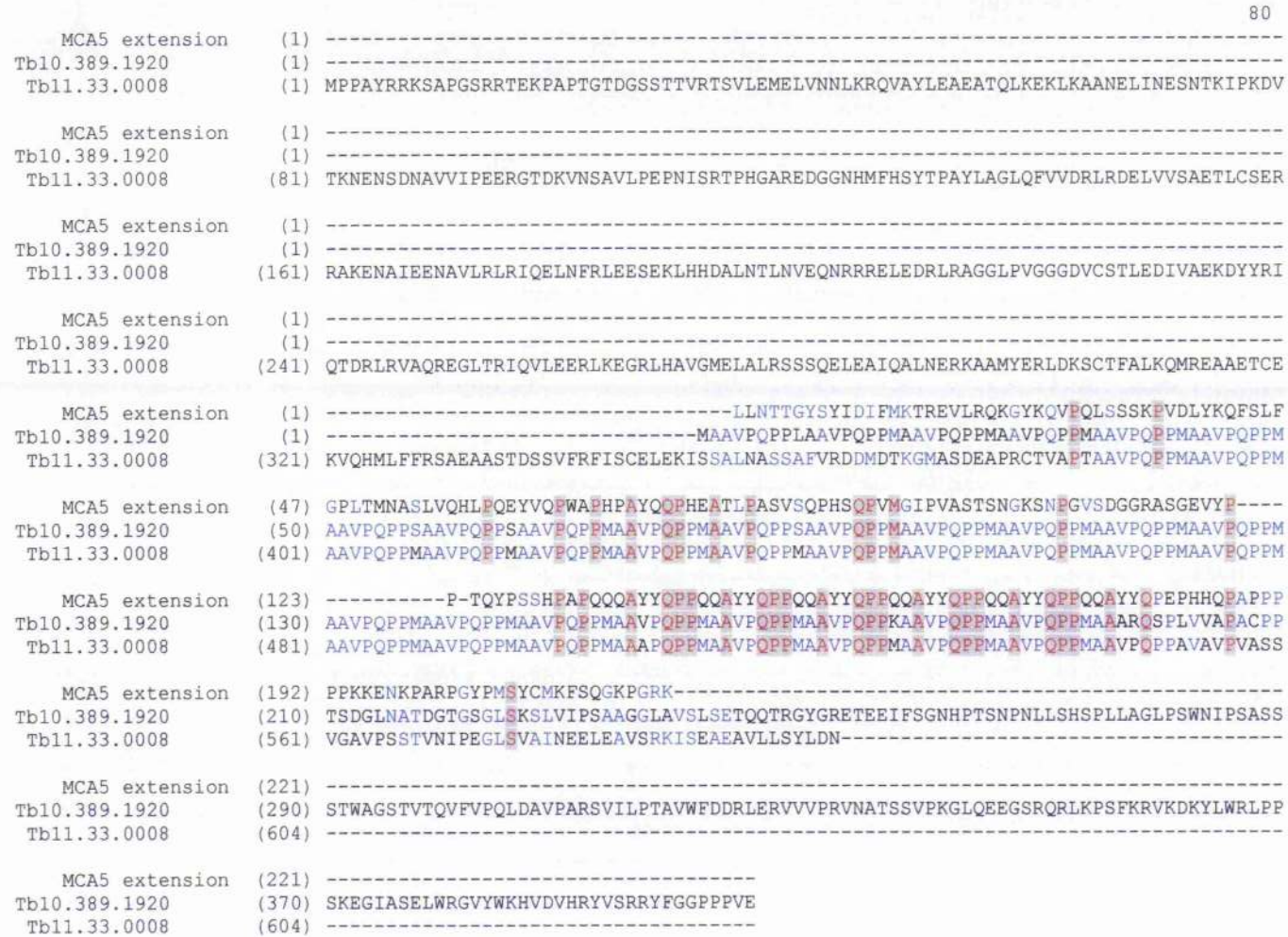
80
MCA5 extension (1) ----------
Tb10.389.1920 (1) ----------
Tb11.33.0008 (1) MPPAYRRKSAPGSRRTEKPAPTGTDGSSTTVRTSVLEMELVNNLKRQVAYLEAEATQLKEKLKAANELINESNTKIPKDV
MCA5 extension (1) ----------
Tb10.389.1920 (1) ----------
Tb11.33.0008 (81) TKNENSDNAVVIPEERGTDKVNSAVLPEPNISRTPHGAREDGGNHMFHSYTPAYLAGLQFVVDRLRDELVVSAETLCSER
MCA5 extension (1) ----------
Tb10.389.1920 (1) ----------
Tb11.33.0008 (161) RAKENAIEENAVLRLRIQELNFRLEESEKLHHDALNTLNVEQNRRRELEDRLRAGGLPVGGGDVCSTLEDIVAEKDYYRI
MCA5 extension (1) ----------
Tb10.389.1920 (1) ----------
Tb11.33.0008 (241) QTDRLRVAQREGLTRIQVLEERLKEGRLHAVGMELALRSSSQELEAIQALNERKAAMYERLDKSCTFALKQMREAAETCE
MCA5 extension (1) ----------LLNTTGYSYIDIFMKTREVLRQKGYKQVPQLSSSKPVDLYKQFSLF
Tb10.389.1920 (1) ----------MAAVPQPPLAAVPQPPMAAVPQPPMAAVPQPPMAAVPQPPMAAVPQPPM
Tb11.33.0008 (321) KVQHMLFFRSAEAASTDSSVFRFISCELEKISSALNASSAFVRDDMDTKGMASDEAPRCTVAPTAAVPQPPMAAVPQPPM
MCA5 extension (47) GPLTMNASLVQHLPQEYVQPWAPHPAYQQPHEATLPASVSQPHSQPVMGIPVASTSNGKSNPGVSDGGRASGEVYP----
Tb10.389.1920 (50) AAVPQPPSAAVPQPPSAAVPQPPMAAVPQPPMAAVPQPPSAAVPQPPMAAVPQPPMAAVPQPPMAAVPQPPMAAVPQPPM
Tb11.33.0008 (401) AAVPQPPMAAVPQPPMAAVPQPPMAAVPQPPMAAVPQPPMAAVPQPPMAAVPQPPMAAVPQPPMAAVPQPPMAAVPQPPM
MCA5 extension (123) ----------P-TQYPSSHPAPQQQAYYQPPQQAYYQPPQQAYYQPPQQAYYQPPQQAYYQPPQQAYYQPEPHHQPAPPP
Tb10.389.1920 (130) AAVPQPPMAAVPQPPMAAVPQPPMAAVPQPPMAAVPQPPMAAVPQPPKAAVPQPPMAAVPQPPMAAARQSPLVVAPACPP
Tb11.33.0008 (481) AAVPQPPMAAVPQPPMAAVPQPPMAAAPQPPMAAVPQPPMAAVPQPPMAAVPQPPMAAVPQPPAVAVPVASS
MCA5 extension (192) PPKKENKPARPGYPMSYCMKFSQGKPGRK----------
Tb10.389.1920 (210) TSDGLNATDGTGSGLSKSLVIPSAAGGLAVSLSETQQTRGYGRETEEIFSGNHPTSNPNLLSHSPLLAGLPSWNIPSASS
Tb11.33.0008 (561) VGAVPSSTVNIPEGLSVAINEELEAVSRKISEAEAVLLSYLDN----------
MCA5 extension (221) ----------
Tb10.389.1920 (290) STWAGSTVTQVFVPQLDAVPARSVILPTAVWFDDRLERVVVPRVNATSSVPKGLQEEGSRQRLKPSFKRVKDKYLWRLPP
Tb11.33.0008 (604) ----------
MCA5 extension (221) ----------
Tb10.389.1920 (370) SKEGIASELWRGVYWKHVDVHRYVSRRYFGGPPPVE
Tb11.33.0008 (604) ----------

Figure 3.4: Comparison of the metacaspases identified in parasitic protozoa and yeast.

Alignment of metacaspase sequences spanning the putative active site residues (indicated by arrows) were generated using Align X (InforMax Inc.). Non-similar residues are black, conservative or similar residues are blue and identical residues are red with grey background. *T. brucei*, *T. cruzi*, *Leishmania major*, *Plasmodium falciparum*, *P. berghei*, *Theileria annulata*, *Saccharomyces cerevisiae* and *Schizosaccharomyces pombe* sequences are shown.

A)

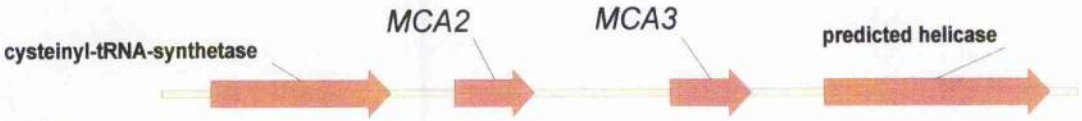

B)

```
MCA3     (1) MAVDPRCLLSLCSTISKASSAKGTNDFVKIGMELWQTAQPYLVQALGLQP
MCA2     (1) ----------MCSLITQLCDAGQLADYVGLGWLNAVSSQPYLVQALGLQP

MCA3    (51) PPPKVDVDAAVANAGDAHGEQPWVATPLPGQTVRALFIGINYYGTSAALS
MCA2    (41) PPRRVDVDAAFRDAKGLHGHQPWVATPLPGQTVRALFIGINYYGTSAALS

MCA3   (101) GCCNDVKQMLATLQKKGLPINEAVILVDEDNFPGRTDQPTRDNIVRYMAW
MCA2    (91) GCCNDVKQMLATLQKRGLPINEAVILVDEDNFPGRTDQPTRDNIVRYMAW

MCA3   (151) LVKDAKPGDVLFFHYSGHGTQCKSRGDSDEKYDQCIAPVDFQKSGCIVDD
MCA2   (141) LVKDAKPGDVLFFHYSGHGTQCKSRGDSDEKYDQCIAPVDFQKSGCIVDD

MCA3   (201) DIHKLLFSRLPEKVRLTAVFDCCHSGSIMDLPFTYVCSGGEQASGTPHMK
MCA2   (191) DIHKLLFSRLPEKVRLTAVFDCCHSGSIMDLPFTYVCSGGEQASGTPHMK

MCA3   (251) RIREGNDVLGDVMMISGCADEQTSADVKNTATFGTGSTGAGGAATQCITC
MCA2   (241) RIREGNDVLGDVMMISGCADEQTSADVKNTATFGTGSTGAGGAATQCITC

MCA3   (301) MLMNNQSLSYGKLLIETRDMLKRKRFKQAPQLSASKAIDLDQTFSLTEMF
MCA2   (291) MLMNNQSLSYGKLLIETRDMLKRKRFKQVPQLSASKAIDLDQTFSLTEMF

MCA3   (351) SVDRSIQ
MCA2   (341) SVDRSIQ
```

Figure 3.5: Genomic locus of *T. brucei MCA2* and *MCA3* and amino acid sequence comparison of MCA2 and MCA3.
A) *MCA2* and *MCA3* are located in tandem on chromosome 6 with approximately 1.8 kb separating the two genes. **B)** Alignment of MCA2 and MCA3 was performed using Align X (InforMax Inc.). Identical residues are red while non-similar residues are black. Putative active site residues are blue. The green line illustrates the region of MCA2 chosen for generation of a peptide for antibody production. The black line indicates a possible glycosylation site on each protein.

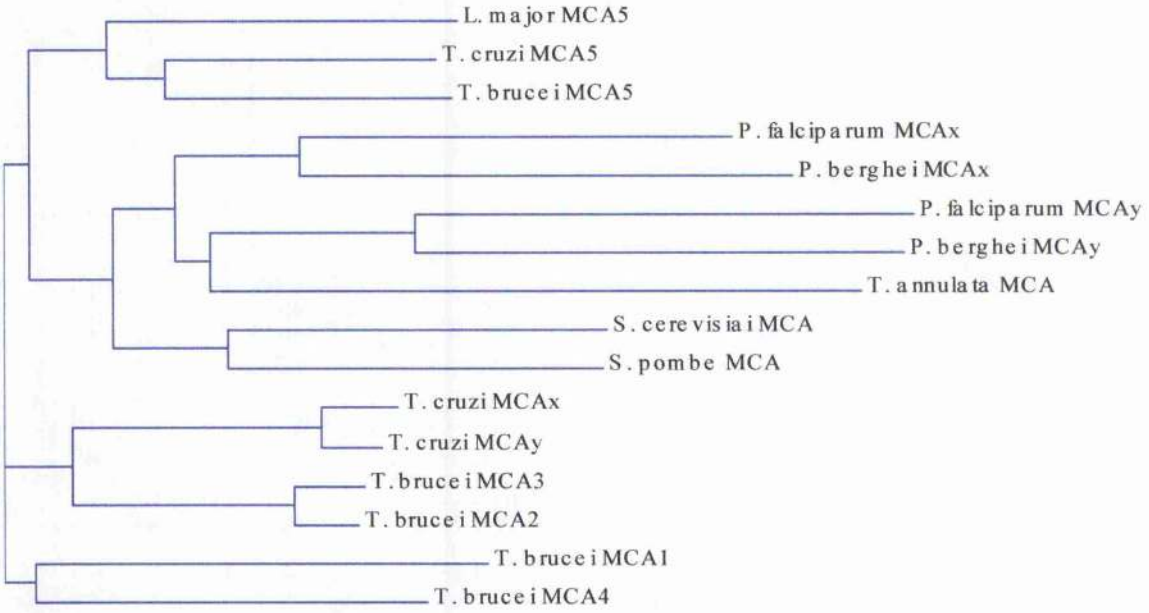

Figure 3.6: Phylogenetic tree of metacaspases identified in parasitic protozoa and yeast.
The central domains of *T. brucei*, *T. cruzi*, *L. major*, *Plasmodium falciparum*, *P. berghei*, *Theileria annulata*, *Saccharomyces cerevisiae* and *Schizosaccharomyces pombe* metacaspases were used to generate a phylogenetic tree using Align X (InforMax Inc.).

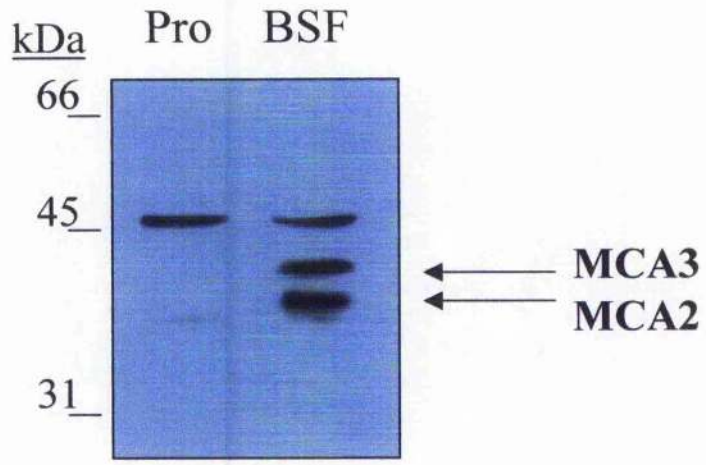

Figure 3.7: Analysis of *MCA2* and *MCA3* expression in *T. brucei*.
Total cell lysates were prepared from *T. brucei* PCF (strain EATRO 795) and BSF (strain 427). $5x10^6$ cell equivalents were then subjected to SDS-PAGE and transferred to PVDF membrane prior to immunoblotting with immunopurifed polyclonal rabbit anti-MCA2/3 antibodies. MCA2 and MCA3 are indicated, they were detected at around their predicted sizes of 38 and 39 kDa, respectively.

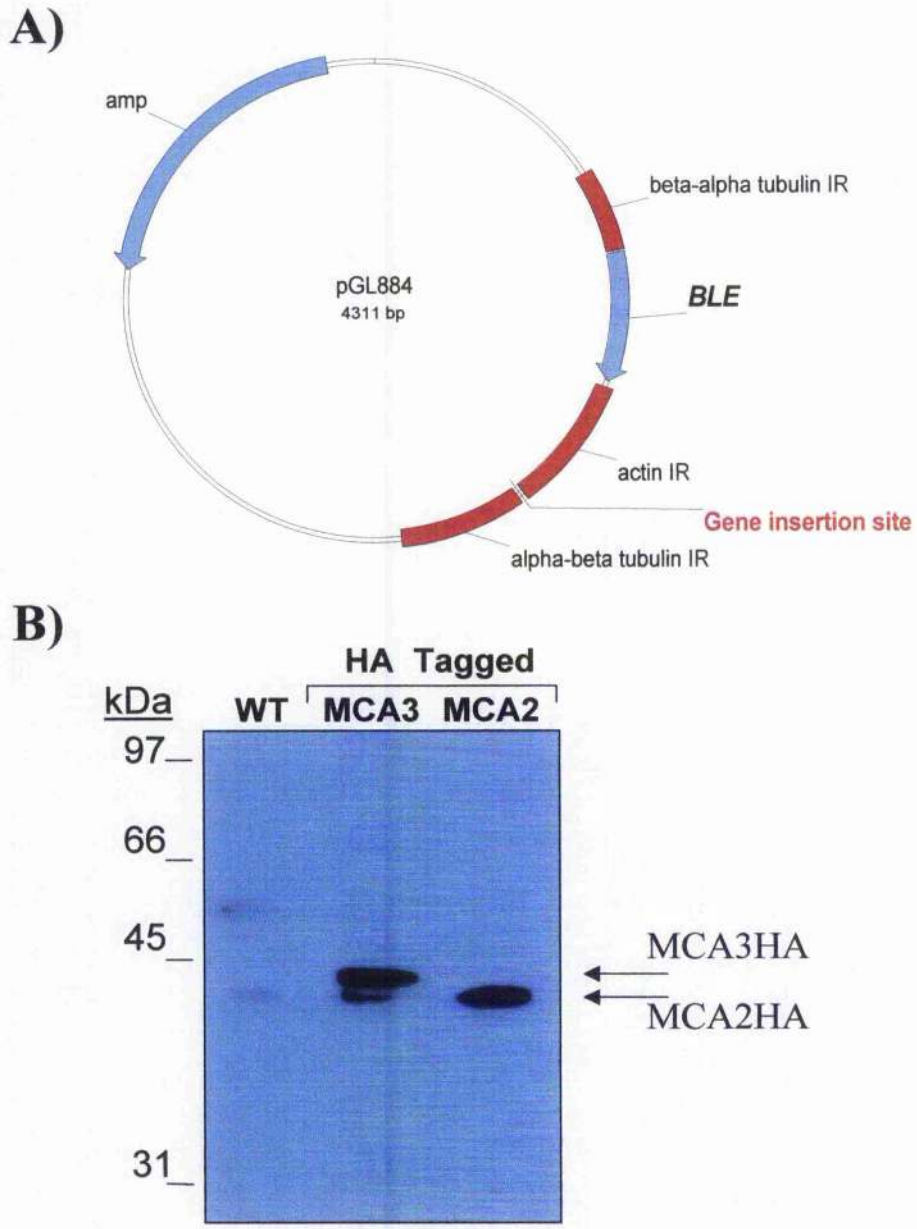

Figure 3.8: Vector used to express *MCA2* and *MCA3* HA-tagged genes and analysis of MCA2HA and MCA3HA expression in BSF *T. brucei*.
A) *MCA2* and *MCA3* with the addition a C-terminal HA tag were cloned individually into pGL884. This vector is designed for integration within the βα-tubulin array, driving expression of inserted metacaspase gene and *BLE* from this locus. **B)** Total cell lysates were prepared from BSF wild type (strain 427) and transgenic BSF (strain 427) parasites expressing an ectopic copy of either *MCA2HA* or *MCA3HA* from the tubulin locus. $5x10^6$ cell equivalents were then subjected to SDS-PAGE and transferred to PVDF membrane prior to immunoblotting with a mouse monoclonal anti-HA antibody. MCA2HA and MCA3HA protein species are indicated at around their predicted sizes of 40 and 41 kDa, respectively.

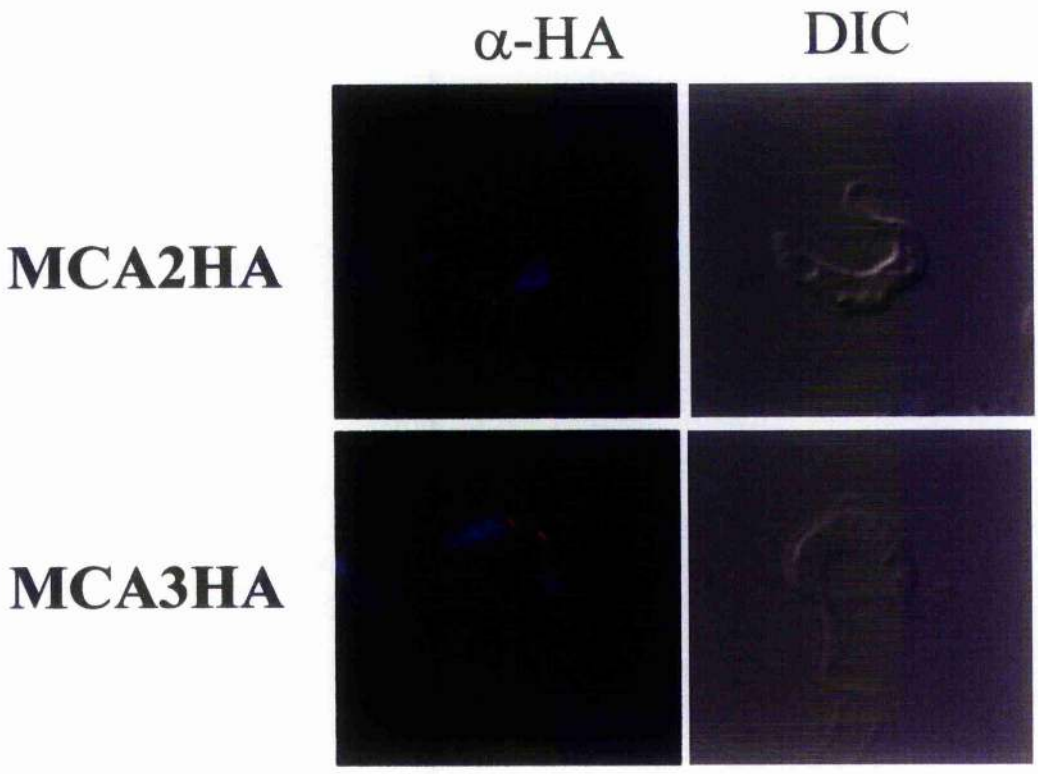

Figure 3.9: Immunofluorescence detection of MCA2HA and MCA3HA in BSF *T. brucei*.

BSF parasites were fixed in -20°C methanol for 15 mins and permeabilised in -20°C acetone for 2 mins, prior to blocking with 5% (w/v) skimmed milk for 30 mins. Slides were then incubated with a 1/200 dilution of monoclonal mouse anti-HA antibody, followed by anti-mouse TRITC conjugate and 1 μg/ml DAPI. A merged image of anti-HA and DAPI labelling is shown together with a DIC image of parasites.

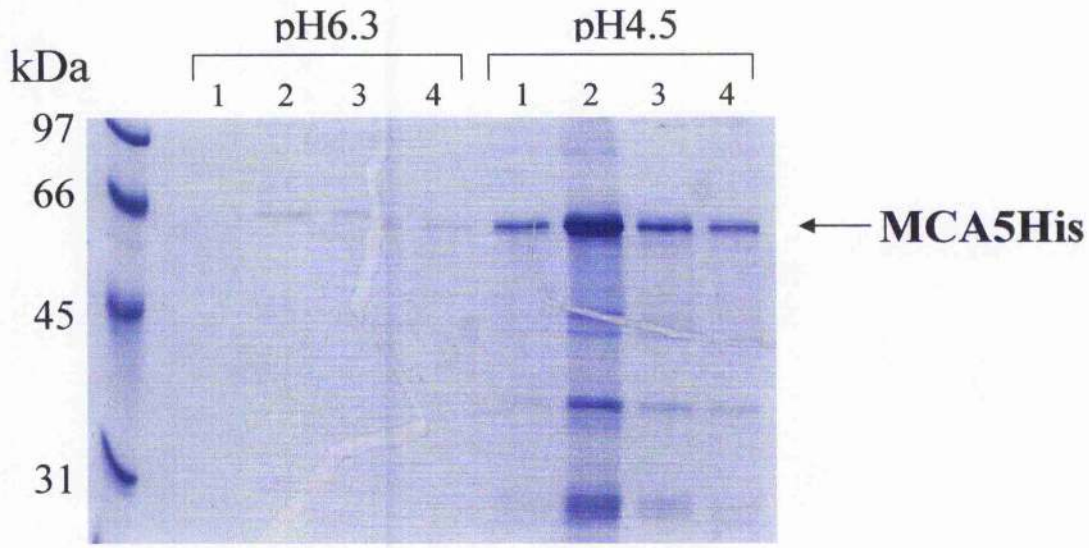

Figure 3.10: Coomassie blue stain of purified MCA5-His.
Total cell lysates of BL21 *E. coli* expressing full-length *T. brucei* MCA5-His were lysed and the pellet, containing MCA5-His, solubilised in 8 M Urea. This material was then bound to a nickel-agarose column and elution fractions 1 - 4 at pH 6.3 and pH 4.5 collected.

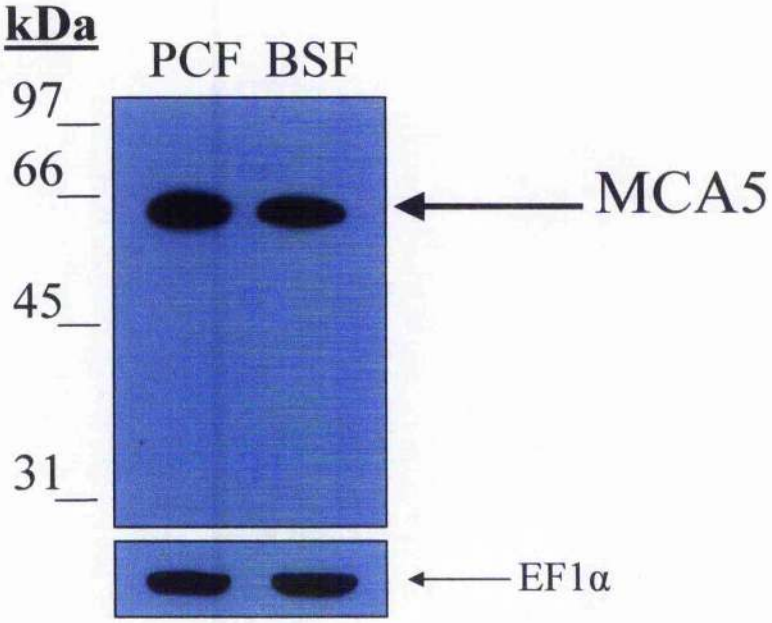

Figure 3.11: Analysis of *MCA5* expression in *T. brucei*.
Total cell lysates were prepared from *T. brucei* PCF (strain EATRO795) and BSF (strain 427) forms. $5x10^6$ cell equivalents were then subjected to SDS-PAGE and transferred to PVDF membrane prior to immunoblotting with sheep polyclonal anti-MCA5 antiserum. MCA5 is indicated at around the 55 kDa predicted size. Equal loading is demonstrated by an antibody against EF1α..

Figure 3.12: Immunofluorescence detection of MCA5 in BSF and PCF *T. brucei*.

T. brucei BSF and PCF parasites were fixed in -20°C methanol for 15 mins and permeabilised in -20°C acetone for 2 mins, prior to blocking with 5% (w/v) skimmed milk for 30 mins. Slides were then incubated with a 1/1000 dilution of sheep polyclonal anti-MCA5 antiserum, followed by anti-sheep FITC conjugate and 1 μg/ml DAPI. A merged image of anti-MCA5 and DAPI labelling is shown, together with DIC image of parasites.

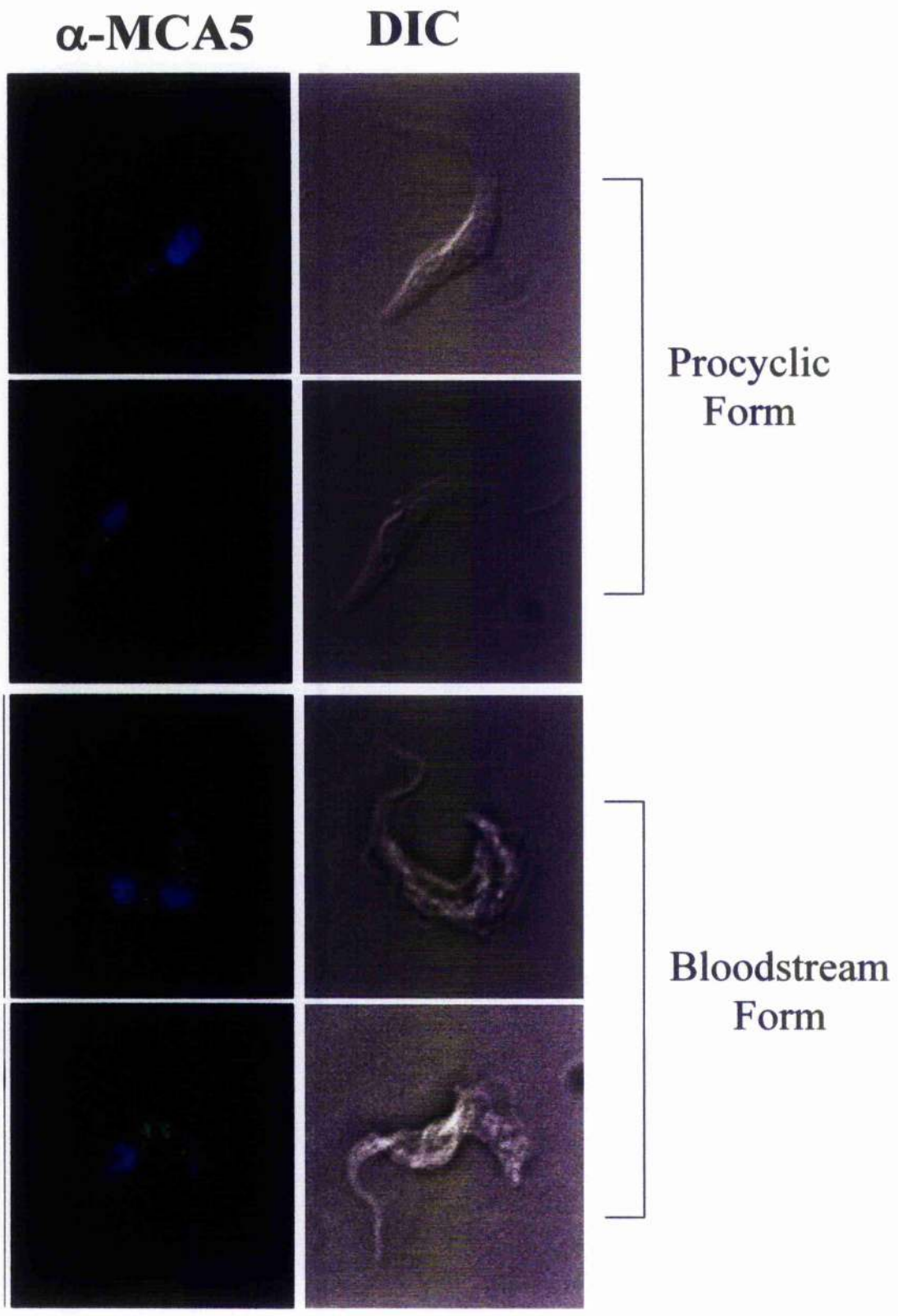
α-MCA5
DIC
Procyclic Form
Bloodstream Form

Figure 3.13: Immunofluorescence detection of co-localisation between MCA2HA and MCA3HA with MCA5 in BSF *T. brucei*.
T. brucei BSF parasites expressing either MCA2HA or MCA3HA proteins were fixed in -20°C methanol and permeabilised in -20°C acetone prior to blocking with 5% (w/v) skimmed milk. Slides were then incubated with the following; 1/200 dilution of mouse monoclonal anti-HA, 1/1000 dilution of sheep polyclonal anti-MCA5 antiserum, followed by anti-mouse TRITC and anti-sheep FITC conjugates together with 1 μg/ml DAPI. Labelling of anti-HA and anti-MCA5 is shown, together with a merged image of both signals, DAPI is included in all images. A DIC image of the parasites is also shown.

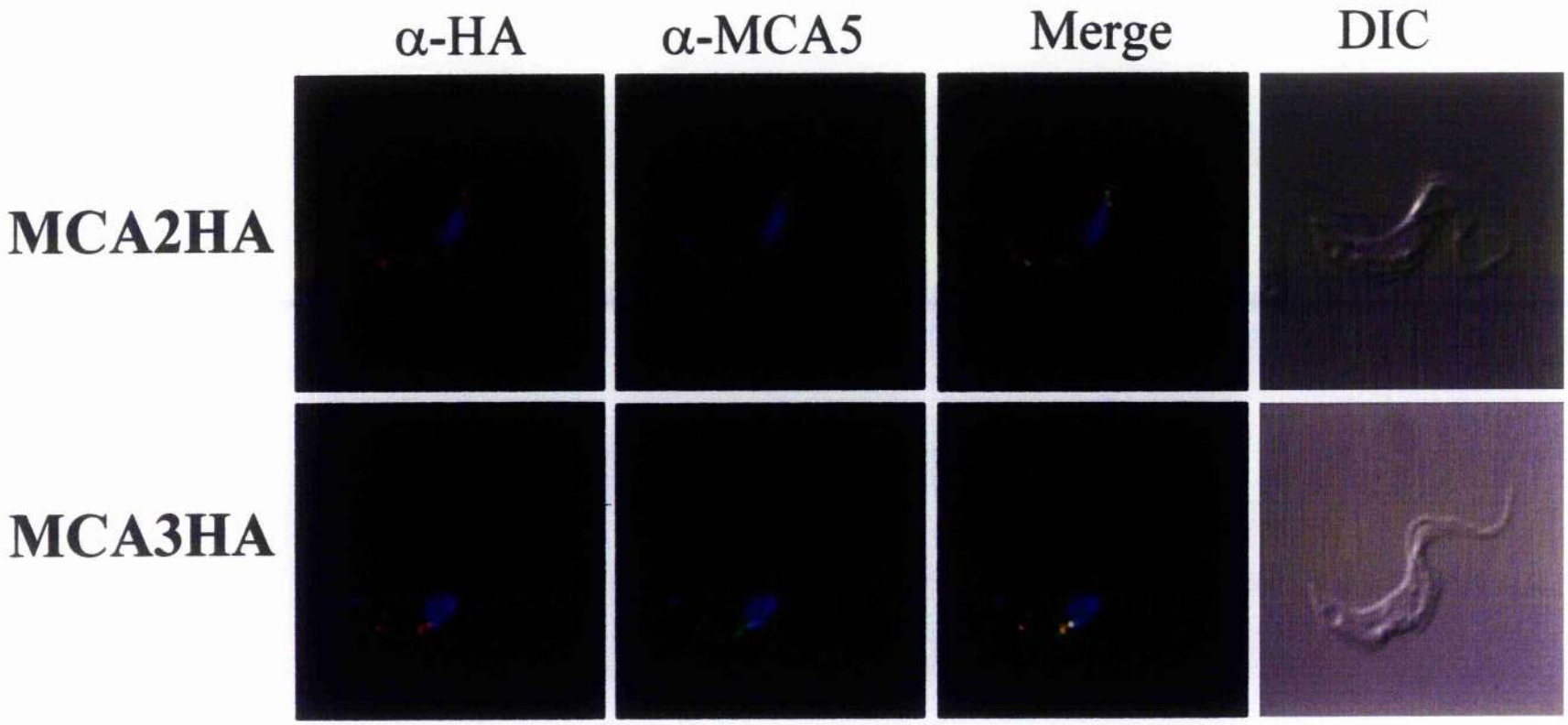
α-HA
α-MCA5
Merge
DIC
MCA2HA
MCA3HA

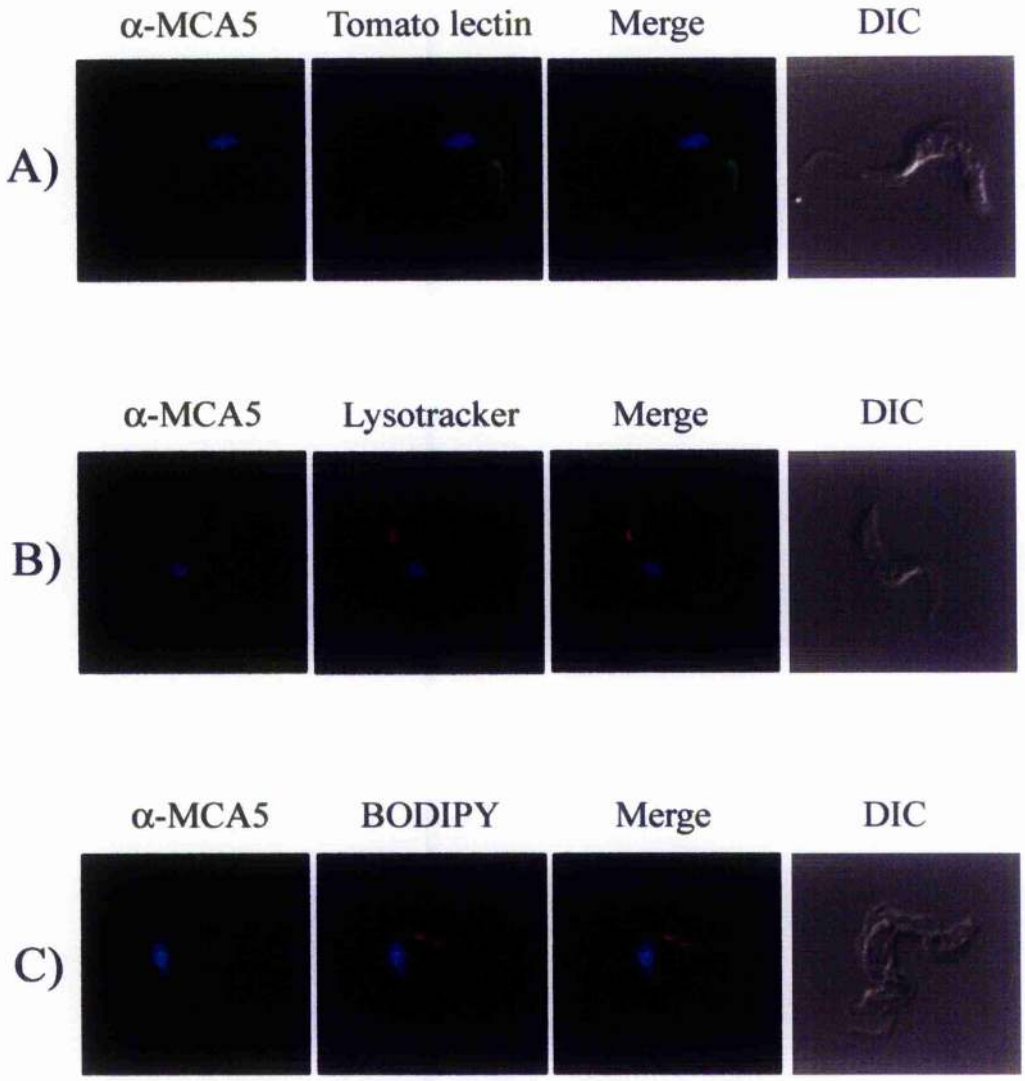

Figure 3.14: Immunofluorescence analyses attempting to localise *T. brucei* MCA5 with characterised organellar markers.
BSF parasites were incubated with several probes to specifically label organellar compartments. A) Early endosomes were labelled with a tomato lectin FITC conjugate (green), B) lysosomes were stained using Lysotracker (red), C) the Golgi apparatus was stained using BODIPY Ceramide (Red). Parasites were then fixed in -20°C methanol and permeabilised in -20°C acetone, prior to blocking with 5% skimmed milk. Slides were then incubated with sheep anti-MCA5 antiserum and anti-sheep FITC or TRITC conjugates together with 1 μg/ml DAPI. Individual images of MCA5 and probe labelling are shown for the separate experiments, together with a merged image. DAPI labelling is also included together with a DIC image of parasites.

Figure 3.15: Metacaspases are associated with Rab11 positive recycling endosomes in *T. brucei*.
PCF and BSF wild type parasites were fixed in -20°C methanol and permeabilised in -20°C acetone, prior to blocking with 5% (w/v) skimmed milk. Slides were then incubated with the following; 1/200 dilution of immunopurified rabbit polyclonal anti-*Tb*Rab11, 1/1000 dilution of sheep polyclonal anti-MCA5 antiserum, followed by anti-rabbit TRITC and anti-sheep FITC conjugates together with 1 µg/ml DAPI. Labelling of anti-*Tb*Rab11 and anti-*Tb*MCA5 is shown, together with a merged image of both signals, DAPI is included in all images. A DIC image of parasites is also shown.

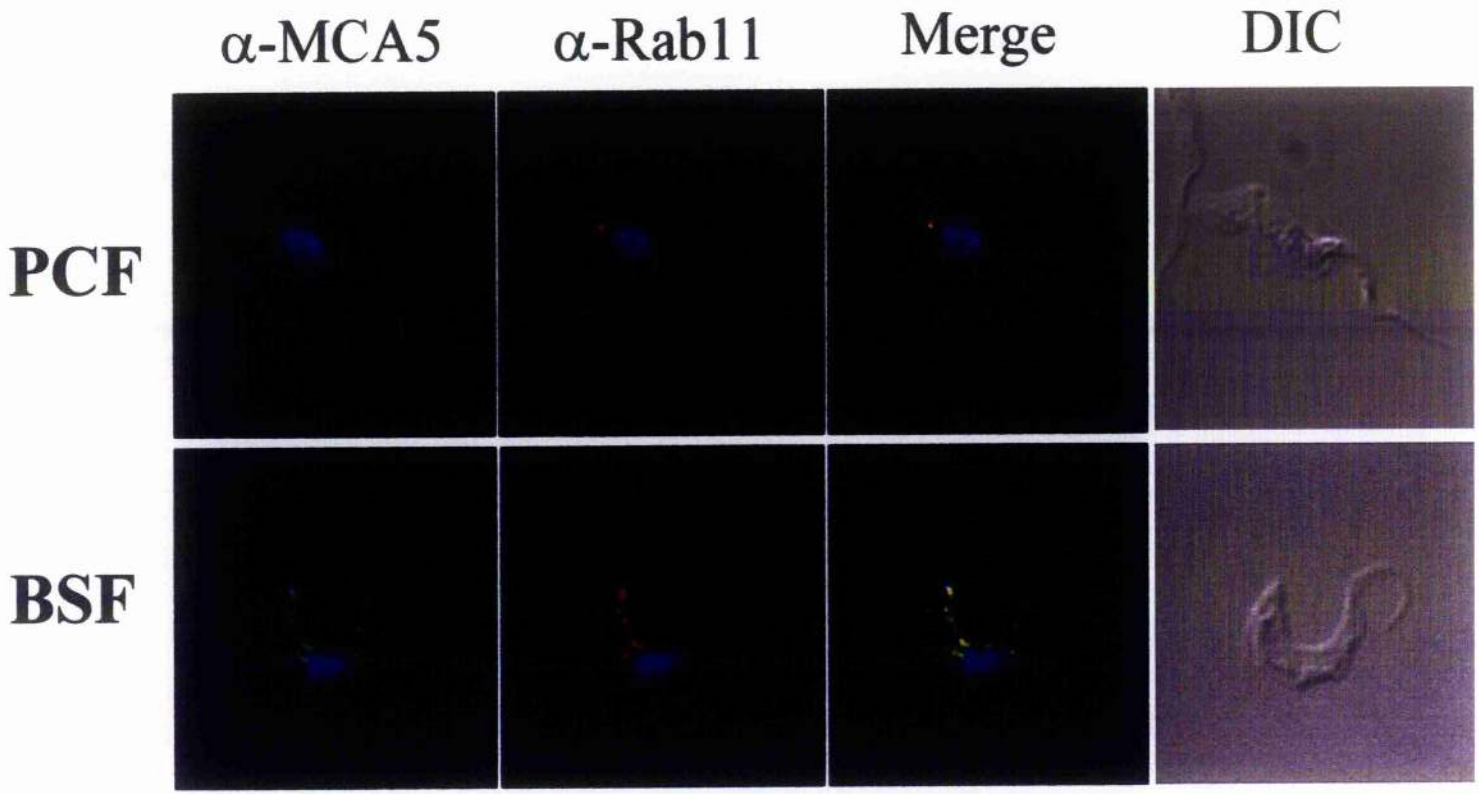
α-MCA5
α-Rab11
Merge
DIC
PCF
BSF

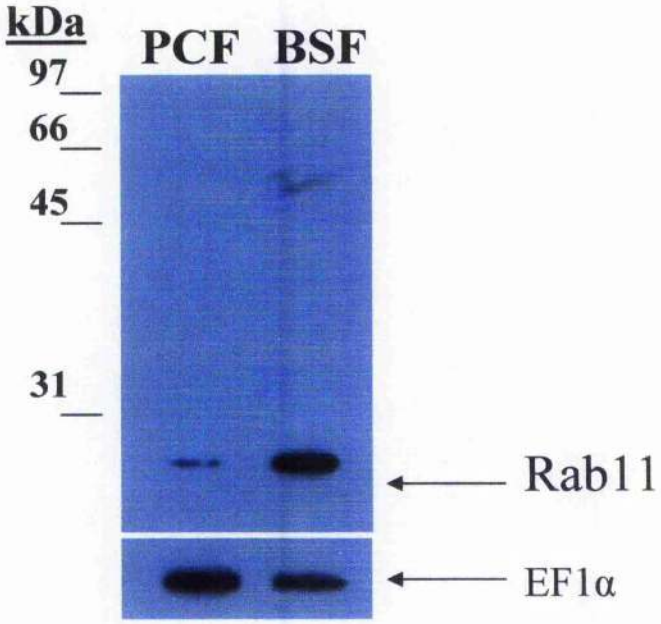

Figure 3.16: Comparison of Rab11 expression in PCF and BSF *T. brucei*. Total cell lysates were prepared from BSF wild type (strain 427) and PCF wild type (stain EATRO 795). $5x10^6$ cell equivalents were then subjected to SDS-PAGE and transferred to PVDF membrane prior to immunoblotting with an immunopurified rabbit polyclonal anti-Rab11 antibody. Rab11 is indicated; antibodies against EF1α were used to indicate equivalent loading.

Figure 3.17: Metacaspases positive structures traffic anti-VSG antibodies. BSF wild type parasites were incubated with rabbit anti-VSG221 antisera at 4°C for 30 mins, and subsequently returned to 37°C for 30 mins. Parasites were fixed in -20°C methanol and permeabilised in -20°C acetone, prior to blocking with 5% (w/v) skimmed milk. Slides were then incubated with the following; 1/1000 dilution of sheep polyclonal anti-MCA5 antiserum, followed by anti-rabbit TRITC and anti-sheep FITC conjugates together with 1 µg/ml DAPI. Labelling of internalised anti-VSG221 antibodies and anti-MCA5 is shown, together with a merged image of both signals, DAPI is included in all images and a DIC image is shown.

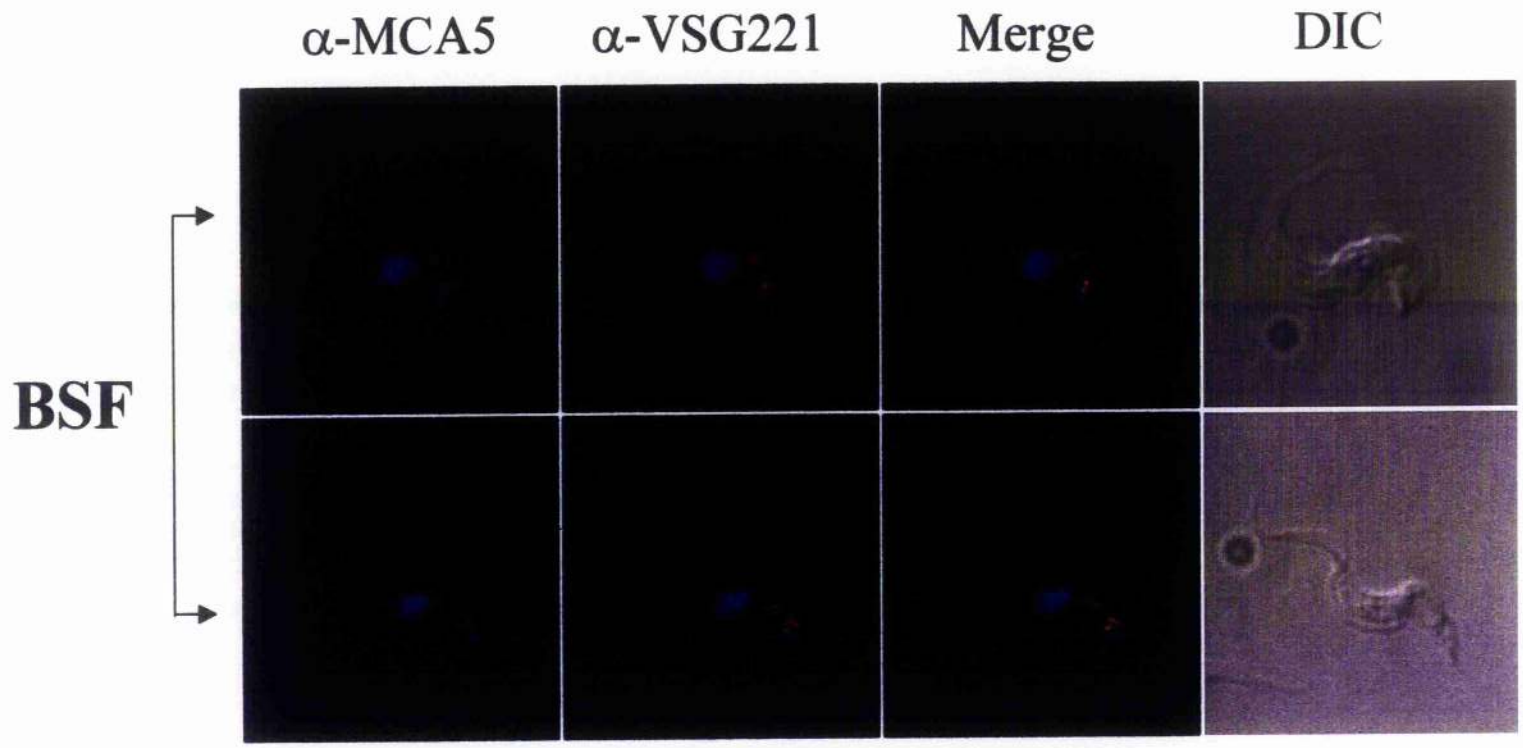
α-MCA5
α-VSG221
Merge
DIC
BSF

Chapter 4

RNAi on metacaspases

4.1 Mechanism of RNA interference (RNAi).

In 1998 it was reported that, in *Caenorhabditis elegans*, double stranded RNA (dsRNA) was more effective at gene silencing than the more commonly used technique of antisense RNA (Fire *et al.*, 1998). Since this discovery, the technique of RNAi has become an extremely useful tool to analyse gene function in a wide variety of eukaryotic organisms. For the mechanism of RNAi to function, the first step is the introduction of gene-specific dsRNA to the target cells. This dsRNA is then cleaved into 20-26 base-pair fragments, termed siRNAs, by an RNAse III-related enzyme termed Dicer (Bernstein *et al.*, 2001). These siRNA fragments are then transferred to a multi-protein complex termed RISC, or RNAi-induced silencing complex (Hammond *et al.*, 2000). In *Drosophila*, a protein with two dsRNA binding domains, named R2D2, and which is also homologous to the *C. elegans* RNAi protein RDE-4, was shown to associate with DICER and facilitate siRNA transfer from Dicer to RISC (Liu *et al.*, 2003). The bound siRNA fragments are then unwound in an ATP-dependent reaction (Nykanen *et al.*, 2001), resulting in exposure of the antisense gene sequence, complex activation, followed by recognition and degradation of target mRNA. The universal components of RNAi have been identified, through biochemical and genetic studies, as the previously described DICER enzyme and members of the Argonaute (AGO) family that are components of RISC. The Argonaute family was first identified in *Arabidopsis thaliana* (Bohmert *et al.*, 1998) and has been shown to be linked to RNAi through studies in both *C. elegans* (Tabara *et al.*, 1999) and *Drosophila* (Hammond *et al.*, 2001). AGO family members possess two characteristic domains. The first is a PAZ domain, which structural studies have defined as an RNA binding module (Yan *et al.*, 2003) thought to possibly function as the siRNA attachment site (Ma *et al.*, 2004). The second is a Piwi domain, displaying similarities to a RNase H domain leading to speculation that AGO proteins function as the nuclease responsible for mRNA degradation (Liu *et al.*, 2004; Song *et al.*, 2004). The RNAi mechanism is thought to be highly specific, mismatches of more than one nucleotide within the siRNA fragments were shown to effectively disrupt degradation of the target mRNA (Elbashir *et al.*, 2001). It is also believed that RNAi evolved as a protective mechanism against parasitic DNA

sequences such as transposons (Sijen and Plasterk, 2003) and viruses (Joost Haasnoot *et al.*, 2003).

The discovery that RNAi was also functional in *T. brucei* (Ngo *et al.*, 1998) followed quickly after the initial identification within *C. elegans* (Fire *et al.*, 1998). It was observed that expression or introduction of dsRNA homologous to α-tubulin mRNA resulted in a dramatic drop in tubulin expression, and that this was due to mRNA degradation. In *T. brucei*, the mechanism by which RNAi occurs is less well characterised than in other organisms. Although siRNAs have been identified and a DICER activity detected (Djikeng *et al.*, 2001), a putative DICER homologue has not been identified in the genome database. One AGO member, termed *Tb*AGO1, has been identified in *T. brucei*, however, and shown to be essential for RNAi (Shi *et al.*, 2004). Shortly after the discovery of RNAi in *T. brucei*, several groups independently developed vectors designed for production of dsRNA within the parasites (LaCount *et al.*, 2000; Shi *et al.*, 2000; Wang *et al.*, 2000; Bastin *et al.*, 2000). In our study, the production of dsRNA within *T. brucei* utilised the p2T7^{Ti} vector, constructed by Doug la Count and John Donelson (LaCount *et al.*, 2000) (Figure 4.1A). This vector uses opposing T7 RNA polymerase promoters to drive the production of dsRNA, insertion of the chosen sequence between these promoters specifies the dsRNA produced. T7 polymerase terminators have also been engineered to ensure that only the inserted gene sequences are transcribed into RNA. To allow the production of dsRNA to be inducible, a tetracycline operator was engineered downstream of the T7 promoters. For selection purposes, the bleomycin resistance gene is present under the control of a trypanosomal ribosomal RNA (rRNA) promoter and the vector is designed for integration within transcriptionally silent ribosomal DNA (rDNA) spacer regions of the *T. brucei* genome. For the RNAi system to function, parasite cell lines are required that have been engineered to express both T7 RNA polymerase and the tetracycline repressor protein (TetR). In these experiments, we have used both PCF (427 pLew13pLew29) and BSF (427 pLew13pLew90-6) cell lines which already contains both of these proteins (Wirtz *et al.*, 1999) (Figure 4.1B).

T7 RNA polymerase, a bacterial polymerase, is non-toxic in *T. brucei* and is able to produce high levels of expression from T7 promoter sites in the parasite (Wirtz *et al.*, 1994). The TetR protein, which forms a homodimer, is also a vital component of this system, binding with a high affinity to the tetracycline operator (Wirtz and Clayton, 1995). Once the RNAi cassette has been integrated within the parasite genome, the TetR protein binds to the tetracycline operator and blocks transcription. The TetR protein also has an affinity for tetracycline (in complex with a divalent cation), which upon binding results in a conformational change in the TetR protein and loss of DNA binding affinity. This removal of repression allows the T7 RNA polymerase to begin transcribing the inserted DNA sequence and dsRNA is produced. Thus the production of dsRNA can be controlled via the addition of tetracycline to the parasite culture medium.

4.2 RNA interference on *MCA2* and *MCA3* in *T. brucei*.

RNAi on *MCA2* and *MCA3* was performed only in the BSF parasites due to the stage-regulated expression of these two genes. As previously discussed, *MCA2* and *MCA3* are located as a tandem repeat on chromosome 6, displaying 91% identity at the DNA level with the only divergence occurring within the 5' region of the two genes (Chapter 3). This high level of homology, with the two genes being 100% identical over the majority of their DNA sequences, allowed us to silence both genes simultaneously. Two oligonucleotides, OL904 and OL905, were designed to amplify by PCR a 668 base-pair fragment for which there is 100% sequence identity between both *MCA2* and *MCA3* (Figure 4.2). This fragment was subsequently cloned from *T. brucei* genomic DNA (strain 427), sequenced to ensure fidelity, and sub-cloned into the p2T7^{ti} RNAi vector. Following linearisation, this vector was used to transfect the BSF RNAi parasite cell line (427 pLew13pLew90-6) and clonal populations attained by limiting dilution using bleomycin as the selection marker. Three separate clones were chosen and RNAi induced by the addition of 50 ng ml^{-1} tetracycline to the culture medium. Growth curves were generated over a four-day period to determine if the silencing of *MCA2* and *MCA3* was detrimental to the parasites (Figure 4.3). Of

the three clones induced with tetracycline, two distinct growth effects were observed. Clones 1 and 3 showed no alteration in growth rate following induction, with the growth curves almost exactly mirroring the non-induced controls over the course of the induction. In addition, there were no obvious gross morphological changes to the parasites following the induction. In clone 2 however, the addition of tetracycline resulted in a pronounced reduction in growth rate, while control parasites continued to grow normally. This reduction in growth rate was accompanied by a drastic alteration in the parasites morphology, the cells becoming large, misshapen and multiflagellate. It was also observed that a small proportion of parasites in the non-induced cultures of clone 2 displayed these morphological alterations, although the majority of parasites had a normal appearance.

Western blot analysis was then performed to determine whether *MCA2* and *MCA3* expression had been successfully silenced in all of the clones. Whole cell extracts were prepared from induced and non-induced parasites at 24 hours post addition of tetracycline or ethanol controls, respectively. These extracts were then subjected to SDS-PAGE, transferred to PVDF membrane and probed with the immunopurified anti-MCA2/3 antibodies (Figure 4.4). In extracts prepared from clones 1 and 3, for which no alteration in either growth rate or morphology had been observed, it was clear that silencing of *MCA2* and *MCA3* expression had been successful. The probing of non-induced extracts detected four proteins and two of these were absent in the induced extracts. It is worth noting, that previous Western blots using this anti-MCA2/3 antibody detected three major proteins in BSF parasite extracts, with the fourth protein detected being at a low level (Figure 3.7). Whether this difference in level of expression of the fourth protein has any relation to the transfection of parasites with the RNAi cassette or is due to a strain difference is unknown. The proteins that had disappeared in the induced extracts closely corresponded with the predicted sizes of MCA2 and MCA3 of 38 and 39 kDa, respectively. Clearly the RNAi technique was functioning effectively as MCA2 and MCA3 were silenced specifically, compared to the other two proteins detected. The situation with clone 2, for which both a rapid onset reduction in growth rate and alterations in morphology

had been observed, was shown to be distinct from clones 1 and 3. Examination of these extracts by Western blotting revealed that both MCA2 and MCA3 were absent from not just the induced but also from the non-induced parasites, while the cross reacting proteins were present in both extracts. Therefore it appeared that *MCA2* and *MCA3* expression had been silenced prior to induction in this clone.

4.3 RNA interference on *MCA5* in *T. brucei*.

While the *MCA2/3* RNAi was performed exclusively in the BSF, *MCA5* was known to be expressed in both BSF and PCF parasites (Chapter 3). This permitted RNAi experiments to be performed in both life stages. To target *MCA5*, oligonucleotides OL944 and OL945 were generated to amplify by PCR a 416 base-pair fragment of *MCA5* (Figure 4.5). Following amplification from *T. brucei* genomic DNA (strain 427), the fragment was sequenced to ensure fidelity and subsequently sub-cloned into the p2T7^{ti} RNAi vector. Following linearisation, this vector was used to transfect both PCF (427 pLew13pLew29) and BSF (427 pLew13pLew90-6) RNAi cell lines and clonal populations obtained by limiting dilution using bleomycin as the selection marker. Induction of RNAi was performed by the addition of 50 ng ml^{-1} tetracycline in both life stages.

4.3.1 RNA interference on *MCA5* in PCF *T. brucei*.

Four clones were chosen for the PCF *MCA5* RNAi induction and growth curves were generated over a period of seven days. Two distinct phenotypes were seen (Figure 4.6). A reduction in growth rate in clones 2 and 4 (clone 2 is shown) was observed. Clones 1 and 3, however, displayed no alteration in growth rate over the period of the experiment with induced cultures mirroring their non-induced counterparts (clone 3 is shown). No morphological alterations were observed in any of the clones either before or after induction.

Western blot analysis was then performed to determine whether *MCA5* expression was effectively being silenced. Whole cell extracts were prepared from clones 2 and 3 at 0, 2 and 4 days post-induction with tetracycline or ethanol controls. Extracts

were then subjected to SDS-PAGE and transferred to PVDF membrane and probed with anti-MCA5 antiserum (Figure 4.7). The analysis revealed that the induction of RNAi resulted in the sole protein detected by the anti-serum being absent from induced parasites, while the expression was unchanged in non-induced parasite extracts. This confirmed the specificity of the antiserum and demonstrated that the RNAi of *MCA5* was functioning efficiently in both clones.

While both clones showed that MCA5 levels were reduced following addition of tetracycline, there does appear to be a difference in expression levels of *MCA5* between the two clones. By loading $5x10^6$ cell equivalents for both clones 2 and 3, it is clear that the expression of *MCA5* in non-induced parasites was lower within the former (Figure 4.7). It is interesting to note that clone 2 was also the clone for which a growth phenotype was detected.

4.3.2 RNA interference on *MCA5* in BSF *T. brucei*.

To examine the effect of *MCA5* RNAi in the BSF, three clones were selected, induced, and growth curves generated over a 24 hour period. Again, two distinct growth phenotypes were observed (Figure 4.8). One in which the addition of tetracycline had no effect on parasite growth, and a second, in which this induction resulted in a rapid growth arrest. Clones A and C (clone C shown in figure 4.8) showed no adverse affects of tetracycline addition with growth rates mirroring those of the control parasites. With clone B, however, following the addition of tetracycline the parasites failed to increase in number over the next 24 hour period. In addition, these parasites took on a mutant morphology highly similar to that described previously for the *MCA2* and *MCA3* BSF RNAi, the parasites becoming large, misshaped and multiflagellate. Again, similarly to *MCA2* and *MCA3* BSF RNAi, it was observed that a small proportion of the clone B uninduced cells also displayed this mutant morphology.

To analyse the effectiveness of the silencing of *MCA5*, whole cell extracts were prepared from clones B and clone C following an 18-hour induction with either

tetracycline or ethanol control. These were then subjected to SDS-PAGE, transferred to PVDF membrane and probed with anti-MCA5 antiserum (Figure 4.9). This demonstrated that the RNAi mechanism was functioning effectively, with an equivalent reduction in protein levels at the 18 hour time point observed for both clones.

4.4 Specificity of RNAi.

The RNAi mechanism is believed to be highly specific, the siRNA fragments must almost exactly match the mRNA to cause degradation of the message (Elbashir *et al.*, 2001). Although unlikely, it was possible that targeting of *MCA2* and *MCA3* by RNAi may also target the *MCA5* mRNA and *vice versa*. To determine if this was the case, Western blot analysis on the whole cell lysates from the previous RNAi experiments was performed. To check the specificity of the *MCA5* RNAi, BSF clones B and C cell extracts were subjected to SDS-PAGE, transferred to PVDF and probed with anti-MCA2/3 antibodies (Figure 4.10A). This demonstrated that upon induction of *MCA5* RNAi, which was shown to drastically reduce MCA5 levels within the parasites, there was no alteration in the level of MCA2 or MCA3 within the parasites. The reverse experiment was also performed to check specificity of the *MCA2/3* RNAi. BSF clones 1 and 3 extracts were subjected to SDS-PAGE, transferred to PVDF and probed with the anti-MCA5 antiserum (Figure 4.10B). It was clear from this analysis that the *MCA2* and *MCA3* RNAi was also specific, as no alteration in MCA5 levels were observed in the induced extracts compared to controls.

4.5 RNA interference on *MCA2*, *MCA3* and *MCA5*.

Having performed RNAi on both *MCA2/3* and *MCA5* successfully, a construct was generated that would be able to target all three genes simultaneously. Due to the stage-regulated expression of *MCA2* and *MCA3*, this was only attempted in BSF parasites. Having shown that the individual fragments chosen for both the *MCA2/3* and *MCA5* RNAi worked successfully, a fusion vector containing both of these gene fragments was created. To achieve this, the 668 base-pair *MCA2/3* fragment was

cloned into the *MCA5* RNAi vector so that it was immediately adjacent to the 408 base-pair *MCA5* fragment (Figure 4.11). Therefore this new construct, following transfection and induction with tetracycline, should produce dsRNA from both *MCA2/3* and *MCA5* fragments.

The generation of clonal populations with this linearised vector, however, was found to be more difficult than the generation of *MCA2/3* or *MCA5* RNAi clones. Although an equivalent amount of linearised DNA was used in the transfection, as compared to the previous *MCA2/3* and *MCA5* RNAi transfections, there was a large discrepancy in the number of clones attained. When the single RNAi BSF transfections were performed, typically it was possible to generate in excess of 10 clonal transformants. However, when the *MCA2/3/5* RNAi transfection was performed the number of transformants generated was very low. The transfection was performed twice with only a single clone generated in each attempt. Although not a controlled experiment, these observations suggest that either the integration efficiency of this vector was reduced or that the background expression of the vector, without induction, may be toxic to the parasites. In addition, although the two clones generated generally appeared healthy, it was notable that a small proportion of the parasites displayed a similar mutant phenotype to that described previously in both the *MCA2/3* and *MCA5* RNAi experiments in the BSF.

With two clones generated, it was possible to perform the triple MCA RNAi experiments in the BSF. Clones 1 and 2 were induced with 50 ng ml^{-1} tetracycline and growth curves generated over a three-day period (Figure 4.12). Induced parasites underwent a rapid onset growth arrest, while controls continued to grow normally. Also notable was that the parasites took on the by now familiar morphological alterations, becoming large, misshaped and multiflagellate. These observations were highly similar to the phenotype described upon induction in the *MCA2/3* and *MCA5* RNAi experiments.

To validate that all three genes were being silenced, Western blot analysis on clone 1 was performed. Whole cell lysates were prepared at 0, 24 and 48 hours post-induction with tetracycline or ethanol controls. These extracts were then subjected to SDS-PAGE, transferred to PVDF and probed with both anti-MCA2/3 antibodies and anti-MCA5 antiserum (Figure 4.13). These results showed that the simultaneous silencing of *MCA2*, *MCA3* and *MCA5* had been successful. MCA5 was not detected following 24 hours induction, while expression was unaffected within the control parasites. The silencing of *MCA2* and *MCA3* was, however, distinct, at 24 hours post-induction it was still possible to detect MCA2 although MCA3 was absent. After 48 hours the amount of MCA2 had also fallen to barely detectable levels, while expression of both proteins was unaffected in control extracts. This differential reduction in *MCA2* and *MCA3* expression had not been observed when *MCA2/3* RNAi had been performed previously, as both MCA2 and MCA3 could not be detected at 24 hours post-induction (Figure 4.4).

4.6 Discussion.

Of the five metacaspase genes identified in *T. brucei*, this study has examined the function of *MCA2*, *MCA3* and *MCA5* by the technique of RNAi. These are the three metacaspases for which antibodies have been raised and their expression profile determined, thus allowing direct quantification of the functionality of the RNAi. *MCA1* and *MCA4*, for which antibodies are not available against the gene products, have not been examined in this study.

Our analysis of the *MCA2/3* RNAi clones generated within BSF parasites revealed that the silencing of *MCA2/3* resulted in two distinct phenotypes. Of the three clones examined, two showed no detrimental effects in terms growth rate or gross morphology, while Western blot analysis revealed that levels of MCA2 and MCA3 were dramatically reduced. In the remaining clone, however, the results obtained were very different: upon induction, parasites underwent a rapid onset reduction in growth rate and took on a highly mutant morphology with the cells becoming large, misshaped and multiflagellate. In addition, Western analysis revealed that *MCA2* and *MCA3* expression had also been effectively silenced in the non-induced parasites. Based upon the observations that two of the clones analysed were able to withstand silencing of both *MCA2* and *MCA3* without the detection of any obvious detrimental effects, it seems reasonable to conclude that the growth arrest and altered morphology phenotype observed within the one clone is most likely a non-specific artefact.

These results raise several possibilities. Firstly, that the silencing of *MCA2* and *MCA3* expression did not affect the parasite's normal cellular process in such a way that was immediately obvious or detrimental. The lack of an observable phenotype does not mean that one was not present, the silencing of the two genes might have resulted in a subtle phenotype that was not detected by the gross analysis performed. Alternatively, it may be that the level of expression of *MCA2* and *MCA3* within the induced parasites, although drastically reduced, was sufficient to retain normal functions. Indeed, longer exposures of the Western blots revealed that MCA2 and

MCA3 remained detectable in the parasite extracts following induction. These are not physical knockouts, and it has been reported that it is not possible to completely ablate target mRNA within *T. brucei* using RNAi (Shi *et al.*, 2000). Therefore the production of gene products can never fully be switched off and the reduced level of expression may still be enough to prevent any detrimental effects of gene silencing becoming evident. With *T. brucei*, RNAi has been used successfully against enzymes (Besteiro *et al.*, 2002; Lillico *et al.*, 2003; Luo *et al.*, 2004), structural proteins (Bastin *et al.*, 2000; Hutchings *et al.*, 2002; Allen *et al.*, 2003; McKean *et al.*, 2003) and non-catalytic components of complexes (Hammarton *et al.*, 2003; Hammarton *et al.*, 2004). However, a resistant mRNA component could theoretically place limitations on the RNAi system, particularly with regard to enzymes which may be able to operate adequately at highly reduced concentrations. Moreover, as negative results are rarely published, it is difficult to assess whether this is the case. It remains a possibility therefore, that, despite a large decrease in *MCA2* and *MCA3* expression, the nominal amount remaining within the parasites retains the ability to function sufficiently. The third possibility is that other metacaspases are able to functionally compensate for the reduction in *MCA2* and *MCA3* expression. We have shown previously that MCA2 and MCA3 are associated with the same compartment as MCA5 in BSF parasites (Chapter 3). It is possible, therefore, that MCA5 is able to offset any detrimental effects resulting from the silencing of *MCA2* and *MCA3*. It is known that multi-gene families can compensate for each other from previous RNAi studies. It has been shown that GLH-1 and GLH-4, RNA helicases involved in germline development in *C. elegans*, were able to compensate for each other. To induce sterility, the silencing of both genes simultaneously was required (Kuznicki *et al.*, 2000). Also in *C. elegans*, three redundant CCCH-type zinc-finger genes were identified which when silenced singly produced no phenotype, while double or triple RNAi induced defects in oocyte maturation (Shimada *et al.*, 2002). Additionally, *MCA5* is not the only other metacaspase that could theoretically negate the silencing of *MCA2* and *MCA3* expression. *T. brucei* also possesses two other metacaspase genes, *MCA1* and *MCA4*, for which expression profiles are unknown. It

is possible, therefore, that these two genes might provide further levels of redundancy and be responsible for the lack of an observable phenotype.

Induction of *MCA5* RNAi in the BSF yielded similar results to that which had been previously observed for the *MCA2* and *MCA3* RNAi. Of the three clones induced, two showed no ill effects, while the remaining clone underwent a rapid onset reduction in growth rate and took on highly similar morphological alterations to those seen with the *MCA2* and *MCA3* RNAi. Upon analysis of parasite extracts, it became apparent that the silencing of *MCA5* was occurring independently of the two distinct effects. The tentative conclusion drawn is that the mutant phenotype observed was another non-specific artefact of the RNAi system.

Therefore it appears that the silencing of *MCA5* does not result in any obviously detrimental effects to the BSF parasites. The possible explanations for this are identical to those described for the *MCA2* and *MCA3* RNAi. A more detailed analysis may have been required to detect a phenotype or alternatively the reduced levels of *MCA5* expression may be sufficient to maintain normal cellular functions. It was suggested that there might have been compensation in the *MCA2* and *MCA3* RNAi experiments, similarly, it is possible that there were compensatory mechanisms for *MCA5* also. This could feasibly occur via *MCA2* or *MCA3*, which we know are expressed, or *MCA1* and *MCA4* for which expression has not been determined.

On performing *MCA5* RNAi in the PCF, the results, although not identical, were similar to those observed for both the *MCA2/3* RNAi and *MCA5* RNAi in the BSF. Upon induction, again two distinct phenotypes were observed. Of the four clones for which growth curves were generated, two showed no reduction in growth rate over the period of the induction, while in the remaining two clones a reduction in growth rate was apparent. However, unlike in the BSF, there were no morphological alterations associated with the reduced growth rate. Similarly, an analysis of protein levels revealed that these two separate phenotypes appeared to be independent of the

silencing of *MCA5*. We can conclude from this that, similarly to the BSF RNAi experiments, the silencing of *MCA5* in the PCF does not appear to have any obviously detrimental effects and, based on the information available, it appears that the clones where a reduction in growth rate was observed are most likely artefactual.

It is possible that the *MCA5* RNAi induces a subtle phenotype that was not revealed by our analysis or that the reduced level of protein expression retains enough enzymatic activity to maintain normal functions. It has been shown, however, that *MCA2* and *MCA3* are not expressed in the PCF parasites (Chapter 3), thus there is no possibility that MCA2 and MCA3 can complement for the loss of MCA5 in the PCF. However, as *MCA1* and *MCA4* expression has yet to be determined there remains the possibility that these two genes could nullify any detrimental effects of *MCA5* silencing.

The *MCA2/3* and *MCA5* RNAi investigations did demonstrate, however, that the RNAi-induced gene silencing was specific for the target metacaspases. No reduction in *MCA2* or *MCA3* expression was detected when *MCA5* RNAi was performed and *vica versa*. This was not too surprising as an alignment of the DNA sequences of the two fragments revealed that the largest domain of homology between the two regions chosen extends for only 7 base pairs. It is believed that for RNAi to function the siRNA fragments may only differ by one or two base pairs (Elbashir *et al.*, 2001). Also of note, is that the silencing of *MCA2/3* or *MCA5* does not result in the up regulation of *MCA5* or *MCA2/3* expression, respectively. If the metacaspase family is redundant, we might have expected to see increased expression of the remaining metacaspases upon RNAi induced silencing, which was not observed. The RNAi data so far discussed is suggestive that *MCA2* and *MCA3* in the BSF and *MCA5* in both the BSF and PCF are non-essential to general parasite health or survival *in vitro*. As this study does not examine the other identified metacaspase genes *MCA1* and *MCA4*, this was as far as the work was taken in the PCF.

It was possible, however, to investigate the possibility of complementation or redundancy in the BSF through the triple RNAi of *MCA2*, *MCA3* and *MCA5*. Upon induction, both of the clones generated underwent a rapid growth arrest and took on the familiar mutant morphology - parasites becoming large, misshaped and multiflagellate. Examination of protein levels revealed that the silencing of both the *MCA2/3* and *MCA5* loci had been successful. Taken in isolation, the triple metacaspase RNAi observations might have appeared an attractive and promising phenotype to study. However, as the same morphological alterations and rapid growth arrest had been observed in the previous RNAi experiments which were concluded to be artefactual, it was felt that this phenotype may also be artefactual. Additionally, while the growth arrest and mutant phenotype occurred extremely rapidly, the analysis of protein levels revealed that MCA2 remained detectable at 24 hours post-induction, a time at which the mutant morphology was apparent. This result further questioned the validity of the phenotype. If as hypothesised, *MCA2*, *MCA3* and *MCA5* are redundant, then a phenotype resulting from their silencing should only become apparent once all three genes had been effectively silenced.

While the RNAi study has illustrated that the metacaspases do not appear to be essential genes *in vitro*, the results have highlighted several points of concern regarding the technique of RNAi in *T. brucei*. As described, in both the *MCA2/3* and *MCA5* RNAi experiments, the mutant phenotypes were independent of gene silencing and therefore must reflect other events. Our hypothesis to explain this is that following induction, and switching on of dsRNA production, the parasites experience a non-specific toxic effect. Non-specific toxic effects of dsRNA production have been reported. The introduction of dsRNA has been shown to evoke a strong antiviral mechanism, including stimulation of the interferon synthesis, in higher eukaryotes, resulting in an inhibition of cell growth or activation (Kumar and Carmichael, 1998). The apparent toxicity in *T. brucei* appeared to manifest differentially between the BSF and PCF parasites. In the BSF there appeared to be a failure in the cellular division process, the increase in size of the parasites and appearance of many flagella suggesting that the parasites were continuing to attempt

replication but for some reason are unable to physically divide. In the PCF, a less severe growth reduction with no associated morphological changes was observed. The differential manifestation may be due to the PCF being better able to withstand high levels of dsRNA production. It is known that the PCF is better able to withstand higher concentrations of antibiotics than the BSF, indicating that it may be generally more resistant to toxic conditions.

However, attempting to understand the reasons why this effect was detected in some but not all of the clones generated is arguably more important. The ability to silence *MCA2* and *MCA3* expression in the BSF, and *MCA5* expression in both the BSF and PCF, without any detrimental effects illustrates that the production of high concentrations of metacaspase specific dsRNA are not inherently toxic to the parasites. Therefore, there must be something distinct occurring to explain the mutant phenotypes observed in the some of the clones generated. The situation with the *MCA2/3* RNAi provides some clues as to what this might be. The lower level of *MCA2* and *MCA3* expression prior to induction indicates that sufficient levels of dsRNA are being produced to silence both genes without the addition of tetracycline, and therefore that the inducible control of the RNAi cassette had either been lost or was not functioning. The level of dsRNA being produced must have been at least equivalent to that produced in the two clones where no phenotype was observed upon induction. In fact it may even have been higher, the small proportion of mutant parasites observed within the non-induced cultures suggests that the level of dsRNA production prior to induction were approaching toxic levels. Although only speculation, it is plausible to suggest that following addition of tetracycline, with the removal of the TetR protein from the tetracycline operator site likely to remove any remaining barriers to dsRNA production, the production of dsRNA would have crossed a toxicity threshold. If massive amounts of dsRNA were then being produced, there are several possible reasons as to why this may have caused toxicity to the parasites. The very presence of this much dsRNA may simply have swamped the cell and prevented normal metabolism from occurring, or alternatively the energy

required to produce this much dsRNA may have placed a drain on other essential resources required to maintain normal cellular processes.

The silencing of both *MCA2* and *MCA3* from the non-induced parasites for which no tetracycline had been added suggests that there is leaky expression of the RNAi cassette within this clone. Leaky expression from the RNAi system refers to the production of dsRNA without the addition of exogenous tetracycline and switching on of T7 RNAse polymerase transcription. There are several possible explanations for such leaky expression. It is possible that tetracycline from external sources may have found its way into the experiment. A possible route with which this may have occurred is via the foetal calf serum (FCS) used to supplement the culture medium. However, the same media preparations were used for all of the *MCA2* and *MCA3* RNAi clones analysed, ruling out the possibility that changes in exogenous tetracycline were behind the leaky expression. If tetracycline concentrations were the same in all non-induced cultures, there must be another explanation for the leaky expression from the RNAi cassette. All three clones were generated from the same RNAi cassette preparation, and indeed were generated from the same transfection. This would appear to rule out the possibility that the apparent differential level of leaky expression was the result of alterations in the expression or functionality of either the TetR protein or T7 RNA polymerase genes already present within the parasites.

Although only the *MCA2* and *MCA3* RNAi has been used to suggest possible explanations for the differential phenotypes observed, parallels can easily be drawn for the *MCA5* RNAi in both BSF and PCF parasites. In the BSF, although there was no evidence of leaky expression, the phenotype observed was virtually indistinguishable, suggesting the same process of dsRNA toxicity was the cause. In the PCF, there was also evidence of leaky expression from the RNAi cassette prior to induction in the clones which presented a growth phenotype.

It is likely, that the distinct phenotypes observed in this RNAi study are the result of differential integration positions of the RNAi cassette within the genome. The RNAi cassette used in this study was designed for integration within the ribosomal DNA (rDNA) spacer region. The *T. brucei* genome contains numerous ribosomal loci which the RNAi cassette vector may integrate into, and all of these are believed to be transcriptionally silent. From these sites the production of dsRNA should therefore be under the sole control of the T7 RNA polymerase driven from the T7 promoter site. However, one explanation for the silencing observed prior to induction may be that not all of the ribosomal spacer regions are completely silent. If this is the case, read through may occur from the ribosomal locus and this maybe strong enough to overcome the TetR system. Alternatively, the insertion of the RNAi vector into certain ribosomal spacer loci may result in instability, resulting somehow in the disruption of the tetracycline repression system. This might de-regulate control over the RNAi cassette and could explain the apparent constitutive expression of dsRNA in the *MCA2/3* RNAi. However, the addition of tetracycline clearly induced further changes to the parasites and, as previously discussed, is most likely due to further increases in dsRNA production. For this increase to occur upon tetracycline addition, the repression system must retain a certain level of functionality, with the addition of tetracycline pushing levels of dsRNA production above a toxicity threshold.

It is also possible that the RNAi cassette integrated into a locus other than the ribosomal spacer region. It has been reported that vectors utilising these rDNA spacer regions for targeted homologous recombination occasionally integrate at other loci within the genome that are homologous to the insert rather than the rDNA spacer region (Bastin *et al.*, 1998; Motyka *et al.*, 2004). The result of such integrations would be difficult to predict due to orientational rearrangement of the elements within the RNAi cassette. No analysis was performed to check whether integration of the RNAi cassette occurred at the rDNA spacer region in the clones analysed, and a future analysis to examine this possibility may be of interest.

One unfortunate result of these apparently artefactual results is that it is not possible to be sure whether the silencing of *MCA2*, *MCA3* and *MCA5* is lethal or detrimental to the parasites. It cannot be said with certainty whether the observed phenotype is artefactual, or real, or whether there is a real phenotype which is being masked. The similarity of the growth arrest and morphological changes does strongly suggest that the hypothesised non-specific dsRNA toxicity is the reason behind the observed phenotype, while the difficulty in achieving clones suggests that disruption of these three genes may be detrimental to the parasites. To further these investigations, null mutants were generated and these are discussed later (Chapter 5).

What is clear from these RNAi investigations is that while this technique clearly can work efficiently in *T. brucei*, and no clones were generated where silencing of target metacaspase did not occur, there are clearly problems associated with the technique which need addressing. These artefacts may be specific to the vector itself and not the technique of RNAi as no similar artefacts have been reported by other researchers working on *T. brucei*. Additionally, although the vector used in this study might have problems associated with it, it is still suitable for RNAi studies. The generation of clones that did not display signs of the artefact were generated, and had an obvious phenotype been present these could have been used to analyse metacaspase function. Additionally there are several publications were this vector has been used successfully (LaCount *et al.*, 2000; Lillico *et al.*, 2003; Hammarton *et al.*, 2004) highlighting the usefulness of this technique.

A)

RNAi cassette: p2T7^{Ti}

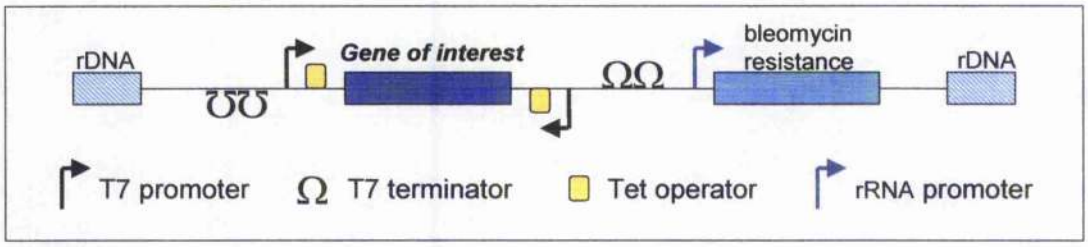

B)

Strains: PCF: 427 pLew13 pLew29
BSF: 427 pLew13 pLew90-6

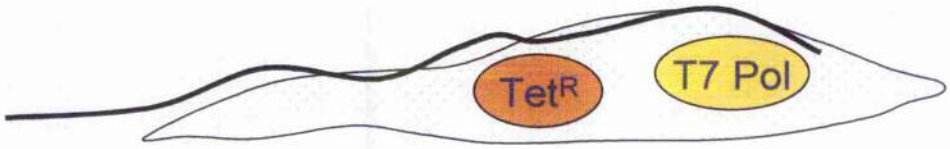

Figure 4.1: Illustration of the domain structure of the inducible RNAi vector and parasite cell lines required for this system.
A) The RNAi cassette from the p2T7^{Ti} vector (LaCount *et al.*, 2000). B) The cell lines used in this study were: PCF (427 pLew13pLew29) and BSF (427 pLew13pLew90-6) (Wirtz *et al.*, 1999).

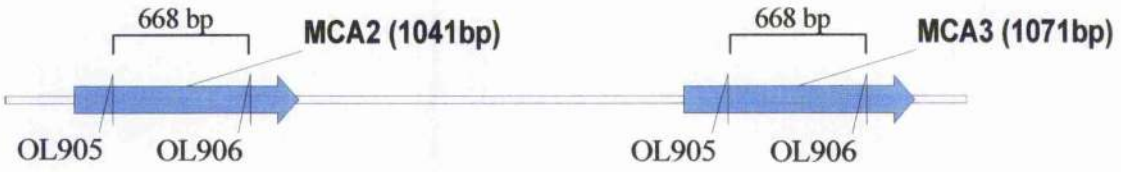

Figure 4.2: Region of *MCA2* & *MCA3* chosen for RNAi.
MCA2 & *MCA3* are located as a tandem repeat, sharing 91% identity at the DNA level. A 668 bp stretch of *MCA2* and *MCA3* was chosen over which the two genes share 100% identity. The oligonucleotides OL905 and OL905 were used to amplify this gene fragment by PCR from genomic DNA (strain 427) for subsequent cloning into the p2T7^{Ti} RNAi vector.

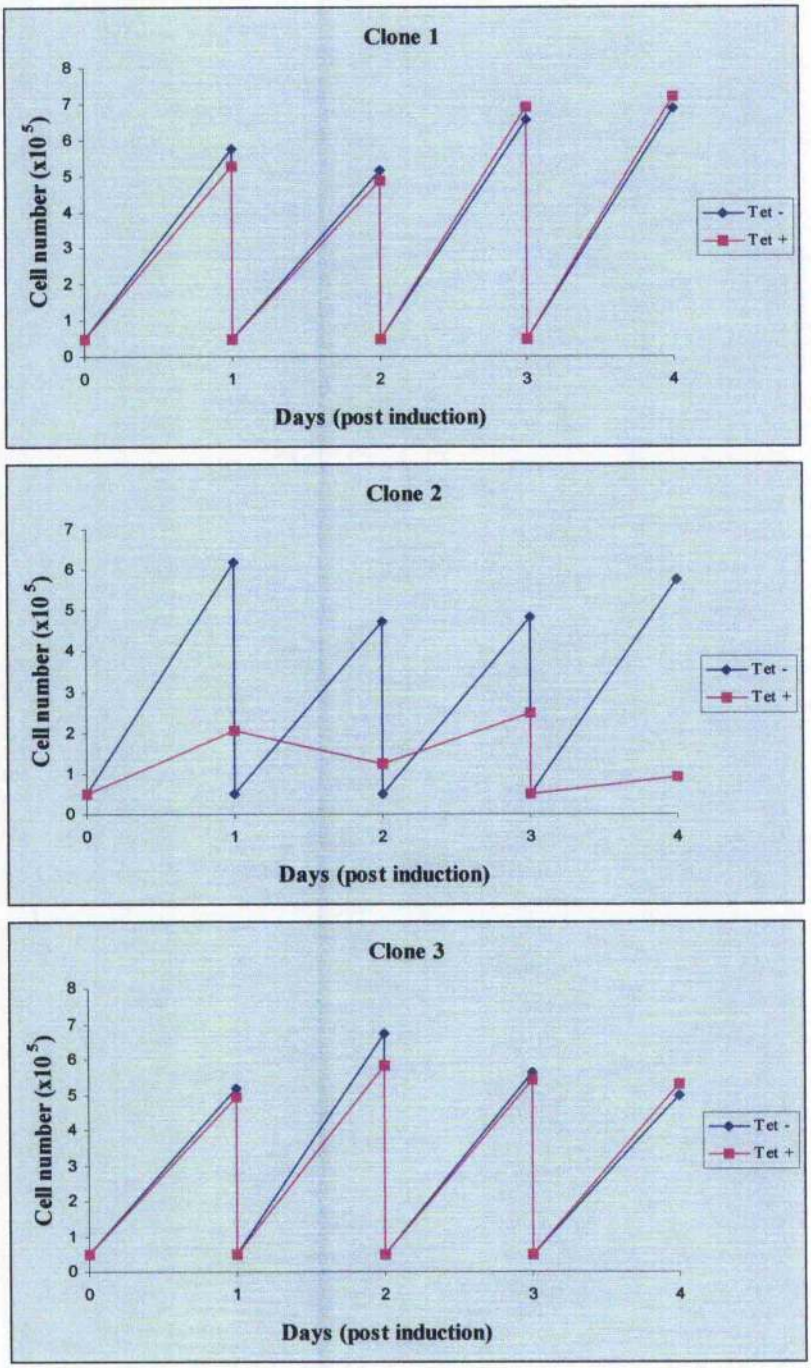

Figure 4.3: Analysis of growth rates following induction of *MCA2/3* RNAi in BSF *T. brucei*.

MCA2/3 BSF RNAi clones 1, 2 and 3 were grown in the absence or presence of 50 ng ml^{-1} tetracycline and cell numbers monitored over a period of 4 days. Initial cultures were seeded at $5x10^4$ cells ml^{-1} and cell counts made daily, with cultures being re-seeded to $5x10^4$ cells ml^{-1} as and when required to maintain cultures in a logarithmic growth phase.

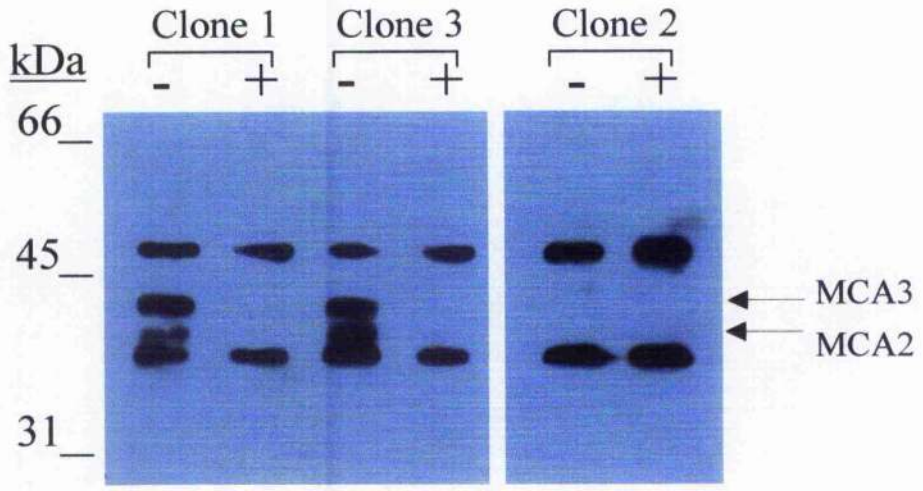

Figure 4.4: Analysis of MCA2 and MCA3 expression following RNAi induction in BSF *T. brucei*.

Total cell lysates were prepared from *MCA2/3* BSF RNAi clones 1, 2 and 3 following a 24 hour induction with 50 ng ml^{-1} tetracycline or ethanol control. $5x10^6$ cell equivalents were then subjected to SDS-PAGE and transferred to PVDF membrane prior to immunoblotting with immunopurified polyclonal rabbit anti-MCA2/3 antibodies. MCA2 and MCA3 are indicated.

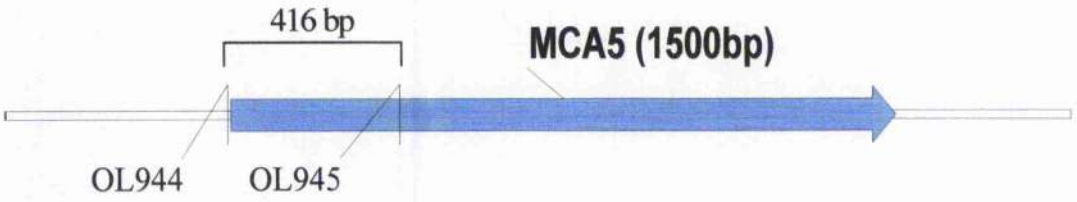

Figure 4.5: Region of *MCA5* chosen for RNAi.
A 416 bp stretch of *MCA5* was chosen as the region of the gene to target by RNAi. The oligonucleotides OL944 and OL945 were used to amplify this gene fragment by PCR from genomic DNA (strain 427) for subsequent cloning into the p2T7^{Ti} RNAi vector.

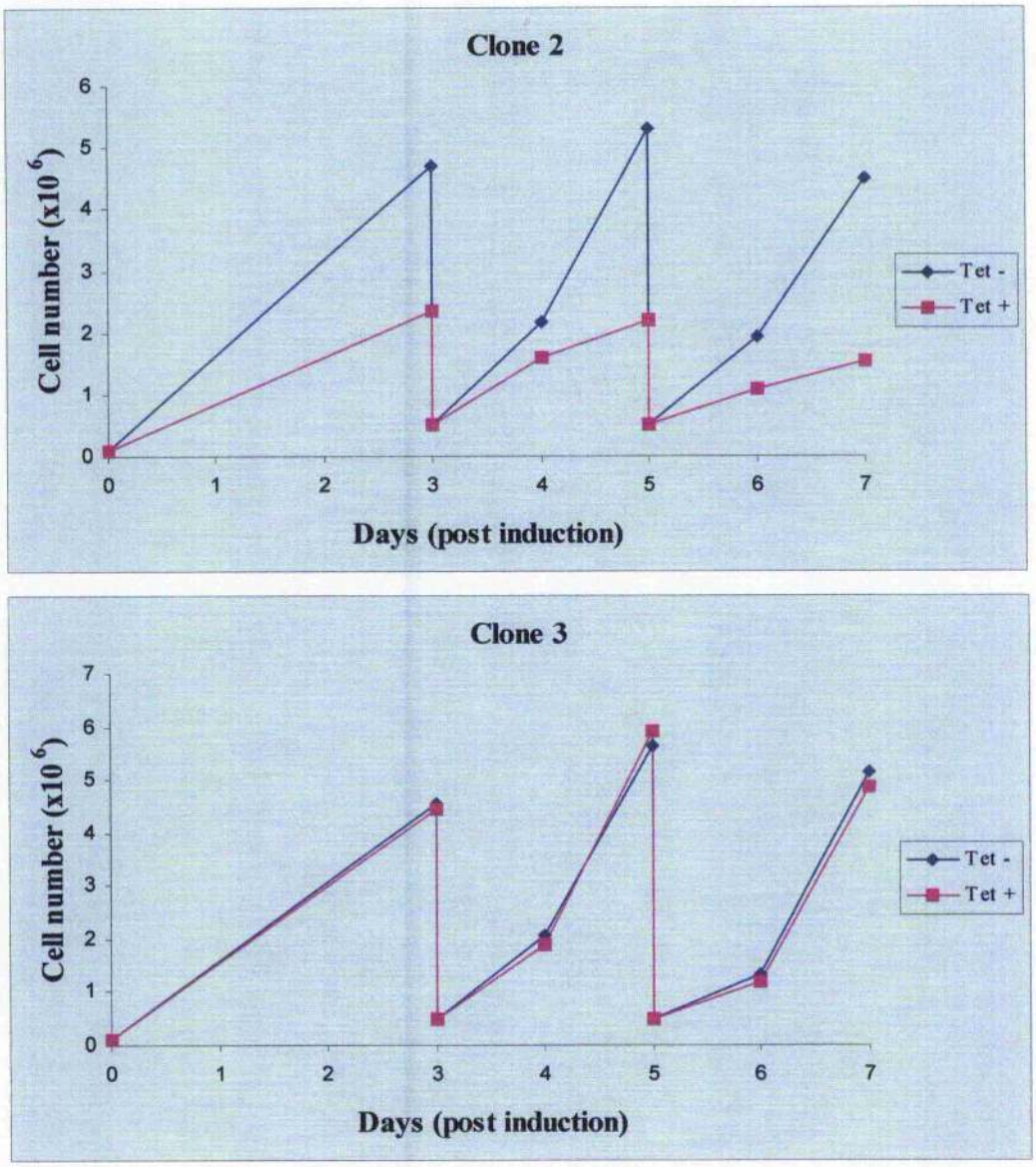

Figure 4.6: Analysis of growth rates following induction of *MCA5* RNAi in PCF *T. brucei*.

MCA5 PCF RNAi clones 2 and 3 were grown in the absence or presence of 50 ng ml^{-1} tetracycline and cell numbers monitored over a period of 7 days. Initial cultures were seeded at 1x10^5 cells ml^{-1} and cell counts made, with cultures being re-seeded to 5x10^5 cells ml^{-1} as and when required to maintain cultures in a logarithmic growth phase.

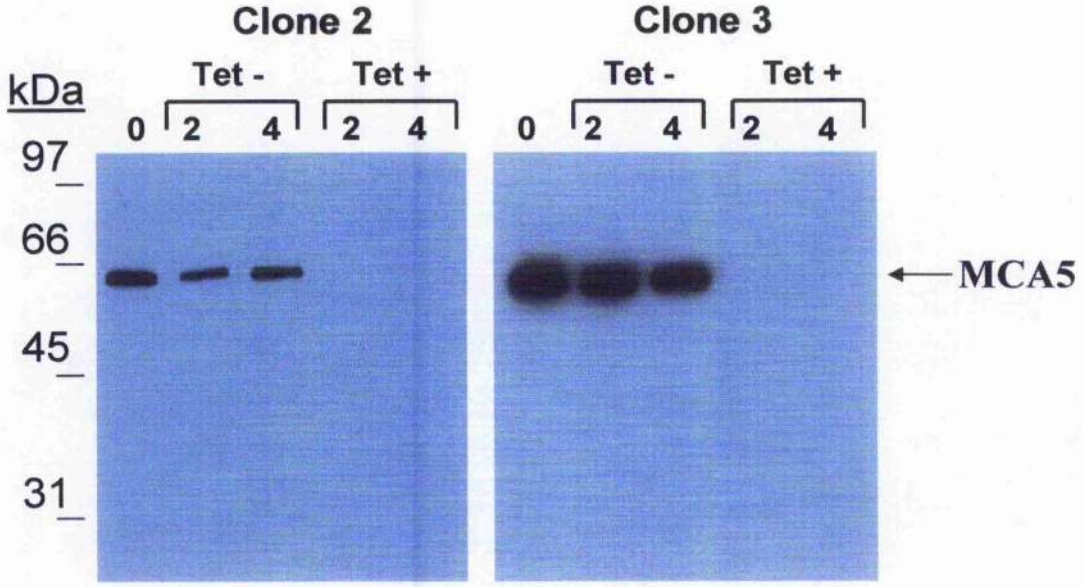

Figure 4.7: Analysis of MCA5 expression following RNAi induction in PCF *T. brucei*.

Total cell lysates were prepared from *MCA5* PCF RNAi clones 2 and 3 induced with 50 ng ml^{-1} tetracycline or ethanol control for 0, 2 and 4 days. $5x10^6$ cell equivalents were then subjected to SDS-PAGE and transferred to PVDF membrane prior to immunoblotting with sheep anti-MCA5 antiserum. MCA5 is indicated.

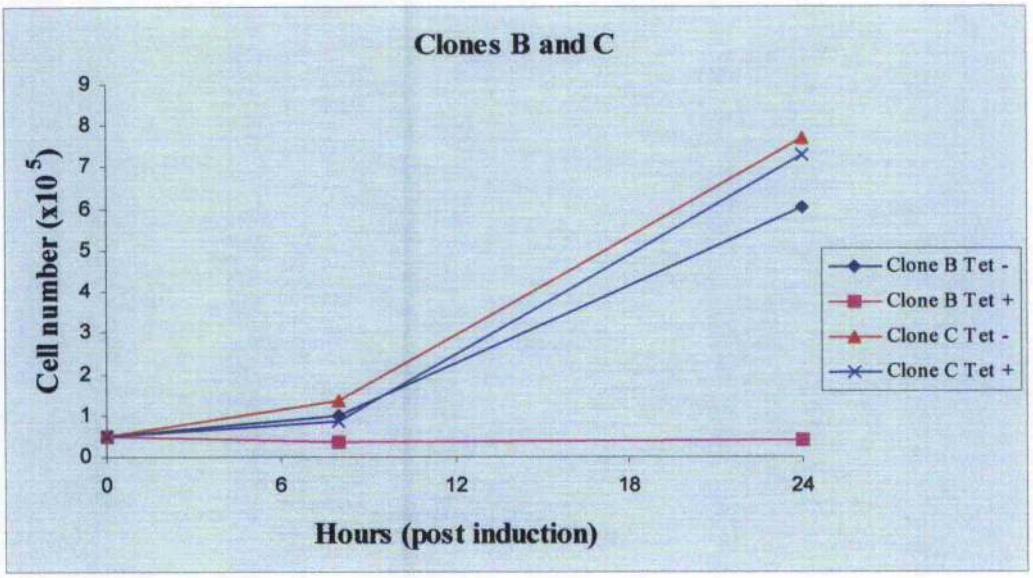

Figure 4.8: Analysis of growth rates following induction of *MCA5* specific RNAi in BSF *T. brucei*.

MCA5 BSF RNAi clones B and C were grown in the absence or presence of 50 ng ml^{-1} tetracycline and cell numbers monitored over 24 hour period. Initial cultures were set up at $5x10^4$ cells ml^{-1} and cell counts made after 7 and 24 hours.

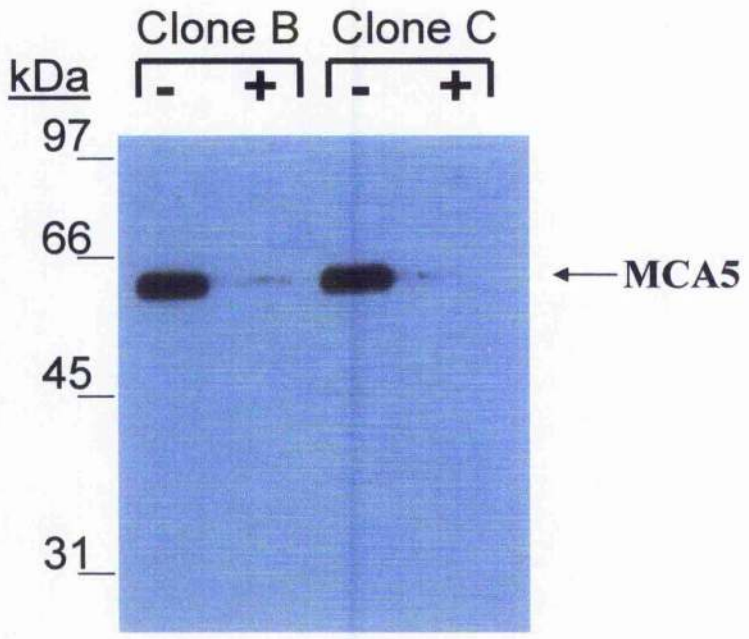

Figure 4.9: Analysis of MCA5 expression following RNAi induction in BSF *T. brucei*.
Total cell lysates were prepared from *MCA5* BSF RNAi clones B and C following an 18 hour induction with 50 ng ml^{-1} tetracycline or ethanol control. $5x10^6$ cell equivalents were then subjected to SDS-PAGE and transferred to PVDF membrane prior to immunoblotting with sheep anti-MCA5 antiserum. MCA5 is indicated.

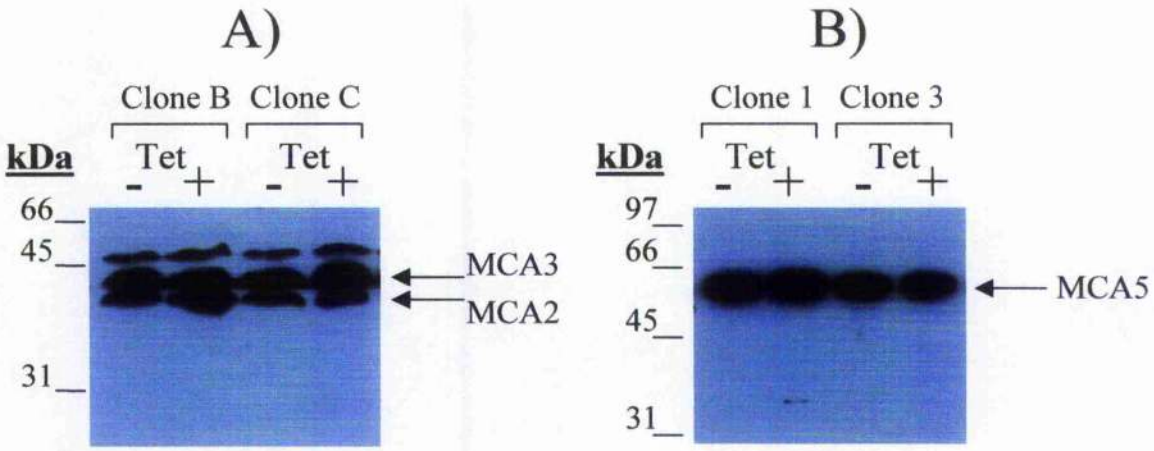

Figure 4.10: Analysis of RNAi specificity in BSF *T. brucei*.
A) Total cell lysates were prepared from *MCA5* BSF RNAi clones B and C following a 18 hour induction with 50 ng ml^{-1} tetracycline or ethanol control. $5x10^6$ cell equivalents were then subjected to SDS-PAGE and transferred to PVDF membrane prior to immunoblotting with immunopurified polyclonal rabbit anti-MCA2/3 antibodies. MCA2 and MCA3 are indicated. B) Total cell lysates were prepared from *MCA2/3* BSF RNAi clones 1 and 3 following a 24 hour induction with 50 ng ml^{-1} tetracycline or ethanol control. $5x10^6$ cell equivalents were then subjected to SDS-PAGE and transferred to PVDF membrane prior to immunoblotting with sheep polyclonal anti-MCA5 antibodies. MCA5 is indicated.

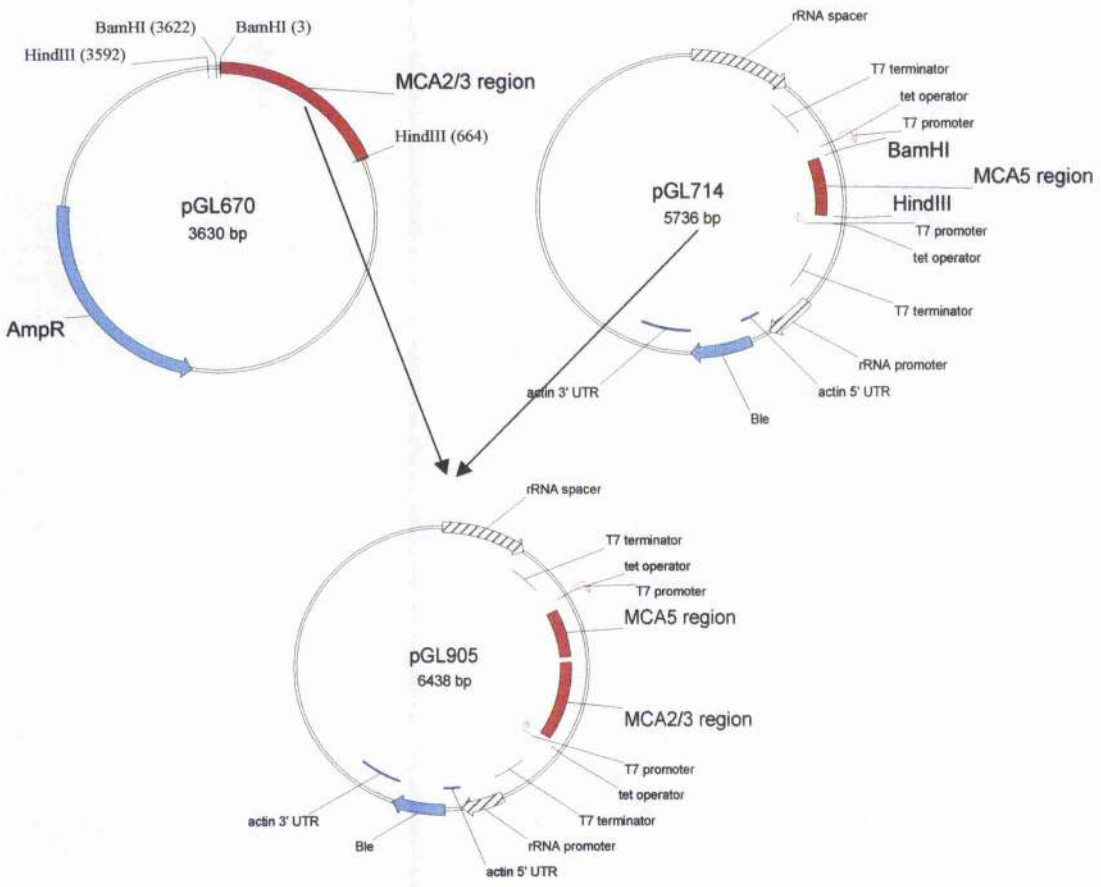

Figure 4.11: Strategy utilised to enable knockdown of *MCA2*, *MCA3* and *MCA5* by RNAi.

The fragment of *MCA5* previously used in the single RNAi studies was cloned into the *MCA2/3* RNAi vector, so that both fragments were located back to back and between the two T7 RNA polymerase promoters. pGL670 was digested with *Hind*III and the *MCA2/3* fragment cloned into pGL714 pre-digested with *Hind*III. This vector, upon integration and induction will produce dsRNA specific to both the *MCA2/3* and *MCA5* mRNA.

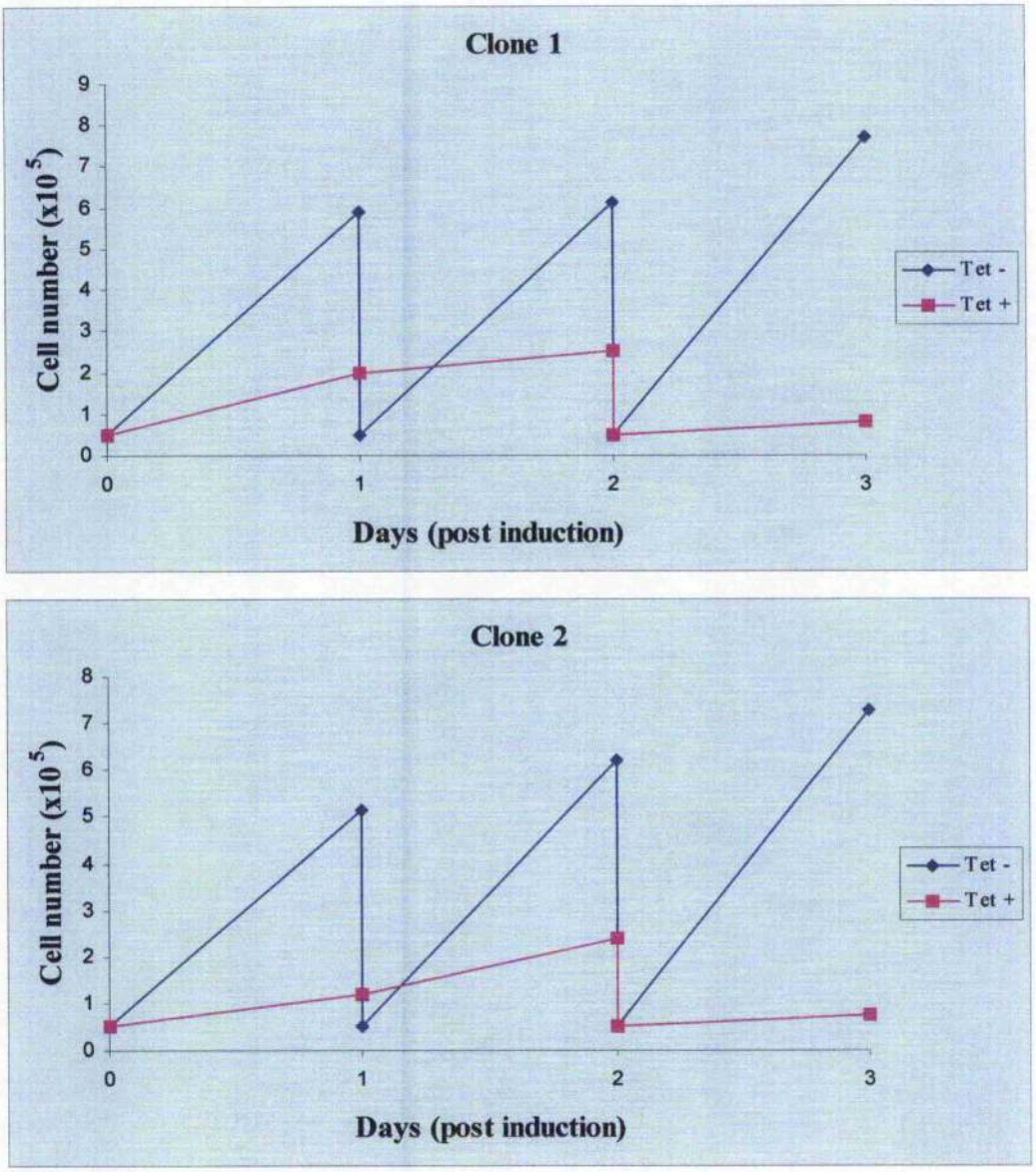

Figure 4.12: Analysis of growth rates following induction of *MCA2*, *MCA3* and *MCA5* RNAi in BSF *T. brucei*.

MCA2, MCA3 and *MCA5* BSF RNAi clones 1 and 2 were grown in the presence or absence of 50 ng ml^{-1} of tetracycline and cell numbers monitored over a 3 day period. Initial cultures were seeded at $5x10^4$ cells ml^{-1} and cell counts made daily, with cultures being re-seeded to $5x10^4$ cells ml^{-1} as and when required to maintain cultures in a logarithmic growth phase.

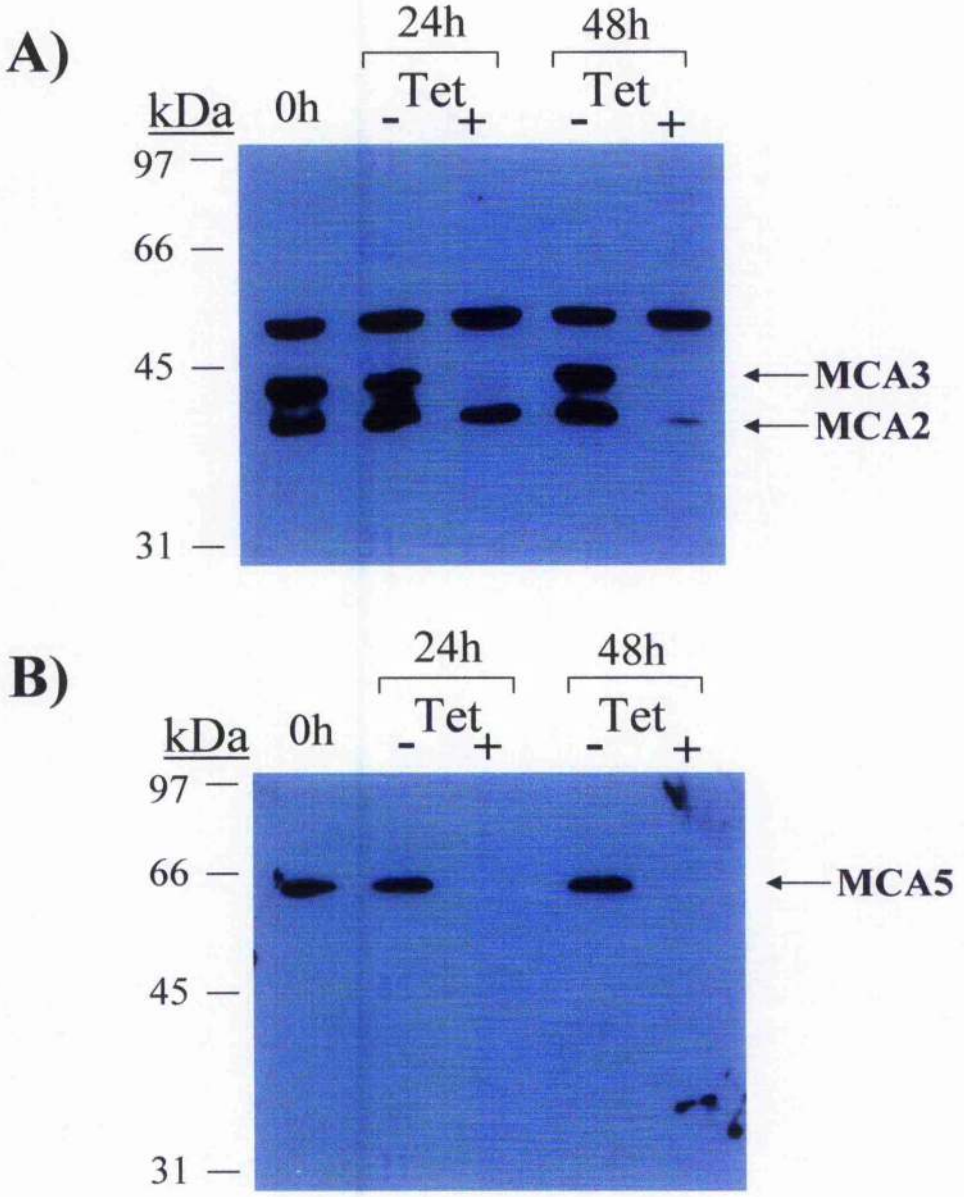

Figure 4.13: Analysis of MCA2, MCA3 and MCA5 expression following RNAi induction in BSF *T. brucei*.

Total cell lysates were prepared from *MCA2, MCA3 and MCA5* BSF RNAi clone 1 following induction with 50 ng ml^{-1} tetracycline or ethanol control for 0, 24 and 48 hours. $5x10^6$ cell equivalents were then subjected to SDS-PAGE and transferred to PVDF membrane prior to immunoblotting with A) immunopurified polyclonal rabbit anti-MCA2/3 antibodies or B) polyclonal sheep anti-MCA5 antiserum. MCA2, MCA3 and MCA5 are indicated.

Chapter 5

Gene knockouts and phenotype analysis

5.1. Knockout of *MCA2* and *MCA3* in BSF *T. brucei*.

The study of *MCA2* and *MCA3* by RNAi had suggested that these were non-essential genes for the BSF *in vitro* (Chapter 4). To test this hypothesis and gain further insights into metacaspase function, the generation of *MCA2* and *MCA3* deletion mutants was attempted. *MCA2 and MCA3*, being both single copies genes and located sequentially on chromosome 6, enabled a strategy to be pursued whereby both genes could be simultaneously deleted. Utilising flanking regions surrounding the *MCA2* and *MCA3* locus, the targeted deletion of both genes in a single recombination event would theoretically be possible. Examination of the *MCA2* and *MCA3* locus, however, revealed that not only are the genes highly homologous, as previously discussed (Chapter 3), but so too are the immediate 5' and 3' flanking regions of both genes. Therefore, the utilisation of regions immediately adjacent to *MCA2* and *MCA3* as flanking regions would result in a variety of recombination events being possible and the deletion of both genes simultaneously would not be guaranteed. To avoid these complications and ensure knockout of both *MCA2* and *MCA3*, unique flanking regions were chosen outside of these homologous regions while avoiding encroachment into the reading frames of either the upstream or downstream genes (Figure 5.1A).

Oligonucleotides were synthesised and PCR performed on genomic DNA (strain 427) to generate these flanking regions, which were then sequenced to ensure fidelity and cloned into a *T. brucei* knockout vector (Figure 5.1B) first described by Cross *et al.* (2002). These vectors contain tubulin intergenic regions to facilitate trans-splicing and polyadenylation of mNRA and ensure translation of the resistance markers. The two markers utilised to delete the native alleles were the *blasticidin* (*BSD)* and *puromycin* (*PAC*) resistance genes. Wild type BSF (strain 427) parasites were transfected with one of the knockout cassettes excised from either the *BSD*- or *PAC*-containing knockout vector. Clones were attained by limiting dilution in 24-well plates, using the appropriate antibiotics. The replacement of the *MCA2* and *MCA3* locus with the *BSD* knockout construct was straightforward, the construct integrating efficiently with approximately 90% of transformants having the correct

integration as assessed by PCR. The generation of single allele replacement mutants using the *PAC*-containing knockout cassette, however, was not so straightforward. The generation of resistant clones required a much-increased DNA concentration and the percentage of correct recombination events was reduced to approximately 15%.

Due to the difficulties, described above, encountered with the use of the *PAC*-knockout construct, attempts at generating *MCA2* and *MCA3* null mutants were performed only with the *PAC*-containing heterozygotes already generated. Two independent *PAC* heterozygotes were transfected with the *BSD* knockout cassette and clones attained, by limiting dilution, that were resistant to both antibiotics. Analysis demonstrated that two, of the six clones generated, had lost both copies of the *MCA2* and *MCA3* locus. The remaining four clones, although resistant to both antibiotics, still possessed a copy of the native *MCA2/3* locus.

To illustrate both the correct integration of the knockout cassettes and deletion of the *MCA2* and *MCA3* locus, a PCR analysis was performed on genomic DNA isolated from the mutant parasites (Figure 5.2). To confirm the correct integration of the knockout cassettes, oligonucleotide primers were designed to be specific to regions immediately upstream and downstream, respectively, of the 5' and 3' flanking regions used in the knockout strategy. These were then used in combination with *BSD* and *PAC* gene-specific primers to illustrate the correct integration of the knockout cassettes in both the single allele heterozygotes and Δ*mca2/3* mutants. To show loss of the *MCA2* and *MCA3* locus, PCR was performed using primers specific to these genes. The predicted product sizes for the 5' and 3' *BSD* integration PCRs were 792 and 900 base pairs, respectively. For the 5' and 3' *PAC* integration PCRs the predicted products were 792 and 1052 base pairs, respectively, while the *MCA2* and *MCA3* specific primers produce a product of 641 base pairs. The analysis revealed that both the single allele and two independent knockout mutants had the correct integration of resistance markers, and also that *MCA2* and *MCA3* were no longer detectable in the Δ*mca2/3* parasites.

To further confirm these knockouts, a Southern blot analysis was performed on genomic DNA prepared from mutant parasites. Physical maps of the native locus, and the modified locus upon replacement with either *BSD* or *PAC* knockout cassettes were generated, allowing prediction of the fragment sizes generated upon digestion with the restriction enzyme *Kpn*I (Figure 5.3A). Upon probing the Southern blot with the 5' flanking region used in the knockout strategy, gene fragments of the predicted sizes were detected. A fragment of approximately 9 kb, as predicted for the native locus, was detected in both wild type and the single allele heterozygotes, but was absent from the two independent null mutants. Fragments of 1.7 and 1.9 kb, as predicted for the *BSD* and *PAC* replacement loci, respectively, were detected in the appropriate single allele heterozygotes and the two independent null mutants (Figure 5.3B). Despite a high stringency wash step, an additional faint band of approximately 4 kb, of unknown identity, was also detected in all extracts. These data further confirmed the correct integration of the knockout cassettes and deletion of both *MCA2* and *MCA3*.

Western blot analysis was also performed on wild type and the two independent Δ*mca2/3* mutants to confirm loss of protein. Whole cell lysates were prepared, subjected to SDS-PAGE and transferred to PVDF membrane prior to probing with anti-*MCA2/3* specific antibodies (Figure 5.4). Proteins running at approximately the predicted sizes of MCA2 and MCA3, of 38 and 39 kDa respectively, were detected in wild type extracts but were absent from the two independent Δ*mca2/3* parasites, termed clones 1 and 2. This analysis further illustrated the deletion of *MCA2* and *MCA3* from the Δ*mca2/3* parasites. The non-specific cross-reacting protein detected in the Western blots acts as an in built loading control and demonstrates equal loading.

5.2 Re-expression of *MCA2* and *MCA3* in Δ*mca2/3* BSF parasites.

The generation of Δ*mca2/3* mutants made it possible to generate parasites re-expressing either MCA2 or MCA3 independently. Both *MCA2 and MCA3* had previously been cloned, sequenced to ensure fidelity and used in *E. coli* expression

work by Gareth Westrop and Sanya Sanderson (University of Glasgow). These genes were individually sub-cloned into the *T. brucei* re-expression vector designed for integration into the αβ tubulin array, as previously described in chapter 3. Δ*mca2/3* clone 1 was transfected with each of these constructs and clones obtained by limiting dilution using bleomycin as the selection drug. Whole cell extracts were then prepared from both Δ*mca2/3*:*MCA2* and Δ*mca2/3*:*MCA3* clones, subjected to SDS-PAGE, transferred to PVDF membrane and probed with anti-*MCA2*/3 antibodies (Figure 5.5). The Western blot analysis illustrated that the re-expression of both genes was successful and that the protein levels were similar to wild type parasites. This experiment further confirmed the identity of MCA2 and MCA3.

5.3 *In vitro* and *in vivo* analysis of Δ*mca2/3* parasites.

The ability to generate Δ*mca2/3* parasites demonstrated that these two genes are non-essential *in vitro*, as the previous RNAi experiments had suggested. These mutant parasites displayed no obvious phenotypic or morphological alterations as a result of loss of the two metacaspase genes, and a comparative analysis of growth rates *in vitro* revealed no pronounced alterations (Figure 5.6A). To determine whether *MCA2* and *MCA3* might be more important in a natural infection, wild type parasites were compared to Δ*mca2*/3 clone 1 *in vivo* using the mouse strain BALB/c as a model. Both wild type and Δ*mca2*/3 clone 1 parasites were initially passaged through mice, parasitaemia determined and a group of six mice for both lines injected interperitoneally with a parasite load of $1x10^3$ per animal and parasitaemia monitored over the course of the infection. Only two time points could be recorded (days 3 and 4 (Figure 5.6B)), as the experiment had to be terminated on day 4 due to the high parasitaemia within the animals and numbers were too low on day 2 to make a recording. The data obtained illustrate that the deletion of *MCA2* and *MCA3* from BSF parasites does not appear to affect either the virulence or growth rate of Δ*mca2/3* parasites in BALB/c mice.

5.4 Knockout of *MCA5* in BSF and PCF *T. brucei*.

MCA5 is a single copy gene and is expressed in both PCF and BSF parasites (Chapter 3). Previous RNAi experiments had suggested that knockout of *MCA5* in both of these life stages would be possible. However, the RNAi experiments also suggested that generation of a triple metacaspase null mutant might not be possible (Chapter 4). To test this hypothesis a similar strategy was adopted for the knockout of *MCA5* to that which had been used successfully for the deletion of *MCA2* and *MCA3*. Oligonucleotides were designed to amplify regions of approximately 750 base pairs flanking the *MCA5* gene (Figure 5.7A) and PCR performed on genomic DNA (strain 427). These flanking regions were then sequenced to ensure fidelity and exchanged for the *MCA2/3* flanking regions in pGL802, the *BSD* knockout vector used in the Δ*mca2/3* generation. To allow for the possible generation of Δ*mca2/3*Δ*mca5* parasites it was necessary to replace the two resistance genes used previously, *BSD* and *PAC*, with two distinct markers. The two chosen were *HYG* and *NEO*, and the sequences for these genes were exchanged for the *BSD* gene in pGL802 to generate pGL906 and pGL907 (Figure 5.7B).

Initially these constructs were used to attempt deletion of *MCA5* from both wild type BSF (strain 427) and PCF (EATRO 795) parasites. Both BSF and PCF parasites were transfected with the knockout cassettes excised from pGL906 and pGL907, and clones attained by limiting dilution using the appropriate antibiotics. Single allele *MCA5* replacements were generated easily in both BSF and PCF parasites with all clones analysed having the correct integration as assessed by PCR. These heterozygotes were then used for a second round of transfections to generate Δ*mca5* parasites in both life stages. Two independent clones, termed clones 1 and 2, were generated for both life stages.

To illustrate both the correct integration of the knockout cassettes and deletion of the *MCA5* locus, a PCR analysis was performed on parasite genomic DNA isolated from mutant parasites. Oligonucleotide primers were designed to be specific for regions immediately upstream and downstream of the 5' and 3' flanking regions used in the

knockout strategy. These were used in combination with *HYG*- and *NEO*- specific primers to test for correct integration of the knockout cassettes in both the single allele heterozygotes and Δ*mca5* mutants (Figure 5.8). The predicted product sizes for the 5' and 3' *HYG* integration PCRs are 2246 and 2545 base pairs, respectively. For the 5' and 3' *NEO* integration PCRs the predicted products were 2023 and 2098 base pairs, respectively, while the *MCA5* gene-specific primers produce a product of 1500 base pairs. The analysis revealed that both the Δ*mca5* clones generated in the BSF and PCF had the correct integration of resistance markers, and also that *MCA5* was no longer detectable (Figure 5.9). All further discussion related to the Δ*mca5* BSF and PCF parasites will refer to clone 1 unless otherwise stated.

To confirm the deletion of *MCA5*, whole cell lysates were prepared from BSF and PCF wild type and Δ*mca5* parasites. These were then subjected to SDS-PAGE, transferred to PVDF membrane and immunoprobed with anti-*MCA5* antiserum (Figure 5.9). The Western analysis shows that the single protein running at approximately the predicted size of MCA5, 55 kDa, was present in wild type but absent from the Δ*mca5* extracts. This confirmed that *MCA5* deletion was possible in both life stages.

5.5 *In vitro* analysis of Δ*mca5* parasites.

The generation of Δ*mca5* mutants in both BSF and PCF parasites confirmed that, as suspected, *MCA5* is a non-essential gene in both life stages. Δ*mca5* parasites displayed no gross morphological alterations relative to wild type and a comparison of the growth rates of wild type and Δ*mca5* in both the PCF and BSF parasites revealed that there were no pronounced alterations in growth rate (Figure 5.10). Therefore it appears that the deletion of *MCA5* results in no obviously detrimental effect to *T. brucei in vitro*.

5.6 Knockout of *MCA5* in Δ*mca2/3* BSF parasites.

While the ability to generate single Δ*mca2/3* and Δ*mca5* parasites had been predicted from the RNAi studies (Chapter 4), the situation with the triple deletion of all three

genes in the BSF was less clear. Unlike the *MCA2/3* and *MCA5* RNAi studies, no clones had been analysed where silencing of the all three metacaspases using RNAi did not adversely affect the parasites. Although this was suspected to be at least partially due to an artefact of the technique, the data available were insufficient to conclude this with certainty.

To address these questions, the Δ*mca2/3* BSF clone 1 previously generated was transfected with either the *HYG* and *NEO MCA5* knockout cassettes and clones attained by limiting dilution using the appropriate antibiotics. Analysis of resistant parasites illustrated that all of the heterozygotes generated had the correct integration of the knockout cassettes as assessed by PCR. Second round transfections were then subsequently performed in both the *HYG* and *NEO* heterozygotes and two independent, double-resistant clones attained, termed clones 1 and 2. A PCR analysis, using the same strategy as illustrated in figure 5.8, was performed to demonstrate correct integration of the knockout cassettes and loss of *MCA5* (Figure 5.12). The analysis revealed that both the Δ*mca2/3*Δ*mca5* clones generated had the correct integration of resistance markers, and also that *MCA5* was no longer detectable. All further discussion related to the Δ*mca2/3*Δ*mca5* parasites will refer to clone 1 unless otherwise stated.

To confirm the deletion of *MCA5*, whole cell lysates were prepared from both wild type and Δ*mca2/3*Δ*mca5* clone 1 BSF parasites, subjected to SDS-PAGE, transferred to PVDF membrane and immunoprobed with both anti-*MCA2/3* antibodies and anti-*MCA5* antiserum (Figure 5.13B). The Western analysis confirmed that the parasites lacked MCA5 and illustrated that *MCA5* deletion is possible in Δ*mca2/3* parasites.

5.7 Re-expression of *MCA2*, *MCA3* and *MCA5* in Δ*mca2/3*Δ*mca5* BSF parasites.

With the generation of Δ*mca2/3*Δ*mca5* mutants, it was possible to generate parasites expressing any of *MCA2*, *MCA3* or *MCA5* independently. The constructs required for *MCA2* and *MCA3* re-expression had already been generated (pGL867 and pGL868 (Chapter 3)), although it was necessary to create a vector for the *MCA5* re-

expression. *MCA5* had already been cloned, sequenced to ensure fidelity and used to produce recombinant protein within *E. coli* for the generation of antibodies (Chapter 3). The sequence for *MCA5* was now sub-cloned into the *T. brucei* re-expression vector designed for integration into the αβ tubulin array (previously described in chapter 3) to generate pGL927. Δ*mca2/3*Δ*mca5* parasites were transfected individually with the three re-expression cassettes, excised from their respective vectors, and clones obtained by limiting dilution using bleomycin as the selection drug. Whole cell extracts were then prepared from Δ*mca2/3*Δ*mca5*:*MCA2*, Δ*mca2/3*Δ*mca5*:*MCA3* and Δ*mca2/3*Δ*mca5*:*MCA5*, subjected to SDS-PAGE, transferred to PVDF membrane and probed with both anti-MCA2/3 antibodies and anti-MCA5 antiserum (Figure 5.13). The Western blot analysis illustrated that the re-expression of all three genes had been successful and at similar protein levels to wild type parasites.

5.8 *In vitro* and *in vivo* analysis of Δ*mca2/3*Δ*mca5* BSF parasites.

The ability to generate Δ*mca2/3*Δ*mca5* parasites demonstrates that *MCA2*, *MCA3* and *MCA5* are non-essential genes (at least under the conditions tested) and further questions the validity of the RNAi phenotype discussed in chapter 4. Interestingly, while the generation of Δ*mca2/3*Δ*mca5* BSF parasites was possible, a phenotype was observed upon their generation. Δ*mca2/3mca5* mutants initially displayed a reduced growth rate, taking a longer time than expected for the clones to grow following the transfection. Usually BSF (strain 427) parasites require passaging approximately six days after transfection and cloning, due the rapid growth rate of this strain. In the Δ*mca2/3*Δ*mca5* parasites, however, this period was extended to 13 days. This phenomenon was also observed in Δ*mca2/3*Δ*mca5* clone 2. A comparison of growth rate of the Δ*mca2/3*Δ*mca3* and wild type parasites was performed, which highlighted this reduced growth rate (Figure 5.14A). This reduced growth rate was not permanent, however, and after approximately two weeks of culturing and successive passages the growth rate returned to wild-type levels (Figure 5.14B). This phenomenon had not been observed in the single *MCA5* knockouts in either the BSF or PCF.

To determine whether there might be a difference between wild type and Δ*mca2/3*Δ*mca5* with regard to infectivity or growth rate *in vivo*, a comparison between growth of the two lines in ICR mice was performed. This was carried out following the apparent adaptation period, and at which time both wild type and Δ*mca2/3*Δ*mca5* had equivalent growth rates *in vitro*. Each cell line was passaged once through a mouse, parasitaemia determined and a group of six mice for both lines injected interperitoneally with a total of $1x10^2$ parasites per animal. The course of infection was followed by 24-hourly assessments of infected blood from the third day post injection onwards (Figure 5.14C). The data illustrate that the Δ*mca2/3*Δ*mca5* parasites showed no reduction in either virulence or growth rate compared to wild type parasites.

5.9 Analysis of recycling processes in Δ*mca2/3*Δ*mca5* BSF parasites.

As the metacaspases were found to be associated with Rab11 positive recycling endosomes (Chapter 3), further phenotype analysis on the Δ*mca2/3*Δ*mca5* parasites focused upon recycling processes. Recycling of surface molecules has been well characterised in the BSF, while in the PCF very little is known and no molecules that are actively recycled have been identified. In the BSF there are two cell surface molecules known to be actively recycled, VSG (Seyfang *et al.*, 1990) and the transferrin receptor (Kabiri and Steverding, 2000).

5.9.1 VSG recycling is unaffected in Δ*mca2/3*Δ*mca5* parasites.

The rapid recycling of VSG is considered essential for survival of the BSF *in vivo*, as it is viewed as a secondary defence against the immune response by clearing host anti-VSG antibodies from the cell surface. It has been reported that the rate of endocytosis in *T. brucei* is extremely rapid, the total VSG cell surface pool can be turned over in 12 minutes (Engstler *et al.*, 2004). Due to the high stability of VSG, the majority of this internalised VSG is recycled back to the surface (Seyfang *et al.*, 1990), while host anti-VSG antibodies are degraded and secreted (O'Beirne *et al.*, 1998) via Rab11 positive endosomes (Pal *et al.*, 2003).

A comparison between wild type and *Δmca2/3Δmca5* parasites was performed to determine whether the metacaspases might be involved in the recycling of VSG. To examine VSG recycling, the parasite's surface coat was biotinylated with NHS-SS-Biotin at 4°C for 10 mins prior to returning to 37°C for 5 mins to allow endocytosis to reach a steady state (Grünfelder *et al.*, 2003). The removal of any biotin label remaining on the cell surface was facilitated through the incubation of parasites with 50 mM glutathione for 7 mins at 4°C, resulting in the cleavage of the disulphide bond present within the biotin label. Whole cell extracts were prepared at this point, subjected to SDS-PAGE, transferred to PVDF membrane and probed with a streptavidin-HRP conjugate (Figure 5.15A). A single protein, with an equivalent intensity, was detected in both wild type and *Δmca2/3Δmca5* extracts, demonstrating that the endocytosis of Biotin-VSG was still functional following deletion of the metacaspases. Following the cleavage of cell surface biotin, parasites were resuspended in HMI-9 at 37°C for 1 hour to allow time for internalised Biotin-VSG to be recycled back to the cell surface. Parasites were then prepared for IFA and Biotin-VSG detected using a streptavidin-TexasRed conjugate. Parasites were also co-stained using rabbit anti-Rab11 antibodies (Figure 5.15B). This analysis revealed that in both wild type and *Δmca2/3Δmca5* parasites internalised Biotin-VSG co-localised with Rab11. Additionally, following the 1 hour chase period, both wild type and *Δmca2/3Δmca5* parasites were able to recycle this internalised VSG and return it to the cell surface. Therefore, it appears that the loss of MCA2, MCA3 and MCA5 does not prevent endocytosis of VSG, the trafficking through Rab11 positive vesicles or its subsequent return to the cell surface.

5.9.2 Anti-VSG antibody degradation is unaffected in *Δmca2/3Δmca5* parasites.

Having shown that MCA2, MCA3 and MCA5 do not appear to be essential for the recycling of VSG, the possibility of a role in anti-VSG antibody degradation was examined. It has been documented previously that internalised anti-VSG antibodies partially co-localised with Rab11 recycling endosomes (Jeffries *et al.*, 2001) and therefore, by inference, with MCA5, which we have confirmed (Chapter 3).

To study these processes, it was first necessary to determine the VSG isoform expression in both the wild type and *Δmca2/3Δmca5* parasites. The BSF 427 strain, in which the knockouts were performed, is a monomorphic laboratory-adapted cell line. The VSG switching rate in this cell line is extremely low, estimated to be around 1 per 10^6 cells, compared to a pleomorphic line, where switching occurs at around 1 per 10^3 cells (Turner and Barry, 1989). Additionally, the absence of selective pressure *in vitro* will result in the VSG expression remaining highly stable. Previous work on this strain has identified that VSG221 is the predominant isoform expressed, and polyclonal antibodies against this are readily available. As the generation of null mutants required several rounds of transfection and subsequent cloning, there was a possibility that the *Δmca2/3Δmca5* parasites, which had been cloned four times, may have switched to a differential VSG isoform. To examine this possibility, whole cell lysates prepared from wild type, *Δmca2/3*, *Δmca5*, and *Δmca2/3Δmca5* parasites were subjected to SDS-PAGE, transferred to PVDF membrane and probed with polyclonal rabbit anti-VSG221 antibodies (Figure 5.16). Although overexposed, the Western blot revealed that all of the metacaspase knockout mutants generated were expressing the same VSG isoform as wild type parasites, namely VSG221. This observation was important, as a direct comparison of wild type and mutant parasites with regard to anti-VSG degradation requires them to be expressing the same VSG isoform.

The peptidases responsible for the degradation of anti-VSG antibodies have not been characterised, nor has the compartment where this occurs been identified. The localisation of the metacaspases within recycling endosomes, which traffic these anti-VSG antibodies, raises the possibility that they might be involved in the process. To investigate this hypothesis, parasites were labelled with a polyclonal rabbit anti-VSG221 antibody at 4°C for 30 mins, washed extensively and incubated at 37°C for a further 30 mins. Following this period, parasites were examined by IFA to confirm that no significant amounts of antibody remained on the surface (Figure 5.17A). Whole cell lysates (Figure 5.17B) and TCA precipitations of the culture medium (Figure 5.18) were then subjected to SDS-PAGE, transferred to PVDF membrane

and probed with an anti-rabbit HRP conjugate to determine the fate of these antibodies.

Examination of cell-associated anti-VSG221 antibodies illustrated that there was no build up of anti-VSG221 antibodies within *Δmca2/3Δmca5* parasites compared to wild type parasites (Figure 5.17B). A single protein was detected at equivalent levels in both cell lines. It is believed to be rabbit heavy chain IgG, which has a predicted size of 45 kDa. Analysis of the secreted products illustrated that the degradation of the anti-VSG antibodies was unaffected in *Δmca2/3Δmca5* parasites (Figure 5.18). While there was some intact heavy chain detected, there were degradation products as well. However, the degradation profile is identical in both wild type and *Δmca2/3Δmca5* parasites. These data show that the *Δmca2/3Δmca5* parasites are still functional with regard to anti-VSG antibody internalisation, degradation and secretion and shows that the absence of MCA2, MCA3 and MCA5 from recycling endosomes does not affect this process.

5.9.3 Transferrin uptake is unaffected in *Δmca2/3Δmca5* parasites.

Rab11 positive recycling endosomes have also been characterised with regard to the recycling of the *T. brucei* transferrin receptor (Pal *et al.*, 2003). The *T. brucei* transferrin receptor is a low abundance protein, encoded by two homologous genes ESAG6 and ESAG7 (Steverding *et al.*, 1994; Salmon *et al.*, 1994), limited in its distribution to the flagellar pocket (Steverding *et al.*, 1994). Following internalisation of the receptor-transferrin complex, the reduction in pH within the endosomal system is believed to cause dissociation of transferrin from the receptor (Dautry-Varsat *et al.*, 1983; Maier and Steverding, 1996). The transferrin receptor is then recycled back to the flagellar pocket via Rab11 positive recycling endosomes (Jeffries *et al.*, 2001) and degraded transferrin secreted (Steverding *et al.*, 1995; Pal *et al.*, 2003). To investigate whether the metacaspases might be involved in this pathway, a comparison of transferrin uptake, degradation and secretion was performed in wild type and *Δmca2/3Δmca5*. BSF parasites were incubated with a human transferrin-biotin conjugate and whole cell lysates prepared following 5, 10,

15 and 60 mins, together with a 10 mins chase. These lysates were then subjected to SDS-PAGE, transferred to PVDF and probed with a streptavidin-HRP conjugate (Figure 5.19A). The Western analysis revealed that both wild type and *Δmca2/3Δmca3* parasites were able to internalise approximately equal levels of transferrin over the time points examined. If a defect in transferrin receptor recycling was evident we might have expected to see less internalised transferrin over the period, this was not observed. Following the 10 mins chase period no transferrin was detectable in either wild type or *Δmca2/3Δmca5* parasites, suggesting that the degradation of transferrin was also unaffected by loss of MCA2, MCA3 and MCA5. To examine the degradation products of transferrin, TCA precipitation was also performed on the culture medium following the chase period. Upon probing, however, there were found to be barely detectable levels of the transferrin biotin conjugate and no detectable degradation products, as had been seen in the comparable anti-VSG antibody experiment (not shown). It has been reported that *T. brucei* is able to regulate the expression of the transferrin receptor dependent on the availability of transferrin within the culture medium (Fast *et al.*, 1999; Mussmann *et al.*, 2004). If the transferrin uptake pathway was detrimentally affected by metacaspase deletion, then the expression of the transferrin receptor might, theoretically, be up regulated. Therefore, whole cell lysates were prepared from wild type and *Δmca2/3Δmca5* clones 1 and 2. These lysates were then subjected to SDS-PAGE, transferred to PVDF membrane and immunoprobed with anti-transferrin receptor antibodies (Figure 5.19B). The Western analysis detected both ESAG6 and ESAG7 at approximately equivalent levels in wild type and mutant parasites. The presence of double bands represents differential glycoyslation of the proteins (Steverding D. 2004). In conclusion, the data gathered on the transferrin pathway suggest that the deletion of *MCA2*, *MCA3* and *MCA5* does not affect normal transferrin uptake or degradation in BSF parasites.

5.10 Responses to stressful stimuli in wild type and *Δmca2/3Δmca5* parasites.

Having been unable to detect any differences between wild type and *Δmca2/3Δmca5* with regard to recycling processes, other possibilities for metacaspase function were

investigated. As discussed earlier there have been reports of metacaspase involvement in apoptotic-like phenomenon in yeast (Madeo *et al.*, 2002; Szallies *et al.*, 2002; Ilerker *et al.*, 2004; Wadskog *et al.*, 2004), although none specifically within *T. brucei*. Additionally there have been numerous reports of apoptotic-like cell death occurring within protozoa, including *T. brucei*, following a variety of stressful stimuli, although none of these have been linked directly with metacaspase function (for review see Debrabant *et al.*, 2003).

The exposure of parasites to such stimuli had previously been performed when attempts were made to activate processing of the metacaspases in wild type parasites (Chapter 3). The stimuli used to compare wild type and Δ*mca2/3*Δ*mca5* parasites responses to stressful conditions were heat shock and exposure of parasites to salt stress.

5.10.1 Comparison of response to heat shock.

It has been reported that *L. amazonensis* upon heat shock undergo cell death displaying markers of apoptosis similar to higher eukaryotes (Moreira *et al.*, 1996). Although such a process has not been characterised in *T. brucei*, a comparative analysis of wild type and Δ*mca2/3*Δ*mca5* BSF parasites was performed following an exposure to elevated temperatures. Both cell lines, at the same density, were incubated for 2 hours at 42°C and subsequently returned to normal growth conditions of 37°C. The 2 hour incubation period was chosen as incubations under this period had little apparent effect on parasite growth. Cell densities were counted on return to the 37°C temperature and again after a 4 hour period (Figure 5.20A). The control cells, which had not been subjected to the heat shock, continued to grow normally, while the density of the parasites exposed to the 2 hour heat shock did not increase over the 4 hours recovery at 37°C. Parasites were then re-suspended at $5x10^4$ cells ml^{-1} in fresh medium with cell counts and re-seeding performed at 24 hour intervals (Figure 5.20B). The analysis revealed that during the three-day period over which growth rates were monitored, the parasites exposed to the heat shock began to recover and approach control parasite growth levels. Importantly, however,

both wild type and Δ*mca2/3*Δ*mca5* parasites behaved in a similar manor with regard to the initial response to the heat shock and the more long term recovery.

5.10.2 Comparison of response to salt stress.

It has recently been documented that apoptotic-like cell death in yeast induced via salt stress was inhibited following metacaspase deletion (Wadskog *et al.*, 2004). In an attempt to determine if a similar relationship exists in *T. brucei*, a comparative analysis between wild type and Δ*mca2/3*Δ*mca5* BSF parasites was performed. Cultures of both cell lines were set up at equal densities and grown in normal HMI-9 or with the addition of 125 mM NaCl (Figure 5.21A). Cell densities were monitored over a 5 hour period with the analysis revealing that this salt concentration was highly toxic to the parasites. However, reducing the concentration to 62.5 mM was observed to have little effect on parasite culture densities over the same period (not shown). A comparison of the growth curves for both wild type and Δ*mca2/3*Δ*mca5* revealed that cell death occurred at a similar rate in both cell lines over the period examined. Parasites were then washed extensively and re-seeded at $5x10^4$ cells ml^{-1} in fresh medium with cell counts and re-seeding performed at 24 hour intervals (Figure 5.21B). The analysis revealed that the recovery from salt stress, although not completed during the period of examination, occurred similarly in both wild type and Δ*mca2/3*Δ*mca5* parasites.

5.10.3 Recovery from high cell densities.

While maintaining BSF wild type and Δ*mca2/3*Δ*mca5* mutants in culture it was observed that mutant parasites upon reaching late log growth phase took longer to recover when re-seeded than their wild type counterparts. BSF parasites cultures *in vitro* begin to plateau, with regard to growth rate, when cell density exceeds $1.5x10^6$ cells ml^{-1}. It is possible to grow parasites to densities in excess of $5x10^6$ cells ml^{-1}, although cultures rapidly begin to die at this stage. To investigate these observations further, a comparison of this phenomenon was performed in wild type, Δ*mca2/3*, Δ*mca5* and Δ*mca2/3*Δ*mca5* BSF mutants. Parasites were maintained in culture until apparent stationary phase was reached. Although it was not possible to have all

cultures reaching the exact same density, all cultures were grown in excess of $4x10^6$ cells ml^{-1}. These cultures were then re-seeded in fresh medium at $5x10^4$ cells ml^{-1}, cell counts made and re-seeded at $5x10^4$ cells/ ml^{-1} every 24 hours to monitor the recovery (Figure 5.22A).

An analysis of the growth curves revealed that the wild types parasites were able to return to normal growth rates fairly rapidly. The growth rate over the first 24 hour period after re-seeding was much reduced but after this period growth rate returned to normal levels. This was not observed, however, in either the Δ*mca2/3* or Δ*mca2/3*Δ*mca5* parasites. The return to *status quo* took much longer, growth rates in these two mutants not returning to wild type levels until 7 days after the initial re-seeding. Both of these clones behaved very similarly, suggesting that this phenotype is the result of *MCA2* and *MCA3* deletion alone. The Δ*mca2/3*Δ*mca5* parasites, generated from the Δ*mca2/3 parasites*, showed no further reduction in their ability to recover. As further evidence that this phenotype was the result of *MCA2* and *MCA3* deletion, the Δ*mca5* mutant behaved much more similarly to wild type parasites with a return to normal growth occurring after 48 hours.

Having previously generated individual *MCA2* and *MCA3* re-expressers in the Δ*mca2/3* parasites, experiments were performed to test if expression of individual genes could complement this phenotype. The growth curves were repeated with wild type, Δ*mca2/3* clone 1, together with Δ*mca2/3:MCA2* and Δ*mca2/3:MCA3* parasites, with recovery rates monitored over 4 days (Figure 5.22B). As shown previously, Δ*mca2/3* parasites did not return to the same growth rate as wild type, however no complementation of this phenotype was observed as both of the re-expressers showed similar growth rates to the Δ*mca2/3* parasites.

5.10.4 Ability to adapt to reduced serum concentrations.

In addition to observations regarding recovery from high densities, another phenotype identified with the mutant parasites was an inability to adapt to reduced serum concentrations. Normal BSF HMI-9 medium contains a final volume of 20%

(v/v) serum; this is made up of 10% FCS and 10% serum plus. The rationale for performing these experiments was that the metacaspases, shown to be associated with the Rab11 positive recycling compartment, might have been involved in the transferrin uptake pathway. Transferrin is provided to the parasites exclusively in serum and by reducing the serum concentration the amount of available transferrin will be reduced. For these experiments it was decided to reduce serum concentration by 10-fold from 20% (v/v) to a final concentration of 2%. Wild type, Δ*mca2/3*, Δ*mca5* and Δ*mca2/3*Δ*mca5* parasites were seeded at $5x10^4$ cells/ml in HMI9 containing a final serum concentration of 2%. Growth rates were followed with re-seeding at $5x10^4$ cells/ml performed daily (Figure 5.23A).

This analysis revealed that all of the parasite cultures showed a much decreased growth rate over the first 24 hours. However, while *Δmca2/3* and *Δmca2/3*Δ*mca5* parasites continued to grow at this reduced rate, wild type and Δ*mca5* parasites seemed better able to adapt to these conditions and in subsequent periods the growth rate increased significantly. Therefore this phenotype again appeared to be dependent only upon *MCA2* and/or *MCA3* deletion and not *MCA5* deletion. Additionally, this phenotype was detected in the two independent Δ*mca2/3* clones generated (Figure 5.23B). This further analysis also highlighted that this apparent adaptation in wild type parasites was not permanent. On day 4 it was observed that growth rate began to decline in the wild type parasites and it was observed that maintenance in conditions of reduced serum for an extended period ultimately resulted in death of all cultures.

This again appeared a promising phenotype to investigate, however all attempts to complement this phenotype also failed. The Δ*mca2/3:MCA2* and *Δmca2/3:MCA3* parasites showed no complementation (Figure 5.23C), with the growth rate of the re-expressers closely matching those of the Δ*mca2/3* parasites.

5.11 Dual re-expression of *MCA2* and *MCA3* in Δ*mca2/3* parasites.

Whilst none of the attempts to complement either of the observed phenotypes had been successful, we wondered whether the re-expression of both *MCA2* and *MCA3* might be required for complementation. This was attempted in the Δ*mca2/3* parasites for several reasons. Firstly, as described both phenotypes were present in Δ*mca2/3* parasites and the additional deletion of *MCA5* did not acerbate either phenotype. Secondly, the dual re-expression of *MCA2* and *MCA3* in the Δ*mca2/3* parasites would return the full complement of metacaspase genes to the parasites and therefore should enable a determination of the reality of this phenotype. Thirdly, for practical reasons the re-expression of *MCA2* and *MCA3* in the Δ*mca2/3*Δ*mca5* parasites would require the use of six drug resistance markers, four used to generate the mutant and one for each of the re-expressed genes. There are not currently this many drug resistance markers for use in *T. brucei* BSF.

To perform the dual re-expression of *MCA2* and *MCA3*, Δ*mca2/3:MCA2* parasites were transfected with the *MCA3* re-expression cassette. However, to permit selection it was necessary to exchange the *BLE* resistance gene within the *MCA3* re-expression construct for the *HYG* resistance gene, the Δ*mca2/3:MCA2* parasites already being resistant to bleomycin. The modified MCA3 re-expression cassette was then excised from the vector (pGL1079), used to transfect Δ*mca2/3:MCA2* parasites and clones attained by limiting dilution.

To determine if the re-expression of *MCA3* had been successful, whole cell lysates were prepared from wild type, Δ*mca2/3*, Δ*mca2/3:MCA2*, Δ*mca2/3:MCA3* and the newly generated Δ*mca2/3:MCA2:MCA3* parasites. These extracts were then subjected to SDS-PAGE, transferred to PVDF and probed with anti-MCA2/3 antibodies (Figure 5.24). The Western blot analysis confirmed that the dual re-expression of *MCA2* and *MCA3* in the Δ*mca2/3* parasites had been successful, with the expression from the tubulin locus producing levels of expression similar to wild type parasites. With the generation of dual re-expressers it was possible to test the hypothesis that both genes might be required for complementation of the observed

phenotypes. Both the recovery from high densities and reduced serum experiments were repeated in wild type, Δ*mca2/3*, Δ*mca2/3:MCA2*, Δ*mca2/3:MCA3* and Δ*mca2/3:MCA2:MCA3* parasites (Figure 5.25). However, despite the re-expression of both metacaspases genes, and a return to a full complement of metacaspases, there was no rescue of either of the phenotypes.

5.12 Discussion.

5.12.1 Generation of mutants.

The genetic knockouts of the metacaspases were able to answer some of the questions raised from the RNAi studies. The RNAi experiments on *MCA2* and *MCA3* in the BSF had suggested that these were non-essential genes. This could not be claimed definitively, however, because the possibility remained that even with a highly reduced expression of *MCA2* and *MCA3* their functions might still be sufficiently fulfilled. The generation of knockout mutants however, confirmed that *MCA2* and *MCA3* are non-essential genes *in vitro*, the clones generated being indistinguishable from their wild type progenitors in terms of growth rate and gross morphology. Similarly the deletion of MCA5 in both PCF and BSF parasites confirmed what had been suggested by the RNAi studies, namely that *MCA5* is also a non-essential gene *in vitro*. The deletion of *MCA5* having no obviously apparent affects on either growth rate or morphology. We have previously speculated that there might be redundancy within the metacaspase family, particularly in the BSF where all three of the studied metacaspases are expressed. The knockout of *MCA5* in the PCF without any apparent detriment to the parasites suggests that these parasites can function adequately in the absence of the metacaspases. However, with no information of the expression profile of the two remaining metacaspases, *MCA1* and *MCA4*, this tentative conclusion may not hold up to further study.

Due to the expression of a larger number of the studied metacaspases, and the more active recycling system that the proteins have been shown to co-localise with, the analysis of mutants concentrated on the BSF. Although the *Δmca2/3* parasites showed no obvious phenotype *in vitro*, it was plausible to suggest that the metacaspases might be involved in interactions with the host *in vivo*. Cysteine peptidases of parasitic protozoa have been implicated in a variety of biological events, including immune evasion, pathogenesis and virulence. The CPB array of *Leishmania mexicana*, for example, has been shown to be involved in successful invasion and establishment *in vivo* (Denise *et al.*, 2003), with a marked decrease in

lesion size and parasite growth in mice observed upon deletion of this array. In *Plasmodium falciparum*, specific falcipain-1 inhibitors blocked parasite invasion of host erythrocytes (Greenbaum *et al.*, 2002). Metacaspase association with Rab11 positive recycling endosomes also suggested that a role *in vivo* might be important. One of the features absent under normal *in vitro* culturing is an immune challenge. The removal of host antibodies bound to the parasite surface is facilitated during the active recycling of VSG for which Rab11 positive recycling endosomes are intimately involved (Jeffries *et al.*, 2001). If metacaspases were involved only in immune evasion, for example, the deletion of *MCA2* and *MCA3* might not be expected to manifest *in vitro*. However, when a comparison of wild type and Δ*mca2/3* was performed in an *in vivo* mouse model of infection there was no difference between the two lines, the Δ*mca2/3* parasites being able to establish an infection and grow at wild type levels. This suggests that *MCA2* and *MCA3* are truly non-essential genes and their functions are either not majorly important or can be compensated for. Upon generation of Δ*mca2/3*Δ*mca5* BSF parasites, the *in vivo* study was repeated. It was decided to use adapted Δ*mca2/3*Δ*mca5* parasites that were growing at wild type levels so any differences between the cell lines could be distinguished from the initial slow growth phenotype observed *in vitro*. However, as had been seen with the Δ*mca2/3* parasites, the mutants were able to establish an infection and showed no reduction in growth rate *in vivo*.

There are limitations, however, with the *in vivo* model that was used in this study. The BSF 427 strain used to generate the null mutants is a laboratory-adapted monomorphic cell line (Cross and Manning, 1973) and is thus easy to maintain *in vitro*, which is obviously advantageous when performing work *in vitro* such as gene knockouts or RNAi studies. Unfortunately, this strain is not particularly practical *in vivo*, due to its rapid growth rate. The parasites replicate so rapidly that the mouse's immune system is unable to react fast enough to control the infection and parasitaemia very rapidly reaches a point were the animal has to be killed. Natural *T. brucei* infections are typically chronic, with waves of parasitaemia occurring periodically. Chronic infections can be modelled in mice *in vivo* using pleomorphic

parasites (Turner, 1999) although these are typically much more demanding with regard to *in vitro* culturing. It is debatable, therefore, whether the immune challenge is a major factor during the period in which the infections were followed in the BSF 427 parasites. If the metacaspases are somehow involved in clearing host immune antibodies, as the subcellular location might suggest, it may be that the model used was simply not sensitive enough to detect this.

While a detailed analysis of Δ*mca2/3* parasites had not been performed *in vitro*, as at least one further metacaspase is expressed in the BSF (namely MCA5) it seemed prudent to attempt the further gene deletion of *MCA5* before further phenotype analysis was performed. Whether the deletion of *MCA5* would actually be possible from Δ*mca2/3* parasites was open to question as the RNAi experiments suggested that the deletion of *MCA2, MCA3* and *MCA5* from the BSF might be either seriously detrimental or result in lethality (Chapter 4). Associated with this hypothesis was the idea of functional redundancy within the metacaspase family and it remained to be seen whether this redundancy hypothesis would hold up when the knockout of *MCA5* in the Δ*mca2/3* background was performed. The ability to generate Δ*mca2/3*Δ*mca5* mutants, however, illustrated that deletion of all three metacaspase genes was not lethal and that they are therefore non-essential genes *in vitro*. One observation of note, however, was the reduced initial growth rate (and the subsequent return to normal growth rate after successive passages) that was observed in two independent Δ*mca2/3*Δ*mca5* clones. This phenomenon had not been observed when *MCA5* was deleted from BSF and PCF wild type parasites.

These observations would appear to suggest that the metacaspase do indeed have some level of functional redundancy, with the reduction in growth rate only being observed upon deletion of all three genes. It might be that in the BSF *MCA2*, *MCA3* and *MCA5* fulfil similar roles, such that if *MCA5* is deleted then *MCA2* and *MCA3* are able to compensate and *vica versa*. However, when all three genes are deleted this creates a deficiency which manifests as a reduced growth rate. This could also

be taken as evidence that *MCA1* and *MCA4* are either not expressed or have separate functions to those of *MCA2*, *MCA3* and *MCA5*.

It was unfortunate for our analysis that this effect on growth rate was only a transient phenotype, with parasites apparently adapting to deletion of the metacaspases. One conclusion that can be drawn from this phenotype, however, is that, whatever the function of the metacaspases, they are active as full-length proteins and do not appear to be inducible, but are constitutively active. Caspases typically remain inactive within the cytoplasm and are only activated following cell surface receptor activation (Cohen, 1997) or cytochrome C release from mitochondria (Cai *et al.*, 1998) - at which point cleavage into two subunits occurs. It has been reported that the single metacaspase (YCA1) in yeast was activated following exposure to reactive oxygen species (Madeo *et al.*, 2002). They reported both the processing of the metacaspase, concurrent increase in caspases-like activity and concluded therefore that YCA1 acts similarly to caspases. Additionally, processing of *Arabidopsis thaliana* type II metacaspases following expression in *E. coli* has been reported (Vercammen *et al.*, 2004). Our data conflicts with these observations, the *T. brucei* metacaspases being apparently active without the requirement of processing.

The apparent adaptation of these mutants to loss of *MCA2*, *MCA3* and *MCA5* is intriguing. When the growth rate of the newly generated Δ*mca2/3*Δ*mca5* parasites was initially compared to wild type there was a marked reduction. However, gradually over the subsequent period of around 2 weeks the growth rate of the parasites increased to match wild type levels. A simple selection process could explain how this occurred, with sequential passages positively selecting faster growing parasites. However, the mechanism underpinning this increased growth rate is uncertain. Adaptation has previously been discussed in the guise of complementation. The hypothesis formed was that the loss of *MCA2* and *MCA3* or *MCA5* would not detrimentally affect the parasites, or the remaining metacaspases could fill in for their absence, or, in other words, adapt to the deletion. This type of adaptation occurred either immediately or extremely rapidly as no prominent

phenotype was detected in either the Δ*mca2/3* or Δ*mca5* parasites. The adaptation following Δ*mca2/3*Δ*mca5* generation occurred over an extended period, suggesting a distinct process is occurring. The most obvious explanation for adaptation to loss of *MCA2*, *MCA3* and *MCA5* would be *MCA1* and *MCA4*. These two metacaspases have not been examined in this study and nothing is known about them except their gene sequences. *MCA1* and *MCA4* may have been upregulated in Δ*mca2/3*Δ*mca5* parasites, but no antibodies are available at present to investigate this possibility.

5.12.2 Potential role in recycling endosomes.

In an attempt to discover a more robust and less transient phenotype than the sole observation of an initial reduction in growth rate, a detailed analysis of mutants was performed in relation to recycling endosomal functions. There are only two characterised recycling processes in *T. brucei* - involving VSG (Seyfang *et al.*, 1990) and the transferrin receptor (Kabiri and Steverding, 2000). VSG, the major surface coat molecule in *T. brucei*, is the primary defence against the immune response in the mammalian host through the process of antigenic variation (Cross *et al.*, 1980). The transferrin receptor, involved in the uptake of transferrin in the BSF, is a heterodimer encoded by ESAG6 and ESAG7 and its surface distribution is limited to the flagellar pocket (Steverding *et al.*, 1994).

The ability to generate Δ*mca2/3*Δ*mca5* BSF parasites suggested that deletion of the metacaspases, whatever their possible functions, did not severely affect the recycling system. If the system had been affected, it is reasonable to assume that an adverse effect might manifest either *in vitro* or *in vivo*. Due to the high rate of endocytosis of VSG, the total surface pool being turned over in 12 mins (Engstler *et al.*, 2004), and its metabolic stability, it has been suggested that >95% of the internalised protein is recycled to the cell surface (Seyfang *et al.*, 1990; Engstler *et al.*, 2004). If this recycling was completely disrupted, the energy demands placed on the parasite through the *de novo* synthesis of sufficient VSG molecules would presumably be rather constrictive and wasteful. There remained the possibility, however, that the

recycling processes may have been hindered in a way which could be detected through a more detailed analysis of the mutants.

An analysis of VSG recycling *in vitro*, however, revealed that the *Δmca2/3Δmca5* parasites were still fully functional with regard to VSG recycling. This pathway was studied through the following of internalised Biotin-VSG, trafficking through Rab11 positive recycling endosomes and subsequent return to the cell surface in both wild type and *Δmca2/3Δmca5* BSF parasites. With no defect in the recycling of the VSG detected, the analysis shifted to the process of removal and degradation of host anti-VSG antibodies. The exact mechanism by which anti-VSG antibodies are separated from VSG and degraded during the recycling process is unknown. Whether the dissociation of antibodies from VSG occurs via a proteolytic clipping event or via a pH reduction has not been determined. Additionally, the peptidases involved in the degradation of these antibodies and the compartment where this occurs have yet to be characterised. Anti-VSG antibodies are known to be recycled via Rab11 positive recycling endosomes (Pal *et al.*, 2003; Grunfelder *et al.*, 2003) and we believe that the metacaspases are located within the lumen of these endosomes (Tetley, unpublished). Therefore, the metacaspases may physically interact with material present within these structures. Additionally, it has been reported that incubation of parasites with a cocktail of peptidase inhibitors resulted in a build up of internalised anti-VSG antibodies detected within vacuoles situated between the nucleus and the flagellar pocket (Russo *et al.*, 1993). This cocktail of inhibitors was made up of leupeptin, E64, chymostatin and antipain; a combination which should inhibit a wide range of both serine and cysteine peptidases. Our analysis revealed, however, that the *Δmca2/3Δmca5* parasites displayed no equivalent build up of internalised anti-VSG antibodies and so suggests that inhibition of the metacaspases were not responsible for the build up of antibodies reported.

An analysis of antibody degradation products also revealed that the metacaspase are not required for the degradation of anti-VSG antibodies. The profile of the secreted antibody fragments exactly matching in both wild type and *Δmca2/3Δmca5*

parasites. This result was not too unexpected based, on what is known about the substrate specificities of other Clan CD peptidases. Unlike general proteolytic cysteine peptidases, Clan CD peptidases are more specific with regard to substrate specificity. Clostripain and asparaginyl endopeptidases are specific for asparagine at the P1 position, gingipain R and separase show specificity toward arginine, while for the caspases an aspartate is preferred (Mottram *et al.*, 2003). Additionally, it has been reported that the metacaspases also follow this rule of P1 specificity, the *A. thaliana* metacaspases cleaving exclusively after arginine or lysine residues (Vercammen *et al.*, 2004).

As the data showed that metacaspases were not apparently involved in VSG and anti-VSG antibody recycling, we next examined the transferrin pathway. It is possible to directly follow transferrin receptor recycling through expression of tagged versions of the receptor with an inducible gene expression (Kabiri and Steverding, 2000). However, due to a lack of further resistance markers this strategy could not be pursued in the Δ*mca2/3*Δ*mca5* parasites already generated. The strategy utilised to investigate transferrin receptor recycling pathway had to be indirect, therefore, and was performed via the following of transferrin uptake. The *T. brucei* transferrin receptor is a relatively low abundance protein estimated to be present at approximately 3000 molecules per cell (Steverding *et al.*, 1995) and the cycling time has been estimated at around 11 mins (Kabiri and Steverding, 2000). It was assumed in our analysis that a defect in recycling of the receptor would result in a reduced rate of transferrin uptake over time. However, no difference in the levels of cell associated Biotin-transferrin were detected between wild type and Δ*mca2/3*Δ*mca5* parasites over the course of the experiment (1 hour). This suggests that there is no defect in the recycling of the transferrin receptor, although due to the indirectness of the analysis this cannot be stated with certainty. It might be that the *de novo* synthesis of receptors is able to match any defect in recycling.

The rate of degradation of the transferrin-biotin conjugate was also not altered in the Δ*mca2/3*Δ*mca5* parasites relative to wild type. Following a 10 mins chase period, no

transferrin biotin conjugate was detected within the parasites. This suggests that the degradation of transferrin occurs very rapidly within the parasites and that the metacaspases are not involved in the degradation process. Like the anti-VSG antibodies, the compartment in which transferrin is degraded has not been fully categorised. It has been reported that transferrin, following internalisation is routed to lysosomal-like structures for degradation (Grab *et al.*, 1992; Steverding *et al.*, 1995). However, more recently it has been suggested that the degradation of transferrin occurs within either the early or recycling endosomes. The proteolysis of transferrin was increased by the expression of the mutant Rab proteins that slowed the overall recycling rate, while a decrease in proteolysis was observed by the over expression of Rab11 which accelerated recycling (Pal *et al.*, 2003).

Despite questions regarding the compartment where degradation takes place it is accepted that the degraded products are secreted from the parasites (Steverding *et al.*, 1995; Pal *et al.*, 2003). Attempts to detect these fragments and perform a comparison between wild type and Δ*mca2/3*Δ*mca5* were unsuccessful. No degradation products were detected within the parasites similar to what was seen with the anti-VSG antibodies experiment. However, unlike the anti-VSG antibody experiment, no degradation products were detected in the TCA medium precipitations. In previous experiments degradation products of transferrin have been detected in the medium (Pal *et al.*, 2003), although these utilised FITC-transferrin and the failure to detect degraded fragments may be due to the biotin probe not being suitable for this purpose.

This phenotype analysis was performed on the Δ*mca2/3*Δ*mca5* after the apparent adaptation period, and once the growth rate had returned to wild type levels. With hindsight, it might have been more prudent to perform these experiments on newly generated Δ*mca2/3*Δ*mca5* parasites which were still exhibiting the reduced growth rate. It is feasible to suggest that a defect in either VSG or transferrin receptor recycling might manifest as a reduced growth rate. With regard to VSG pathway, this could be through an increased *de novo* synthesis of VSG, while for the

transferrin pathway this could theoretically occur via a reduction in available iron, an essential co-factor in a variety of enzymes. One possible explanation for the adaptation observed could be that the parasites are able to compensate by returning recycling rates to wild type levels. Therefore, future work could address this possibility by repeating these experiments in newly generated *Δmca2/3Δmca5* parasites. Stringent controls would be required, however, as any reduction in recycling rate might simply be a secondary effect of metacaspase deletion and not directly related to a defect in the actual recycling process.

One possible route of adaptation that could be tested was upregulation of transferrin receptor expression. It has been reported that BSF parasites are able to upregulate expression of the transferrin receptor under conditions of reduced transferrin availability (Mussmann *et al.*, 2004). An analysis of transferrin receptor expression in the *Δmca2/3Δmca5* parasites did not show any such increase following the apparent adaptation period, however, appearing to rule this out as a possible explanation. Alternatively another nutrient that is taken up, trafficked through, and its receptor recycled via Rab11 positive endosomes may be responsible for the reduction in growth rate. Transferrin is the only such nutrient molecule known in T. *brucei* that is taken up via this route, although it is possible that there are others that are as yet unidentified.

Despite the failure to detect a phenotype directly related to categorised recycling processes, the identification of two phenotypes in the BSF *Δmca2/3* parasites (a reduced ability to recover from high densities and a diminished ability to adapt to low serum concentrations) were initially promising. These phenotypes were initially identified in *Δmca2/3Δmca5* parasites although later it was discovered that these phenotypes were also present in the *Δmca2/3* but not the *Δmca5* parasites. These phenotypes appeared therefore to be specific to the deletion of *MCA2* and/or *MCA3*.

With regard to the reduced ability to recover from high densities, a similar phenomenon has been claimed for metacaspase function in yeast. The deletion of

the yeast metacaspase resulted in an initial increased survival of chronologically aged cultures, however these surviving cells lost the ability to re-grow (Herker *et al.*, 2004). It was suggested that the yeast metacaspase is involved in the elimination of unfit cells by apoptosis, thus leaving only the youngest, fittest, and best adapted cells for further growth. How this is related to our observations is unclear, *Δmca2/3* parasites did not show an initial increased survival although they did display a reduced ability to re-grow.

However, conjecture about what these phenotypes might represent is only important if some form of complementation can be achieved and unfortunately this was not possible. Even the dual re-expression of both *MCA2* and *MCA3* in the *Δmca2/3* mutants did not result in complementation the two phenotypes. The pertinent question therefore is whether these detected phenotypes are related to metacaspase function. It is clear that the re-expression of the metacaspases to approximately wild type levels was successful, thus ruling out differences in expression levels as the reason behind the failure to complement the phenotypes. All of the metacaspases used in the re-expressions had been cloned from wild type (strain 427) genomic DNA and sequenced to ensure that there were no introduced errors. The failure of complementation therefore is unlikely to be the result of a loss of activity. It was also shown that HA-tagged version of MCA2 and MCA3 were targeted to their native location (Chapter 3), therefore we can assume that the re-expressed untagged versions should also target to the correct compartment. This leads to the distinct possibility that the described phenotypes are not directly related to the deletion of *MCA2* and *MCA3*.

Although these experiments were performed in the absence of antibiotics, it is possible that the presence of the *PAC* and *BSD* gene products may be causing these effects through a non-specific mechanism unrelated to *MCA2* and *MCA3* deletion. It is difficult to determine what the reasons for these phenotypes are, although for the time being will have to be classified as artefactual. In addition, do the two different phenotypes stem from the route cause and are they simply different manifestations of

the same deficiency. This being that the *Δmca2/3* mutants are unable to cope with stressful conditions for some reason, but one which is not related to absence of MCA2 and MCA3 from recycling endosomes.

Another possible role for the metacaspase, that has not been investigated, may be that they are not involved in recycling processes themselves but are involved in the cleavage or processing of nascent proteins destined for the cell surface or secretion. The endosomal system of yeast is believed to sit at a junction between the endocytic and secretory pathways (Lemmon and Traub, 2000). In *T. brucei*, the return of internalised VSG and transferrin receptor to the cell surface has been shown to occur via Rab11 positive recycle endosomes (Pal *et al.*, 2003; Grunfelder *et al.*, 2003), although the route for the delivery of *de novo* cell surface proteins in trypanosomatids is not well defined. It is believed to occur directly from the trans Golgi network (TGN) to flagellar pocket, although the nature of the transport intermediates are not well defined (McConville *et al.*, 2002). In *Leishmania*, however, it has been suggested that the secretory and endocytic pathways converge (Ghedin *et al.*, 2001). Rab11 positive recycling endosomes may therefore be at a cross roads between the recycling of cell surface molecules and the normal secretory system. It is plausible to suggest that the metacaspases are located within Rab11 positive endosomes to facilitate the activation of an unknown secreted protein. A future comparative analysis of the secretion profile of wild type and *Δmca2/3Δmca5* parasites may be able to address this possibility.

5.12.3 Potential involvement in cell death processes.

Due to the failure to detect any phenotypes related to recycling processes, the possibility of metacaspase involvement in cell death, as have been claimed in the literature (Szallies *et al.*, 2002; Hoeberichts *et al.*, 2003; Wadskog *et al.*, 2004; Suarez *et al.*, 2004), was investigated. Deciding on suitable stimuli to use was difficult as the evidence for apoptotic-like machinery or a process being present in any single cellular organism is far from concrete, and there have been no such reported experiments performed in BSF *T. brucei*. As detailed in chapter 1, claims

of detection of some form of regulated cell death in single cell organisms have usually involved some form of stressful stimuli in order to induce the reported responses. The inherent problem with the stimuli used in these reports is that they are usually themselves toxic. In contrast, apoptosis in higher eukaryotes can be stimulated via the activation of specific receptors, but none of the reports of apoptotic-like death in single cell organisms have been shown to be due to stimulation of such a specific pathway. The induction of an apoptotic-like mechanism in single cell organisms with inherently toxic stimuli could therefore be considered a questionable approach. Despite these reservations, attempts were made to reproduce several toxic stimuli that have been claimed to induce such phenomena. The only stimuli used in this limited study were heat shock and salt stress, adapted from studies in *Leishmania* (Moreira *et al.*, 1996) and yeast (Wadskog *et al.*, 2004), respectively.

In these experiments the determination of whether the stressful stimuli were actually resulting in features associated with apoptotic-like cell death, such a chromatin condensation, phosphatidyl serine externalisation or DNA fragmentation were not evaluated. These experiments were simply a quick determination of whether the metacaspases might be involved in cell death. *Δmca2/3Δmca5* parasites showed no significant differences in response to the stressful stimuli or the subsequent recovery as compared to wild type parasites. To rule out the possibility that the metacaspases might be involved in a cell death pathway, however, would be premature. These investigations were far from thorough and the stimuli used may have been too harsh to determine any subtle differences between the wild type and *Δmca2/3Δmca5* parasites. If an apoptotic-like phenomenon does exist in *T. brucei* it might be that the trigger is only present *in vivo* and that mimicking of this *in vitro* may not be possible. More detailed studies on cell death in trypanosomatids are required before it will be possible to determine if the metacaspases are involved.

In general, however, what has been identified in *T. brucei* about the metacaspases does not immediately stand out as suggesting an involvement in an apoptotic-like

pathway. Firstly, the association with recycling endosomes is not immediately suggestive of a role in such a phenomenon. Secondly, the observation of an initial slow growth upon Δ*mca2/3*Δ*mca5* generation would tend to suggest that the metacaspases are constitutively active. A role in cell death would presumably require them to remain inactive until stimulated and this does not appear to be the case.

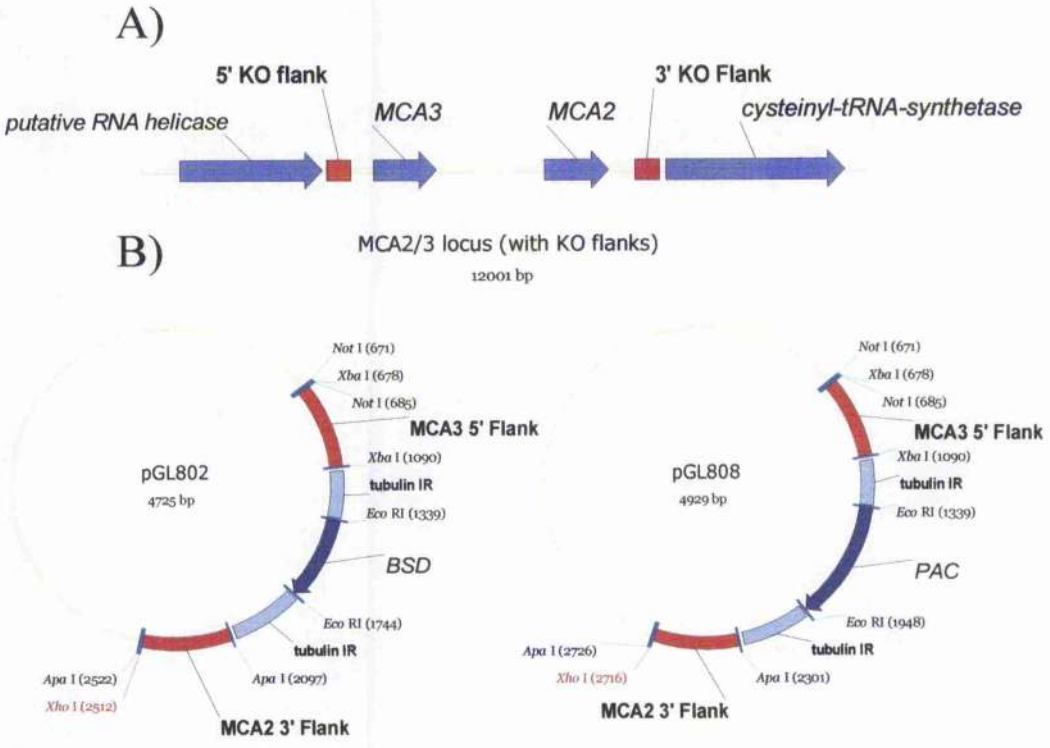

Figure 5.1: Illustration of knockout strategy for *MCA2* and *MCA3*.
A) To permit replacement of the *MCA2/3* locus, flanking regions downstream of *MCA2* and upstream of *MCA3* were chosen (highlighted in red) avoiding the regions of homology immediately surrounding both genes and avoiding encroachment into the adjacent ORFs. B) These 5' and 3' regions were then amplified by PCR and subsequently subcloned into the knockout vectors shown using *Xba*I and *Apa*I, respectively. The knockout cassette was cleaved from the vector using *Not*I and *Xho*I. This knockout vector contains tubulin intergenic regions to facilitate trans-splicing and polyadenlylation and to ensure translation of the two resistance genes used, *BSD* and *PAC*.

Figure 5.2: Strategy used to show correct integration of *MCA2/3* knockout cassettes and the PCR analysis.
Cartoon illustration of A) *MCA2/3* native locus and the loci following replacement with knockout cassettes containing B) *PAC* and C) *BSD* resistance genes. Open reading frames are highlighted in blue, while flanks used for targeting of knockout cassettes are highlighted in red. Also shown are primers used to confirm correct integration of knockout cassettes at both the 5' and 3' regions together with primers used to show deletion of both *MCA2* and *MCA3*. D) Genomic DNA was prepared from 1) wild type, 2) *BSD* heterozygote, 3) *PAC* heterozygote, 4) Δ*mca2/3* clone 1 and 5) Δ*mca2/3* clone 2. PCR analysis was performed to confirm the correct integration of the knockout cassettes at both the 5' and 3' regions and to illustrate loss of the *MCA2/3* locus in Δ*mca2/3* mutants.

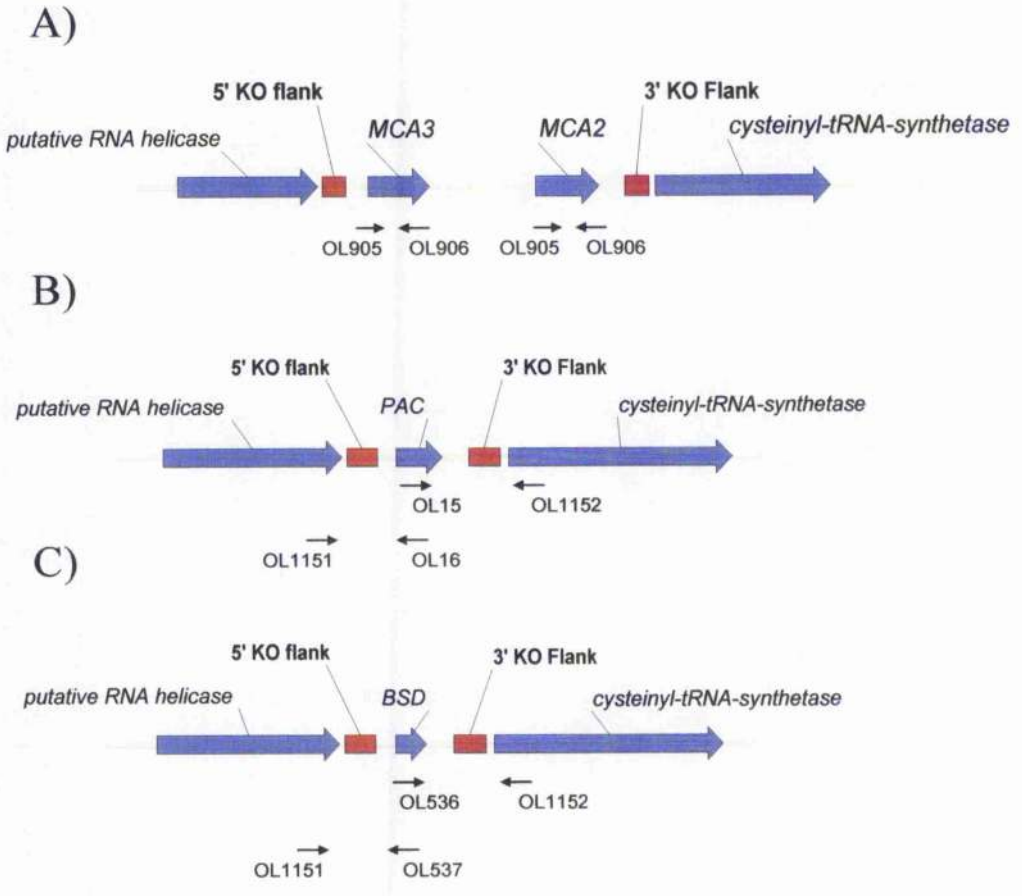
A)
5' KO flank
3' KO Flank
putative RNA helicase
MCA3
MCA2
cysteinyl-tRNA-synthetase
OL905
OL906
OL905
OL906
B)
5' KO flank
3' KO Flank
putative RNA helicase
PAC
cysteinyl-tRNA-synthetase
OL15
OL1152
OL1151
OL16
C)
5' KO flank
3' KO Flank
putative RNA helicase
BSD
cysteinyl-tRNA-synthetase
OL536
OL1152
OL1151
OL537

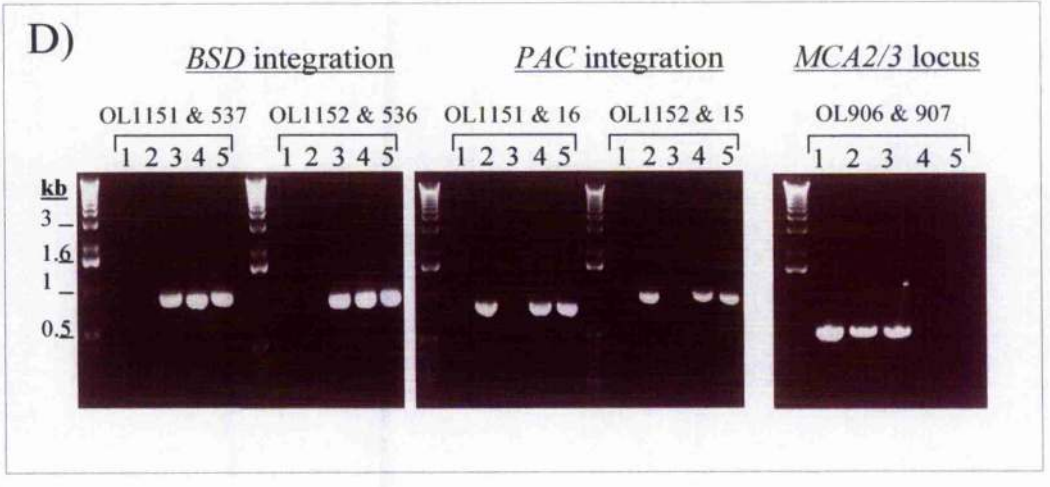
D)
BSD integration
PAC integration
MCA2/3 locus
OL1151 & 537
OL1152 & 536
OL1151 & 16
OL1152 & 15
OL906 & 907
1 2 3 4 5
kb
3
1.6
1
0.5

Figure 5.3: Predicted fragments sizes and Southern blot analysis confirming *MCA2/3* knockout.
Cartoon illustration of A) *MCA2/3* native locus and the loci following replacement with knockout cassettes containing B) *PAC* and C) *BSD* resistance genes. Open reading frames are highlighted in blue, while flanks used for targeting of knockout cassettes are highlighted in red. Predicted *Kpn*I restriction sites are indicated together with size of fragments resulting from digestion with this enzyme. D) Genomic DNA was prepared from BSF (strain 427) 1) wild type, 2) *PAC* heterozygotes, 3) *BSD* heterozygotes, 4) Δ*mca2/3* clone 1 and 5) Δ*mca2/3* clone 2. 3 µg of DNA were digested with *Kpn*I, genomic fragments separated by electrophoresis, transferred to Hybond-P and probed with the *MCA2/3* 5' flanking region.

A)

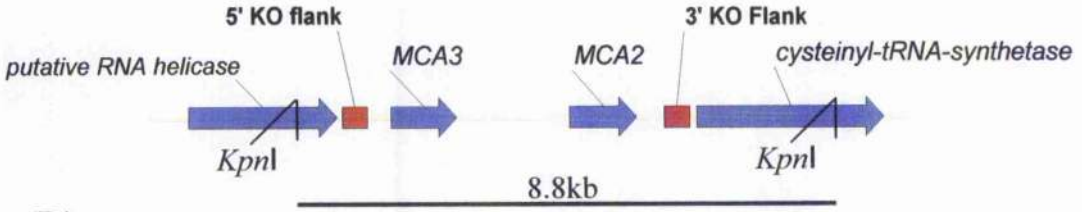
5' KO flank
3' KO Flank
putative RNA helicase
MCA3
MCA2
cysteinyl-tRNA-synthetase
KpnI
KpnI
8.8kb

B)

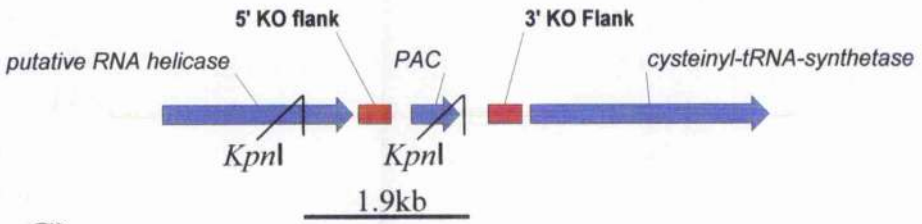
5' KO flank
3' KO Flank
putative RNA helicase
PAC
cysteinyl-tRNA-synthetase
KpnI
KpnI
1.9kb

C)

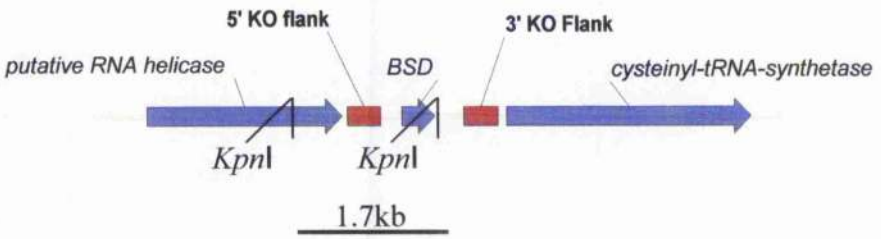
5' KO flank
3' KO Flank
putative RNA helicase
BSD
cysteinyl-tRNA-synthetase
KpnI
KpnI
1.7kb

D)

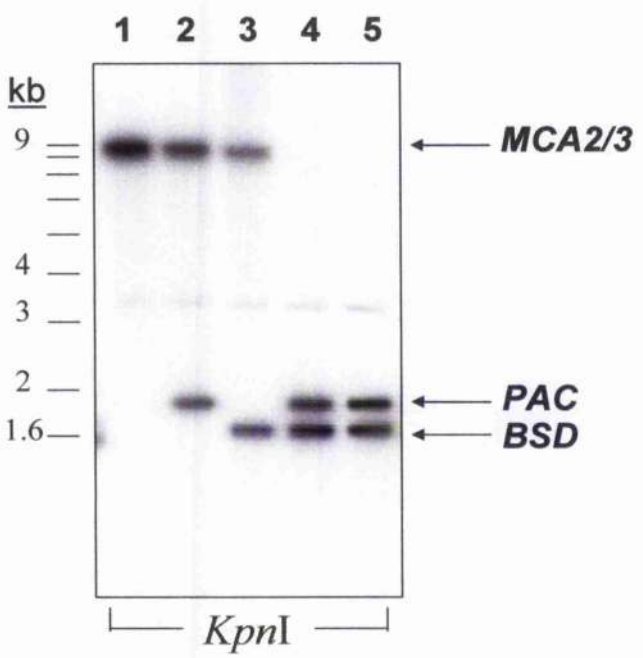
1
2
3
4
5
kb
9
4
3
2
1.6
MCA2/3
PAC
BSD
KpnI

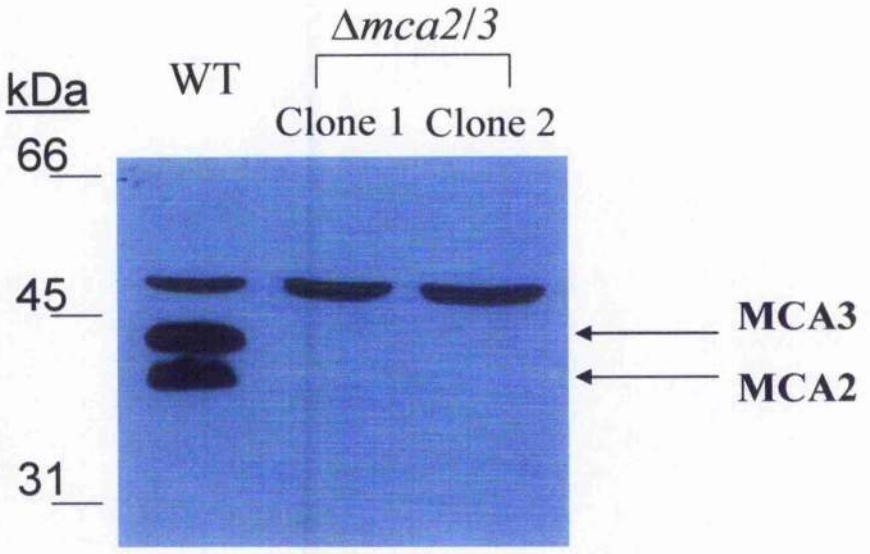

Figure 5.4: Confirmation of *MCA2* and *MCA3* deletion in BSF *T. brucei*. Total cell lysates were prepared from *T. brucei* BSF (strain 427) wild type and Δ*mca2/3* clones 1 and 2. $5x10^6$ cell equivalents were then subjected to SDS-PAGE and transferred to PVDF membrane prior to immunoblotting with immunopurified polyclonal rabbit anti-MCA2/3 antibodies. MCA2 and MCA3 are indicated, the upper protein also detected by the antibody acting as a loading control.

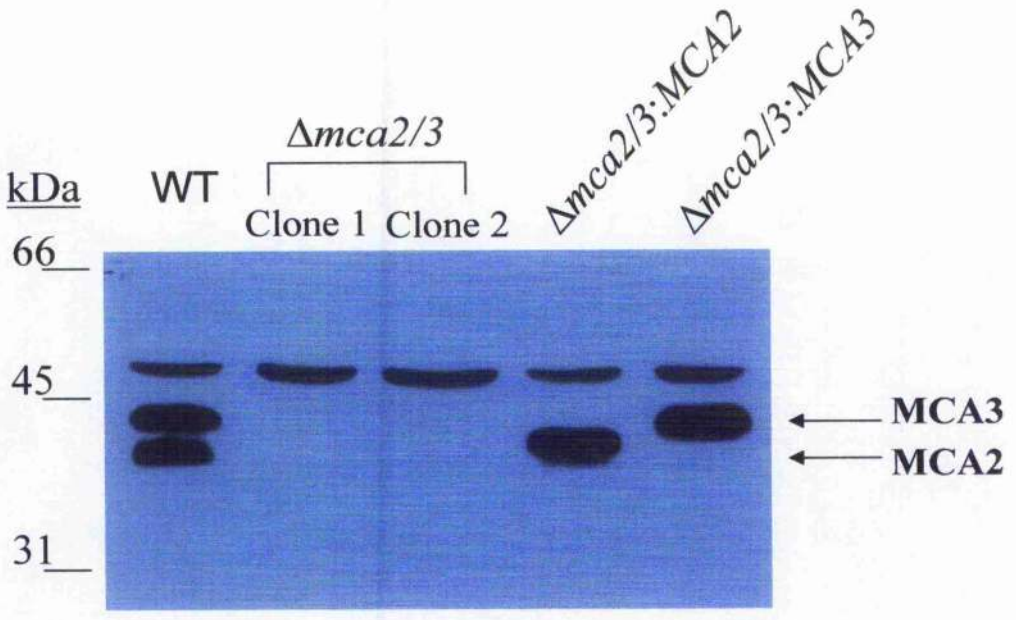

Figure 5.5: Re-expression of *MCA2* and *MCA3* in Δ*mca2/3* BSF parasites. Total cell lysates were prepared from *T. brucei* BSF (strain 427) wild type, Δ*mca2/3* clone 1, Δ*mca2/3* clone 2, Δ*mca2/3*:*MCA2* and Δ*mca2/3:MCA3* parasites. $5x10^6$ cell equivalents were then subjected to SDS-PAGE and transferred to PVDF membrane prior to immunoblotting with immunopurifed polyclonal rabbit anti-MCA2/3 antibodies. MCA2 and MCA3 are indicated, the upper protein also detected by the antibody acting as a loading control.

A)

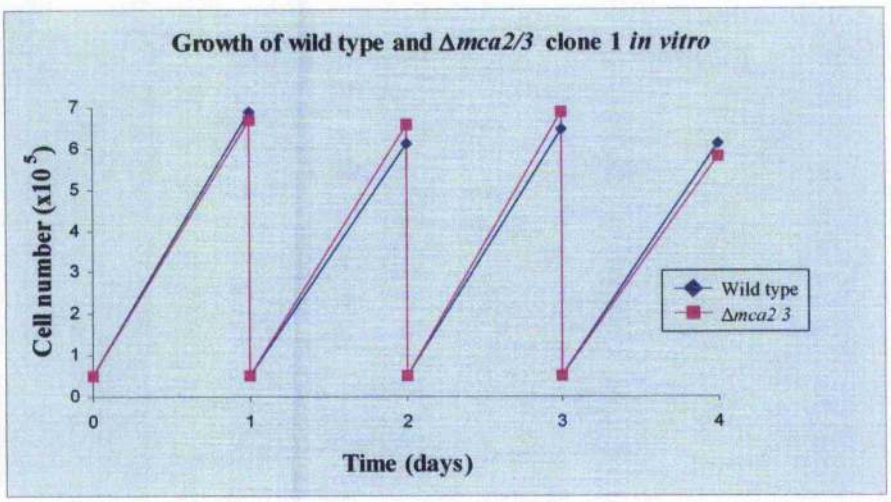

B)

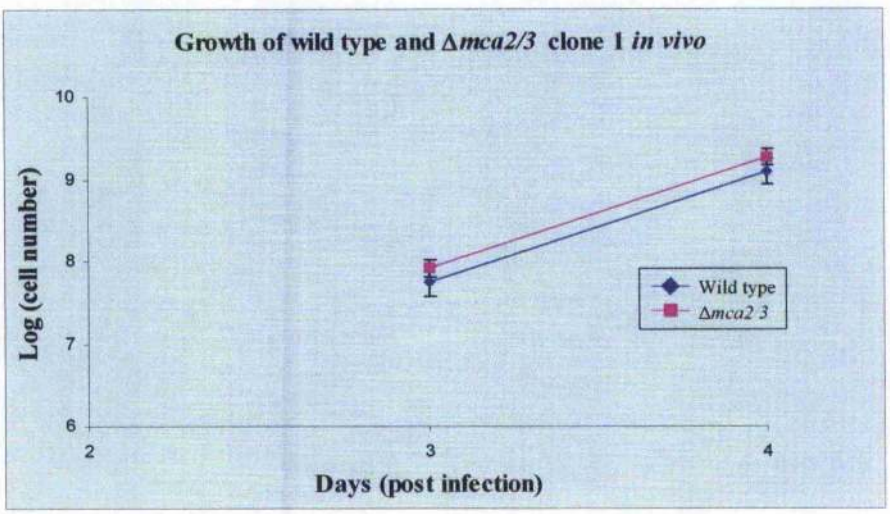

Figure 5.6: *In vitro* and *in vivo* growth curve analysis of wild type and *Δmca2/3*.

A) The growth rate of BSF (strain 427) wild type and *Δmca2/3* clone 1 *in vitro* were monitored over a period of 4 days. Cultures were seeded at $5x10^4$ cells ml^{-1} and cell counts made daily, with cultures being re-seeded to $5x10^4$ cells ml^{-1} each day to maintain cultures in a logarithmic growth phase. B) The growth rate of BSF (strain 427) wild type and *Δmca2/3* clone 1 were evaluated *in vivo*. Both lines were passaged once through mice and $1x10^3$ parasites injected into a group of six mice. Parasitaemia was determined on days 3 and 4 post-infection. Average parasites densities, converted into logarithms, are plotted together with error bars indicating standard deviation.

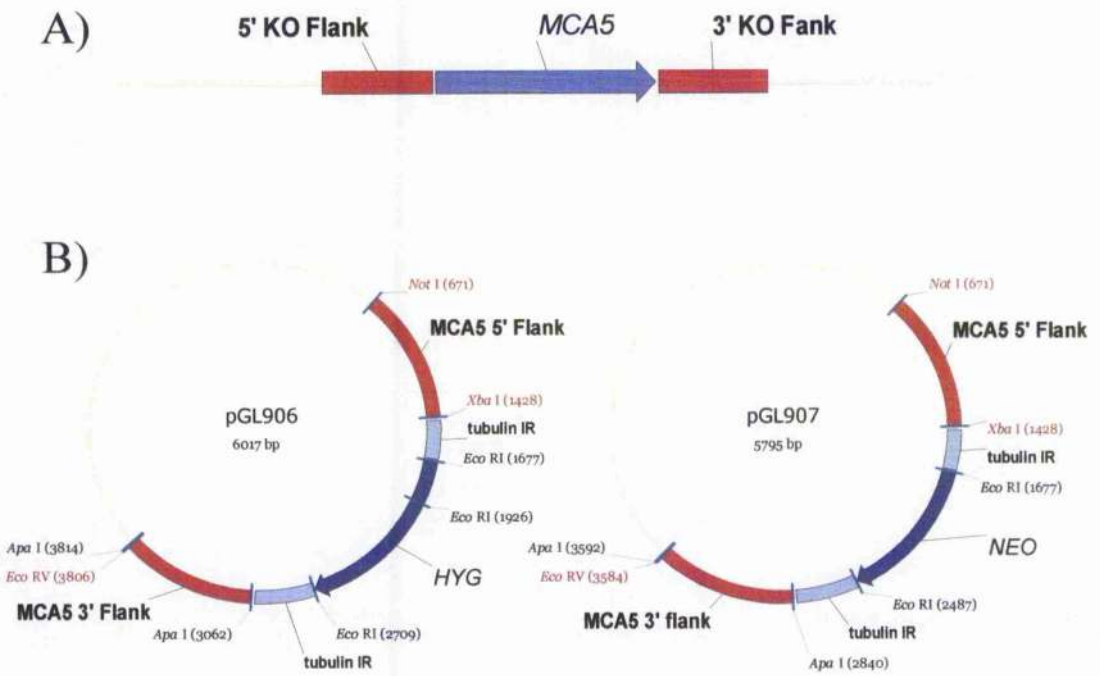

Figure 5.7: Illustration of knockout strategy for *MCA5*.
A) 5' and 3' flanking regions were chosen (highlighted in red) immediately surrounding the *MCA5* locus. B) These 5' and 3' regions were then amplified by PCR and subsequently subcloned into the knockout vectors shown using *Not*I/XbaI and *Apa*I, respectively. The knockout cassette was cleaved from the vector using *Not*I and *EcoR*V. This knockout vector contains tubulin intergenic regions to facilitate trans-splicing and polyadenlylation and to ensure translation of the two resistance genes used, *HYG* and *NEO*.

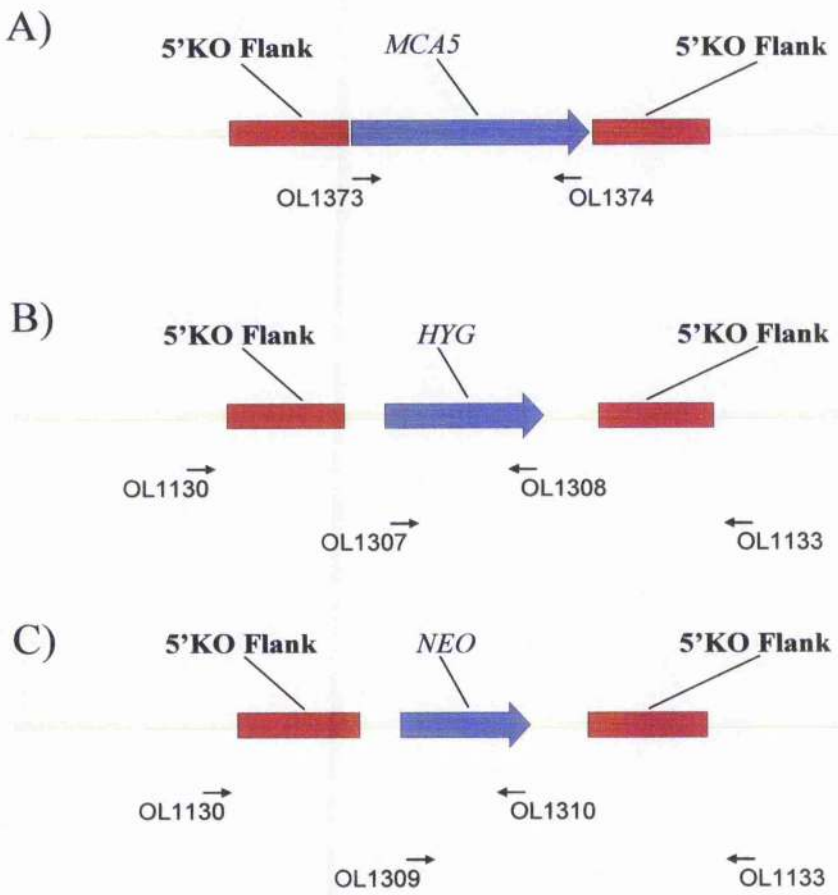

Figure 5.8: Illustration of strategy used to show correct integration of *MCA5* knockout cassettes.
Cartoon illustration of A) *MCA2/3* native locus and the loci following replacement with knockout cassettes containing B) *HYG* resistance gene and B) *NEO* resistance gene. Open reading frames are highlighted in blue, while flanks used for targeting of knockout cassettes are highlighted in red. Also shown are primers used to confirm correct integration of knockout cassettes at both the 5' and 3' regions, together with primers used to show deletion of both *MCA2* and *MCA3*.

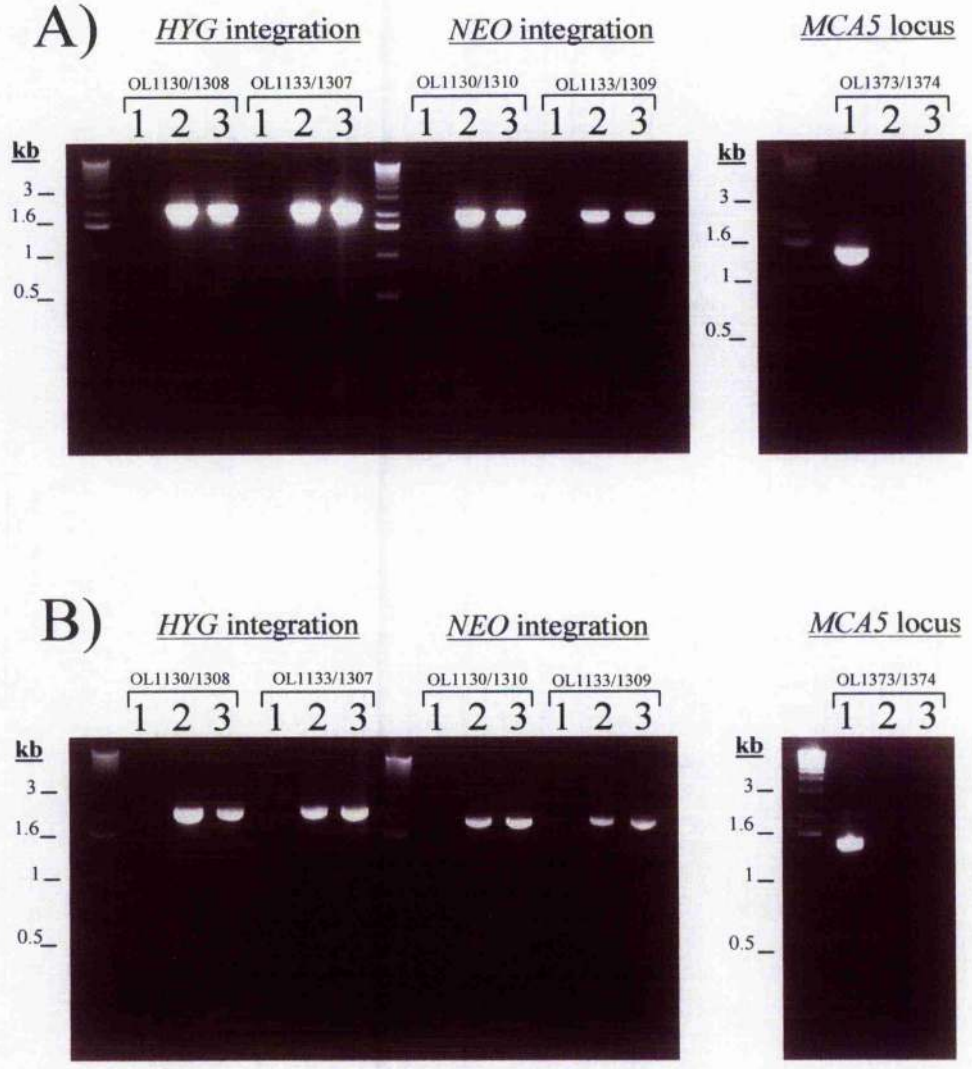

Figure 5.9: PCR analysis confirming correct integration of *MCA5* knockout cassettes and deletion of *MCA5* in PCF and BSF.

A) Genomic DNA was prepared from BSF (strain 427) 1) wild type, 2) Δ*mca5* clone 1 and 3) Δ*mca5* clone 2. B) Genomic DNA was prepared from PCF (EATRO 795) 1) wild type, 2) Δ*mca5* clone1 and 3) Δ*mca5* clone 2. PCR analysis was performed to confirm the correct integration of the knockout cassettes at both the 5' and 3' regions and to illustrate loss of the *MCA5* locus in Δ*mca5* mutants as illustrated in figure 5.8.

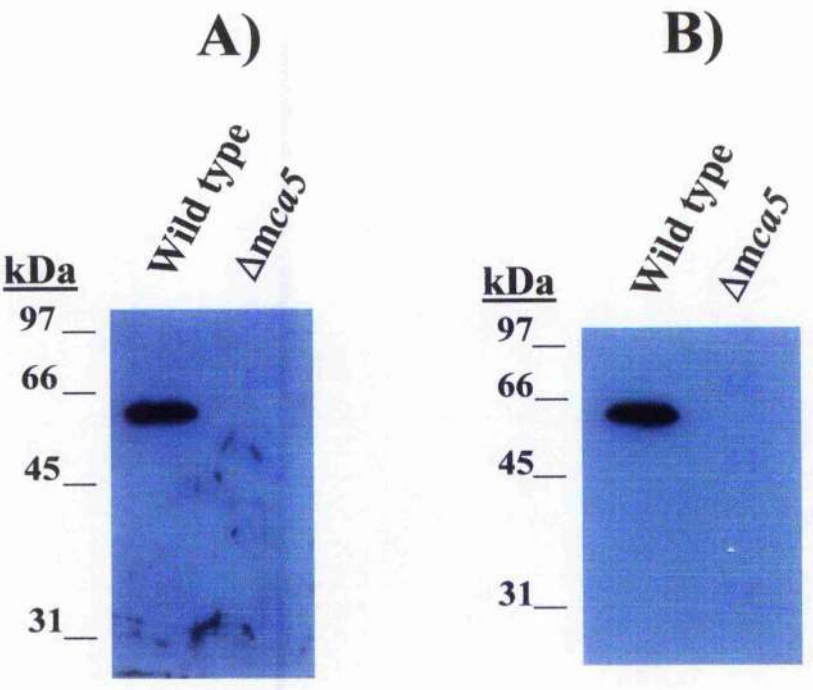

Figure 5.10: Confirmation of *MCA5* deletion in PCF and BSF *T. brucei*. Total cell lysates were prepared from A) BSF (strain 427) wild type and Δ*mca5* clone 1. B) PCF (EATRO 795) wild type and Δ*mca5* clone 1. $5x10^6$ cell equivalents were subjected to SDS-PAGE and transferred to PVDF membrane prior to immunoblotting with polyclonal sheep anti-MCA5 antibodies.

A)

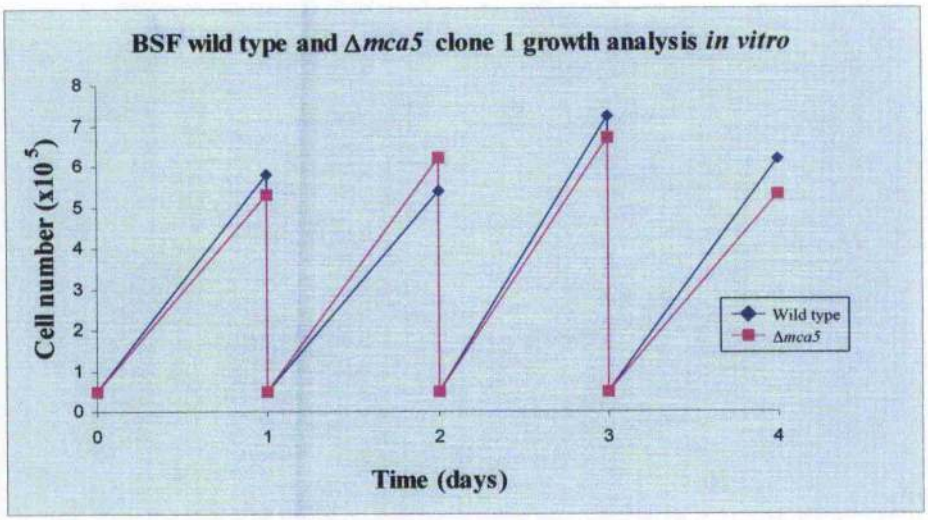

B)

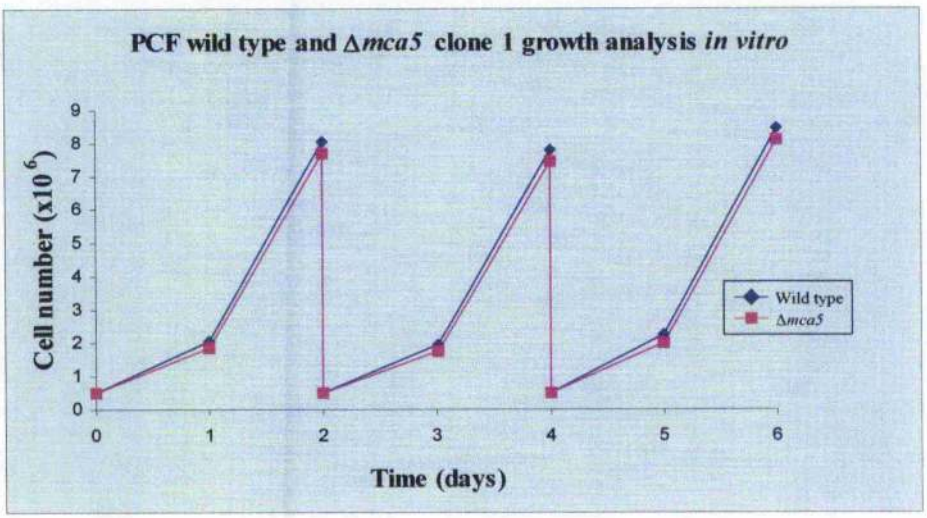

Figure 5.11: *In vitro* growth analysis of wild type and Δ*mca5* in both BSF and PCF parasites.

A) The growth rate of BSF (strain 427) wild type and Δ*mca5* clone 1 were monitored over a period of 4 days. Cultures were seeded at $5x10^4$ cells ml^{-1} and cell counts made every 24 hours, cultures were re-seeded to $5x10^4$ cells ml^{-1} daily to maintain cultures in a logarithmic growth phase. B) The growth rate of PCF (EATRO 795) wild type and Δ*mca5* clone 1 were monitored over a period of six days. Cultures were seeded at $5x10^5$ cells ml^{-1} and cell counts made every 24 hours, cultures were re-seeded to $5x10^5$ cells ml^{-1} every 2 days to maintain cultures in a logarithmic growth phase.

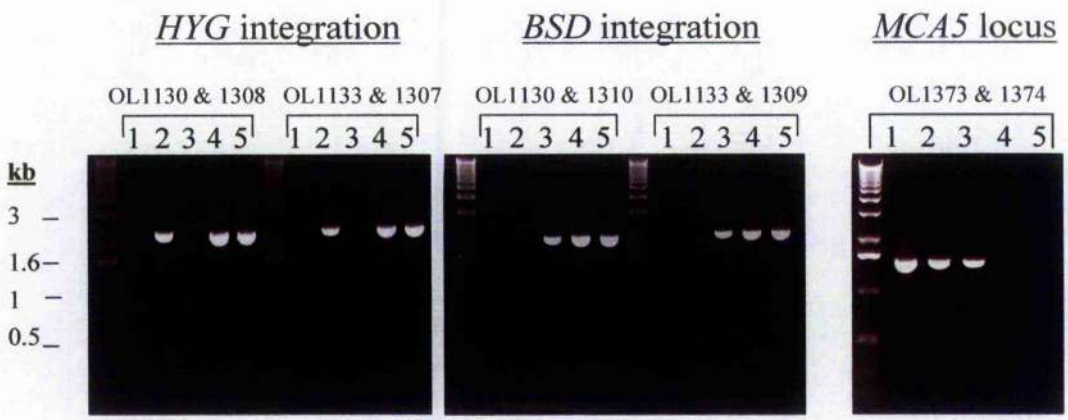

Figure 5.12: PCR analysis confirming correct integration of *MCA5* knockout cassettes and deletion of *MCA5* in BSF Δ*mca2/3* clone 1.
Genomic DNA was prepared from BSF (strain 427) 1) Δ*mca2/3*, 2) *HYG* heterozygote, 3) *NEO* heterozygote, 4) *Δmca2/3Δmca5* clone 1 and 5) Δ*mca2/3Δmca5* clone 2. PCR analysis was performed to confirm the correct integration of the knockout cassettes at both the 5' and 3' regions and to illustrate loss of the *MCA5* locus in Δ*mca5* mutants as illustrated in figure 5.8.

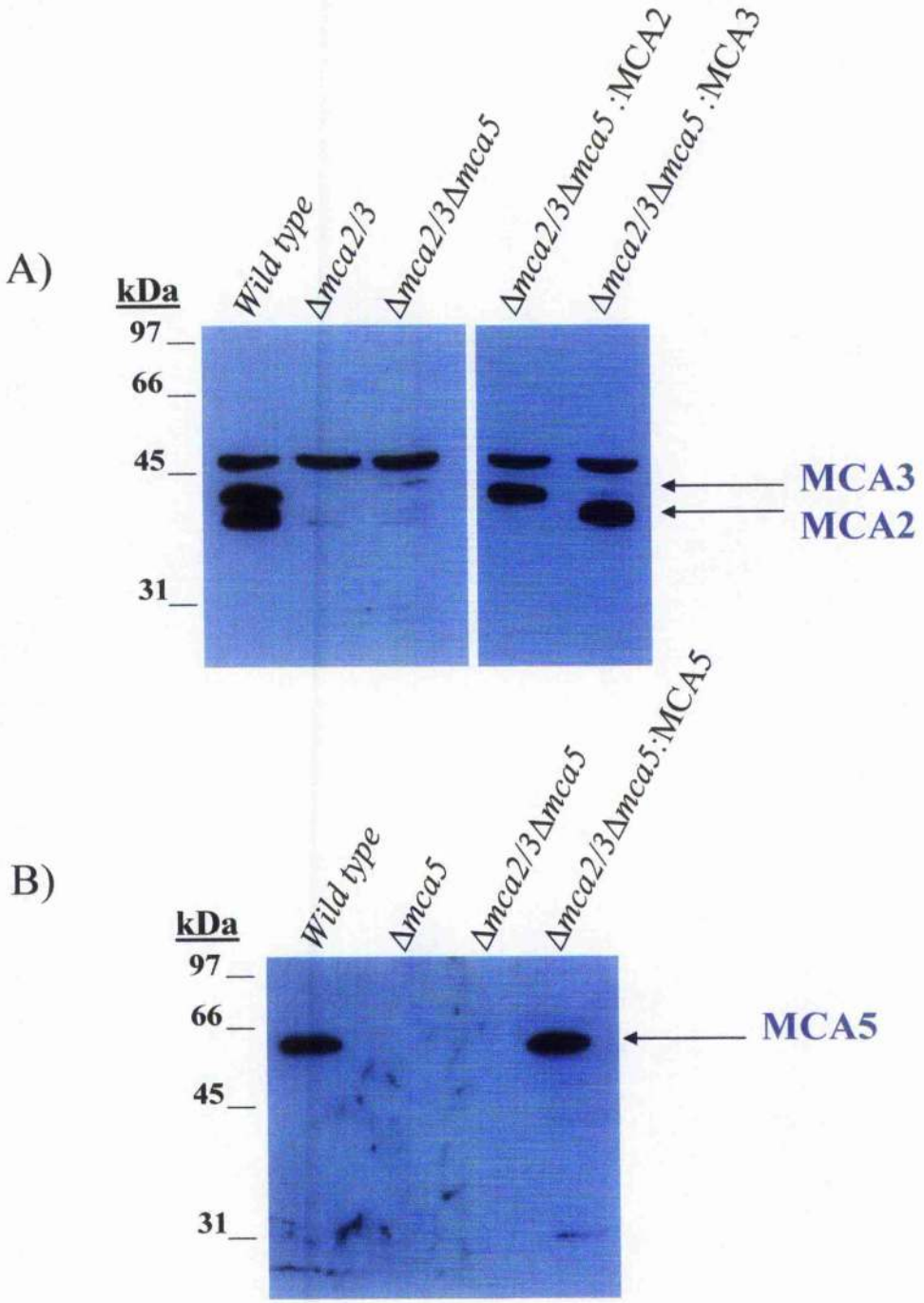

Figure 5.13: Western blot of Δ*mca2/3*Δ*mca5* parasites.
Total cell lysates were prepared from BSF (strain 427) wild type, Δ*mca2/3* clone 1, Δ*mca5* clone 1, Δ*mca2/3*Δ*mca5* clone 1, Δ*mca2/3*Δ*mca5:MCA2*, Δ*mca2/3*Δ*mca5:MCA3* and Δ*mca2/3*Δ*mca5:MCA5* parasites. $5x10^6$ cell equivalents were then subjected to SDS-PAGE and transferred to PVDF membrane prior to immunoblotting with A) polyclonal rabbit anti-MCA2/3 antibodies and B) polyclonal sheep anti-MCA5 antiserum. MCA2, MCA3 and MCA5 are indicated.

Figure 5.14: Growth analysis of *Δmca2/3Δmca5* parasites *in vitro* and *in vivo*.

A) The growth rate of BSF (strain 427) wild type and *Δmca2/3Δmca5* clone 1 was monitored *in vitro* over a period of 6 days immediately following generation of mutant parasites. Cultures were seeded at $5x10^4$ cells ml^{-1} and cell counts made daily, with cultures being re-seeded to $5x10^4$ cells ml^{-1} each day, to maintain cultures in a logarithmic growth phase. B) The growth rate of BSF (strain 427) wild type and *Δmca2/3Δmca5* clone 1 following successive passages *in vitro* were monitored over a period of 4 days. Cultures were seeded at $5x10^4$ cells ml^{-1} and cell counts made daily, with cultures being re-seeded to $5x10^4$ cells ml^{-1} each day, to maintain cultures in a logarithmic growth phase. C) The growth rate of BSF (strain 427) wild type and *Δmca2/3Δmca5* clone 1 was evaluated *in vivo* following *in vitro* adaptation period and return to wild type growth levels. Each line was passaged once through a mouse and $1x10^2$ parasites then injected into a group of six mice. Parasitaemia was determined on days 3, 4 and 5 post-infection. The average cell counts are plotted together with error bars indicating standard deviation.

A)

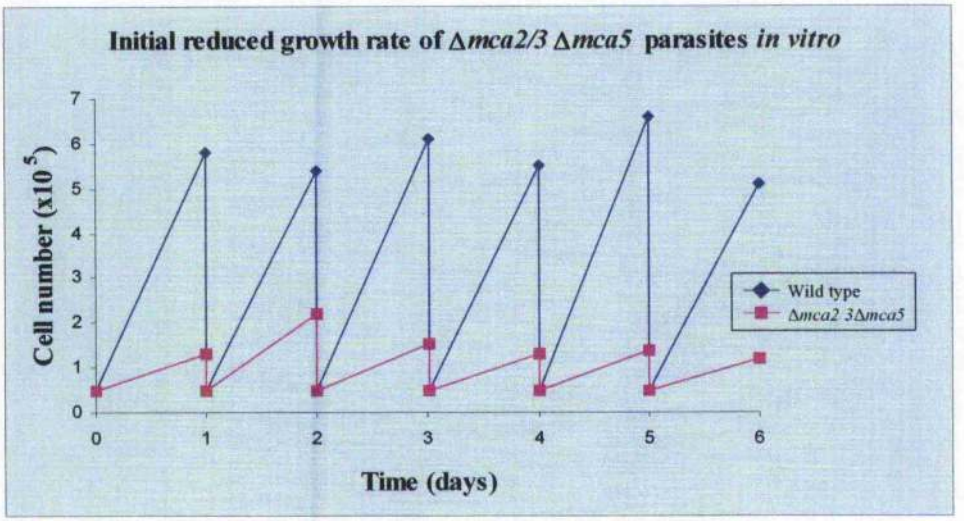
Initial reduced growth rate of Δmca2/3 Δmca5 parasites in vitro
Cell number (x10^5)
Time (days)
Wild type
Δmca2 3Δmca5

B)

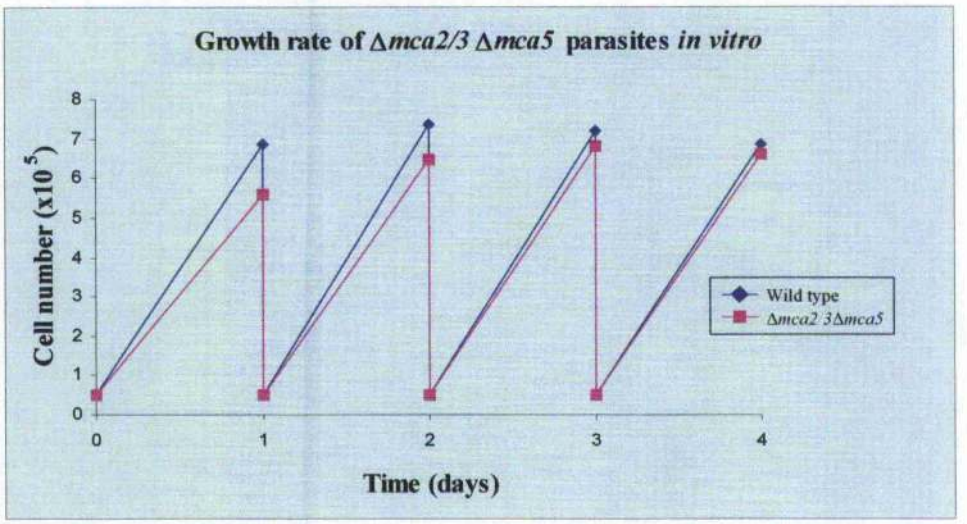
Growth rate of Δmca2/3 Δmca5 parasites in vitro
Cell number (x10^5)
Time (days)
Wild type
Δmca2 3Δmca5

C)

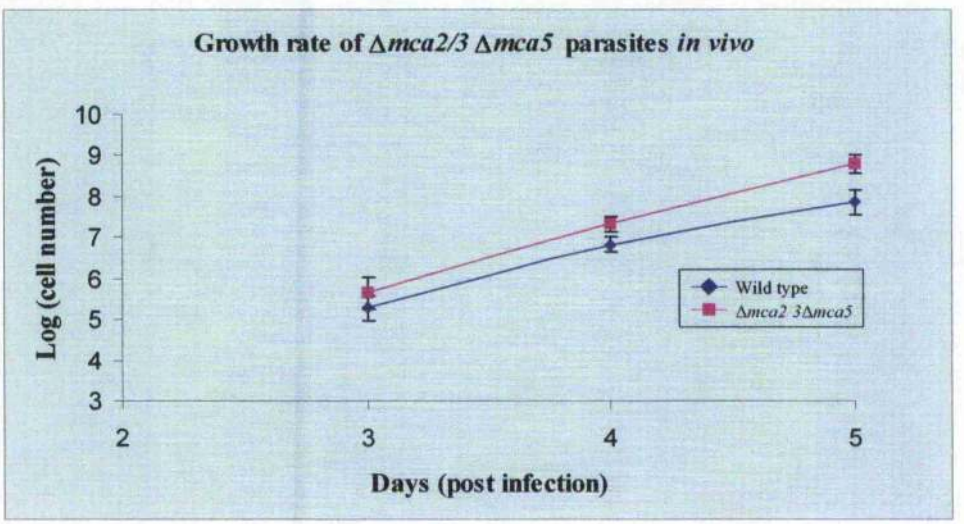
Growth rate of Δmca2/3 Δmca5 parasites in vivo
Log (cell number)
Days (post infection)
Wild type
Δmca2 3Δmca5

Figure 5.15: Analysis of VSG recycling in BSF *T. brucei*.
BSF (strain 427) wild type and Δ*mca2/3*Δ*mca5* clone 1 were biotinylated at 4°C in TDB prior to incubation at 37°C for 5 mins in HMI-9. Remaining surface label was then cleaved by incubation with 50 mM glutathione for 7 mins at 4°C. A) Whole cell lysates were prepared and $5x10^6$ cell equivalents subjected to SDS-PAGE and transferred to PVDF membrane prior to immunoblotting with a streptavidin-HRP conjugate. EF-1α serves as loading control to illustrate equivalent loading. B) Parasites were prepared for IFA both immediately after the glutathione incubation and following a 1 hour chase period in HMI-9. Parasites were fixed in -20°C methanol for 15 mins and permeabilised in -20°C acetone for 2 mins, prior to blocking with 1% (w/v) BSA for 30 mins. Slides were then incubated with a 1/1000 dilution of streptavidin-TexasRed conjugate, 1/200 dilution of rabbit anti-Rab11 antibodies, followed by anti-rabbit-FITC conjugate and 1 μg/ml DAPI. Biotin-VSG and Rab11 labelling is shown together with a merged image, DAPI labelling is also shown. A DIC image of parasites is also provided.

A)

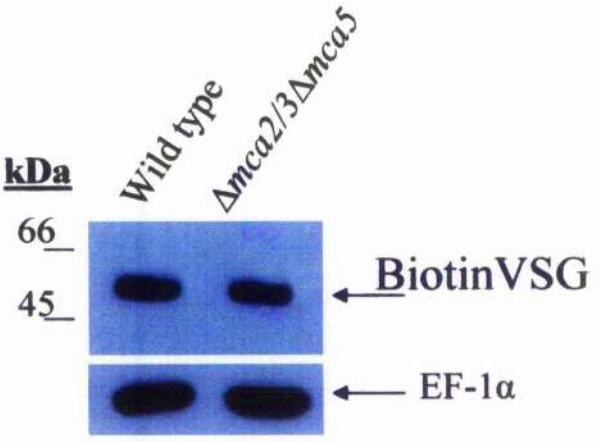
kDa
Wild type
Δmca2/3Δmca5
66
45
BiotinVSG
EF-1α

B)

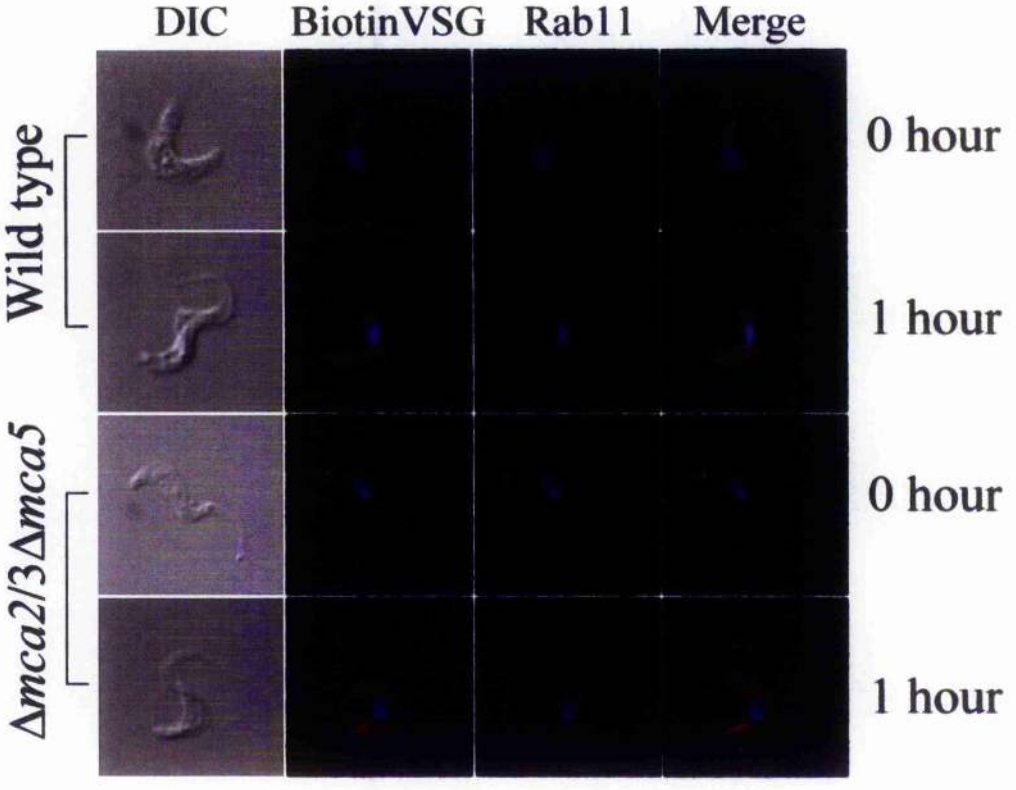
DIC
BiotinVSG
Rab11
Merge
Wild type
Δmca2/3Δmca5
0 hour
1 hour
0 hour
1 hour

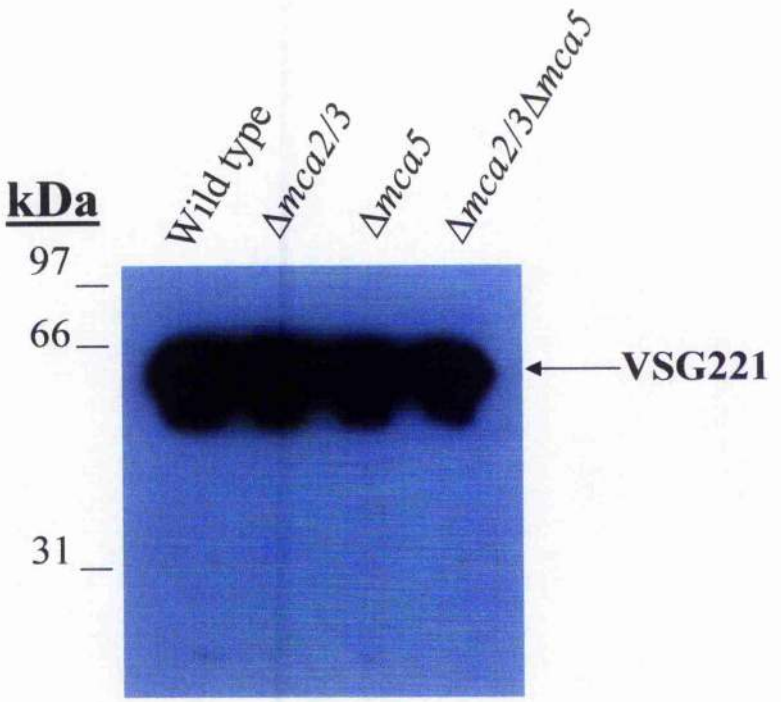

Figure 5.16: Confirmation of VSG221 expression.
Total cell lysates were prepared from BSF (strain 427) wild type, Δ*mca2/3*, Δ*mca5* and Δ*mca2/3*Δ*mca5* parasites. $5x10^6$ cell equivalents were subjected to SDS-PAGE and transferred to PVDF membrane prior to immunoblotting with polyclonal rabbit anti-VSG221 antiserum. The position of VSG221 is indicated.

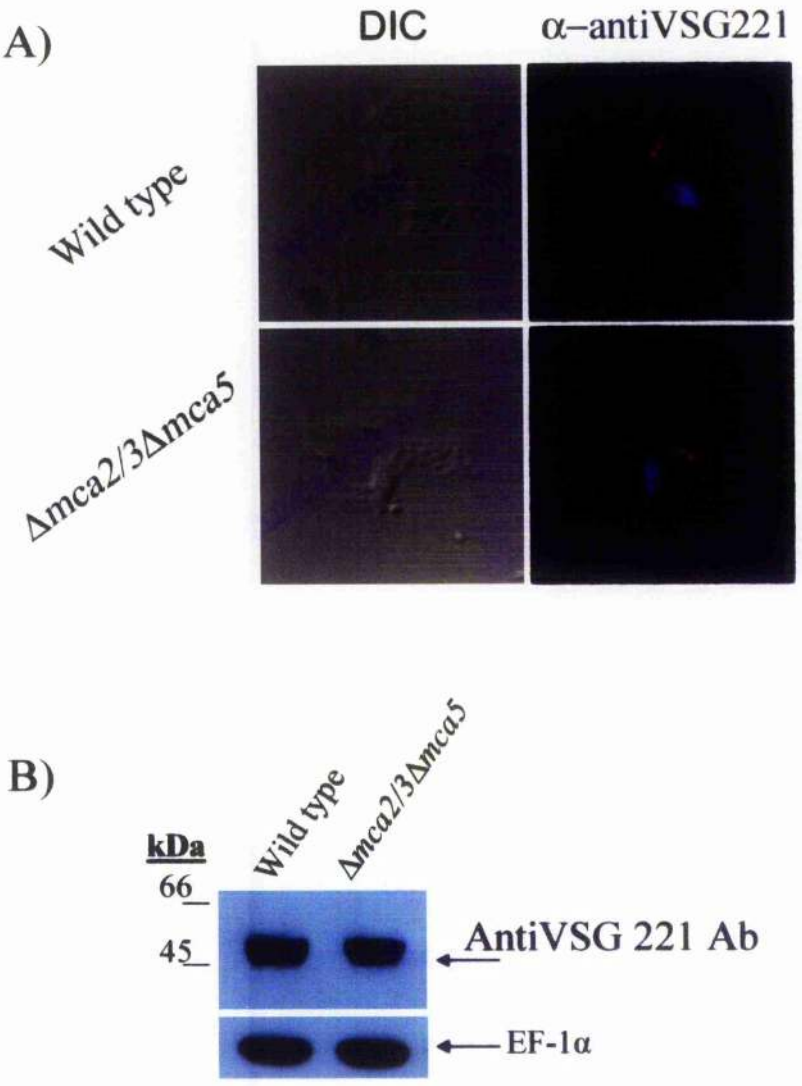

Figure 5.17: Analysis of cell associated anti-VSG antibodies.
BSF (strain 427) wild type and *Δmca2/3Δmca5* clone 1 were labelled with polyclonal rabbit anti-VSG221 antibodies for 30 mins at 4°C in HMI-9. Parasites were then extensively washed and incubated at 37°C for 30 mins in HMI-9 to allow parasites to internalise and clear the surface coat of antibodies. A) Parasites were fixed in -20°C methanol for 15 mins and permeabilised in -20°C acetone for 2 mins, prior to blocking with 5% (w/v) skimmed milk powder for 30 mins. Slides were then incubated with an anti rabbit-TexasRed conjugate and 1 μg/ml DAPI. Anti-VSG221 and DAPI labelling is shown together with DIC images of the parasites. B) Whole cell lysates were prepared and $5x10^6$ cell equivalents subjected to SDS-PAGE and transferred to PVDF membrane prior to immunoblotting with anti rabbit-HRP conjugate. EF-1α serves as a loading control to illustrate equivalent loading. Anti-VSG antibodies are indicated.

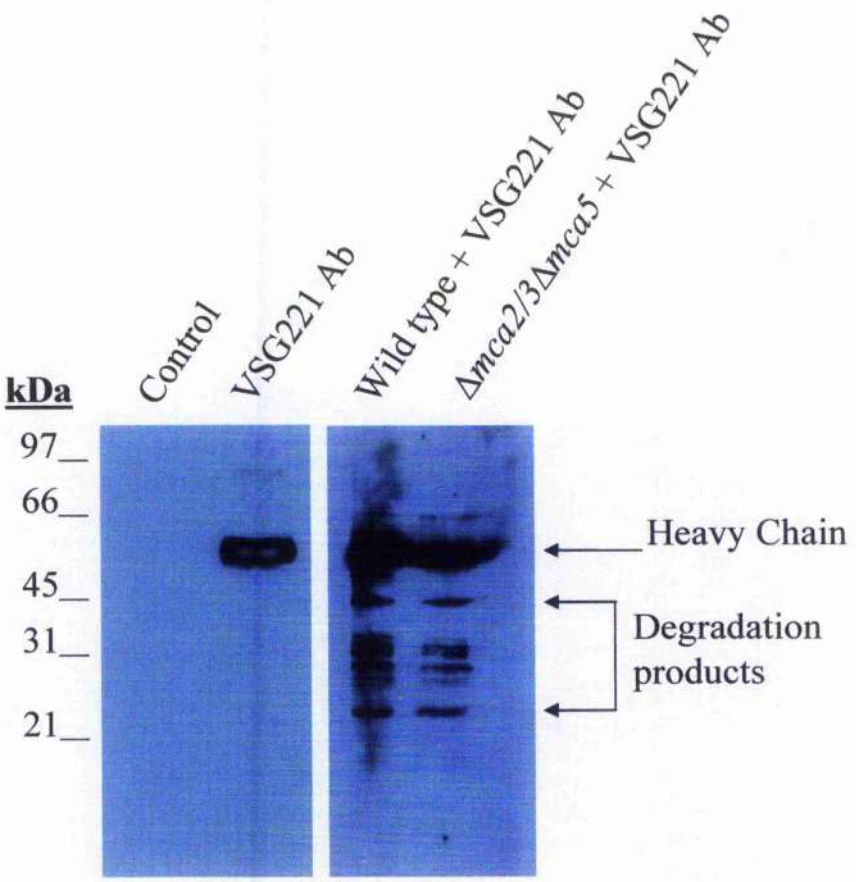

Figure 5.18: Analysis of secreted anti-VSG221 degradation products.
BSF (strain 427) wild type and *Δmca2/3Δmca5* parasites were labelled with polyclonal rabbit anti-VSG221 antibodies for 30 mins at 4°C in HMI-9. Parasites were then extensively washed and incubated at 37°C for 30 mins in HMI-9 to allow parasites to internalise and clear the surface coat of antibodies. TCA precipitations of culture medium were resuspended and subjected to SDS-PAGE and transferred to PVDF membrane prior to immunoblotting with an anti rabbit-HRP conjugate. Also shown are negative (control) and positive (VSG221 Ab) controls. Rabbit immunoglobulin heavy chain and degradation products are indicated.

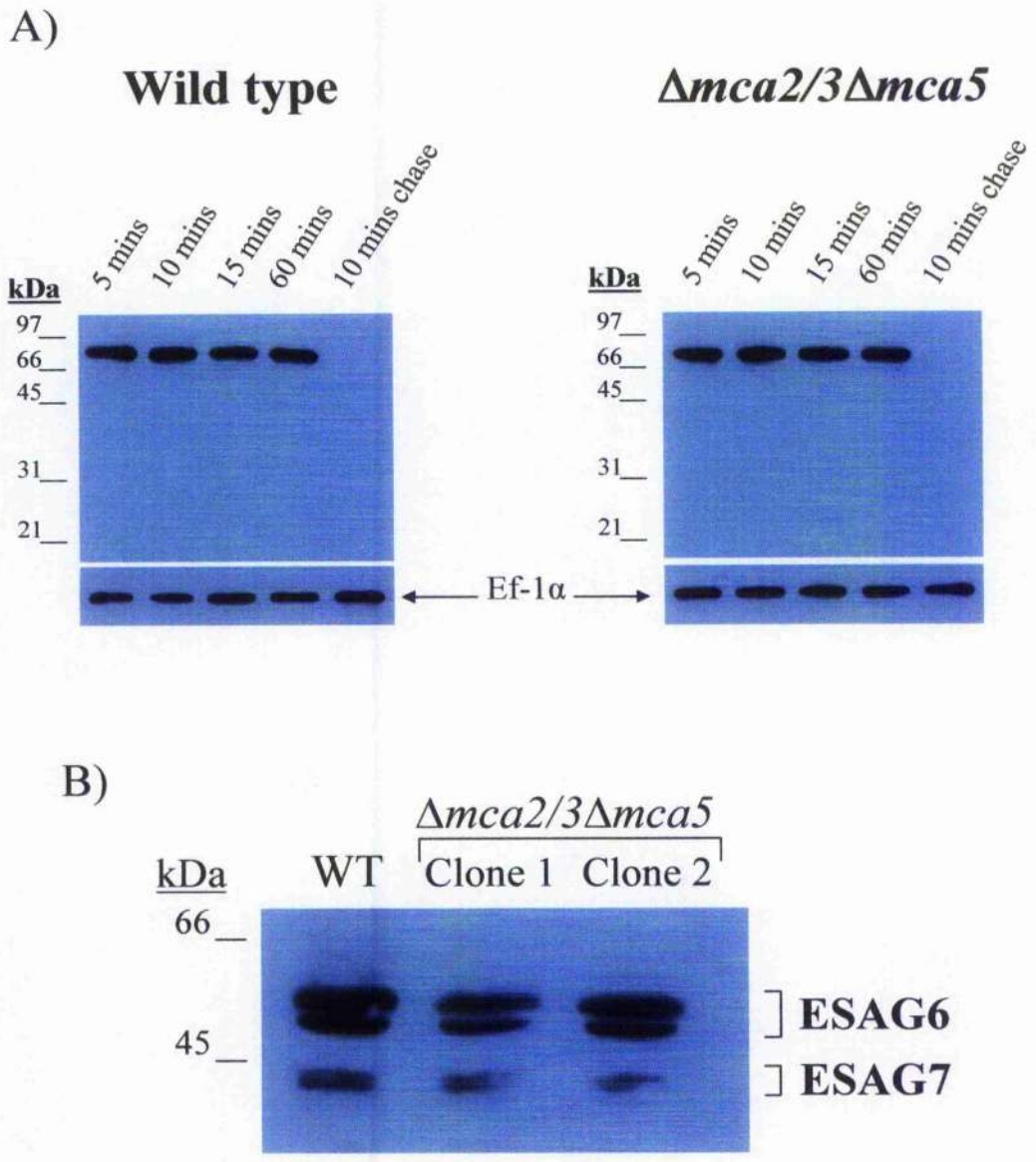

Figure 5.19: Analysis of transferrin uptake and receptor expression.
A) BSF (strain 427) wild type and *Δmca2/3Δmca5* clone 1 were incubated with 50 mM transferrin-biotin conjugate for 5, 10, 15 and 60 mins in serum free HMI-9 followed by a 10-mins chase. Whole cell lysates were prepared and $5x10^6$ cell equivalents subjected to SDS-PAGE and transferred to PVDF membrane prior to immunoblotting with a streptavidin-HRP conjugate. EF-1α serves as a loading control to demonstrate equivalent loading. B) Whole cell lysates were prepared form BSF wild type and *Δmca2/3Δmca5* clones 1 and 2. $5x10^6$ cell equivalents were subjected to SDS-PAGE, transferred to PVDF membrane prior to immunoblotting with anti-transferrin receptor antibodies. The positions of ESAG6 and ESAG7 are indicated.

A)

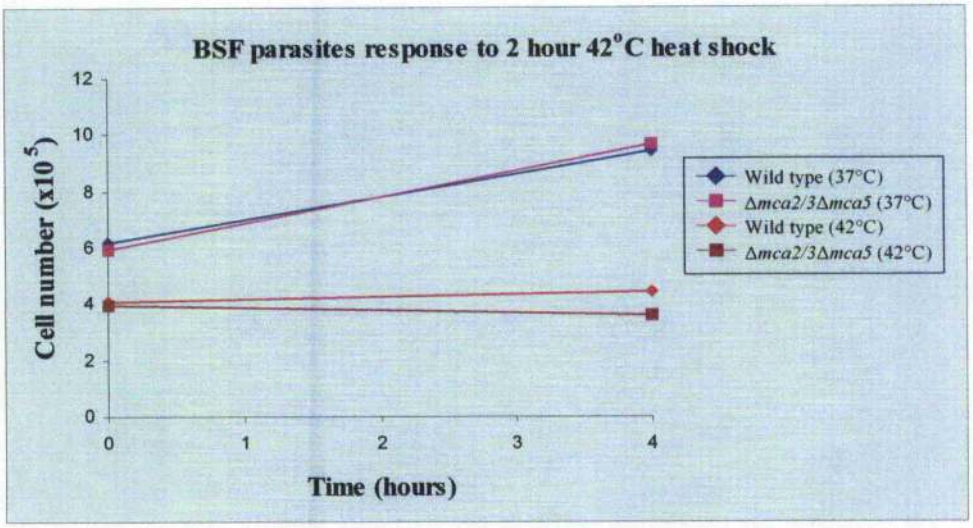

B)

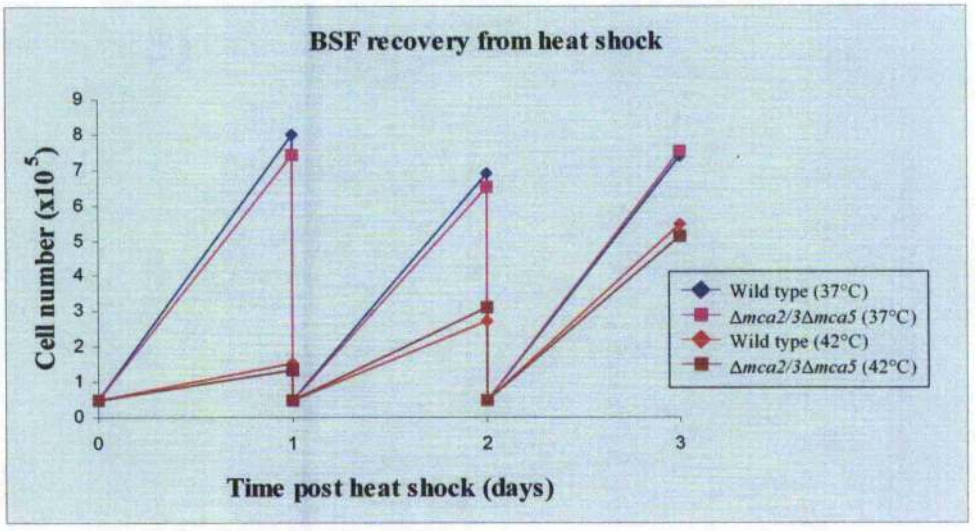

Figure 5.20: Response of *T. brucei* to a 2 hour heat shock at 42°C.
BSF (strain 427) wild type and *Δmca2/3Δmca5* clone 1, at a density of $5x10^5$ cells ml^{-1}, were exposed to a 42°C heat shock for 2 hours or control at 37°C. A) Parasite densities were determined following this 2 hour period and counts made 4 hours subsequently. B) The rate of recovery of parasites following this heat shock relative to controls was also determined. Parasites were re-seeded at $5x10^4$ cells ml^{-1} and counts made every 24 hours with re-seeding at $5x10^4$ cells ml^{-1} daily.

A)

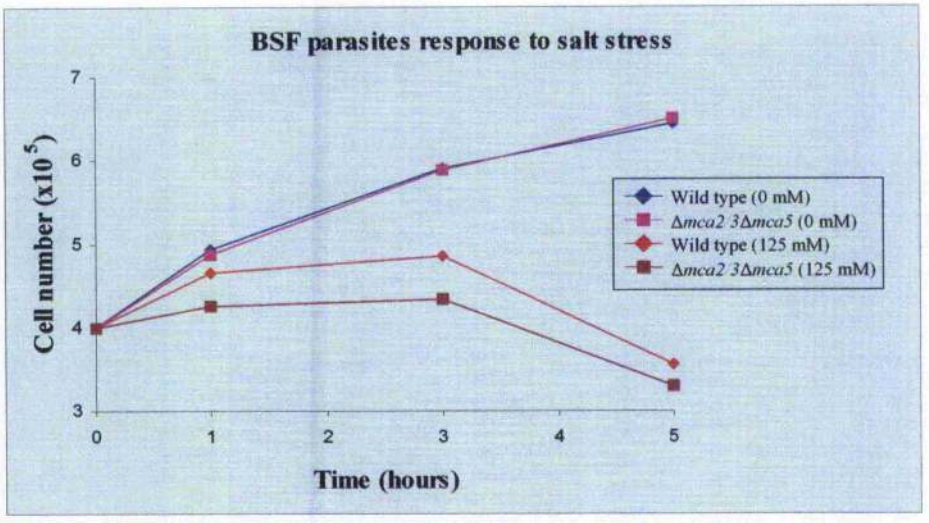

B)

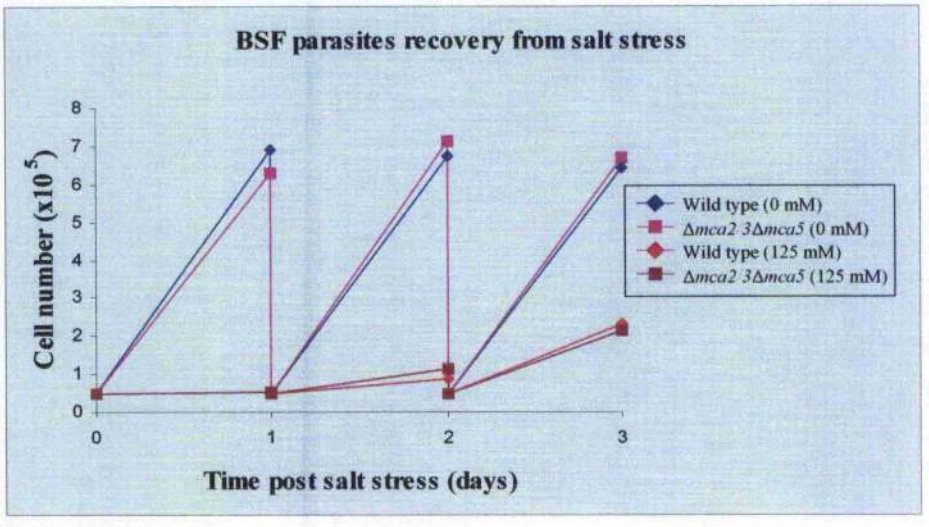

Figure 5.21: Response of *T. brucei* to salt stress.
BSF (strain 427) wild type and *Δmca2/3Δmca5* clone 1 at a density of $4x10^5$ cells ml^{-1} were exposed to 125 mM NaCl in HMI-9. A) Parasite densities were determined following 1, 3 and 5 hour exposure periods. B) The rate of recovery of parasites following this salt stress was also determined. Parasites were extensively washed in HMI-9 prior to re-seeding at $5x10^4$ cells ml^{-1} and counts made every 24 hours with re-seeding at $5x10^4$ cells ml^{-1} daily.

A)

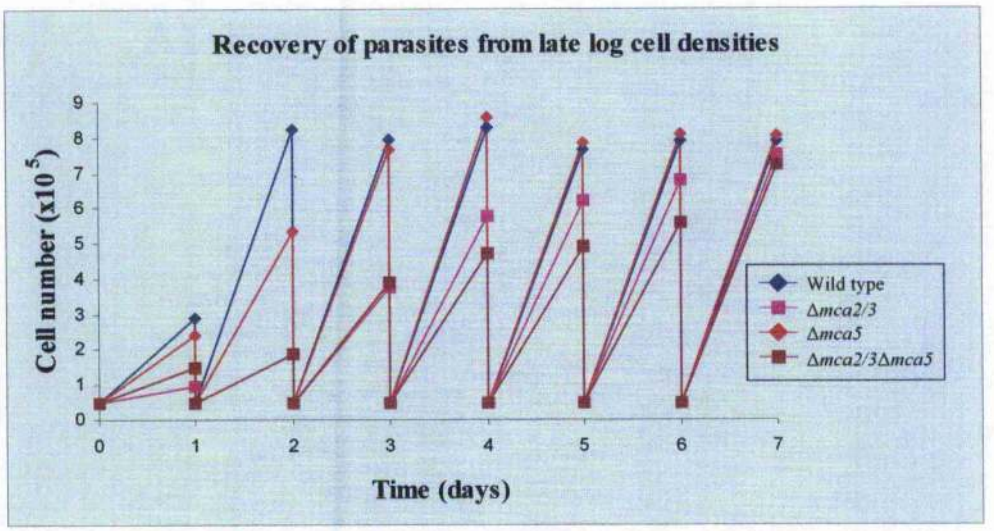

B)

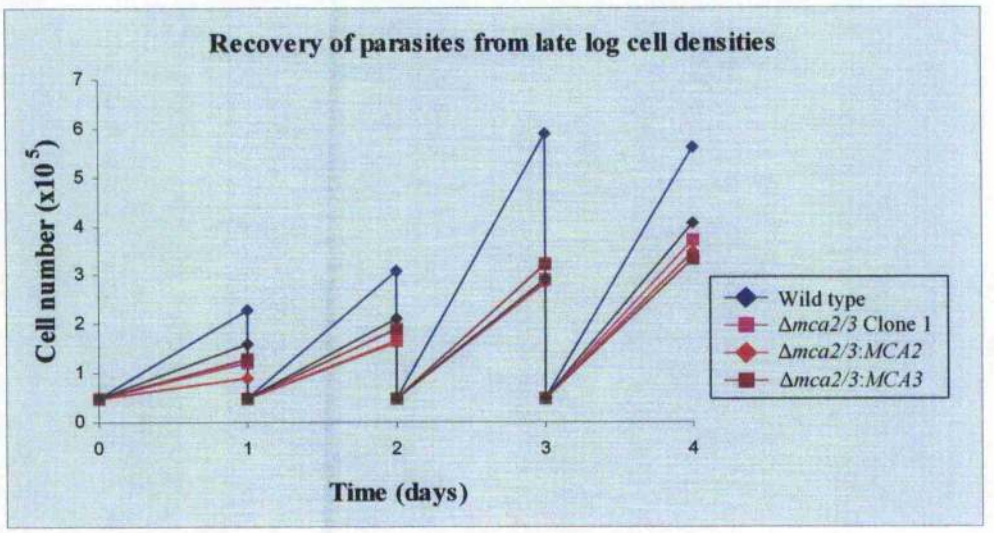

Figure 5.22: Analysis of recovery following growth to late log densities.
BSF (strain 427) parasites were cultured to densities in excess of $4x10^6$ cells ml^{-1}, reaching an apparent stationary growth phase. Cultures were then re-seeded at $5x10^4$ cells/ml and counts made every 24 hours with re-seeding daily to $5x10^4$ cells ml^{-1}. A) Wild type, *Δmca2/3* clone 1, *Δmca5* clone 1 and *Δmca2/3Δmca5* clone 1. B) Wild type, *Δmca2/3* clone 1, *Δmca2/3:MCA2* and *Δmca2/3:MCA3*.

A)

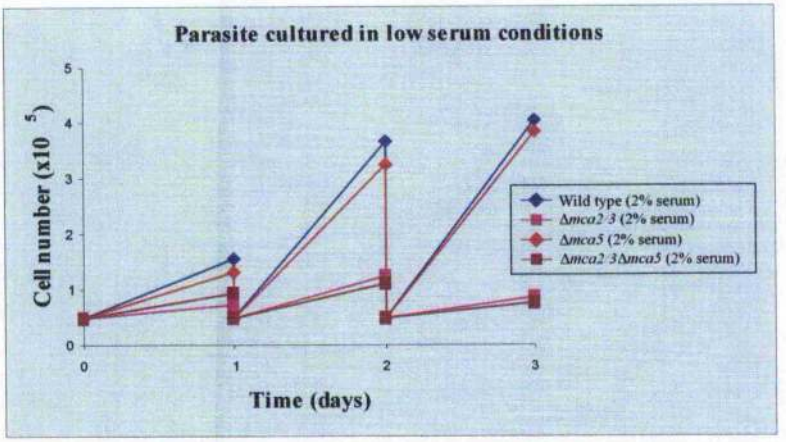

B)

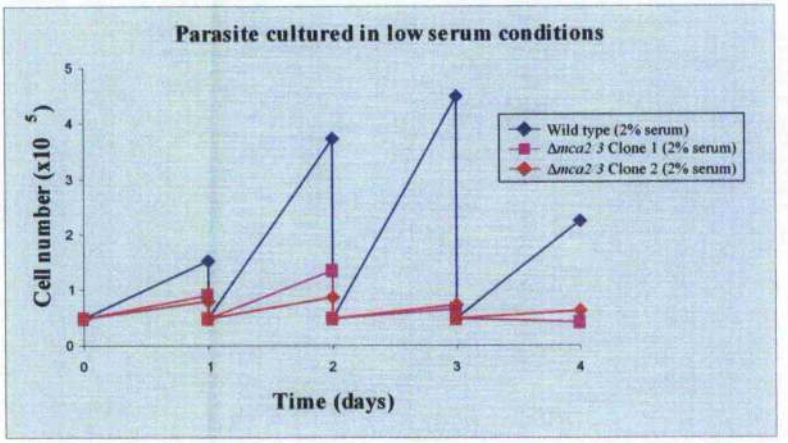

C)

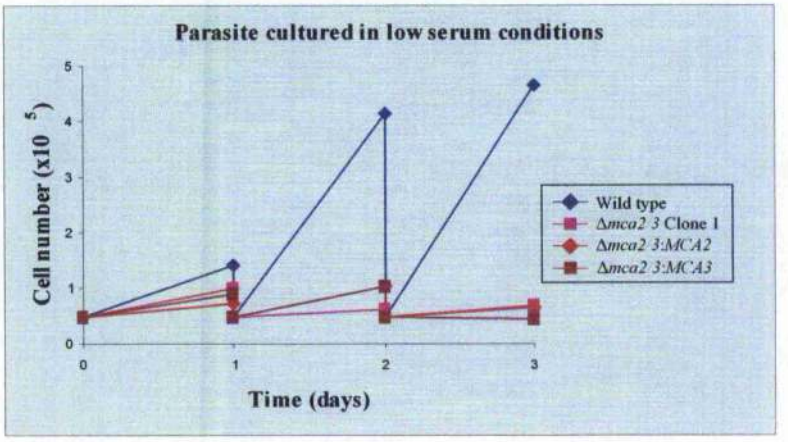

Figure 5.23: Analysis of growth rate under conditions of serum deprivation. The growth rate of BSF (strain 427) parasites was monitored in culture medium with a 10-fold reduction in serum to a final concentration of 2% (v/v). Parasites cultures were seeded at $5x10^4$ cells ml^{-1} and counts made every 24 hours with re-seeding at $5x10^4$ cells ml^{-1} daily. A) Wild type, *Δmca2/3* clone 1, *Δmca5* clone 1 and *Δmca2/3Δmca5* clone1. B) Wild type, *Δmca2/3* clone 1 and clone 2. C) Wild type, *Δmca2/3* clone 1, *Δmca2/3:MCA2* and *Δmca2/3:MCA3*.

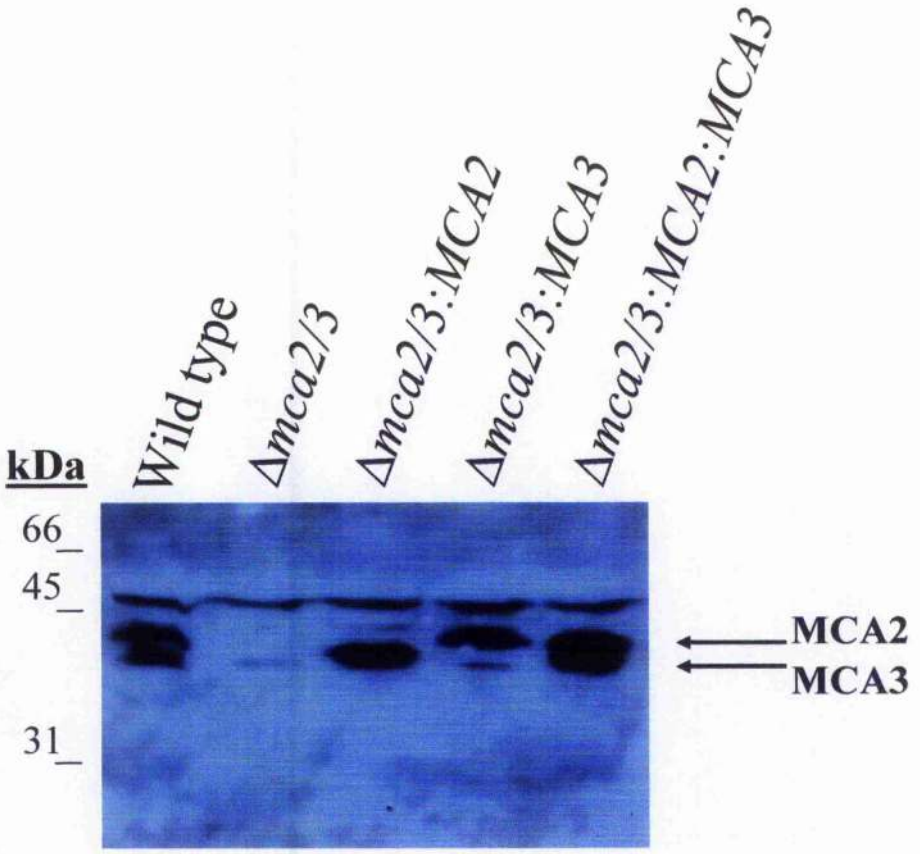

Figure 5.24: Dual re-expression of *MCA2* and *MCA3* in BSF *Δmca2/3*.
Total cell lysates were prepared from *T. brucei* BSF (strain 427) wild type, *Δmca2/3* clone 1, *Δmca2/3:MCA2*, *Δmca2/3:MCA3* and *Δmca2/3:MCA2:MCA3* parasites. $5x10^6$ cell equivalents were then subjected to SDS-PAGE and transferred to PVDF membrane prior to immunoblotting with immunopurified polyclonal rabbit anti-MCA2/3 antibodies. The upper protein also detected by the antibody acts as a loading control. MCA2 and MCA3 are indicated.

A)

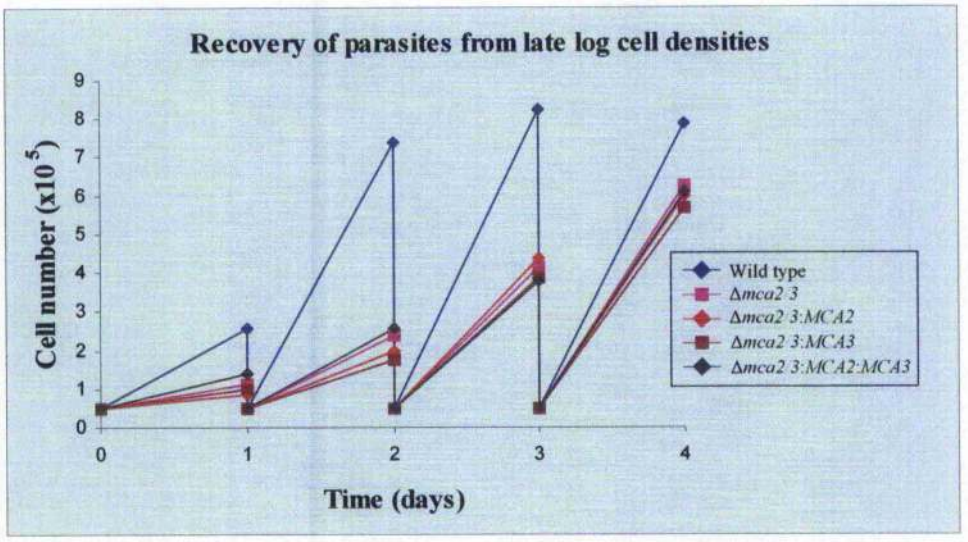

B)

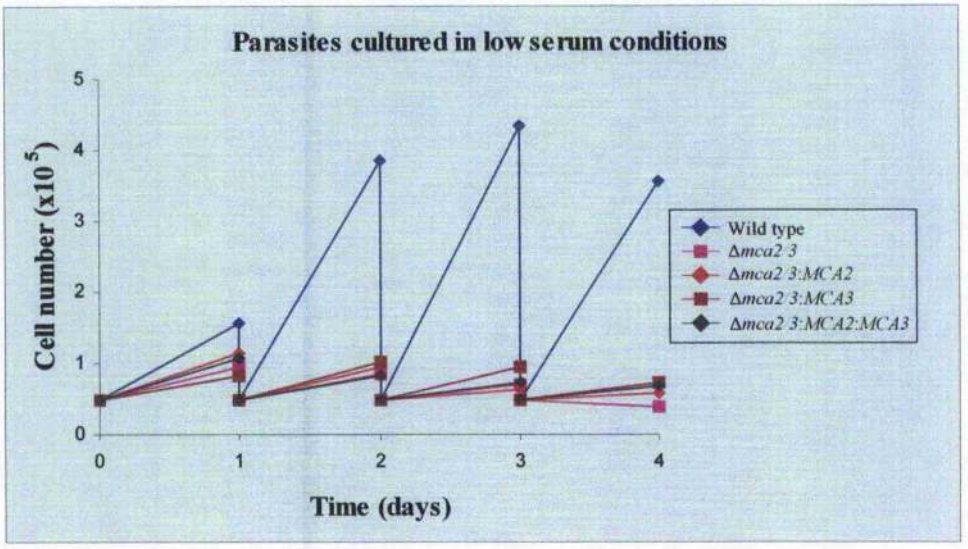

Figure 5.25: Attempts to complement phenotypes in dual re-expressers.
A) BSF (strain 427) wild type, *Δmca2/3* clone 1, *Δmca2/3:MCA2*, *Δmca2/3:MCA3* and *Δmca2/3*:MCA2:*MCA3* were cultured to densities in excess of $4x10^6$ cells ml^{-1} reaching an apparent stationary growth phase. Cultures were then re-seeded at $5x10^4$ cells ml^{-1} and counts made every 24 hours with re-seeding daily to $5x10^4$ cells ml^{-1}. B) The growth rate of BSF (strain 427) wild type, *Δmca2/3*, *Δmca2/3:MCA2*, *Δmca2/3:MCA3* and *Δmca2/3:MCA2:MCA3* parasites was monitored in culture medium with a 10-fold reduction in serum to a final concentration of 2% (v/v). Parasites cultures were seeded at $5x10^4$ cells ml^{-1} and counts made every 24 hours with re-seeding at $5x10^4$ cells ml^{-1} daily.

Chapter 6

Discussion

6.1 Do the metacaspases function similarly to caspases?

At the beginning of this investigation nothing was known about metacaspase function in any organism. Insights into their possible functions have been attained during the three years of this study, and other researchers have also published their findings in this time. Various links between apoptotic-like phenomena and metacaspases have been drawn from studies on yeast and it has been suggested that the metacaspases may have caspase-like activity and functions (Madeo et al., 2002; Szallies et al., 2002; Herker et al., 2004; Wadskog et al., 2004). Similarly it has also been suggested that the metacaspases are involved in the hypersensitivity response of plants, a phenomenon of developmentally regulated cell death with some similarities to programmed cell death (PCD) (Suarez et al., 2004; Bozhkov et al., 2004).

It is easy to see why this path of investigation for metacaspase function has been pursued, as no true caspase genes have been identified in either yeast or plants despite continued reports of PCD/apoptotic-like phenomenon (Eisler et al., 2004; Fabrizio et al., 2004; Chen and Dickman, 2004; Hatsugai et al., 2004). Indeed, it is also an attractive proposition to postulate that the metacaspases in trypanosomatids might be responsible for the reports of apoptotic-like cell death that have been reported in the literature (Moreira et al., 1996; Ameisen et al., 1996; Welburn et al., 1997; Ridgley et al., 1999; Das et al., 2001; Lee et al., 2002; Arnoult et al., 2002; Sen et al., 2004). To believe that the metacaspases are involved in some form of PCD/apoptotic-like pathway is to presumably assume that the metacaspases are able to bring about cell death, and over the course of evolution became modern day caspases found in multicellular organisms. If the reports in both yeast and plants are to be believed, this would imply that a common ancestor that possessed metacaspases also had at least a rudimentary suicidal mechanism. This is a controversial hypothesis as many people believe that apoptosis/PCD is only a plausible phenomenon in multicellular organisms.

The basis for hypothesising that the metacaspases may have similar functions to the caspases stems from the fact that of all the other Clan CD peptidases, they are predicted to be most similar to the caspases in regards to evolutionary

origins (Uren et al., 2000). However, the precedent set from another family in Clan CD, C13, which contains both the legumains and the glycosylphosphatidylinositol (GPI) transamidases, suggests that attempting to extrapolate functions based upon sequence similarities can not always be relied upon. These two classes of peptidase, although having widely distinct functions are grouped in the same family. While the legumains are proteolytic enzymes, GPI transamidases, although still proteolytic, catalyse the nucleophilic attack of the activated carbonyl group with an NH_2 group of a pre-formed GPI anchor. Additionally, legumains have been characterised as having seperate functions in different organisms. In human B-cells they are lysosomal enzymes, involved in foreign antigen degradation and the generation of suitable peptides to form complexes with the class II major histocompatibility complex (Manoury et al., 1998). In the blood fluke *Schistosoma mansoni*, it has been proposed that they proteolytic activate CB1, the major papain-like cysteine peptidase detected in the lumen of the schistosome gut and which is involved in haemoglobin degradation (Sajid et al., 2003). In plants they can be localised to the vacuole, where they have been implicated in storage protein breakdown during germination and seedling growth (Muntz and Shutov, 2002).

Cleary there are precedents then for Clan CD peptidases within families to have different functions, and even for different organisms to use homologous proteins for divergent roles. Therefore, while hypothesising that the metacaspases might have a role in apoptosis or PCD-like phenomena based upon their evolutionary relationship to caspases might be attractive, the reality may be different. Indeed, this study has provided evidence that MCA2, MCA3 and MCA5 are associated with recycling endosomes in *T. brucei*. However, the deletion of *MCA2*, *MCA3* and *MCA5* did not appear to affect either of the characterised recycling processes in BSF parasites, with no disruption of the VSG and transferrin receptor recycling pathways being detectable. There are several possible reasons as to why no phenotypes related to recycling were detected in this study. The metacaspases may either be involved in an uncharacterised recycling process, or be involved in a component of the VSG or transferrin pathway not examined in our analysis. Additionally, there is the possibility that that the metacaspases have a high level of redundancy and that MCA1 and/or

MCA4 may be compensating for the deletion of *MCA2*, *MCA3* and *MCA5*. Another possibility is that despite association with recycling endosomes, metacaspase function might be unrelated to recycling processes.

Although a specific function has not been assigned to the metacaspases in this investigation, their association with recycling endosomes does not immediately suggest a role in cell death or other cellular processes that are known to involve caspase functions. Indeed, our investigations into possible metacaspase involvement in cell death in *T. brucei*, although far from extensive, were unable to detect any differences between wild type and Δ*mca2/3*Δ*mca5* parasites. As previously discussed, the only suggestions made in the literature for metacaspase function relate to apoptotic/PCD-like phenomena. In *Saccharomyces cerevisiae* a global analysis of protein localisation, using GFP as a label, localised the single yeast metacaspase to both the nucleus and cytoplasm (Huh et al., 2003), and the ectopic expression of a *Tb*MCA4-GFP fusion in yeast also revealed apparent nuclear localisation (Szallies et al., 2002). If this localisation is to be believed, this is markedly different from what we have observed in *T. brucei* in that no nuclear or cytosolic localisation was detected for MCA2, MCA3 or MCA5. It is possible, therefore, that the different localisations could represent divergent function of the metacaspases between yeast and *T. brucei*.

The lack of any apparent processing of the metacaspases in our study is also different to what has been reported in yeast and plants. Processing has been reported following overexpression of the FLAG-tagged single yeast metacaspase (Madeo et al., 2002), and has also been observed following expression of polyhistidine tagged *Arapidopsis thialiana* type II metacaspases in *E. coli* (Vercammen et al., 2004). In both of these reports the processing was dependent on the putative active site residues, as no processing was observed when these were mutated. This evidence suggests that the metacaspases have similarities to caspases in that they appear to autocatalytically process. Determination of the *A. thialiana* type II metacaspase activity also suggested that this processing was required to generate active peptidase (Vercammen et al., 2004). However, in our study no large scale processing events were

observed for any of the metacaspases examined. MCA2, MCA3 and MCA5 were invariably detected at sizes closely corresponding to the full-length protein predictions, despite various attempts to induce processing through exposure to stressful stimuli. Additionally, the initial slow growth rate phenotype observed in the newly generated Δ*mca2/3*Δ*mca5* parasites suggests that they are active under normal *in vitro* conditions and do not require processing. We hypothesise, therefore, that unlike the plant type II metacaspases the *T. brucei* metacaspases are active as full-length proteins. Plant type II metacaspases are categorised by the possession of an insertion of approximately 200 amino acids (Uren et al., 2000). This insertion appears to be unique to plant type II metacaspases and is not present in any other the metacaspases identified in yeast or protozoa. The autocatalytic cleavage site identified with the type II metacaspases is found within this insertion domain (Vercammen et al., 2004), and the *A. thaliana* type I metacaspases which lack this insertion did not display processing when expressed in *E. coli*. This might explain the absence of processing in the *T. brucei* metacaspases, as they do not possess a similar cleavage site.

6.2 Comparison of RNAi versus gene knockout to study function

The functions of the metacaspases were examined in this study by two techniques. Initially, RNAi was performed on *MCA2*, *MCA3* and *MCA5* and then later various null mutants were generated. The RNAi system used in this study, as previously discussed, appears to be prevalent with non-specific artefacts. These artefacts, present in the *MCA2/3* and *MCA5* RNAi were shown to be independent of gene silencing, which was further confirmed when the generation of both the *MCA2/3*-deficient and *MCA5*-deficient mutants were shown to be possible without any detrimental effects. However, there was a question regarding the growth arrest and difficulty in attaining clones when the triple RNAi of *MCA2*, *MCA3* and *MCA5* was performed. It was hypothesised that the silencing of all three genes might indeed be detrimental to the parasites. Indeed, the slow initial growth rate observed upon generation of Δ*mca2/3*Δ*mca5* parasites suggests that metacaspase function is important to parasite growth, even though they appear to be able to adapt to the loss over time and regain normal growth rates. As suspected, however, the morphology changes seen in

the triple RNAi would appear to be nothing to do with metacaspase deletion, as no similar changes were observed in the triple null mutants.

6.3 Possible role of "dead peptidases"

The identification of metacaspase genes that appear to have substitutions at the putative active site residues raised the possibility that they might have a function independent of cysteine peptidase activity. This has echos with a recent study, which has identified numerous inactive enzyme homologues in metazoan databases, and for which their presence was suggested to be the rule rather than the exception (Pils and Schultz, 2004b). For example, it was demonstrated that within the protein tyrosine phosphatase family some members possess putative non-catalytic phosphatase domains (Pils and Schultz, 2004a). These variants were still able to bind substrates, and due to the loss of catalytic activity, these become trapped and were protected from other active phosphatases. Another example is phospholipase A2 (PLA2) and its inhibitor. These share two out of the three catalytic residues, with the third having been substituted in the inhibitor (Bartlett et al., 2003). This inhibitor no longer possesses catalytic activity, but forms an inactive heterodimeric complex with PLA2, and thus regulates the enzyme. The majority of these inactive enzyme homologues identified were involved in regulatory processes (Pils and Schultz, 2004b). Their effects are achieved either directly, with the inactive enzyme homologue acting as a regulatory subunit as in the PLA2 example, or alternatively via antagonisation of the active enzyme, as in the phosphatase example. In MCA1 and MCA4, which are predicted to have active site substitutions, there remains a high conservation of residues around these sites. This suggests that if these two proteins are acting as modulators of metacaspase activity, this is likely to be occurring through the antagonisation model.

6.4 Future studies

The identification of predicted WW binding domains within MCA2, MCA3 and MCA5 suggests that the metacaspases may interact with other cellular proteins via this domain, and WW domains have been identified within nine annotated proteins in *T. brucei* (www.genedb.org). To further our understanding of metacaspase function, attempts to identify interacting partners may be useful.

Within yeast there have been several independent comprehensive studies performed examining protein-protein interactions through the yeast two-hybrid system (Uetz et al., 2000; Ito et al., 2001; Hazbun et al., 2003). The most recent study, Hazbun *et al.* 2003, identified 10 proteins with which the yeast metacaspase interacted (Table 6.1).

Systematic Name	Standard Name	Description	Homologue in *T. brucei*
YBL106C	*SRO77*	Suppressor of defect in the small GTPase Rho3p	No
YIL113W	*SDP1*	Stress-inducible dual specificity phosphatase	Yes (*Tb*04.1H19.900)
YKL012W	*PRP40*	U1 snRNP protein involved in splicing	No
YKR096W		Unknown	Hypothetical (*Tb*11.02.2360)
YLR371W	*ROM2*	GDP/GTP exchange protein for Rho1p and Rho2p	No
YLR410W	*VIP1*	Interactions with actin	No
YMR257C	*PET111*	Specific translational activator for the COX2 mRNA	No
YNL075W	*IMP4*	Component of the SSU processome	Yes (*Tb*06.5F5.280)
YNL339C	*YRF1*	Helicase	Yes (*Tb*11.12.0011)
YPL137C		Unknown	Hypothetical (*Tb*08.10J17.380)

Table 6.1: List of proteins thought to interact with yeast metacaspase (from Hazbun *et al.* 2003).

While none of these potential partners have been validated through co-localisation studies, this type of approach may further aid in the understanding of metacaspase function. Attempts to identify interacting partners of the *T. brucei* metacaspases could be pursued through either immunoprecipitations or via the tandem affinity purification (TAP) method (Rigaut et al., 1999). If successful, any proteins identified could be subjected to mass spectrometry and identified from the *T. brucei* database. These could also be compared to what has been found in yeast as several of the interacting proteins identified in yeast are homologous to *T. brucei* proteins (Table 6.1).

A theme running throughout this study has been the possible redundancy within the metacaspase family, and in particular through the uncharacterised *MCA1*

and *MCA4*. The production of specific antibodies to determine the expression profile of these two genes could provide insights into this possibility. It would be interesting to determine whether they are expressed, and, if they are, if there is a differential expression profile between the life stages - as there is for MCA2 and MCA3. Additionally, it would be interesting to determine whether MCA1 and/or MCA4 also localise to the same compartment as the other characterised metacaspases.

Assuming that MCA1 and/or MCA4 are expressed in the parasites, it would be attractive to further delete these genes to investigate this redundancy hypothesis. Expanding upon the strategy already utilised, it is theoretically possible to delete one further gene from the PCF Δ*mca5* parasites, although no further deletions will be possible in the BSF Δ*mca2/3*Δ*mca5* parasites. This is due to the limited number of antibiotic resistance markers available for the generation of transgenic parasites. However, the generation of multiple null mutants via the recycling of resistance markers might be possible. This could be achieved through the utilisation of a similar strategy as has been reported for *Leishmania* (Denise et al., 2004). This technique used the hygromycin resistance gene as a positive marker and a thymidine kinase gene as a negative marker. This technique allows null mutants to be generated without the addition of any exogenous DNA, and thus allows the resistance marker to be re-used. If this strategy was shown to be successful in *T. brucei*, it would be possible to delete multiple metacaspase genes. Alternatively, it should be possible to silence all five genes by RNAi. While this study has highlighted problems with the RNAi technique utilised, it may be that these were vector-specific and performing RNAi with another vector may not have the same problems. We were able to show that the silencing of three metacaspase genes was possible by RNAi and therefore it should be possible to silence five simultaneously in the BSF if required.

Unfortunately, biochemical characterisation of the metacaspases was not pursued in this study due to problems of solubility with the recombinant enzymes. The successful refolding of cysteine peptidases from inclusion bodies has been performed successfully (Sanderson et al., 2000), although attempts to

perform this with the metacaspases were unsuccessful (S. Sanderson – unpublished). Further attempts at generating soluble recombinant enzymes in *E. coli* or *Pichia* could be pursued to solve these problems. While the *A. thaliana* type II metacaspases have been shown to be specific for arginine/lysine at the P1 position (Vercammen et al., 2004), it would be interesting to perform a similar study on the *T. brucei* metacaspases. This could answer whether they possess the same specificity and whether they are active as full-length proteins or require processing. Additionally, this could also address the question of whether MCA1 and/or MCA4 are active peptidases or inactive enzyme homologues.

Reference List

Al Olayan, E.M., Williams, G.T., and Hurd, H. (2002). Apoptosis in the malaria protozoan, *Plasmodium berghei*: a possible mechanism for limiting intensity of infection in the mosquito. Int. J. Parasitol. *32*, 1133-1143.

Alexandre, S., Guyaux, M., Murphy, N.B., Coquelet, H., Pays, A., Steinert, M., and Pays, E. (1988). Putative genes of a variant-specific antigen gene transcription unit in *Trypanosoma brucei*. Mol. Cell Biol. *8*, 2367-2378.

Allen, C.L., Goulding, D., and Field, M.C. (2003). Clathrin-mediated endocytosis is essential in *Trypanosoma brucei*. EMBO J. *22*, 4991-5002.

Ameisen, J.C., Idziorek, T., Billaut-Multo, O., Loyens, M., Yissier, J.P., Potentier, A., and Ouaissi, A. (1996). Apoptosis in a unicellular eukaryote (*Trypanosoma cruzi*): Implications for the evolutionary origin and role of programmed cell death in the control of cell proliferation, differentiation and survival. Parasitol. Today *12*, 49.

Andre, B. and Springael, J.Y. (1994). WWP, a new amino acid motif present in single or multiple copies in various proteins including dystrophin and the SH3-binding Yes-associated protein YAP65. Biochem. Biophys. Res. Commun. *205*, 1201-1205.

Aravind, L., Dixit, V.M., and Koonin, E.V. (1999). The domains of death: evolution of the apoptosis machinery. Trends Biochem. Sci. *24*, 47-53.

Arnoult, D., Akarid, K., Grodet, A., Petit, P.X., Estaquier, J., and Ameisen, J.C. (2002). On the evolution of programmed cell death: apoptosis of the unicellular eukaryote *Leishmania major* involves cysteine proteinase activation and mitochondrion permeabilization. Cell Death Differ. *9*, 65-81.

Asgian, J.L., James, K.E., Li, Z.Z., Carter, W., Barrett, A.J., Mikolajczyk, J., Salvesen, G.S., and Powers, J.C. (2002). Aza-peptide epoxides: A new class of inhibitors selective for clan CD cysteine proteases. J. Med. Chem. *45*, 4958-4960.

Balber, A.E. (1990). The pellicle and the membrane of the flagellum, flagellar adhesion zone, and flagellar pocket: functionally discrete surface domains of the bloodstream form of African trypanosomes. Crit. Rev. Immunol. *10*, 177-201.

Bangs, J.D., Uyetake, L., Brickman, M.J., Balber, A.E., and Boothroyd, J.C. (1993). Molecular cloning and cellular localization of a BiP homologue in *Trypanosoma brucei*. Divergent ER retention signals in a lower eukaryote. J. Cell Sci. *105*, 1101-1113.

Barrett, A.J. (2004). Bioinformatics of proteases in the MEROPS database. Curr. Opin. Drug Discov. Devel. *7*, 334-341.

Barrett, A.J. and Rawlings, N.D. (2001). Evolutionary lines of cysteine peptidases. Biol. Chem. *382*, 727-733.

Barry, J.D. and McCulloch, R. (2001). Antigenic variation in trypanosomes: Enhanced phenotypic variation in a eukaryotic parasite. Adv. Parasitol. *49*, 1-70.

Bart, G., Coombs, G.H., and Mottram, J.C. (1995). Isolation of *lmcpc*, a gene encoding a *Leishmania mexicana* cathepsin B-like cysteine proteinase. Mol. Biochem. Parasitol. *73*, 271-274.

Bartlett, G.J., Borkakoti, N., and Thornton, J.M. (2003). Catalysing new reactions during evolution: economy of residues and mechanism. J. Mol. Biol. *331*, 829-860.

Bastin, P., Ellis, K., Kohl, L., and Gull, K. (2000). Flagellum ontogeny in trypanosomes studied via an inherited and regulated RNA interference system. J. Cell Sci. *113*, 3321-3328.

Bastin, P., Sherwin, T., and Gull, K. (1998). Paraflagellar rod is vital for trypanosome motility. Nature *391*, 548.

Benghezal, M., Benachour, A., Rusconi, S., Aebi, M., and Conzelmann, A. (1996). Yeast Gpi8p is essential for GPI anchor attachment onto proteins. EMBO J. *15*, 6575-6583.

Benne, R., Vandenburg, J., Brakenhoff, J.P.J., Sloof, P., Vanboom, J.H., and Tromp, M.C. (1986). Major transcript of the frameshifted coxII gene from trypanosome mitochondria contains 4 nucleotides that are not encoded in the dna. Cell *46*, 819-826.

Bernstein, E., Caudy, A.A., Hammond, S.M., and Hannon, G.J. (2001). Role for a bidentate ribonuclease in the initiation step of RNA interference. Nature *409*, 363-366.

Besteiro, S., Biran, M., Biteau, N., Coustou, V., Baltz, T., Canioni, P., and Bringaud, F. (2002). Succinate secreted by *Trypanosoma brucei* is produced by a novel and unique glycosomal enzyme, NADH-dependent fumarate reductase. J. Biol. Chem. *277*, 38001-38012.

Bienen, E.J., Saric, M., Pollakis, G., Grady, R.W., and Clarkson, A.B. (1991). Mitochondrial development in *Trypanosoma brucei brucei* transitional blood-stream forms. Mol. Biochem. Parasitol. *45*, 185-192.

Bilder, D., Li, M., and Perrimon, N. (2000). Cooperative regulation of cell polarity and growth by *Drosophila* tumor suppressors. Science *289*, 113-116.

Boatright, K.M., Renatus, M., Scott, F.L., Sperandio, S., Shin, H., Pedersen, I.M., Ricci, J.E., Edris, W.A., Sutherlin, D.P., Green, D.R., and Salvesen, G.S. (2003). A unified model for apical caspase activation. Mol. Cell *11*, 529-541.

Bohmert, K., Camus, I., Bellini, C., Bouchez, D., Caboche, M., and Benning, C. (1998). AGO1 defines a novel locus of *Arabidopsis* controlling leaf development. EMBO J. *17*, 170-180.

Boldin, M.P., Goncharov, T.M., Goltsev, Y.V., and Wallach, D. (1996). Involvement of MACH, a novel MORT1/FADD-interacting protease, in Fas/APO-1- and TNF receptor-induced cell death. Cell *85*, 803-815.

Bork, P. and Sudol, M. (1994). The WW domain: a signalling site in dystrophin? Trends Biochem. Sci. *19*, 531-533.

Borst, P. and Fairlamb, A.H. (1998). Surface receptors and transporters of *Trypanosoma brucei*. Annu. Rev. Microbiol. *52*, 745-778.

Bozhkov, P.V., Filonova, L.H., Suarez, M.F., Helmersson, A., Smertenko, A.P., Zhivotovsky, B., and von Arnold, S. (2004). VEIDase is a principal caspase-like activity involved in plant programmed cell death and essential for embryonic pattern formation. Cell Death. Differ. *11*, 175-182.

Brickman, M.J. and Balber, A.E. (1993). *Trypanosoma brucei rhodesiense*: membrane glycoproteins localized primarily in endosomes and lysosomes of bloodstream forms. Exp. Parasitol. *76*, 329-344.

Brooks, D.R., Tetley, L., Coombs, G.H., and Mottram, J.C. (2000). Processing and trafficking of cysteine proteases in *Leishmania mexicana*. J. Cell Sci. *113*, 4035-4041.

Brun, R. and Schonenberger, M. (1979). Cultivation and *in vitro* cloning of procyclic forms of *Trypanosoma brucei* in a semi-defined medium. Acta Trop. *36*, 289-292.

Bucci, C., Parton, R.G., Mather, I.H., Stunnenberg, H., Simons, K., Hoflack, B., and Zerial, M. (1992). The small GTPase rab5 functions as a regulatory factor in the early endocytic pathway. Cell *70*, 715-728.

Burri, C. and Brun, R. (2003). Eflornithine for the treatment of human African trypanosomiasis. Parasitol. Res. *90 Supp 1*, S49-S52.

Cai, J., Yang, J., and Jones, D.P. (1998). Mitochondrial control of apoptosis: the role of cytochrome c. Biochim. Biophys. Acta *1366*, 139-149.

Chang, H.Y. and Yang, X. (2000). Proteases for cell suicide: functions and regulation of caspases. Microbiol. Mol. Biol. Rev. *64*, 821-846.

Chen, J.M., Dando, P.M., Rawlings, N.D., Brown, M.A., Young, N.E., Stevens, R.A., Hewitt, E., Watts, C., and Barrett, A.J. (1997). Cloning, isolation, and characterization of mammalian legumain, an asparaginyl endopeptidase. J. Biol. Chem. *272*, 8090-8098.

Chen, S. and Dickman, M.B. (2004). Bcl-2 family members localize to tobacco chloroplasts and inhibit programmed cell death induced by chloroplast-targeted herbicides. J. Exp. Bot.

Cheng, E.H., Kirsch, D.G., Clem, R.J., Ravi, R., Kastan, M.B., Bedi, A., Ueno, K., and Hardwick, J.M. (1997). Conversion of Bcl-2 to a Bax-like death effector by caspases. Science *278*, 1966-1968.

Cheng, J., Park, T.S., Chio, L.C., Fischl, A.S., and Ye, X.S. (2003). Induction of apoptosis by sphingoid long-chain bases in *Aspergillus nidulans*. Mol. Cell Biol. *23*, 163-177.

Choi, D.W. (1988). Calcium-mediated neurotoxicity: relationship to specific channel types and role in ischemic damage. Trends Neurosci. *11*, 465-469.

Clayton, C.E. and Michels, P. (1996). Metabolic compartmentation in African trypanosomes. Parasitol. Today *12*, 465-471.

Cohen, G.M. (1997). Caspases: the executioners of apoptosis. Biochem. J. *326*, 1-16.

Coppens, I., Opperdoes, F.R., Courtoy, P.J., and Baudhuin, P. (1987). Receptor-mediated endocytosis in the blood-stream form of *trypanosoma-brucei*. J. Protozool. *34*, 465-473.

Cornillon, S., Foa, C., Davoust, J., Buonavista, N., Gross, J.D., and Golstein, P. (1994). Programmed cell death in *Dictyostelium*. J. Cell Sci. *107*, 2691-2704.

Cross, G.A. (1975). Identification, purification and properties of clone-specific glycoprotein antigens constituting the surface coat of *Trypanosoma brucei*. Parasitology *71*, 393-417.

Cross, G.A., Holder, A.A., Allen, G., and Boothroyd, J.C. (1980). An introduction to antigenic variation in trypanosomes. Am. J. Trop. Med. Hyg. *29*, 1027-1032.

Cross, G.A. and Manning, J.C. (1973). Cultivation of *Trypanosoma brucei* sspp. in semi-defined and defined media. Parasitology *67*, 315-331.

Cross, M., Kieft, R., Sabatini, R., Dirks-Mulder, A., Chaves, I., and Borst, P. (2002). J-binding protein increases the level and retention of the unusual base J in trypanosome DNA. Mol. Microbiol. *46*, 37-47.

Cully, D.F., Ip, H.S., and Cross, G.A.M. (1985). Coordinate transcription of variant surface glycoprotein genes and an expression site associated gene family in *Trypanosoma brucei*. Cell *42*, 173-182.

Das, M., Mukherjee, S.B., and Shaha, C. (2001). Hydrogen peroxide induces apoptosis-like death in *Leishmania donovani* promastigotes. J. Cell Sci. *114*, 2461-2469.

Dautry-Varsat, A., Ciechanover, A., and Lodish, H.F. (1983). pH and the recycling of transferrin during receptor-mediated endocytosis. Proc. Natl. Acad. Sci. U. S. A *80*, 2258-2262.

Davis, M.C., Ward, J.G., Herrick, G., and Allis, C.D. (1992). Programmed nuclear death: apoptotic-like degradation of specific nuclei in conjugating *Tetrahymena*. Dev. Biol. *154*, 419-432.

Debrabant, A., Lee, N., Bertholet, S., Duncan, R., and Nakhasi, H.L. (2003). Programmed cell death in trypanosomatids and other unicellular organisms. Int. J Parasitol. *33*, 257-267.

Denise, H., Coombs, G.H., and Mottram, J.C. (2004). Generation of *Leishmania* mutants lacking antibiotic resistance genes using a versatile hit-and-run targeting strategy. FEMS Microbiol. Lett. *235*, 89-94.

Denise, H., McNeil, K.S., Brooks, D.R., Alexander, J., Coombs, G.H., and Mottram, J.C. (2003). The expression of multiple *CPB* cysteine protease genes is required for *Leishmania mexicana* virulence *in vivo*. Infect. Immun. *71*, 3190-3195.

Denny, P.W., Lewis, S., Tempero, J.E., Goulding, D., Ivens, A.C., Field, M.C., and Smith, D.F. (2002). *Leishmania* RAB7: characterisation of terminal endocytic stages in an intracellular parasite. Mol. Biochem. Parasitol *123*, 105-113.

Dhir, V., Goulding, D., and Field, M.C. (2004). TbRAB1 and TbRAB2 mediate trafficking through the early secretory pathway of *Trypanosoma brucei*. Mol. Biochem. Parasitol. *137*, 253-265.

Djikeng, A., Shi, H., Tschudi, C., and Ullu, E. (2001). RNA interference in *Trypanosoma brucei*: cloning of small interfering RNAs provides evidence for retroposon-derived 24-26-nucleotide RNAs. RNA. *7*, 1522-1530.

Drenth, J., Jansonius, J.N., Koekoek, R., Swen, H.M., and Wolthers, B.G. (1968). Structure of papain. Nature *218*, 929-932.

Duan, H. and Dixit, V.M. (1997). RAIDD is a new 'death' adaptor molecule. Nature *385*, 86-89.

Eakin, A.E., Mills, A.A., Harth, G., McKerrow, J.H., and Craik, C.S. (1992). The sequence, organization, and expression of the major cysteine protease (cruzain) from *Trypanosoma cruzi*. J. Biol. Chem. *267*, 7411-7420.

Eichinger, A., Beisel, H.G., Jacob, U., Huber, R., Medrano, F.J., Banbula, A., Potempa, J., Travis, J., and Bode, W. (1999). Crystal structure of gingipain R: an Arg-specific bacterial cysteine proteinase with a caspase-like fold. EMBO J. *18*, 5453-5462.

Eisenhaber, B., Bork, P., and Eisenhaber, F. (2001). Post-translational GPI lipid anchor modification of proteins in kingdoms of life: analysis of protein sequence data from complete genomes. Protein Eng. *14*, 17-25.

Eisler, H., Frohlich, K.U., and Heidenreich, E. (2004). Starvation for an essential amino acid induces apoptosis and oxidative stress in yeast. Exp. Cell Res. *300*, 345-353.

Elbashir, S.M., Martinez, J., Patkaniowska, A., Lendeckel, W., and Tuschl, T. (2001). Functional anatomy of siRNAs for mediating efficient RNAi in *Drosophila melanogaster* embryo lysate. EMBO J. *20*, 6877-6888.

Ellis, H.M. and Horvitz, H.R. (1986). Genetic control of programmed cell death in the nematode *C. elegans*. Cell *44*, 817-829.

Engstler, M., Thilo, L., Weise, F., Grunfelder, C.G., Schwarz, H., Boshart, M., and Overath, P. (2004). Kinetics of endocytosis and recycling of the GPI-anchored variant surface glycoprotein in *Trypanosoma brucei*. J. Cell Sci. *117*, 1105-1115.

Evans, D.A. and Brown, R.C. (1972). The utilization of glucose and proline by culture forms of *Trypanosoma brucei*. J. Protozool. *19*, 686-690.

Evans, D.A. and Ellis, D.S. (1983). Recent observations on the behaviour of certain trypanosomes within their insect hosts. Adv. Parasitol. *22*, 1-42.

Fabrizio, P., Battistella, L., Vardavas, R., Gattazzo, C., Liou, L.L., Diaspro, A., Dossen, J.W., Gralla, E.B., and Longo, V.D. (2004). Superoxide is a mediator of an altruistic aging program in *Saccharomyces cerevisiae*. J. Cell Biol. *166*, 1055-1067.

Fast, B., Kremp, K., Boshart, M., and Steverding, D. (1999). Iron-dependent regulation of transferrin receptor expression in *Trypanosoma brucei*. Biochem. J. *342*, 691-696.

Feagin, J.E., Jasmer, D.P., and Stuart, K. (1986). Differential mitochondrial gene-expression between slender and stumpy bloodforms of *Trypanosoma brucei*. Mol. Biochem. Parasitol. *20*, 207-214.

Ferguson, M.J. (1997). The surface glycoconjugates of trypanosomatid parasites. Philosophical Transactions Of The Royal Society Of London Series B- Biological Sciences *352*, 1295-1302.

Field, H., Ali, B.R., Sherwin, T., Gull, K., Croft, S.L., and Field, M.C. (1999). TbRab2p, a marker for the endoplasmic reticulum of *Trypanosoma brucei*, localises to the ERGIC in mammalian cells. J. Cell Sci. *112*, 147-156.

Field, H., Farjah, M., Pal, A., Gull, K., and Field, M.C. (1998). Complexity of trypanosomatid endocytosis pathways revealed by Rab4 and Rab5 isoforms in *Trypanosoma brucei*. J. Biol. Chem. *273*, 32102-32110.

Field, H., Sherwin, T., Smith, A.C., Gull, K., and Field, M.C. (2000). Cell-cycle and developmental regulation of TbRAB31 localisation, a GTP-locked Rab protein from *Trypanosoma brucei*. Mol. Biochem. Parasitol. *106*, 21-35.

Field, M.C., Menon, A.K., and Cross, G.A.M. (1991). A glycosylphosphatidylinositol protein anchor from procyclic stage *trypanosoma-brucei* - lipid structure and biosynthesis. EMBO J. *10*, 2731-2739.

Filonova, L.H., Bozhkov, P.V., Brukhin, V.B., Daniel, G., Zhivotovsky, B., and von Arnold, S. (2000). Two waves of programmed cell death occur during formation and development of somatic embryos in the gymnosperm, Norway spruce. J. Cell Sci. *113*, 4399-4411.

Fire, A., Xu, S., Montgomery, M.K., Kostas, S.A., Driver, S.E., and Mello, C.C. (1998). Potent and specific genetic interference by double-stranded RNA in *Caenorhabditis elegans*. Nature *391*, 806-811.

Fischer, U., Janicke, R.U., and Schulze-Osthoff, K. (2003). Many cuts to ruin: a comprehensive update of caspase substrates. Cell Death. Differ. *10*, 76-100.

Fox, T., de Miguel, E., Mort, J.S., and Storer, A.C. (1992). Potent slow-binding inhibition of cathepsin B by its propeptide. Biochemistry *31*, 12571-12576.

Frame, M.J., Mottram, J.C., and Coombs, G.H. (2000). Analysis of the roles of cysteine proteinases of *Leishmania mexicana* in the host-parasite interaction . Parasitology *121*, 367-377.

Francis, S.E., Gluzman, I.Y., Oksman, A., Banerjee, D., and Goldberg, D.E. (1996). Characterization of native falcipain, an enzyme involved in *Plasmodium falciparum* hemoglobin degradation. Mol. Biochem. Parasitol. *83*, 189-200.

Garay-Arroyo, A., Colmenero-Flores, J.M., Garciarrubio, A., and Covarrubias, A.A. (2000). Highly hydrophilic proteins in prokaryotes and eukaryotes are common during conditions of water deficit. J. Biol. Chem. *275*, 5668-5674.

Ghedin, E., Debrabant, A., Engel, J.C., and Dwyer, D.M. (2001). Secretory and endocytic pathways converge in a dynamic endosomal system in a primitive protozoan. Traffic. *2*, 175-188.

Gorvel, J.P., Chavrier, P., Zerial, M., and Gruenberg, J. (1991). Rab5 controls early endosome fusion in vitro. Cell *64*, 915-925.

Govrin, E.M. and Levine, A. (2000). The hypersensitive response facilitates plant infection by the necrotrophic pathogen *Botrytis cinerea*. Curr. Biol. *10*, 751-757.

Grab, D.J., Wells, C.W., Shaw, M.K., Webster, P., and Russo, D.C. (1992). Endocytosed transferrin in African trypanosomes is delivered to lysosomes and may not be recycled. Eur. J. Cell Biol. *59*, 398-404.

Green, E.G., Ramm, E., Riley, N.M., Spiro, D.J., Goldenring, J.R., and Wessling-Resnick, M. (1997). Rab11 is associated with transferrin-containing recycling compartments in K562 cells. Biochem. Biophys. Res. Commun. *239*, 612-616.

Greenbaum, D.C., Baruch, A., Grainger, M., Bozdech, Z., Medzihradszky, K.F., Engel, J., DeRisi, J., Holder, A.A., and Bogyo, M. (2002). A role for the protease falcipain 1 in host cell invasion by the human malaria parasite. Science *298*, 2002-2006.

Greenbaum, D.C., Mackey, Z., Hansell, E., Doyle, P., Gut, J., Caffrey, C.R., Lehrman, J., Rosenthal, P.J., McKerrow, J.H., and Chibale, K. (2004). Synthesis and structure-activity relationships of parasiticidal thiosemicarbazone cysteine protease inhibitors against *Plasmodium falciparum, Trypanosoma brucei,* and *Trypanosoma cruzi*. J. Med. Chem. *47*, 3212-3219.

Greenberg, J.T. (1996). Programmed cell death: a way of life for plants. Proc. Natl. Acad. Sci. U. S. A *93*, 12094-12097.

Grünfelder, C.G., Engstler, M., Weise, F., Schwarz, H., Stierhof, Y.D., Morgan, G.W., Field, M.C., and Overath, P. (2003). Endocytosis of a glycosylphosphatidylinositol-anchored protein via clathrin-coated vesicles, sorting by default in endosomes, and exocytosis via RAB11-positive carriers. Mol. Biol. Cell *14*, 2029-2040.

Gu, Y., Sarnecki, C., Aldape, R.A., Livingston, D.J., and Su, M.S. (1995). Cleavage of poly(ADP-ribose) polymerase by interleukin-1 beta converting enzyme and its homologs TX and Nedd-2. J. Biol. Chem. *270*, 18715-18718.

Hajduk, S., Adler, B., Bertrand, K., Fearon, K., Hager, K., Hancock, K., Harris, M., Leblanc, A., Moore, R., Pollard, V., Priest, J., and Wood, Z. (1992). Molecular Biology of African Trypanosomes - Development of New Strategies to Combat an Old Disease. Am. J. Med. Sci. *303*, 258-270.

Hall, D.H., Gu, G., Garcia-Anoveros, J., Gong, L., Chalfie, M., and Driscoll, M. (1997). Neuropathology of degenerative cell death in *Caenorhabditis elegans*. J. Neurosci. *17*, 1033-1045.

Hammarton, T.C., Clark, J., Douglas, F., Boshart, M., and Mottram, J.C. (2003). Stage-specific differences in cell cycle control in *Trypanosoma brucei* revealed by RNA interference of a mitotic cyclin. J. Biol. Chem. *278*, 22877-22886.

Hammarton, T.C., Engstler, M., and Mottram, J.C. (2004). The *Trypanosoma brucei* cyclin, CYC2, is required for cell cycle progression through G1 phase and maintenance of procyclic form cell morphology. J. Biol. Chem. *279*, 24757-24764.

Hammond, S.M., Bernstein, E., Beach, D., and Hannon, G.J. (2000). An RNA-directed nuclease mediates post-transcriptional gene silencing in *Drosophila* cells. Nature *404*, 293-296.

Hammond, S.M., Boettcher, S., Caudy, A.A., Kobayashi, R., and Hannon, G.J. (2001). Argonaute2, a link between genetic and biochemical analyses of RNAi. Science *293*, 1146-1150.

Hara-Nishimura, I., Takeuchi, Y., and Nishimura, M. (1993). Molecular characterization of a vacuolar processing enzyme related to a putative cysteine proteinase of *Schistosoma mansoni*. Plant Cell *5*, 1651-1659.

Hatsugai, N., Kuroyanagi, M., Yamada, K., Meshi, T., Tsuda, S., Kondo, M., Nishimura, M., and Hara-Nishimura, I. (2004). A plant vacuolar protease, VPE, mediates virus-induced hypersensitive cell death. Science *305*, 855-858.

Hazbun, T.R., Malmstrom, L., Anderson, S., Graczyk, B.J., Fox, B., Riffle, M., Sundin, B.A., Aranda, J.D., McDonald, W.H., Chiu, C.H., Snydsman, B.E., Bradley, P., Muller, E.G., Fields, S., Baker, D., Yates, J.R., III, and Davis, T.N. (2003). Assigning function to yeast proteins by integration of technologies. Mol. Cell *12*, 1353-1365.

Hendriks, E.F., Robinson, D.R., Hinkins, M., and Matthews, K.R. (2001). A novel CCCH protein which modulates differentiation of *Trypanosoma brucei* to its procyclic form. EMBO J. *20*, 6700-6711.

Herker, E., Jungwirth, H., Lehmann, K.A., Maldener, C., Frohlich, K.U., Wissing, S., Buttner, S., Fehr, M., Sigrist, S., and Madeo, F. (2004). Chronological aging leads to apoptosis in yeast. J. Cell Biol. *164*, 501-507.

Hirumi, H. and Hirumi, K. (1989). Continuous cultivation of *Trypanosoma brucei* blood stream forms in a medium containing a low concentration of serum-protein without feeder cell-layers. J. Parasitol. *75*, 985-989.

Hodder, A.N., Drew, D.R., Epa, V.C., Delorenzi, M., Bourgon, R., Miller, S.K., Moritz, R.L., Frecklington, D.F., Simpson, R.J., Speed, T.P., Pike, R.N., and Crabb, B.S. (2003). Enzymic, phylogenetic, and structural characterization of the unusual papain-like protease domain of *Plasmodium falciparum* SERA5. J. Biol. Chem. *278*, 48169-48177.

Hoeberichts, F.A., Ten Have, A., and Woltering, E.J. (2003). A tomato metacaspase gene is upregulated during programmed cell death in *Botrytis cinerea*-infected leaves. Planta *217*, 517-522.

Hong, Y., Ohishi, K., Kang, J.Y., Tanaka, S., Inoue, N., Nishimura, J., Maeda, Y., and Kinoshita, T. (2003). Human PIG-U and yeast Cdc91p are the fifth subunit of GPI transamidase that attaches GPI-anchors to proteins. Mol. Biol. Cell *14*, 1780-1789.

Hornig, N.C.D., Knowles, P.P., McDonald, N.Q., and Uhlmann, F. (2002). The dual mechanism of separase regulation by securin. Curr. Biol. *12*, 973-982.

Hu, S., Vincenz, C., Ni, J., Gentz, R., and Dixit, V.M. (1997). I-FLICE, a novel inhibitor of tumor necrosis factor receptor-1- and CD-95-induced apoptosis. J. Biol. Chem. *272*, 17255-17257.

Huh, G.H., Damsz, B., Matsumoto, T.K., Reddy, M.P., Rus, A.M., Ibeas, J.I., Narasimhan, M.L., Bressan, R.A., and Hasegawa, P.M. (2002). Salt causes ion disequilibrium-induced programmed cell death in yeast and plants. Plant J. *29*, 649-659.

Huh, W.K., Falvo, J.V., Gerke, L.C., Carroll, A.S., Howson, R.W., Weissman, J.S., and O'Shea, E.K. (2003). Global analysis of protein localization in budding yeast. Nature *425*, 686-691.

Hutchings, N.R., Donelson, J.E., and Hill, K.L. (2002). Trypanin is a cytoskeletal linker protein and is required for cell motility in African trypanosomes. J. Cell Biol. *156*, 867-877.

Ingham, R.J., Gish, G., and Pawson, T. (2004). The Nedd4 family of E3 ubiquitin ligases: functional diversity within a common modular architecture. Oncogene *23*, 1972-1984.

Ito, T., Chiba, T., Ozawa, R., Yoshida, M., Hattori, M., and Sakaki, Y. (2001). A comprehensive two-hybrid analysis to explore the yeast protein interactome. Proc. Natl. Acad. Sci. U. S. A *98*, 4569-4574.

Jeffries, T.R., Morgan, G.W., and Field, M.C. (2001). A developmentally regulated Rab11 homologue in *Trypanosoma brucei* is involved in recycling processes. J. Cell Sci. *114*, 2617-2626.

Jeffries, T.R., Morgan, G.W., and Field, M.C. (2002). TbRAB18, a developmentally regulated Golgi GTPase from *Trypanosoma brucei*. Mol. Biochem. Parasitol *121*, 63-74.

Joost Haasnoot, P.C., Cupac, D., and Berkhout, B. (2003). Inhibition of virus replication by RNA interference. J. Biomed. Sci. *10*, 607-616.

Kabiri, M. and Steverding, D. (2000). Studies on the recycling of the transferrin receptor in *Trypanosoma brucei* using an inducible gene expression system. Eur. J. Biochem. *267*, 3309-3314.

Kaufmann, S.H. and Hengartner, M.O. (2001). Programmed cell death: alive and well in the new millennium. Trends Cell Biol. *11*, 526-534.

Kelley, R.J., Alexander, D.L., Cowan, C., Balber, A.E., and Bangs, J.D. (1999). Molecular cloning of p67, a lysosomal membrane glycoprotein from *Trypanosoma brucei*. Mol. Biochem. Parasitol. *98*, 17-28.

Kembhavi, A.A., Buttle, D.J., Knight, C.G., and Barrett, A.J. (1993). The two cysteine endopeptidases of legume seeds: purification and characterization by use of specific fluorometric assays. Arch. Biochem. Biophys. *303*, 208-213.

Kennedy, P.G., Murray, M., Jennings, F., and Rodgers, J. (2002). Sleeping sickness: new drugs from old? [corrected]. Lancet *359*, 1695-1696.

Kerr, J.F., Wyllie, A.H., and Currie, A.R. (1972). Apoptosis: a basic biological phenomenon with wide-ranging implications in tissue kinetics. Br. J. Cancer *26*, 239-257.

Klemba, M.W. and Goldberg, D.E. (2002). Biological roles of proteases in parasitic protozoa. Annu. Rev. Biochem. *71*, 275-305.

Koonin, E.V. and Aravind, L. (2002). Origin and evolution of eukaryotic apoptosis: the bacterial connection. Cell Death. Differ. *9*, 394-404.

Kumar, M. and Carmichael, G.G. (1998). Antisense RNA: function and fate of duplex RNA in cells of higher eukaryotes. Microbiol. Mol. Biol. Rev. *62*, 1415-1434.

Kuznicki, K.A., Smith, P.A., Leung-Chiu, W.M., Estevez, A.O., Scott, H.C., and Bennett, K.L. (2000). Combinatorial RNA interference indicates GLH-4 can compensate for GLH-1; these two P granule components are critical for fertility in *C. elegans*. Development *127*, 2907-2916.

LaCount, D.J., Bruse, S., Hill, K.L., and Donelson, J.E. (2000). Double-stranded RNA interference in *Trypanosoma brucei* using head-to-head promoters. Mol. Biochem. Parasitol. *111*, 67-76.

Lecaille, F., Kaleta, J., and Bromme, D. (2002). Human and parasitic papain-like cysteine proteases: their role in physiology and pathology and recent developments in inhibitor design. Chem. Rev. *102*, 4459-4488.

Lee, N., Bertholet, S., Debrabant, A., Muller, J., Duncan, R., and Nakhasi, H.L. (2002). Programmed cell death in the unicellular protozoan parasite *Leishmania*. Cell Death Differ. *9*, 53-64.

Legros, D., Ollivier, G., Gastellu-Etchegorry, M., Paquet, C., Burri, C., Jannin, J., and Buscher, P. (2002). Treatment of human African trypanosomiasis--present situation and needs for research and development. Lancet Infect. Dis. *2*, 437-440.

Lemmon, S.K. and Traub, L.M. (2000). Sorting in the endosomal system in yeast and animal cells. Curr. Opin. Cell Biol. *12*, 457-466.

Lillico, S.G., Field, M.C., Blundell, P., Coombs, G.H., and Mottram, J.C. (2003). Essential roles for GPI-anchored proteins in African trypanosomes revealed using mutants deficient in GPI8. Mol. Biol. Cell *14*, 1182-1194.

Lipton, S.A. and Nicotera, P. (1998). Calcium, free radicals and excitotoxins in neuronal apoptosis. Cell Calcium *23*, 165-171.

Liu, J., Carmell, M.A., Rivas, F.V., Marsden, C.G., Thomson, J.M., Song, J.J., Hammond, S.M., Joshua-Tor, L., and Hannon, G.J. (2004). Argonaute2 is the catalytic engine of mammalian RNAi. Science *305*, 1437-1441.

Liu, J.Y., Qiao, X.G., Du, D.Y., and Lee, M.G.S. (2000). Receptor-mediated endocytosis in the procyclic form of *Trypanosoma brucei*. J. Biol. Chem. *275*, 12032-12040.

Liu, Q., Rand, T.A., Kalidas, S., Du, F., Kim, H.E., Smith, D.P., and Wang, X. (2003). R2D2, a bridge between the initiation and effector steps of the *Drosophila* RNAi pathway. Science *301*, 1921-1925.

Luo, S., Rohloff, P., Cox, J., Uyemura, S.A., and Docampo, R. (2004). *Trypanosoma brucei* plasma membrane-type Ca(2+)-ATPase 1 (TbPMC1) and 2 (TbPMC2) genes encode functional Ca(2+)-ATPases localized to the acidocalcisomes and plasma membrane, and essential for Ca(2+) homeostasis and growth. J. Biol. Chem. *279*, 14427-14439.

Ma, J.B., Ye, K., and Patel, D.J. (2004). Structural basis for overhang-specific small interfering RNA recognition by the PAZ domain. Nature *429*, 318-322.

Macias, M.J., Hyvonen, M., Baraldi, E., Schultz, J., Sudol, M., Saraste, M., and Oschkinat, H. (1996). Structure of the WW domain of a kinase-associated protein complexed with a proline-rich peptide. Nature *382*, 646-649.

Macias, M.J., Wiesner, S., and Sudol, M. (2002). WW and SH3 domains, two different scaffolds to recognize proline-rich ligands. FEBS Lett. *513*, 30-37.

Madeo, F., Frohlich, E., Ligr, M., Grey, M., Sigrist, S.J., Wolf, D.H., and Frohlich, K.U. (1999). Oxygen stress: a regulator of apoptosis in yeast. J. Cell Biol. *145*, 757-767.

Madeo, F., Herker, E., Maldener, C., Wissing, S., Lachelt, S., Herlan, M., Fehr, M., Lauber, K., Sigrist, S.J., Wesselborg, S., and Frohlich, K.U. (2002). A caspase-related protease regulates apoptosis in yeast. Mol. Cell *9*, 911-917.

Magez, S., Geuskens, M., Beschin, A., del Favero, H., Verschueren, H., Lucas, R., Pays, E., and De Baetselier, P. (1997). Specific uptake of tumor necrosis factor-alpha is involved in growth control of *Trypanosoma brucei*. J. Cell Biol. *137*, 715-727.

Maier, A. and Steverding, D. (1996). Low affinity of *Trypanosoma brucei* transferrin receptor to apotransferrin at pH 5 explains the fate of the ligand during endocytosis. FEBS Lett. *396*, 87-89.

Manoury, B., Hewitt, E.W., Morrice, N., Dando, P.M., Barrett, A.J., and Watts, C. (1998). An asparaginyl endopeptidase processes a microbial antigen for class II MHC presentation. Nature *396*, 695-699.

Marks, M.S., Ohno, H., Kirchhausen, T., and Bonifacino, J.S. (2004). Protein sorting by tyrosine-based signals: adapting to the Ys and wherefores. Trends Cell Biol. 7, 124-128.

McConville, M.J., Mullin, K.A., Ilgoutz, S.C., and Teasdale, R.D. (2002). Secretory pathway of trypanosomatid parasites. Microbiol. Mol. Biol. Rev. *66*, 122-154.

McKean, P.G., Baines, A., Vaughan, S., and Gull, K. (2003). Gamma-tubulin functions in the nucleation of a discrete subset of microtubules in the eukaryotic flagellum. Curr. Biol. *13*, 598-602.

McKerrow, J.H., Engel, J.C., and Caffrey, C.R. (1999). Cysteine protease inhibitors as chemotherapy for parasitic infections. Bioorg. Med. Chem. *7*, 639-644.

McManus, M.T., Shimamura, M., Grams, J., and Hajduk, S.L. (2001). Identification of candidate mitochondrial RNA editing ligases from *Trypanosoma brucei*. RNA. *7*, 167-175.

Medina-Acosta, E. and Cross, G.A.M. (1993). Rapid isolation of DNA from trypanosomatid protozoa using a simple mini-prep procedure. Mol. Biochem. Parasitol. *59*, 327-329.

Michelotti, E.F. and Hajduk, S.L. (1987). Developmental regulation of trypanosome mitochondrial gene expression. J. Biol. Chem. *262*, 927-932.

Miossec, C., Decoen, M.C., Durand, L., Fassy, F., and Diu-Hercend, A. (1996). Use of monoclonal antibodies to study interleukin-1 beta-converting enzyme expression: only precursor forms are detected in interleukin-1 beta-secreting cells. Eur. J. Immunol. *26*, 1032-1042.

Mitchell, W.M. (1977). Cleavage at arginine residues by clostripain. Methods Enzymol. *47*, 165-170.

Mitchell, W.M. and Harrington, W.F. (1968). Purification and properties of clostridiopeptidase B (Clostripain). J. Biol. Chem. *243*, 4683-4692.

Miura, M., Zhu, H., Rotello, R., Hartwieg, E.A., and Yuan, J. (1993). Induction of apoptosis in fibroblasts by IL-1 beta-converting enzyme, a mammalian homolog of the *C. elegans* cell death gene *ced-3*. Cell *75*, 653-660.

Moreira, M.E., Del Portillo, H.A., Milder, R.V., Balanco, J.M., and Barcinski, M.A. (1996). Heat shock induction of apoptosis in promastigotes of the unicellular organism *Leishmania (Leishmania) amazonensis*. J. Cell Physiol. *167*, 305-313.

Mottram, J.C., Brooks, D.R., and Coombs, G.H. (1998). Roles of cysteine proteinases of trypanosomes and *Leishmania* in host-parasite interactions. Curr. Opin. Microbiol. *1*, 455-460.

Mottram, J.C., Helms, M.J., Coombs, G.H., and Sajid, M. (2003). Clan CD cysteine peptidases of parasitic protozoa. Trends Parasitol. *19*, 182-187.

Motyka, S.A., Zhao, Z.X., Gull, K., and Englund, P.T. (2004). Integration of pZJM library plasmids into unexpected locations in the *Trypanosoma brucei* genome. Mol. Biochem. Parasitol. *134*, 163-167.

Mowatt, M.R. and Clayton, C.E. (1987). Developmental regulation of a novel repetitive protein of trypanosoma-brucei. Mol. Cell. Biol. *7*, 2838-2844.

Muntz, K. and Shutov, A.D. (2002). Legumains and their functions in plants. Trends Plant Sci. *7*, 340-344.

Mussmann, R., Engstler, M., Gerrits, H., Kieft, R., Bentin, T.C., Onderwater, J., Koerten, H., Van Luenen, H.G., and Borst, P. (2004). Factors affecting level and localization of the transferrin receptor in *Trypanosoma brucei*. J. Biol. Chem.

Nagamune, K., Ohishi, K., Ashida, H., Hong, Y., Hino, J., Kangawa, K., Inoue, N., Maeda, Y., and Kinoshita, T. (2003). GPI transamidase of *Trypanosoma brucei* has two previously uncharacterized (trypanosomatid transamidase 1 and 2) and three common subunits. Proc. Natl. Acad. Sci. U. S. A *100*, 10682-10687.

Nasirudeen, A.M., Hian, Y.E., Singh, M., and Tan, K.S. (2004). Metronidazole induces programmed cell death in the protozoan parasite *Blastocystis hominis*. Microbiology *150*, 33-43.

Nasirudeen, A.M., Tan, K.S., Singh, M., and Yap, E.H. (2001). Programmed cell death in a human intestinal parasite, *Blastocystis hominis*. Parasitology *123*, 235-246.

Nasmyth, K. (1999). Separating sister chromatids. Trends Biochem. Sci. *24*, 98-104.

Navarro, M. and Gull, K. (2001). A pol I transcriptional body associated with VSG mono-allelic expression in *Trypanosoma brucei*. Nature *414*, 759-763.

Ngo, H., Tschudi, C., Gull, K., and Ullu, E. (1998). Double-stranded RNA induces mRNA degradation in *Trypanosoma brucei*. Proc. Natl. Acad. Sci. U. S. A *95*, 14687-14692.

Nicholson, D.W. and Thornberry, N.A. (1997). Caspases: killer proteases. Trends Biochem. Sci. *22*, 299-306.

Nkemgu, N.J., Grande, R., Hansell, E., McKerrow, J.H., Caffrey, C.R., and Steverding, D. (2003). Improved trypanocidal activities of cathepsin L inhibitors. Int. J. Antimicrob. Agents *22*, 155-159.

Nolan, D.P., Geuskens, M., and Pays, E. (1999). *N*-linked glycans containing linear poly-*N*-acetyllactosamine as sorting signals in endocytosis in *Trypanosoma brucei*. Curr. Biol. *9*, 1169-1172.

Novick, P. and Brennwald, P. (1993). Friends and family: the role of the Rab GTPases in vesicular traffic. Cell *75*, 597-601.

Nuoffer, C. and Balch, W.E. (1994). GTPases: Multifunctional Molecular Switches Regulating Vesicular Traffic. Annu. Rev. Biochem. *63*, 949-990.

Nykanen, A., Haley, B., and Zamore, P.D. (2001). ATP requirements and small interfering RNA structure in the RNA interference pathway. Cell *107*, 309-321.

O'Beirne, C., Lowry, C.M., and Voorheis, H.P. (1998). Both IgM and IgG anti-VSG antibodies initiate a cycle of aggregation-disaggregation of bloodstream forms of *Trypanosoma brucei* without damage to the parasite. Mol. Biochem. Parasitol. *91*, 165-193.

Olie, R.A., Durrieu, F., Cornillon, S., Loughran, G., Gross, J., Earnshaw, W.C., and Golstein, P. (1998). Apparent caspase independence of programmed cell death in *Dictyostelium*. Curr. Biol. *8*, 955-958.

Opperdoes, F.R. and Borst, P. (1977). Localization of nine glycolytic enzymes in a microbody-like organelle in *Trypanosoma brucei*: the glycosome. FEBS Lett. *80*, 360-364.

Overath, P., Czichos, J., Stock, U., and Nonnengaesser, C. (1983). Repression of glycoprotein-synthesis and release of surface-coat during transformation of *trypanosoma-brucei*. EMBO J. *2*, 1721-1728.

Overath, P., Steverding, D., Chaudhri, M., Stierhof, Y.D., and Ziegelbauer, K. (1994). Structure and function of GPI-anchored surface proteins of *Trypanosoma brucei*. Braz. J. Med. Biol. Res. *27*, 343-347.

Overath, P., Stierhof, Y.D., and Wiese, M. (1997). Endocytosis and secretion in trypanosomatid parasites tumultuous traffic in a pocket. Trends Cell Biol. *7*, 27-33.

Pal, A., Hall, B.S., Jeffries, T.R., and Field, M.C. (2003). Rab5 and Rab11 mediate transferrin and anti-variant surface glycoprotein antibody recycling in *Trypanosoma brucei*. Biochem. J. *374*, 443-451.

Pal, A., Hall, B.S., Nesbeth, D.N., Field, H.I., and Field, M.C. (2002). Differential Endocytic functions of *Trypanosoma brucei* Rab5 isoforms reveal a glycosylphosphatidylinositol-specific endosomal pathway. J. Biol. Chem. *277*, 9529-9539.

Panigrahi, A.K., Schnaufer, A., Ernst, N.L., Wang, B., Carmean, N., Salavati, R., and Stuart, K. (2003). Identification of novel components of *Trypanosoma brucei* editosomes. RNA. *9*, 484-492.

Parsons, M., Furuya, T., Pal, S., and Kessler, P. (2001). Biogenesis and function of peroxisomes and glycosomes. Mol. Biochem. Parasitol. *115*, 19-28.

Pays, E., Tebabi, P., Pays, A., Coquelet, H., Revelard, P., Salmon, D., and Steinert, M. (1989). The genes and transcripts of an antigen gene expression site from *T.brucei*. Cell *57*, 835-845.

Pays, E., Vanhamme, L., and Berberof, M. (1994). Genetic controls for the expression of surface antigens in African trypanosomes. Annu. Rev. Microbiol. *48*, 25-52.

Pepin, J. and Milord, F. (1994). The treatment of human African trypanosomiasis. Adv. Parasitol. *33*, 1-47.

Picot, S., Burnod, J., Bracchi, V., Chumpitazi, B.F., and Ambroise-Thomas, P. (1997). Apoptosis related to chloroquine sensitivity of the human malaria parasite *Plasmodium falciparum*. Trans. R. Soc. Trop. Med. Hyg. *91*, 590-591.

Pils, B. and Schultz, J. (2004a). Evolution of the multifunctional protein tyrosine phosphatase family. Mol. Biol. Evol. *21*, 625-631.

Pils, B. and Schultz, J. (2004b). Inactive enzyme-homologues find new function in regulatory processes. J. Mol. Biol. *340*, 399-404.

Potempa, J. and Travis, J. (1996). *Porphyromonas gingivalis* proteinases in periodontitis, a review. Acta Biochim. Pol. *43*, 455-465.

Ramage, P., Cheneval, D., Chvei, M., Graff, P., Hemmig, R., Heng, R., Kocher, H.P., MacKenzie, A., Memmert, K., Revesz, L., and . (1995). Expression, refolding, and autocatalytic proteolytic processing of the interleukin-1 beta-converting enzyme precursor. J. Biol. Chem. *270*, 9378-9383.

Rawlings, N.D., Tolle, D.P., and Barrett, A.J. (2004). MEROPS: the peptidase database. Nucleic Acids Res. *32 Database issue*, D160-D164.

Renatus, M., Stennicke, H.R., Scott, F.L., Liddington, R.C., and Salvesen, G.S. (2001). Dimer formation drives the activation of the cell death protease caspase 9. Proc. Natl. Acad. Sci. U. S. A *98*, 14250-14255.

Richardson, J.P., Beecroft, R.P., Tolson, D.L., Liu, M.K., and Pearson, T.W. (1988). Procyclin: an unusual immunodominant glycoprotein surface antigen from the procyclic stage of African trypanosomes. Mol. Biochem. Parasitol. *31*, 203-216.

Ridgley, E.L., Xiong, Z.H., and Ruben, L. (1999). Reactive oxygen species activate a Ca2+-dependent cell death pathway in the unicellular organism *Trypanosoma brucei brucei*. Biochem. J. *340 (Pt 1)*, 33-40.

Rigaut, G., Shevchenko, A., Rutz, B., Wilm, M., Mann, M., and Seraphin, B. (1999). A generic protein purification method for protein complex characterization and proteome exploration. Nat. Biotechnol. *17*, 1030-1032.

Robertson, C.D. and Coombs, G.H. (1994). Multiple high activity cysteine proteases of *Leishmania mexicana* are encoded by the *Imcpb* gene array. Microbiology *140*, 417-424.

Roisin-Bouffay, C., Luciani, M.F., Klein, G., Levraud, J.P., Adam, M., and Golstein, P. (2004). Developmental cell death in *Dictyostelium* does not require paracaspase. J. Biol. Chem. *279*, 11489-11494.

Rosenthal, P.J. (1999). Proteases of protozoan parasites. Adv. Parasitol. *43*, 105-159.

Ross, K.E. and Cohen-Fix, O. (2002). Separase: a conserved protease separating more than just sisters. Trends Cell Biol. *12*, 1-3.

Rotonda, J., Nicholson, D.W., Fazil, K.M., Gallant, M., Gareau, Y., Labelle, M., Peterson, E.P., Rasper, D.M., Ruel, R., Vaillancourt, J.P., Thornberry, N.A., and Becker, J.W. (1996). The three-dimensional structure of apopain/CPP32, a key mediator of apoptosis. Nat. Struct. Biol. *3*, 619-625.

Rozman-Pungercar, J., Kopitar-Jerala, N., Bogyo, M., Turk, D., Vasiljeva, O., Stefe, I., Vandenabeele, P., Bromme, D., Puizdar, V., Fonovic, M., Trstenjak-Prebanda, M., Dolenc, I., Turk, V., and Turk, B. (2003). Inhibition of papain-like cysteine proteases and legumain by caspase-specific inhibitors: when reaction mechanism is more important than specificity. Cell Death. Differ. *10*, 881-888.

Russo, D.C., Grab, D.J., Lonsdale-Eccles, J.D., Shaw, M.K., and Williams, D.J. (1993). Directional movement of variable surface glycoprotein-antibody complexes in *Trypanosoma brucei*. Eur. J. Cell Biol. *62*, 432-441.

Sajid, M. and McKerrow, J.H. (2002). Cysteine proteases of parasitic organisms. Mol. Biochem. Parasitol. *120*, 1-21.

Sajid, M., McKerrow, J.H., Hansell, E., Mathieu, M.A., Lucas, K.D., Hsieh, I., Greenbaum, D., Bogyo, M., Salter, J.P., Lim, K.C., Franklin, C., Kim, J.H., and Caffrey, C.R. (2003). Functional expression and characterization of *Schistosoma mansoni* cathepsin B and its trans-activation by an endogenous asparaginyl endopeptidase. Mol. Biochem. Parasitol *131*, 65-75.

Salmon, D., Geuskens, M., Hanocq, F., Hanocq-Quertier, J., Nolan, D., Ruben, L., and Pays, E. (1994). A novel heterodimeric transferrin receptor encoded by a pair of VSG expression site-associated genes in *T. brucei*. Cell *78*, 75-86.

Sanderson, S.J., Pollock, K.G., Hilley, J.D., Meldal, M., St.Hilaire, P.M., Juliano, M.A., Juliano, L., Mottram, J.C., and Coombs, G.H. (2000). Expression and characterisation of a recombinant cysteine proteinase of *Leishmania mexicana*. Biochem. J. *347*, 383-388.

Searle, J., Kerr, J.F., and Bishop, C.J. (1982). Necrosis and apoptosis: distinct modes of cell death with fundamentally different significance. Pathol. Annu. *17*, 229-259.

Sen, N., Das, B.B., Ganguly, A., Mukherjee, T., Bandyopadhyay, S., and Majumder, H.K. (2004). Camptothecin induced imbalance in intracellular cation homeostasis regulates programmed cell death in unicellular hemoflagellate *leishmania donovani*. J. Biol. Chem.

Seyfang, A., Mecke, D., and Duszenko, M. (1990). Degradation, recycling, and shedding of *Trypanosoma brucei* variant surface glycoprotein. J. Protozool. *37*, 546-552.

Shenai, B.R., Sijwali, P.S., Singh, A., and Rosenthal, P.J. (2000). Characterization of native and recombinant falcipain-2, a principal trophozoite cysteine protease and essential hemoglobinase of *Plasmodium falciparum*. J. Biol. Chem. *275*, 29000-29010.

Shi, H., Djikeng, A., Tschudi, C., and Ullu, E. (2004). Argonaute protein in the early divergent eukaryote *Trypanosoma brucei*: control of small interfering RNA accumulation and retroposon transcript abundance. Mol. Cell Biol. *24*, 420-427.

Shi, H.F., Djikeng, A., Mark, T., Wirtz, E., Tschudi, C., and Ullu, E. (2000). Genetic interference in *Trypanosoma brucei* by heritable and inducible double-stranded RNA. RNA Publ. RNA Soc. *6*, 1069-1076.

Shimada, M., Kawahara, H., and Doi, H. (2002). Novel family of CCCH-type zinc-finger proteins, MOE-1, -2 and -3, participates in *C. elegans* oocyte maturation. Genes Cells *7*, 933-947.

Sijen, T. and Plasterk, R.H. (2003). Transposon silencing in the Caenorhabditis elegans germ line by natural RNAi. Nature *426*, 310-314.

Son, H.J., Cook, G.A., Hall, T., and Donelson, J.E. (1989). Expression site associated genes of *Trypanosoma brucei rhodesiense*. Mol. Biochem. Parasitol. *33*, 59-66.

Song, J.J., Smith, S.K., Hannon, G.J., and Joshua-Tor, L. (2004). Crystal structure of Argonaute and its implications for RISC slicer activity. Science *305*, 1434-1437.

Souza, A.E., Bates, P.A., Coombs, G.H., and Mottram, J.C. (1994). Null mutants for the *lmcpa* cysteine proteinase gene in *Leishmania mexicana*. Mol. Biochem. Parasitol. *63*, 213-220.

Stadnyk, A.W., Myler, P.J., Lodes, M., and Stuart, K.D. (1991). Characterization of Expression Site Associated Genes (ESAGs) of Trypanosoma brucei. FASEB J. *5*, 1533.

Stennicke, H.R. and Salvesen, G.S. (1998). Properties of the caspases. Biochim. Biophys. Acta *1387*, 17-31.

Steverding, D. (2004). The transferrin receptor of *Trypanosoma brucei*. Parasitol. Int. *48*, 191-198.

Steverding, D., Stierhof, Y.D., Fuchs, H., Tauber, R., and Overath, P. (1995). Transferrin-binding protein complex is the receptor for transferrin uptake in *Trypanosoma brucei*. J. Cell Biol. *131*, 1173-1182.

Steverding, D., Stierhof, Y.-D., Chaudhri, M., Ligtenberg, M., Schell, D., Beck-Sickinger, A.G., and Overath, P. (1994). ESAG 6 and 7 products of *Trypanosoma brucei* form a transferrin binding protein complex. Eur. J. Cell Biol. *64*, 78-87.

Stuart, K. and Panigrahi, A.K. (2002). RNA editing: complexity and complications. Mol. Microbiol. *45*, 591-596.

Suarez, M.F., Filonova, L.H., Smertenko, A., Savenkov, E.I., Clapham, D.H., von Arnold, S., Zhivotovsky, B., and Bozhkov, P.V. (2004). Metacaspase-dependent programmed cell death is essential for plant embryogenesis. Curr. Biol. *14*, R339-R340.

Sudol, M. and Hunter, T. (2000). NeW wrinkles for an old domain. Cell *103*, 1001-1004.

Sudol, M., Sliwa, K., and Russo, T. (2001). Functions of WW domains in the nucleus. FEBS Lett. *490*, 190-195.

Syntichaki, P. and Tavernarakis, N. (2002). Death by necrosis. Uncontrollable catastrophe, or is there order behind the chaos? EMBO Rep. *3*, 604-609.

Szallies, A., Kubata, B.K., and Duszenko, M. (2002). A metacaspase of *Trypanosoma brucei* causes loss of respiration competence and clonal death in the yeast *Saccharomyces cerevisiae*. FEBS Lett. *517*, 144-150.

Tabara, H., Sarkissian, M., Kelly, W.G., Fleenor, J., Grishok, A., Timmons, L., Fire, A., and Mello, C.C. (1999). The rde-1 gene, RNA interference, and transposon silencing in *C. elegans*. Cell *99*, 123-132.

Tetley, L. and Vickerman, K. (1985). Differentiation in *trypanosoma-brucei* - host-parasite cell- junctions and their persistence during acquisition of the variable antigen coat. J. Cell Sci. *74*, 1-19.

Tewari, M., Quan, L.T., O'Rourke, K., Desnoyers, S., Zeng, Z., Beidler, D.R., Poirier, G.G., Salvesen, G.S., and Dixit, V.M. (1995). Yama/CPP32 beta, a mammalian homolog of CED-3, is a CrmA-inhibitable protease that cleaves the death substrate poly(ADP-ribose) polymerase. Cell *81*, 801-809.

Traub, L.M. and Kornfeld, S. (1997). The trans-Golgi network: a late secretory sorting station. Curr. Opin. Cell Biol. *9*, 527-533.

Turner, C.M. (1999). Antigenic variation in *Trypanosoma brucei* infections: an holistic view. J. Cell Sci. *112*, 3187-3192.

Turner, C.M.R. and Barry, J.D. (1989). High frequency of antigenic variation in *Trypanosoma brucei rhodesiense* infections. Parasitology *99*, 67-75.

Uetz, P., Giot, L., Cagney, G., Mansfield, T.A., Judson, R.S., Knight, J.R., Lockshon, D., Narayan, V., Srinivasan, M., Pochart, P., Qureshi-Emili, A., Li, Y., Godwin, B., Conover, D., Kalbfleisch, T., Vijayadamodar, G., Yang, M., Johnston, M., Fields, S., and Rothberg, J.M. (2000). A comprehensive analysis of protein-protein interactions in *Saccharomyces cerevisiae*. Nature *403*, 623-627.

Uhlmann, F., Lottspeich, F., and Nasmyth, K. (1999). Sister-chromatid separation at anaphase onset is promoted by cleavage of the cohesin subunit Scc1. Nature *400*, 37-42.

Ullrich, O., Reinsch, S., Urbe, S., Zerial, M., and Parton, R.G. (1996). Rab11 regulates recycling through the pericentriolar recycling endosome. J. Cell Biol. *135*, 913-924.

Uren, A.G., O'Rourke, K., Aravind, L.A., Pisabarro, M.T., Seshagiri, S., koonin, E.V., and Dixit, V.M. (2000). Identification of paracaspases and metacaspases: two ancient families of caspase-like proteins, one of which plays a key role in MALT lymphoma. Mol. Cell *6*, 961-967.

Utz, P.J. and Anderson, P. (2000). Life and death decisions: regulation of apoptosis by proteolysis of signaling molecules. Cell Death. Differ. *7*, 589-602.

Van der Ploeg, L.H., Valerio, D., de Lange, T., Bernards, A., Borst, P., and Grosveld, F.G. (1982). An analysis of cosmid clones of nuclear DNA from *Trypanosoma brucei* shows that the genes for variant surface glycoproteins are clustered in the genome. Nucleic Acids Res. *10*, 5905-5923.

van Vliet, C., Thomas, E.C., Merino-Trigo, A., Teasdale, R.D., and Gleeson, P.A. (2003). Intracellular sorting and transport of proteins. Prog. Biophys. Mol. Biol. *83*, 1-45.

van Weelden, S.W., Fast, B., Vogt, A., van der, M.P., Saas, J., Van Hellemond, J.J., Tielens, A.G., and Boshart, M. (2003). Procyclic *Trypanosoma brucei* do not use Krebs cycle activity for energy generation. J. Biol. Chem. *278*, 12854-12863.

Vassella, E., Reuner, B., Yutzy, B., and Boshart, M. (1997). Differentiation of African trypanosomes is controlled by a density sensing mechanism which signals cell cycle arrest via the cAMP pathway. J. Cell Sci. *110*, 2661-2671.

Vercammen, D., Van De, C.B., De Jaeger, G., Eeckhout, D., Casteels, P., Vandepoele, K., Vandenberghe, I., Van Beeumen, J., Inze, D., and Van Breusegem, F. (2004). Type-II metacaspases Atmc4 and Atmc9 of *Arabidopsis thaliana* cleave substrates after arginine and lysine. J. Biol. Chem.

Vickerman, K. (1978). Antigenic variation in trypanosomes. Nature *273*, 613-617.

Vickerman, K. (1985). Developmental cycles and biology of pathogenic trypanosomes. Br. Med. Bull. *41*, 105-114.

Wadskog, I., Maldener, C., Proksch, A., Madeo, F., and Adler, L. (2004). Yeast lacking the SRO7/SOP1-encoded tumor suppressor homologue show increased susceptibility to apoptosis-like cell death on exposure to NaCl stress. Mol. Biol. Cell *15*, 1436-1444.

Wang, J., Bohme, U., and Cross, G.A. (2003). Structural features affecting variant surface glycoprotein expression in *Trypanosoma brucei*. Mol. Biochem. Parasitol. *128*, 135-145.

Wang, Z., Morris, J.C., Drew, M.E., and Englund, P.T. (2000). Inhibition of *Trypanosoma brucei* Gene Expression by RNA Interference Using an Integratable Vector with Opposing T7 Promoters. J. Biol. Chem. *275*, 40174-40179.

Wei, Y., Fox, T., Chambers, S.P., Sintchak, J., Coll, J.T., Golec, J.M., Swenson, L., Wilson, K.P., and Charifson, P.S. (2000). The structures of caspases-1, -3, -7 and -8 reveal the basis for substrate and inhibitor selectivity. Chem. Biol. *7*, 423-432.

Weil, M., Jacobson, M.D., Coles, H.S., Davies, T.J., Gardner, R.L., Raff, K.D., and Raff, M.C. (1996). Constitutive expression of the machinery for programmed cell death. J. Cell Biol. *133*, 1053-1059.

Welburn, S.C., Barcinski, M.A., and Williams, G.T. (1997). Programmed cell death in trypanosomatids. Parasitol. Today *13*, 22-26.

Welburn, S.C., Dale, C., Ellis, D., Beecroft, R., and Pearson, T.W. (1996). Apoptosis in procyclic *Trypanosoma brucei rhodesiense* in vitro. Cell Death Differ. *3*, 229-236.

Welburn, S.C., Lillico, S., and Murphy, N.B. (1999). Programmed cell death in procyclic form Trypanosoma brucei rhodesiense --identification of differentially expressed genes during con A induced death. Mem. Inst. Oswaldo Cruz *94*, 229-234.

Welburn, S.C. and Murphy, N.B. (1998). Prohibitin and RACK homologues are up-regulated in trypanosomes induced to undergo apoptosis and in naturally occurring terminally differentiated forms. Cell Death. Differ. *5*, 615-622.

Wirtz, E. and Clayton, C.E. (1995). Inducible gene expression in trypanosomes mediated by a prokaryotic repressor. Science *268*, 1179-1183.

Wirtz, E., Hartmann, C., and Clayton, C. (1994). Gene expression mediated by bacteriophage T3 and T7 RNA polymerases in transgenic trypanosomes. Nucleic Acids Res. *22*, 3887-3894.

Wirtz, E., Leal, S., Ochatt, C., and Cross, G.A. (1999). A tightly regulated inducible expression system for conditional gene knock-outs and dominant-negative genetics in *Trypanosoma brucei*. Mol. Biochem. Parasitol. *99*, 89-101.

Wysocki, R. and Kron, S.J. (2004). Yeast cell death during DNA damage arrest is independent of caspase or reactive oxygen species. J. Cell Biol. *166*, 311-316.

Xue, D. and Horvitz, H.R. (1997). Caenorhabditis elegans CED-9 protein is a bifunctional cell-death inhibitor. Nature *390*, 305-308.

Yan, K.S., Yan, S., Farooq, A., Han, A., Zeng, L., and Zhou, M.M. (2003). Structure and conserved RNA binding of the PAZ domain. Nature *426*, 468-474.

Yu, J.L., Nagarajan, S., Knez, J.J., Udenfriend, S., Chen, R., and Medof, M.E. (1997). The affected gene underlying the class K glycosylphosphatidylinositol (GPI) surface protein defect codes for the GPI transamidase. Proc. Natl. Acad. Sci. USA *94*, 12580-12585.

Yuan, J., Shaman, S., Ledoux, S., Ellis, H.M., and Horvitz, H.R. (1993). The *C. elegans* cell death gene *ced-3* encodes a protein similar to mammalian interleukin-1b-converting enzyme. Cell *75*, 641-652.

Zamzami, N. and Kroemer, G. (1999). Condensed matter in cell death. Nature *401*, 127-128.

Zangger, H., Mottram, J.C., and Fasel, N. (2002). Cell death in *Leishmania* induced by stress and differentiation: Programmed cell death or necrosis? Cell Death Diff. *9*, 1126-1139.